Mechatronics

VISIT…

SOLID MECHANICS AND ITS APPLICATIONS
Volume 136

Series Editor: G.M.L. GLADWELL
Department of Civil Engineering
University of Waterloo
Waterloo, Ontario, Canada N2L 3GI

Aims and Scope of the Series

The fundamental questions arising in mechanics are: *Why?, How?,* and *How much?* The aim of this series is to provide lucid accounts written by authoritative researchers giving vision and insight in answering these questions on the subject of mechanics as it relates to solids.

The scope of the series covers the entire spectrum of solid mechanics. Thus it includes the foundation of mechanics; variational formulations; computational mechanics; statics, kinematics and dynamics of rigid and elastic bodies: vibrations of solids and structures; dynamical systems and chaos; the theories of elasticity, plasticity and viscoelasticity; composite materials; rods, beams, shells and membranes; structural control and stability; soils, rocks and geomechanics; fracture; tribology; experimental mechanics; biomechanics and machine design.

The median level of presentation is the first year graduate student. Some texts are monographs defining the current state of the field; others are accessible to final year undergraduates; but essentially the emphasis is on readability and clarity.

For a list of related mechanics titles, see final pages.

Mechatronics
Dynamics of Electromechanical and Piezoelectric Systems

by

A. PREUMONT
ULB Active Structures Laboratory,
Brussels, Belgium

Springer

A C.I.P. Catalogue record for this book is available from the Library of Congress.

ISBN-10 1-4020-4695-2 (HB)
ISBN-13 978-1-4020-4695-7 (HB)
ISBN-10 1-4020-4696-0 (e-book)
ISBN-13 978-1-4020-4696-4 (e-book)

Published by Springer,
P.O. Box 17, 3300 AA Dordrecht, The Netherlands.

www.springer.com

Printed on acid-free paper

All Rights Reserved
© 2006 Springer
No part of this work may be reproduced, stored in a retrieval system, or transmitted
in any form or by any means, electronic, mechanical, photocopying, microfilming, recording
or otherwise, without written permission from the Publisher, with the exception
of any material supplied specifically for the purpose of being entered
and executed on a computer system, for exclusive use by the purchaser of the work.

Printed in the Netherlands.

"*Tenez, mon ami, si vous y pensez bien,*
vous trouverez qu'en tout,
notre véritable sentiment n'est pas celui
dans lequel nous n'avons jamais vacillé;
mais celui auquel nous sommes le plus
habituellement revenus."

Diderot,
(*Entretien entre D'Alembert et Diderot*)

Contents

Preface xiii

1 Lagrangian dynamics of mechanical systems 1
- 1.1 Introduction 1
- 1.2 Kinetic state functions 2
- 1.3 Generalized coordinates, kinematic constraints 4
  - 1.3.1 Virtual displacements 7
- 1.4 The principle of virtual work 8
- 1.5 D'Alembert's principle 10
- 1.6 Hamilton's principle 11
  - 1.6.1 Lateral vibration of a beam 14
- 1.7 Lagrange's equations 17
  - 1.7.1 Vibration of a linear, non-gyroscopic, discrete system 19
  - 1.7.2 Dissipation function 19
  - 1.7.3 Example 1: Pendulum with a sliding mass 20
  - 1.7.4 Example 2: Rotating pendulum 22
  - 1.7.5 Example 3: Rotating spring mass system 23
  - 1.7.6 Example 4: Gyroscopic effects 24
- 1.8 Lagrange's equations with constraints 27
- 1.9 Conservation laws 29
  - 1.9.1 Jacobi integral 29
  - 1.9.2 Ignorable coordinate 30
  - 1.9.3 Example: The spherical pendulum 32
- 1.10 More on continuous systems 32
  - 1.10.1 Rayleigh-Ritz method 32
  - 1.10.2 General continuous system 34
  - 1.10.3 Green strain tensor 34
  - 1.10.4 Geometric strain energy due to prestress 35
  - 1.10.5 Lateral vibration of a beam with axial loads 37

1.10.6 Example: Simply supported beam in compression ... 38
1.11 References ... 39

2 Dynamics of electrical networks ... 41
2.1 Introduction ... 41
2.2 Constitutive equations for circuit elements ... 42
2.2.1 The Capacitor ... 42
2.2.2 The Inductor ... 43
2.2.3 Voltage and current sources ... 45
2.3 Kirchhoff's laws ... 46
2.4 Hamilton's principle for electrical networks ... 47
2.4.1 Hamilton's principle, charge formulation ... 48
2.4.2 Hamilton's principle, flux linkage formulation ... 49
2.4.3 Discussion ... 51
2.5 Lagrange's equations ... 53
2.5.1 Lagrange's equations, charge formulation ... 53
2.5.2 Lagrange's equations, flux linkage formulation ... 54
2.5.3 Example 1 ... 54
2.5.4 Example 2 ... 57
2.6 References ... 59

3 Electromechanical systems ... 61
3.1 Introduction ... 61
3.2 Constitutive relations for transducers ... 61
3.2.1 Movable-plate capacitor ... 62
3.2.2 Movable-core inductor ... 65
3.2.3 Moving-coil transducer ... 68
3.3 Hamilton's principle ... 71
3.3.1 Displacement and charge formulation ... 71
3.3.2 Displacement and flux linkage formulation ... 72
3.4 Lagrange's equations ... 73
3.4.1 Displacement and charge formulation ... 73
3.4.2 Displacement and flux linkage formulation ... 73
3.4.3 Dissipation function ... 74
3.5 Examples ... 76
3.5.1 Electromagnetic plunger ... 76
3.5.2 Electromagnetic loudspeaker ... 77
3.5.3 Capacitive microphone ... 79
3.5.4 Proof-mass actuator ... 82
3.5.5 Electrodynamic isolator ... 84

3.5.6 The *Sky-hook* damper 86
3.5.7 Geophone 87
3.5.8 One-axis magnetic suspension 89
3.6 General electromechanical transducer 92
3.6.1 Constitutive equations 92
3.6.2 Self-sensing 93
3.7 References 94

4 Piezoelectric systems 95
4.1 Introduction 95
4.2 Piezoelectric transducer 96
4.3 Constitutive relations of a discrete transducer 99
4.3.1 Interpretation of k^2 103
4.4 Structure with a discrete piezoelectric transducer 105
4.4.1 Voltage source 107
4.4.2 Current source 107
4.4.3 Admittance of the piezoelectric transducer 108
4.4.4 Prestressed transducer 109
4.4.5 Active enhancement of the electromechanical coupling 111
4.5 Multiple transducer systems 113
4.6 General piezoelectric structure 114
4.7 Piezoelectric material 116
4.7.1 Constitutive relations 116
4.7.2 Coenergy density function 118
4.8 Hamilton's principle 121
4.9 Rosen's piezoelectric transformer 124
4.10 References 130

5 Piezoelectric laminates 131
5.1 Piezoelectric beam actuator 131
5.1.1 Hamilton's principle 131
5.1.2 Piezoelectric loads 133
5.2 Laminar sensor 136
5.2.1 Current and charge amplifiers 136
5.2.2 Distributed sensor output 136
5.2.3 Charge amplifier dynamics 138
5.3 Spatial modal filters 139
5.3.1 Modal actuator 139
5.3.2 Modal sensor 140

5.4 Active beam with collocated actuator-sensor 141
5.4.1 Frequency response function 142
5.4.2 Pole-zero pattern 143
5.4.3 Modal truncation 145
5.5 Piezoelectric laminate 147
5.5.1 Two dimensional constitutive equations 148
5.5.2 Kirchhoff theory 148
5.5.3 Stiffness matrix of a multi-layer elastic laminate 149
5.5.4 Multi-layer laminate with a piezoelectric layer 151
5.5.5 Equivalent piezoelectric loads 152
5.5.6 Sensor output 153
5.5.7 Remarks 154
5.6 References 156

6 Active and passive damping with piezoelectric transducers 159
6.1 Introduction 159
6.2 Active strut, open-loop FRF 161
6.3 Active damping via IFF 165
6.3.1 Voltage control 165
6.3.2 Modal coordinates 167
6.3.3 Current control 169
6.4 Admittance of the piezoelectric transducer 170
6.5 Damping via resistive shunting 172
6.5.1 Damping enhancement via negative capacitance shunting 175
6.5.2 Generalized electromechanical coupling factor 176
6.6 Inductive shunting 176
6.6.1 Alternative formulation 181
6.7 Decentralized control 183
6.8 General piezoelectric structure 184
6.9 Self-sensing 185
6.9.1 Force sensing 186
6.9.2 Displacement sensing 187
6.9.3 Transfer function 187
6.10 Other active damping strategies 191
6.10.1 Lead control 191
6.10.2 Positive Position Feedback (PPF) 192

6.11 Remark 195
6.12 References 195

Bibliography 199

Index 205

Preface

The objective of my previous book, *Vibration Control of Active Structures*, was to cross the bridge between Structural Dynamics and Automatic Control. To insist on important control-structure interaction issues, the book often relied on "ad-hoc" models and intuition (e.g. a thermal analogy for piezoelectric loads), and was seriously lacking in accuracy and depth on transduction and energy conversion mechanisms which are essential in active structures. The present book project was initiated in preparation for a new edition, with the intention of redressing the imbalance, by including a more serious treatment of the subject. As the work developed, it appeared that this topic was broad enough to justify a book on its own.

This short book attempts to offer a systematic and unified way of analyzing electromechanical and piezoelectric systems, following a Hamilton-Lagrange formulation. The transduction mechanisms and the Hamilton-Lagrange analysis of classical electromechanical systems have been addressed in a few excellent textbooks (e.g. *Dynamics of Mechanical and Electromechanical Systems* by Crandall et al. in 1968), but to the author's knowledge, there has been no similar systematic treatment of piezoelectric systems.

The first three chapters are devoted to the analysis of mechanical systems, electrical networks and classical electromechanical systems, respectively; Hamilton's principle is extended to electromechanical systems following two dual formulations. Except for a few examples, this part of the book closely follows the existing literature. The last three chapters are devoted to piezoelectric systems. Chapter 4 analyzes discrete piezoelectric transducers and their introduction into a structure; the approach parallels that of the previous chapter with the appropriate energy and coenergy functions. Chapter 5 analyzes distributed systems, and focuses on piezoelectric beams and laminates, with particular attention to the way the piezoelectric layers interact with the supporting structure (piezoelectric loads, modal filters, etc...). Chapter 6 examines energy conversion from the perspective of active and passive damping; a unified approach is proposed, leading to a meaningful comparison of various active and passive techniques, and design guidelines for maximizing energy conversion.

This book is intended for mechanical engineers (researchers and graduate students) who wish to get some training in electromechanical and piezoelectric transducers, and improve their understanding of the subtle interplay between mechanical response and electrical boundary condi-

tions, and *vice versa*. In so doing, we follow the famous advice given by Prof. Joseph Henry to Alexander Graham Bell, who had consulted him in connection with his telephone experiments in 1875, and lamented over his lack of the electrical knowledge needed to overcome his mechanical difficulties. Henry simply replied: "*Get it*". The beauty of the Hamilton-Lagrange formulation is that, once the appropriate energy and coenergy functions are used, all the electromagnetic forces (electrostatic, Lorentz, reluctance forces,...) and the multi-physics constitutive equations are automatically accounted for.

Acknowledgements

I am indebted to my present and former graduate students and coworkers who, by their enthusiasm and curiosity, raised many of the questions which have led to this book. Particular thanks are due to Amit Kalyani, Bruno de Marneffe, More Avraam and Arnaud Deraemaeker who helped me in preparing the manuscript, and produced most of the figures. The comments of the Series Editor, Prof. Graham Gladwell, and of my friend Michel Geradin, have been very useful in improving this text. I am also indebted to *ESA/ESTEC*, *EU*, *FNRS* and the *IUAP* program of the *SSTC* for their generous and continuous support of the *Active Structures Laboratory* of *ULB*. This book was partly written while I was visiting professor at *Université de Technologie de Compiègne (Laboratoire Roberval)*.

Notation

Notation is always a source of problems when writing a book, and the difficulty is further magnified as one attempts to address interdisciplinary subjects, which blend disconnected fields with a long history, each with its own, well established notation. This book is no exception to this rule, since mechatronics mixes, analytical mechanics, structural mechanics, electrical networks, electromagnetism, piezoelectricity and automatic control, etc.

The notation has been chosen according to the following rules: *(i)* We shall follow the *IEEE Standard on Piezoelectricity* as much as we can. *(ii)* When there is no ambiguity, we will not make explicit distinction between scalars, vectors and matrices; the meaning will be clear from the context. In some circumstances, when the distinction is felt necessary, column vectors will be made explicit by $\{\quad\}$ (e.g. $\{T\}$ will denote the stress

vector, while T_{ij} denotes the stress tensor). *(iii)* The partial derivative will be denoted either by $\partial/\partial x_i$ or by the subscript $_{,i}$ (the index after the comma indicates the variable with respect to which the partial derivative is taken); the choice of one notation or the other will be guided by clarity, compactness and conformity to the classical literature. Similarly, summation on repeated indexes (Einstein's summation convention) will be assumed even when it is not explicitly mentioned.

André Preumont
Brussels, Decembre 2005.

1

Lagrangian dynamics of mechanical systems

1.1 Introduction

This book considers the modelling of electromechanical systems in an unified way based on Hamilton's principle. This chapter starts with a review of the Lagrangian dynamics of mechanical systems, the next chapter proceeds with the Lagrangian dynamics of electrical networks and the remaining chapters address a wide class of electromechanical systems, including piezoelectric structures.

Lagrangian dynamics has been motivated by the substitution of scalar quantities (energy and work) for vector quantities (force, momentum, torque, angular momentum) in classical vector dynamics. Generalized coordinates are substituted for physical coordinates, which allows a formulation independent of the reference frame. Systems are considered globally, rather than every component independently, with the advantage of eliminating the interaction forces (resulting from constraints) between the various elementary parts of the system. The choice of generalized coordinates is not unique.

The derivation of the variational form of the equations of dynamics from its vector counterpart (Newton's laws) is done through the principle of virtual work, extended to dynamics thanks to d'Alembert's principle, leading eventually to Hamilton's principle and the Lagrange equations for discrete systems.

Hamilton's *principle* is an alternative to Newton's laws and it can be argued that, as such, it is a fundamental law of physics which cannot be derived. We believe, however, that its form may not be immediately comprehensible to the unexperienced reader and that its derivation for a system of particles will ease its acceptance as an alternative formula-

tion of dynamic equilibrium. Hamilton's principle is in fact more general than Newton's laws, because it can be generalized to distributed systems (governed by partial differential equations) and, as we shall see later, to electromechanical systems. It is also the starting point for the formulation of many numerical methods in dynamics, including the finite element method.

1.2 Kinetic state functions

Consider a particle travelling in the direction x with a linear momentum p. According to Newton's law, the force acting on the particle equals the rate of change of the momentum:

$$f = \frac{dp}{dt} \tag{1.1}$$

The increment of work on the particle is

$$f\,dx = \frac{dp}{dt}\,dx = \frac{dp}{dt}\,v\,dt = v\,dp \tag{1.2}$$

where $v = dx/dt$ is the velocity of the particle. The *kinetic energy function* $T(p)$ is defined as the total work done by f in increasing the momentum from 0 to p

$$T(p) = \int_0^p v\,dp \tag{1.3}$$

According to this definition, T is a function of the instantaneous momentum p, with derivative equal to the instantaneous velocity

$$\frac{dT}{dp} = v \tag{1.4}$$

Up to now, no explicit relation between p and v has been assumed; the *constitutive equation of Newtonian mechanics* is

$$p = mv \tag{1.5}$$

Substituting in Equ.(1.3), one gets

$$T(p) = \frac{p^2}{2m} \tag{1.6}$$

A complementary kinetic state function can be defined as the *kinetic coenergy function* (Fig.1.1)

$$T^*(v) = \int_0^v p\, dv \tag{1.7}$$

which, as (1.3), is independent of the velocity-momentum relation. Note, from Fig.1.1, that $T(p)$ and $T^*(v)$ are related by

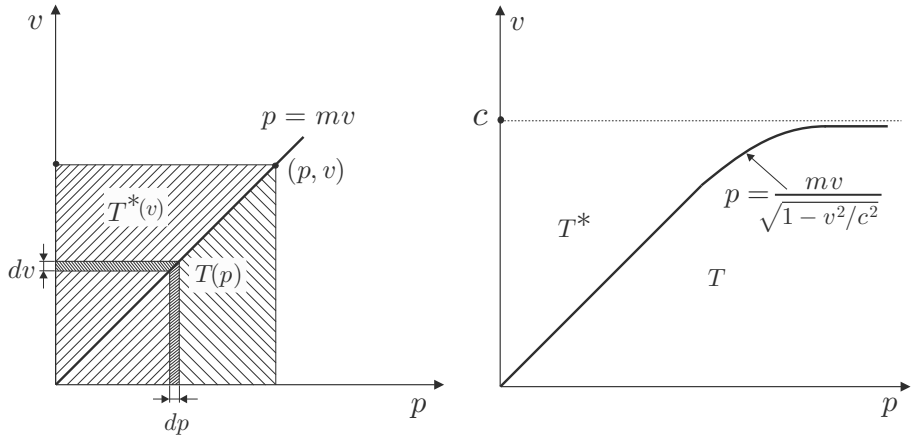

Fig. 1.1. Velocity-momentum relation for (a) Newtonian mechanics (b) special relativity.

$$T^*(v) = pv - T(p) \tag{1.8}$$

The total differential of the kinetic coenergy reads

$$dT^* = p\, dv + v\, dp - \frac{dT}{dp} dp = p\, dv \tag{1.9}$$

if (1.4) is used. It follows that

$$p = \frac{dT^*}{dv} \tag{1.10}$$

Thus, the kinetic coenergy is a function of the instantaneous velocity v, with derivative equal to the instantaneous momentum. Equation(1.8) defines a *Legendre transformation* which allows us to change from one independent variable [p in $T(p)$] to the other [v in $T^*(v)$] without loss of information on the constitutive behavior. For a Newtonian particle, combining (1.5) and (1.7), the kinetic coenergy reads

$$T^*(v) = \frac{1}{2}mv^2 \tag{1.11}$$

This form is usually known as the kinetic energy in most engineering mechanics textbooks. Note, however that $T(p)$ and $T^*(v)$ have different variables, even though they have identical values for a Newtonian particle. Since T and T^* are always identical in Newtonian mechanics, it has been a tradition not to make a distinction between them. This point of view has been reinforced by the fact that the variational methods in mechanics are almost exclusively displacement based (based on virtual displacements). However, in the following chapters, we will extend Hamilton's principle to electromechanical systems and the distinction between electrical and magnetic, energy and coenergy functions will become necessary. This is why we will use the kinetic coenergy $T^*(v)$ instead of the classical notation of the kinetic energy $T(v)$.

To illustrate that T and T^* may have different values, it is interesting to mention that when going from Newtonian mechanics to special relativity, the constitutive equation (1.5) must be replaced by

$$p = \frac{mv}{\sqrt{1 - v^2/c^2}} \tag{1.12}$$

where m is the rest mass and c is the speed of light. Equations (1.5) and (1.12) are almost identical at low speed, but they diverge considerably at high speeds (Fig.1.1.b), and T^* and T are no longer identical. [1]

1.3 Generalized coordinates, kinematic constraints

A *kinematically admissible* motion denotes a spatial configuration that is always compatible with the geometric boundary conditions. The *generalized coordinates* are a set of coordinates that allow a full geometric description of the system with respect to a reference frame. This representation is not unique; Fig.1.2 shows two sets of generalized coordinates for the double pendulum in a plane; in the first case, the relative angles are adopted as generalized coordinates, while the absolute angles are taken in the second case. Note that the generalized coordinates do not always have a simple physical meaning such as a displacement or an angle; they may also represent the amplitude of an assumed mode in a distributed system, as is done extensively in the analysis of flexible structures.

[1] unlike the kinetic coenergy T^*, the potential coenergy V^* is often used in structural engineering; however, it will not be used in this text, because our variational approach will rely exclusively on a displacement formulation.

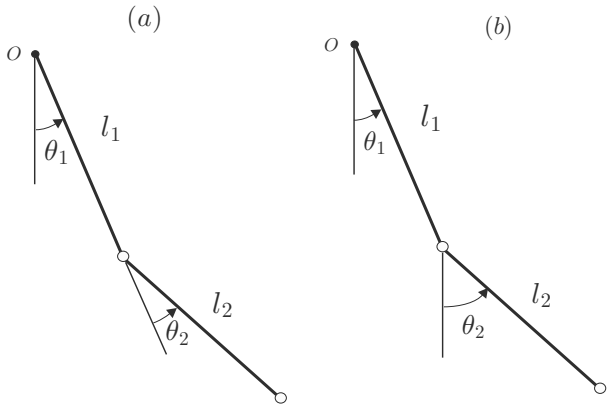

Fig. 1.2. Double pendulum in a plane (a) relative angles (b) absolute angles.

The number of degrees of freedom (d.o.f.) of a system is the minimum number of coordinates necessary to provide its full geometric description. If the number of generalized coordinates is equal to the number of d.o.f., they form a minimum set of generalized coordinates. The use of a minimum set of coordinates is not always possible, nor advisable; if their number exceeds the number of d.o.f., they are not independent and they are connected by kinematic constraints. If the constraint equations between the generalized coordinates q_i can be written in the form

$$f(q_1, ..., q_n, t) = 0 \tag{1.13}$$

they are called *holonomic*. If the time does not appear explicitly in the constraints, they are called *scleronomic*.

$$f(q_1, ..., q_n) = 0 \tag{1.14}$$

The algebraic constraints (1.13) or (1.14) can always be used to eliminate the redundant set of generalized coordinates and reduce the coordinates to a minimum set. This is no longer possible if the kinematic constraints are defined by a (non integrable) differential relation

$$\sum_i a_i dq_i + a_0 dt = 0 \tag{1.15}$$

or

$$\sum_i a_i dq_i = 0 \tag{1.16}$$

if the time is excluded; non integrable constraints such as (1.15) and (1.16) are called *non-holonomic*.

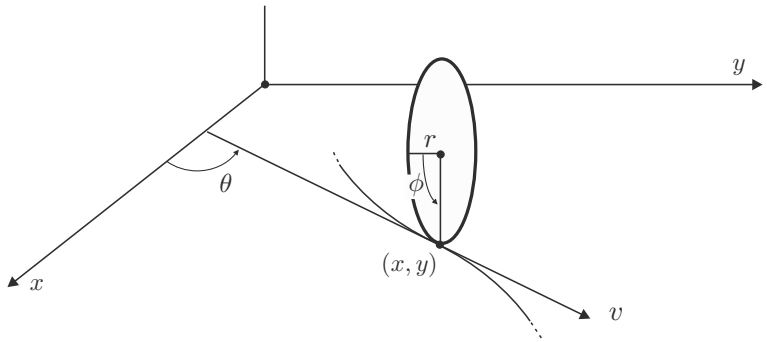

Fig. 1.3. Vertical disk rolling without slipping on an horizontal plane.

As an example of non-holonomic constraints, consider a vertical disk rolling without slipping on an horizontal plane (Fig.1.3). The system is fully characterized by four generalized coordinates, the location (x, y) of the contact point in the plane, and the orientation of the disk, defined by (θ, ϕ). The reader can check that, if the appropriate path is used, the four generalized variables can be assigned *arbitrary* values (i.e. the disc can be moved to all points of the plane with an arbitrary orientation). However, the time derivatives of the coordinates are not independent, because they must satisfy the rolling conditions:

$$v = r\dot{\phi}$$

$$\dot{x} = v\cos\theta$$

$$\dot{y} = v\sin\theta$$

combining these equations, we get the differential constraint equations:

$$dx - r\cos\theta\, d\phi = 0$$

$$dy - r\sin\theta\, d\phi = 0$$

which actually restrict the possible paths to go from one configuration to the other.

1.3.1 Virtual displacements

A *virtual displacement*, or more generally a virtual change of configuration, is an infinitesimal change of coordinates occurring *at constant time*, and consistent with the kinematic constraints of the system (but otherwise arbitrary). The notation δ is used for the virtual changes of coordinates; they follow the same rules as the derivatives, except that time is not involved. It follows that, for a system with generalized coordinates q_i related by holonomic constraints (1.13) or (1.14), the admissible variations must satisfy

$$\delta f = \sum_i \frac{\partial f}{\partial q_i} \delta q_i = 0 \tag{1.17}$$

Note that the same form applies, whether t is explicitly involved in the constraints or not, because the virtual displacements are taken at constant time. For non-holonomic constraints (1.15) or (1.16), the virtual displacements must satisfy

$$\sum_i a_i \delta q_i = 0 \tag{1.18}$$

Comparing Equ.(1.15) and (1.18), we note that, if the time appears explicitly in the constraints, the virtual displacements are not possible displacements. The differential displacements dq_i are along a particular trajectory as it unfolds with time, while the virtual displacements δq_i measure the separation between two different trajectories at a given instant.

Consider a single particle constrained to move on a smooth surface

$$f(x, y, z) = 0$$

The virtual displacements must satisfy the constraint equation

$$\frac{\partial f}{\partial x}\delta x + \frac{\partial f}{\partial y}\delta y + \frac{\partial f}{\partial z}\delta z = 0$$

which is in fact the dot product of the gradient to the surface,

$$\text{grad} f = \nabla f = (\frac{\partial f}{\partial x}, \frac{\partial f}{\partial y}, \frac{\partial f}{\partial z})^T$$

and the vector of virtual displacement $\delta x = (\delta x, \delta y, \delta z)^T$:

$$\text{grad} f.\delta x = (\nabla f)^T \delta x = 0$$

Since ∇f is parallel to the normal n to the surface, this simply states that the virtual displacements belong to the plane tangent to the surface. Let us now consider the reaction force F which constraints the particle to move along the surface. If we assume that the system is smooth and frictionless, the reaction force is also normal to the surface; it follows that

$$F.\delta x = F^T \delta x = 0 \tag{1.19}$$

the virtual work of the constraint forces on any virtual displacements is zero. We will accept this as a general statement for a reversible system (without friction); note that it remains true if the surface equation depends explicitly on t, because the virtual displacements are taken at constant time.

1.4 The principle of virtual work

The principle of virtual work is a variational formulation of the static equilibrium of a mechanical system without friction. Consider a system of N particles with position vectors x_i, $i = 1, .., N$. Since the static equilibrium implies that the resultant R_i of the force applied to each particle i is zero, each dot product $R_i.\delta x_i = 0$, and

$$\sum_{i=1}^{N} R_i.\delta x_i = 0$$

for all virtual displacements δx_i compatible with the kinematic constraints. R_i can be decomposed into the contribution of external forces applied F_i and the constraint (reaction) forces F'_i

$$R_i = F_i + F'_i$$

and the previous equation becomes

$$\sum F_i.\delta x_i + \sum F'_i.\delta x_i = 0$$

For a reversible system (without friction), Equ.(1.19) states that the virtual work of the constraint forces is zero, so that the second term vanishes, it follows that

$$\sum F_i.\delta x_i = 0 \tag{1.20}$$

The virtual work of the external applied forces on the virtual displacements compatible with the kinematics is zero. The strength of this result comes from the fact that *(i)* the reaction forces have been removed from the equilibrium equation, *(ii)* the static equilibrium problem is transformed into kinematics, and *(iii)* it can be written in generalized coordinates:

$$\sum Q_k.\delta q_k = 0 \tag{1.21}$$

where Q_k is the generalized force associated with the generalized coordinate q_k.

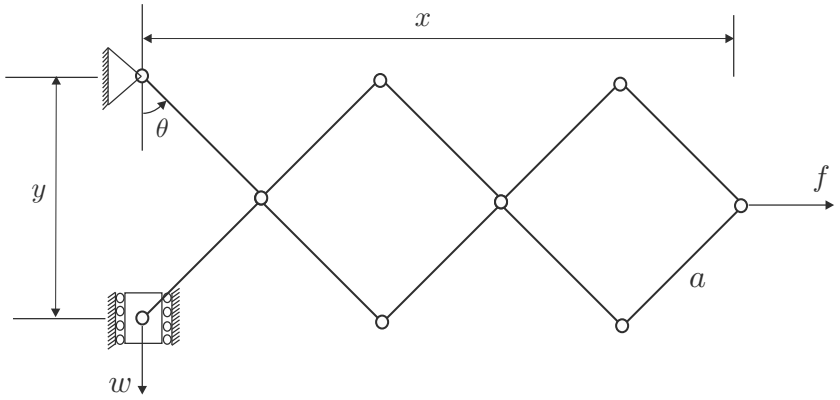

Fig. 1.4. Motion amplification mechanism.

As an example of application, consider the one d.o.f. motion amplification mechanism of Fig.1.4. Its kinematics is governed by

$$x = 5a\sin\theta \qquad y = 2a\cos\theta$$

It follows that

$$\delta x = 5a\cos\theta\,\delta\theta \qquad \delta y = -2a\sin\theta\,\delta\theta$$

The principle of virtual work reads

$$f\,\delta x + w\,\delta y = (f.5a\cos\theta - w.2a\sin\theta)\,\delta\theta = 0$$

for arbitrary $\delta\theta$, which implies that the static equilibrium forces f and w satisfy

$$f = w\frac{2}{5}\tan\theta$$

1.5 D'Alembert's principle

D'Alembert's principle extends the principle of virtual work to dynamics. It states that a problem of dynamic equilibrium can be transformed into a problem of static equilibrium by adding the inertia forces - $m\ddot{x}_i$ to the externally applied forces F_i and constraints forces F'_i.

Indeed, Newton's law implies that, for every particle,

$$R_i = F_i + F'_i - m_i\ddot{x}_i = 0$$

Following the same development as in the previous section, summing over all the particles and taking into account that the virtual work of the constraint forces is zero, one finds

$$\sum_{i=0}^{N}(F_i - m_i\ddot{x}_i).\delta x_i = 0 \tag{1.22}$$

The sum of the applied external forces and the inertia forces is sometimes called the *effective force*. Thus, *the virtual work of the effective forces on the virtual displacements compatible with the constraints is zero*. This principle is most general; unfortunately, it is difficult to apply, because it still refers to vector quantities expressed in an inertial frame and, unlike the principle of virtual work, it cannot be translated directly into generalized coordinates. This will be achieved with Hamilton's principle in the next section.

If the time does not appear explicitly in the constraints, the virtual displacements are possible, and Equ.(1.22) is also applicable for the actual displacements $dx_i = \dot{x}_i dt$

$$\sum_i F_i.dx_i - \sum_i m_i\ddot{x}_i.\dot{x}_i dt = 0$$

If the external forces can be expressed as the gradient of a potential V which does not depend explicitly on t, $\sum F_i.dx_i = -dV$ (if V depends explicitly on t, the total differential includes a partial derivative with respect to t). Such a force field is called *conservative*. The second term in the previous equation is the differential of the kinetic coenergy:

$$\sum_i m_i\ddot{x}_i.\dot{x}_i dt = \frac{d}{dt}\left(\frac{1}{2}\sum_i m_i\,\dot{x}_i.\dot{x}_i\right)dt = dT^*$$

It follows that

$$d(T^* + V) = 0$$

and

$$T^* + V = C^t \tag{1.23}$$

This is the law of *conservation of total energy*. Note that it is restricted to systems where *(i)* the potential energy does not depend explicitly on t and *(ii)* the kinematical constraints are independent of time.

1.6 Hamilton's principle

D'Alembert's principle is a complete formulation of the dynamic equilibrium; however, it uses the position coordinates of the various particles of the system, which are in general not independent; it cannot be formulated in generalized coordinates. On the contrary, Hamilton's principle expresses the dynamic equilibrium in the form of the stationarity of a definite integral of a scalar energy function. Thus, Hamilton's principle becomes independent of the coordinate system. Consider again Equ.(1.22); the first contribution

$$\delta W = \sum F_i.\delta x_i$$

represents the virtual work of the applied external forces. The second contribution to Equ.(1.22) can be transformed using the identity

$$\ddot{x}_i.\delta x_i = \frac{d}{dt}(\dot{x}_i.\delta x_i) - \dot{x}_i.\delta\dot{x}_i = \frac{d}{dt}(\dot{x}_i.\delta x_i) - \delta\frac{1}{2}(\dot{x}_i.\dot{x}_i)$$

where we have used the commutativity of δ and $(\dot{})$. It follows that

$$\sum_{i=1}^{N} m_i\ddot{x}_i.\delta x_i = \sum_{i=1}^{N} m_i\frac{d}{dt}(\dot{x}_i.\delta x_i) - \delta T^*$$

where T^* is the kinetic coenergy of the system. Using this equation, we transform d'Alembert's principle (1.22) into

$$\delta W + \delta T^* = \sum_{i=0}^{N} m_i\frac{d}{dt}(\dot{x}_i.\delta x_i)$$

The left hand side consists of scalar work and energy functions. The right hand side consists of a total time derivative which can be eliminated by

integrating over some interval $[t_1, t_2]$, assuming that the system configuration is known at t_1 and t_2, so that

$$\delta x_i(t_1) = \delta x_i(t_2) = 0 \tag{1.24}$$

Taking this into account, one gets

$$\int_{t_1}^{t_2} (\delta W + \delta T^*) dt = \sum_{i=1}^{N} m_i [\dot{x}_i . \delta x_i]_{t_1}^{t_2} = 0$$

If some of the external forces are conservative,

$$\delta W = -\delta V + \delta W_{nc} \tag{1.25}$$

where V is the potential and δW_{nc} is the virtual work of the nonconservative forces. Thus, Hamilton's principle is expressed by the variational indicator (V.I.):

$$\text{V.I.} = \int_{t_1}^{t_2} [\delta(T^* - V) + \delta W_{nc}] dt = 0 \tag{1.26}$$

or

$$\text{V.I.} = \int_{t_1}^{t_2} [\delta L + \delta W_{nc}] dt = 0 \tag{1.27}$$

where

$$L = T^* - V \tag{1.28}$$

is the *Lagrangian* of the system. The statement of the dynamic equilibrium goes as follows: *The actual path is that which cancels the value of the variational indicator (1.26) or (1.27) with respect to all arbitrary variations of the path between two instants t_1 and t_2, compatible with the kinematic constraints, and such that* $\delta x_i(t_1) = \delta x_i(t_2) = 0$.

Again, we stress that δx_i does not measure displacements on the true path, but the separation between the true path and a perturbed one at a given time (Fig.1.5).

Note that, unlike Equ.(1.23) which requires that the potential V does not depend explicitly on time, the virtual expression (1.25) allows V to depend on t, since the virtual variation is taken at constant time ($\delta V = \nabla V . \delta x$, while $dV = \nabla V . dx + \partial V / \partial t . dt$).

Hamilton's principle, that we derived here from d'Alembert's principle for a system of particles, is the most general statement of dynamic equilibrium, and it is, in many respects, more general than Newton's laws,

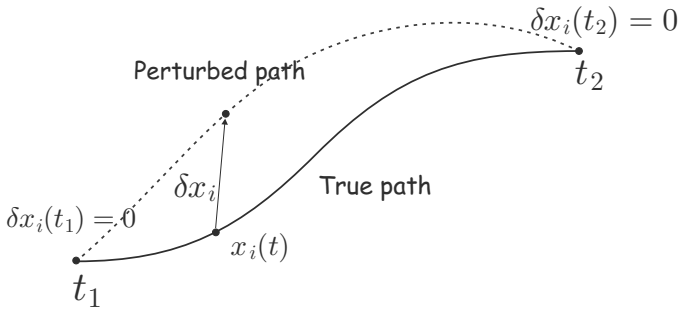

Fig. 1.5. True and perturbed paths.

because it applies to continuous systems and more, as we will see shortly. Some authors argue that, being a fundamental law of physics, it cannot be derived, just accepted. Thus we could have proceeded the opposite way: state Hamilton's principle, and show that it implies Newton's laws. It is a matter of taste, but also of history: 150 years separate Newton's Principia (1687) from Hamilton's principle (1835). From now on, we will consider Hamilton's principle as the fundamental law of dynamics. We stress that when dealing with purely mechanical systems, the distinction between the kinetic energy T and the kinetic coenergy T^* is not necessary; it is motivated here by the subsequent extension to electromechanical systems.

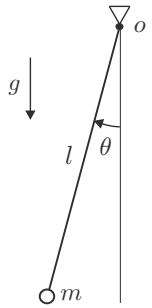

Fig. 1.6. Plane pendulum.

Consider the plane pendulum of Fig.1.6; taking the altitude of the pivot O as reference, we find the Lagrangian

$$L = T^* - V = \frac{1}{2} m (l\dot{\theta})^2 + mgl\cos\theta$$

$$\delta L = ml^2 \dot{\theta}\delta\dot{\theta} - mgl\sin\theta\delta\theta$$

Hamilton's principle states that the variational indicator (V.I).

$$\text{V.I.} = \int_{t_1}^{t_2} [ml^2\dot{\theta}\delta\dot{\theta} - mgl\sin\theta\delta\theta]dt = 0$$

for all virtual variations $\delta\theta$ such that $\delta\theta(t_1) = \delta\theta(t_2) = 0$. As always in variational calculus, $\delta\dot{\theta}$ can be eliminated from the variational indicator by integrating by part over t. Using $\dot{\theta}\delta\dot{\theta} = \dfrac{d}{dt}(\dot{\theta}\delta\theta) - \ddot{\theta}\delta\theta$ one gets

$$\text{V.I.} = [ml^2\dot{\theta}\delta\theta]_{t_1}^{t_2} - \int_{t_1}^{t_2} (ml^2\ddot{\theta} + mgl\sin\theta)\delta\theta dt = 0$$

for all virtual variations $\delta\theta$ such that $\delta\theta(t_1) = \delta\theta(t_2) = 0$. Since the integral appearing in the second term must vanish for arbitrary $\delta\theta$, we conclude that

$$ml^2\ddot{\theta} + mgl\sin\theta = 0$$

which is the differential equation for the oscillation of the pendulum. The Lagrange's equations give a much quicker way of solving this type of problem, as we will see shortly; however, before this, we illustrate the power of Hamilton's principle by deriving the partial differential equation of the lateral vibration of the Euler-Bernoulli beam.

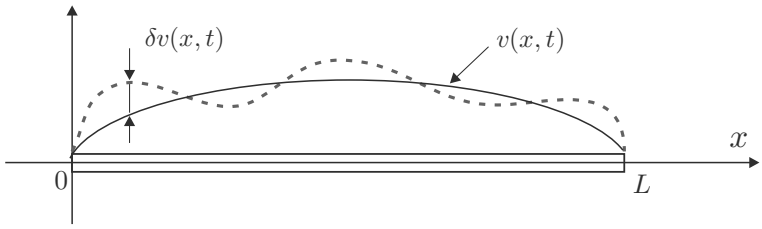

Fig. 1.7. Transverse vibration of a beam.

1.6.1 Lateral vibration of a beam

Consider the transverse vibration of the beam of Fig.1.7, subjected to a transverse distributed load $p(x,t)$. It is assumed that the principal axes of the cross section are such that the vibration takes place in the plane; $v(x,t)$ denotes the transverse displacements; the virtual displacements

$\delta v(x,t)$ satisfy the geometric (kinematic) boundary conditions and are such that

$$\delta v(x,t_1) = \delta v(x,t_2) = 0 \tag{1.29}$$

(the configuration is fixed at the limit times t_1 and t_2).

The Euler-Bernoulli beam theory neglects the shear deformations and assumes that the cross section remains orthogonal to the neutral axis; this is equivalent to assuming that the uniaxial strain distribution S_{11} is a linear function of the distance to the neutral axis, $S_{11} = -zv''$, where v'' is the curvature of the beam. Accordingly, the potential energy, which in this case is the strain energy, reads

$$V(S_{ij}) = \frac{1}{2}\int_V E(S_{11})^2 dV = \frac{1}{2}\int_0^L \int_S E(v'')^2 z^2 dS dx$$

or

$$V = \frac{1}{2}\int_0^L EI(v'')^2 dx \tag{1.30}$$

where v'' is the curvature of the beam, E the Young's modulus and I the geometric moment of inertia of the cross section (EI is called the bending stiffness). If one includes only the translational inertia, the kinetic coenergy is

$$T^* = \frac{1}{2}\int_0^L \varrho A(\dot{v})^2 dx \tag{1.31}$$

where $\dot{v}$ is the transverse velocity, ϱ is the density and A the cross section area. The virtual work of the non-conservative forces is associated with the distributed load:

$$\delta W_{nc} = \int_0^L p\,\delta v\,dx \tag{1.32}$$

From (1.30) and (1.31),

$$\delta V = \int_0^L EIv''\delta v'' dx \qquad \text{and} \qquad \delta T^* = \int_0^L \varrho A\dot{v}\,\delta\dot{v}\,dx$$

As in the previous section, $\delta\dot{v}$ can be eliminated by integrating by part over t, and similarly, $\delta v''$ can be eliminated by integrating twice by part over x; one gets

$$\delta V = \int_0^L EIv''\delta v'' dx = [EIv''\delta v']_0^L - \int_0^L (EIv'')'\delta v' dx$$

$$= [EIv''\delta v']_0^L - [(EIv'')'\delta v]_0^L + \int_0^L (EIv'')''\delta v\,dx$$

and similarly

$$\int_{t_1}^{t_2} \delta T^* dt = \int_{t_1}^{t_2} dt \int_0^L \varrho A \dot{v}\, \delta \dot{v}\, dx = [\int_0^L \varrho A \dot{v}\, \delta v\, dx]_{t_1}^{t_2} - \int_{t_1}^{t_2} dt \int_0^L \varrho A \ddot{v}\, \delta v\, dx$$

The expression in the bracket vanishes because of (1.29). Substituting the above expressions in Hamilton's principle, one gets

$$\int_{t_1}^{t_2} dt \{-[EIv''\delta v']_0^L + [(EIv'')'\delta v]_0^L + \int_0^L [-(EIv'')'' - \varrho A\ddot{v} + p]\delta v\, dx\} = 0 \tag{1.33}$$

This variational indicator must vanish for all arbitrary variations δv compatible with the kinematic constraints and satisfying (1.29). This implies that the dynamic equilibrium is governed by the following partial differential equation

$$(EIv'')'' + \varrho A\ddot{v} = p \tag{1.34}$$

Besides, cancelling the terms within brackets, we find that the following conditions must be fulfilled in $x = 0$ and $x = L$,

$$EIv''.\delta v' = 0 \tag{1.35}$$

$$(EIv'')'.\delta v = 0 \tag{1.36}$$

The first equation expresses that, at both ends, one must have either $\delta v' = 0$, which is the case if the rotation is fixed, or $EIv'' = 0$, which means that the bending moment is equal to 0. Similarly, the second one implies that at both ends, either $\delta v = 0$, which is the case if the displacement is fixed, or $(EIv'')' = 0$, which means that the shear force is equal to 0. $\delta v = 0$ and $\delta v' = 0$ are kinematic (geometric) boundary conditions; $EIv'' = 0$ and $(EIv'')' = 0$ are sometimes called *natural* boundary conditions, because they come naturally from the variational principle. A *free end* allows arbitrary δv and $\delta v'$; this implies $EIv'' = 0$ and $(EIv'')' = 0$. A *clamped end* implies that $\delta v = 0$ and $\delta v' = 0$. A *pinned* end implies that $\delta v = 0$, but $\delta v'$ is arbitrary; it follows that $EIv'' = 0$. Note that the kinematic and the natural boundary conditions are energetically conjugate: displacement-shear force, rotation-bending moment.

The Euler-Bernoulli beam will be reexamined in chapter 5 when we include a piezoelectric layer. More elaborate beam theories are available, which account for shear deformations and the rotary inertia of the cross section; they are based on different kinematic assumptions on the displacement field, leading to new expressions for the strain energy V and the kinetic coenergy T^*; the subsequent application of Hamilton's principle follows closely the discussion above.

1.7 Lagrange's equations

Hamilton's principle relies on scalar work and energy quantities; it does not refer to a particular coordinate system. The system configuration can be expressed in generalized coordinates q_i. If the generalized coordinates are independent, the virtual change of configuration can be represented by independent virtual variations of the generalized coordinates, δq_i. This allows us to transform the variational indicator (1.26) into a set of differential equations which are Lagrange's equations.

First, consider the case where the system configuration is described by a finite set of n independent generalized coordinates q_i. All the material points of the system follow

$$x_i = x_i(q_1, ..., q_n; t) \tag{1.37}$$

We also allow an explicit dependency on time t, which is important for analyzing gyroscopic systems such as rotating machinery. The velocity of the material point i is given by

$$\dot{x}_i = \sum_j \frac{\partial x_i}{\partial q_j}\dot{q}_j + \frac{\partial x_i}{\partial t} \tag{1.38}$$

where the matrix of partial derivatives $\partial x_i/\partial q_j$ has the meaning of a Jacobian. From Equ.(1.38), the kinetic coenergy can be written in the form

$$T^* = \frac{1}{2}\sum_i m_i \dot{x}_i.\dot{x}_i = T_2^* + T_1^* + T_0^* \tag{1.39}$$

where T_2^*, T_1^* and T_0^* are respectively homogeneous functions of order 2,1 and 0 in the generalized velocities $\dot{q}_i$; the coefficients of T_i^* depend on the partial derivatives $\partial x_i/\partial q_j$, which are themselves functions of the generalized coordinates q_i. Note that without explicit dependency on t, the last term in (1.38) disappears and $T^* = T_2^*$ (homogenous quadratic function of $\dot{q}_i$). Being independent of $\dot{q}_i$, the term T_0^* appears as a potential; it is in general related to centrifugal forces, while the linear term T_1^* is responsible for the gyroscopic forces. The general form of the kinetic coenergy is

$$T^* = T^*(q_1, ..., q_n, \dot{q}_1, ..., \dot{q}_n; t) \tag{1.40}$$

The potential energy V does not depend on the velocity; it can be assumed to be of the general form

$$V = V(q_1, ..., q_n; t) \tag{1.41}$$

From these two equations, it can be assumed that the most general form of the Lagrangian is

$$L = T^* - V = L(q_1, ..., q_n, \dot{q}_1, ..., \dot{q}_n; t) \tag{1.42}$$

Let us now examine the virtual work of the non-conservative forces; expressing the virtual displacement δx_i in terms of δq_i, one finds

$$\delta W_{nc} = \sum_i F_i.\delta x_i = \sum_i \sum_k F_i \frac{\partial x_i}{\partial q_k} \delta q_k = \sum_k Q_k \delta q_k \tag{1.43}$$

where

$$Q_k = \sum_i F_i \frac{\partial x_i}{\partial q_k} \tag{1.44}$$

Q_k is the generalized force associated with the generalized variable q_k; they are energetically conjugate (their product has the dimension of energy). Introducing Equ.(1.43) in Hamilton's principle (1.26), one finds

$$\begin{aligned} \text{V.I.} = \delta I &= \int_{t_1}^{t_2} [\delta L(q_1, ..., q_n,\ \dot{q}_1, ..., \dot{q}_n; t) + \sum Q_i \delta q_i] dt \\ &= \int_{t_1}^{t_2} [\sum_i (\frac{\partial L}{\partial q_i} \delta q_i + \frac{\partial L}{\partial \dot{q}_i} \delta \dot{q}_i) + \sum Q_i \delta q_i] dt \end{aligned}$$

and, upon integrating by part to eliminate $\delta \dot{q}_i$, using

$$\frac{\partial L}{\partial \dot{q}_i} \delta \dot{q}_i = \frac{d}{dt}\left(\frac{\partial L}{\partial \dot{q}_i} \delta q_i\right) - \frac{d}{dt}\left(\frac{\partial L}{\partial \dot{q}_i}\right) \delta q_i$$

one finds

$$\delta I = \sum_i [\frac{\delta L}{\delta \dot{q}_i} \delta q_i]_{t_1}^{t_2} - \int_{t_1}^{t_2} \sum_i [\frac{d}{dt}\left(\frac{\partial L}{\partial \dot{q}_i}\right) - \frac{\partial L}{\partial q_i} - Q_i] \delta q_i dt = 0 \tag{1.45}$$

The first term vanishes because $\delta q_i(t_1) = \delta q_i(t_2) = 0$, and since the virtual variations are arbitrary (q_i are independent), one must have

$$\frac{d}{dt}(\frac{\partial L}{\partial \dot{q}_i}) - \frac{\partial L}{\partial q_i} = Q_i \qquad\qquad i = 1, ...n \tag{1.46}$$

These are Lagrange's equations, their number is equal to the number n of independent coordinates. The generalized forces contain all the non-conservative forces; they are obtained from the principle of virtual work (1.43). Once the analytical expression of the Lagrangian in terms of the generalized coordinates has been found, Equ.(1.46) allows us to write the differential equations governing the motion in a straightforward way.

1.7.1 Vibration of a linear, non-gyroscopic, discrete system

The general form of the kinetic coenergy of a linear non-gyroscopic, discrete mechanical system is

$$T^* = \frac{1}{2}\dot{x}^T M \dot{x} \tag{1.47}$$

where x is a set of generalized coordinates, and M is the mass matrix. M is symmetric and semi-positive definite, which translates the fact that any velocity distribution must lead to a non-negative value of the kinetic coenergy; M is strictly positive definite if all the coordinates have an inertia associated to them, so that it is impossible to find a velocity distribution such that $T^* = 0$. Similarly, the general form of the strain energy is

$$V = \frac{1}{2}x^T K x \tag{1.48}$$

where K is the stiffness matrix, also symmetric and semi-positive definite. A rigid body mode is a set of generalized coordinates with no strain energy in the system. K is strictly positive definite if the system does not have rigid body modes.

The Lagrangian of the system reads,

$$L = T^* - V = \frac{1}{2}\dot{x}^T M \dot{x} - \frac{1}{2}x^T K x \tag{1.49}$$

If, in addition, one assumes that the virtual work of the non-conservative external forces can be written $\delta W_{nc} = f^T \delta x$, applying the Lagrange equations (1.46), one gets the equation of motion

$$M\ddot{x} + Kx = f \tag{1.50}$$

1.7.2 Dissipation function

In the literature, it is customary to define the *dissipation function* D such that the dissipative forces are given by

$$Q_i = -\frac{\partial D}{\partial \dot{q}_i} \tag{1.51}$$

If this definition is used, Equ.(1.46) becomes

$$\frac{d}{dt}\left(\frac{\partial L}{\partial \dot{q}_i}\right) + \frac{\partial D}{\partial \dot{q}_i} - \frac{\partial L}{\partial q_i} = Q_i \tag{1.52}$$

where Q_i includes all the non-conservative forces which are not already included in the dissipation function. Viscous damping can be represented by a quadratic dissipation function. If one assumes

$$D = \frac{1}{2}\dot{x}^T C \dot{x} \tag{1.53}$$

in previous section, one gets the equation of motion

$$M\ddot{x} + C\dot{x} + Kx = f \tag{1.54}$$

where C is the viscous damping matrix, also symmetric and semi-positive definite. We now examine a few examples of mechanical systems, to illustrate some of the features of the method.

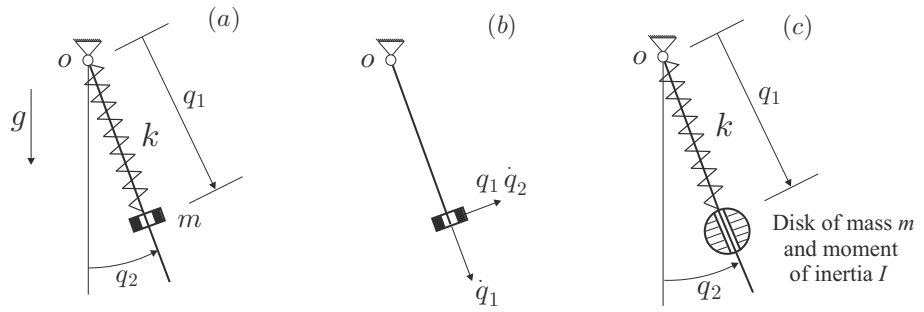

Fig. 1.8. Pendulum with a sliding mass attached with a spring. (a) and (b): Point mass. (c) Disk.

1.7.3 Example 1: Pendulum with a sliding mass

Consider the pendulum of Fig.1.8(a) where a mass m slides without friction on a massless rod in a constant gravity field g; a linear spring of stiffness k connects the mass to the pivot O of the pendulum. This system has two d.o.f. and we select q_1 (position of the mass along the bar) and

q_2 (angle of the pendulum) as the generalized coordinates. It is assumed that, when $q_1 = 0$, the spring force vanishes.

The kinetic coenergy is associated with the point mass m; its velocity can be expressed in two orthogonal directions as in Fig.1.8(b); it follows that

$$T^* = \frac{1}{2} m(\dot{q}_1^2 + \dot{q}_2^2 q_1^2)$$

The potential energy reads

$$V = -m\, g\, q_1 \cos q_2 + \frac{1}{2} k\, q_1^2$$

The first contribution comes from gravity (the reference altitude has been taken at the pivot O) and the second one is the strain energy in the spring (assumed unstretched when $q_1 = 0$). The Lagrange equations are

$$\frac{d}{dt}(m\, q_1^2\, \dot{q}_2) + m\, g\, q_1 \sin q_2 = 0$$

$$m\, \ddot{q}_1 - m\, q_1 \dot{q}_2^2 - m\, g \cos q_2 + k q_1 = 0$$

If one assumes that the mass m is no longer a point mass, but a disk of moment of inertia I sliding along the massless rod [Fig.1.8(c)], it contributes an extra term to the kinetic coenergy, representing the kinetic coenergy of rotation of the disk (the kinetic coenergy of a rigid body is the sum of the kinetic coenergy of translation of the total mass lumped at the center of mass and the kinetic coenergy of rotation around the center of mass):

$$T^* = \frac{1}{2} m(\dot{q}_1^2 + \dot{q}_2^2 q_1^2) + \frac{1}{2} I \dot{q}_2^2$$

The disk has the same potential energy as the point mass. Furthermore, if the rod is uniform with a total mass M and a length l, its moment of inertia with respect to the pivot is

$$I_o = \int_0^l \varrho x^2 dx = \varrho l^3/3 = M l^2/3$$

($M = \varrho l$); the additional contribution to the kinetic coenergy is $I_o \dot{q}_2^2/2$. Note that, this includes the translational energy as well as the rotational energy of the rod, because the moment of inertia I_0 refers to the fixed point at the pivot. The bar has also an additional contribution to the potential energy: $-m\, g\, l \cos q_2/2$ (the center of mass is at mid length).

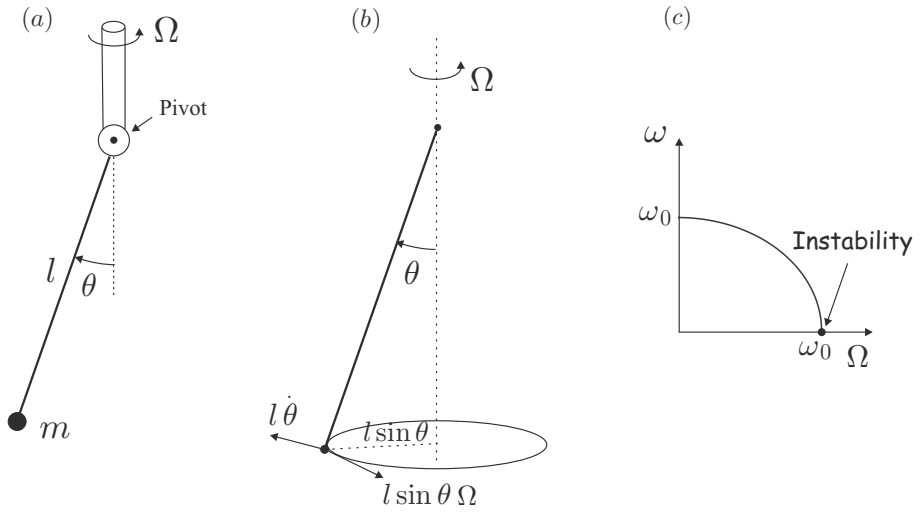

Fig. 1.9. Rotating pendulum.

1.7.4 Example 2: Rotating pendulum

Consider the rotating pendulum of Figure 1.9(a). The point mass m is connected by a massless rod to a pivot which rotates about a vertical axis at constant velocity Ω; the system is in a vertical gravity field g. Because Ω is constant, the system has a single d.o.f., with coordinate θ. In order to write the kinetic coenergy, it is convenient to project the velocity of the point mass in the orthogonal frame shown in Fig.1.9(b). One axis is tangent to the circular trajectory when the pendulum rotates about the vertical axis with θ fixed, while the other one is tangent to the trajectory of the mass in the plane of the pendulum when it does not rotate about the vertical axis; the projected components are respectively $l\Omega \sin\theta$ and $l\dot{\theta}$. Being orthogonal, it follows that

$$T^* = \frac{m}{2}\left[(l\dot{\theta})^2 + (l\Omega\sin\theta)^2\right]$$

Note that the first term is quadratic in $\dot{\theta}$ [$T_2{}^*$ in (1.39)], while the second term is independent of $\dot{\theta}$ and appears as a potential of centrifugal forces [$T_0{}^*$ in (1.39)]. Taking the reference altitude at the pivot, the gravity potential is $V = -gml\cos\theta$ and

$$L = T^* - V = \frac{m}{2}\left[(l\dot{\theta})^2 + (l\Omega\sin\theta)^2\right] + gml\cos\theta$$

The corresponding Lagrange equation reads

$$ml^2\ddot{\theta} - ml^2\Omega^2 \sin\theta\cos\theta + mgl\sin\theta = 0$$

For small oscillations near $\theta = 0$, the equation can be simplified using the approximations $\sin\theta \simeq \theta$ and $\cos\theta = 1$; this leads to

$$\ddot{\theta} + \frac{g}{l}\theta - \Omega^2\theta = 0$$

Introducing $\omega_0^2 = \dfrac{g}{l}$, the pendulum frequency

$$\ddot{\theta} + \left(\omega_0^2 - \Omega^2\right)\theta = 0$$

One sees that the centrifugal force introduces a negative stiffness. Figure 1.9(c) shows the evolution of the frequency of the small oscillations of the pendulum with Ω; the system is unstable beyond $\Omega = \omega_0$.

1.7.5 Example 3: Rotating spring mass system

A spring mass system is rotating in the horizontal plane at a constant velocity Ω, Fig.1.10(a). The system has a single d.o.f., described by the coordinate u measuring the extension of the spring. The absolute velocity of the point mass m can be conveniently projected in the moving frame (x, y); the components are $(\dot{u}, u\Omega)$. It follows that

$$T^* = \frac{1}{2}m\left[\dot{u}^2 + (u\Omega)^2\right]$$

Once again, there is a quadratic contribution, ${T_2}^*$, and a contribution independent of the generalized velocity, ${T_0}^*$ (potential of centrifugal force). It is not necessary to include the kinetic coenergy of the rotating mechanism, because it is constant, and will disappear when writing the Lagrange equation. Since the system is not subjected to gravity, the potential energy is associated with the extension of the spring; assuming that the spring force is equal to zero when $u = 0$,

$$V = \frac{1}{2}ku^2$$

The Lagrangian reads

$$L = T^* - V = \frac{1}{2}m\dot{u}^2 - \frac{1}{2}(k - m\Omega^2)u^2$$

leading to the Lagrange equation

$$m\ddot{u} + (k - m\Omega^2)u = 0$$

or

$$\ddot{u} + (\omega_n^2 - \Omega^2)u = 0$$

after introducing $\omega_n^2 = k/m$. This equation is identical to the linearized form of the previous example; the system becomes unstable for $\Omega > \omega_n$.

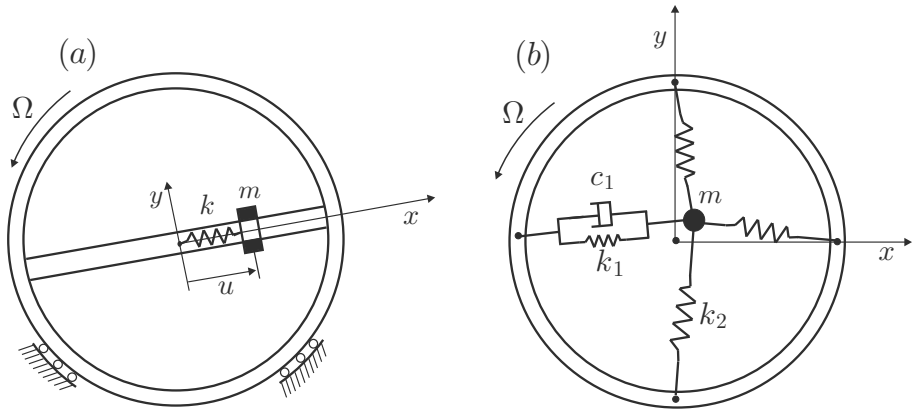

Fig. 1.10. Rotating spring-mass systems (a) Single axis (b) Two-axis.

1.7.6 Example 4: Gyroscopic effects

Next, consider the system of Fig.1.10(b), where the constraint along $y = 0$ has been removed and replaced by another spring orthogonal to the previous one. This system has 2 d.o.f.; it is fully described by the generalized coordinates x and y, the displacements along the moving axes rotating at constant speed Ω. We assume small displacements and, in Fig.1.10(b), the stiffness k_1 and k_2 represent the global stiffness along x and y, respectively. We assume viscous damping along x, with damping coefficient c_1. The absolute velocity in the rotating frame is $(\dot{x} - \Omega y, \dot{y} + \Omega x)$, leading to the kinetic coenergy of the point mass

$$T^* = \frac{1}{2}m\left[(\dot{x} - \Omega y)^2 + (\dot{y} + \Omega x)^2\right]$$

As in the previous example, we disregard the constant term associated with the rotation at constant speed of the supporting mechanism. Upon expanding T^*, one gets

$$T^* = T_2^* + T_1^* + T_0^*$$

with

$$T_2^* = \frac{1}{2}m(\dot{x}^2 + \dot{y}^2)$$

$$T_1^* = m\Omega(x\dot{y} - \dot{x}y)$$

$$T_0^* = \frac{1}{2}m\Omega^2(x^2 + y^2)$$

Note that a contribution T_1^* of the first order in the generalized velocities appears for the first time; it will be responsible for gyroscopic forces [the system of Fig.1.10(b) is actually the simplest, where gyroscopic forces can be illustrated]. The potential V is associated with the extension of the springs; with the assumption of small displacements,

$$V = \frac{1}{2}k_1x^2 + \frac{1}{2}k_2y^2$$

The damping force can be handled either by the virtual work, $\delta W_{nc} = -c_1\dot{x}\delta x$ or with dissipation function (1.53). In this case,

$$D = \frac{1}{2}c_1\dot{x}^2$$

The Lagrange equations read

$$m\ddot{x} - 2m\Omega\dot{y} + c_1\dot{x} + k_1x - m\Omega^2x = 0$$

$$m\ddot{y} + 2m\Omega\dot{x} + k_2x - m\Omega^2y = 0$$

or, in matrix form, with $q = (x, y)^T$,

$$M\ddot{q} + (C + G)\dot{q} + (K - \Omega^2M)q = 0 \tag{1.55}$$

where

$$M = \begin{bmatrix} m & 0 \\ 0 & m \end{bmatrix} \qquad C = \begin{bmatrix} c_1 & 0 \\ 0 & 0 \end{bmatrix} \qquad K = \begin{bmatrix} k_1 & 0 \\ 0 & k_2 \end{bmatrix}$$

are respectively the mass, damping and stiffness matrices, and

$$G = \begin{bmatrix} 0 & -2m\Omega \\ 2m\Omega & 0 \end{bmatrix} \tag{1.56}$$

is the anti-symmetric matrix of gyroscopic forces, which couples the motion in the two directions; its magnitude is proportional to the inertia (m)

and to the rotating speed Ω. The contribution $-\Omega^2 M$ is, once again, the centrifugal force. Note that, with the previous definitions of the matrices M, G, K and C, the various energy terms appearing in the Lagrangian can be written

$$\begin{aligned} T_2^* &= \frac{1}{2}\dot{q}^T M \dot{q} \\ T_1^* &= \frac{1}{2}\dot{q}^T G q \\ T_0^* &= \frac{\Omega^2}{2} q^T M q \\ V &= \frac{1}{2} q^T K q \\ D &= \frac{1}{2}\dot{q}^T C \dot{q} \end{aligned} \tag{1.57}$$

Note that the modified potential

$$V^+ = V - T_0^* = \frac{1}{2} q^T \left(K - \Omega^2 M\right) q \tag{1.58}$$

is no longer positive definite if $\Omega^2 > k_1/m$ or k_2/m.

Let us examine this system a little further, in the particular case where $k_1 = k_2 = k$ and $c_1 = 0$. If $\omega_n^2 = k/m$, the equations of motion become

$$\ddot{x} - 2\Omega\dot{y} + \left(\omega_n^2 - \Omega^2\right) x = 0$$

$$\ddot{y} + 2\Omega\dot{x} + \left(\omega_n^2 - \Omega^2\right) y = 0$$

To analyze the stability of the system, let us assume a solution of the form $x = Xe^{pt}$, $y = Ye^{pt}$; the corresponding eigenvalue problem is

$$\begin{bmatrix} p^2 + \omega_n^2 - \Omega^2 & -2\Omega p \\ 2\Omega p & p^2 + \omega_n^2 - \Omega^2 \end{bmatrix} \begin{Bmatrix} X \\ Y \end{Bmatrix} = 0$$

Nontrivial solutions of this homogenous system of equations require that the determinant be zero, leading to the characteristic equation

$$p^4 + 2p^2(\omega_n^2 + \Omega^2) + (\omega_n^2 - \Omega^2)^2 = 0$$

The roots of this equation are

$$p_1^2 = -(\omega_n - \Omega)^2, \qquad p_2^2 = -(\omega_n + \Omega)^2$$

Thus, the eigenvalues are all imaginary, for all values of Ω. Figure 1.11 shows the evolution of the natural frequencies with Ω (this plot is often called *Campbell diagram*). We note that, in contrast with the previous example, the system does not become unstable beyond $\Omega = \omega_n$; it is stabilized by the gyroscopic forces.

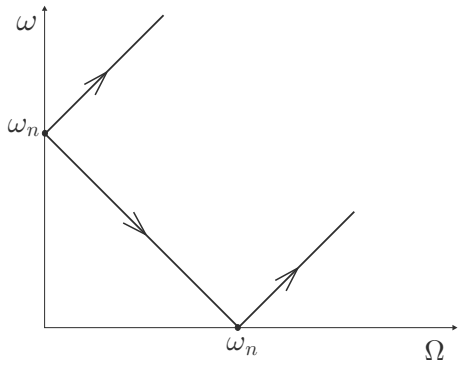

Fig. 1.11. Campbell diagram of the system of Fig.1.10(b), in the particular case $k_1 = k_2$ and $c_1 = 0$.

1.8 Lagrange's equations with constraints

Consider the case where the n generalized coordinates are not independent. In this case, the virtual changes of configuration δq_k must satisfy a set of m constraint equations of the form of Equ.(1.18):

$$\sum_k a_{lk}\delta q_k = 0 \qquad\qquad l = 1, ...m \tag{1.59}$$

The number of degrees of freedom of the system is $n - m$. In Hamilton's principle (1.45), the variations δq_i are no longer arbitrary, because of Equ.(1.59), and the step leading from Equ.(1.45) to (1.46) is impossible. This difficulty can be solved by using *Lagrange multipliers*. The technique consists of adding to the variational indicator a linear combination of the constraint equations

$$\sum_{l=1}^{m} \lambda_l \left(\sum_{k=1}^{n} a_{lk}\delta q_k \right) = \sum_{k=1}^{n} \delta q_k \left(\sum_{l=1}^{m} \lambda_l a_{lk} \right) = 0 \tag{1.60}$$

where the Lagrange multipliers λ_l are unknown at this stage. Equation (1.60) is true for any set of λ_l. Adding to Equ.(1.45), one gets

$$\int_{t_1}^{t_2} \sum_{k=1}^{n} [\frac{d}{dt}(\frac{\partial L}{\partial \dot{q}_k}) - \frac{\partial L}{\partial q_k} - Q_k - \sum_{l=1}^{m} \lambda_l a_{lk}] \delta q_k dt = 0$$

In this equation, $n-m$ variations δq_k can be taken arbitrarily (the independent variables) and the corresponding expressions between brackets must vanish; the m terms left in the sum do not have independent variations δq_k, but we are free to select the m Lagrange multipliers λ_l to cancel them too. Overall, one gets

$$\frac{d}{dt}(\frac{\partial L}{\partial \dot{q}_k}) - \frac{\partial L}{\partial q_k} = Q_k + \sum_{l=1}^{m} \lambda_l a_{lk} \qquad k = 1, ..., n$$

The second term in the right hand side represents the generalized constraint forces, which are linear functions of the Lagrange multipliers. This set of n equations has $n+m$ unknown (the generalized coordinates q_k and the Lagrange multipliers λ_l). Combining with the m constraints equations, we obtain a set of $n+m$ equations. For non-holonomic constraints of the form (1.15), the equations read

$$\sum_k a_{lk} dq_k + a_{l_0} dt \qquad l = 1, ..., m \tag{1.61}$$

$$\frac{d}{dt}(\frac{\partial L}{\partial \dot{q}_k}) - \frac{\partial L}{\partial q_k} = Q_k + \sum_{l=1}^{m} \lambda_l a_{lk} \qquad k = 1, ..., n \tag{1.62}$$

with the unknown $q_k, k = 1, ..., n$ and $\lambda_l, l = 1, ..., m$. If the system is holonomic, with constraints of the form (1.13), the equations become

$$g_l(q_1, q_2, ...q_n; t) = 0 \qquad l = 1, ..., m \tag{1.63}$$

$$\frac{d}{dt}(\frac{\partial L}{\partial \dot{q}_k}) - \frac{\partial L}{\partial q_k} = Q_k + \sum_{l=1}^{m} \lambda_l \frac{\partial g_l}{\partial q_k} \qquad k = 1, ..., n \tag{1.64}$$

This is a system of *algebro-differential* equations. This formulation is frequently met in multi-body dynamics.

1.9 Conservation laws

1.9.1 Jacobi integral

If the generalized coordinates are independent, the Lagrange equations constitute a set of n differential equations of the second order; their solution requires $2n$ initial conditions describing the configuration and the velocity at $t = 0$. In special circumstances, the system admits first integrals of the motion, which contain derivatives of the variables of one order lower than the order of the differential equations. The most celebrated of these first integrals is that of conservation of energy (1.23); it is a particular case of a more general relationship known as a *Jacobi integral*.

If the system is conservative ($Q_k = 0$) and if the Lagrangian does not depend explicitly on time,

$$\frac{\partial L}{\partial t} = 0 \tag{1.65}$$

The total derivative of L with respect to time reads

$$\frac{dL}{dt} = \sum_{k=1}^{n} \frac{\partial L}{\partial q_k}\dot{q}_k + \sum_{k=1}^{n} \frac{\partial L}{\partial \dot{q}_k}\ddot{q}_k$$

On the other hand, from the Lagrange's equations (taking into account that $Q_k = 0$)

$$\frac{\partial L}{\partial q_k} = \frac{d}{dt}\left(\frac{\partial L}{\partial \dot{q}_k}\right)$$

Substituting into the previous equation, one gets

$$\frac{dL}{dt} = \sum_{k=1}^{n}[\frac{d}{dt}\left(\frac{\partial L}{\partial \dot{q}_k}\right)\dot{q}_k + \frac{\partial L}{\partial \dot{q}_k}\ddot{q}_k] = \sum_{k=1}^{n}\frac{d}{dt}[\left(\frac{\partial L}{\partial \dot{q}_k}\right)\dot{q}_k]$$

It follows that

$$\frac{d}{dt}[\sum_{k=1}^{n}\left(\frac{\partial L}{\partial \dot{q}_k}\right)\dot{q}_k - L] = 0 \tag{1.66}$$

or

$$\sum_{k=1}^{n}\left(\frac{\partial L}{\partial \dot{q}_k}\right)\dot{q}_k - L = h = C^t \tag{1.67}$$

Recall that the Lagrangian reads

$$L = T^* - V = T_2^* + T_1^* + T_0^* - V \tag{1.68}$$

where T_2^* is a homogenous quadratic function of $\dot{q}_k$, T_1^* is homogenous linear in $\dot{q}_k$, and T_0^* and V do not depend on $\dot{q}_k$.

According to Euler's theorem on homogenous functions, if T_n^* is an homogeneous function of order n in some variables q_i, it satisfies the identity

$$\sum q_i \frac{\partial T_n^*}{\partial q_i} = n T_n^* \tag{1.69}$$

It follows from this theorem that

$$\sum \left(\frac{\partial L}{\partial \dot{q}_k} \right) \dot{q}_k = 2T_2^* + T_1^*$$

and (1.67) can be rewritten

$$h = T_2^* - T_0^* + V = C^t \tag{1.70}$$

This result is known as a *Jacobi integral*, or also a *Painlevé integral*. If the kinetic coenergy is a homogeneous quadratic function of the velocity, $T^* = T_2^*$ and $T_0^* = 0$; Equ.(1.70) becomes

$$T^* + V = C^t \tag{1.71}$$

which is the integral of *conservation of energy*. From the above discussion, it follows that it applies to conservative systems whose Lagrangian does not depend explicitly on time [Equ.(1.65)] and whose kinetic coenergy is a homogeneous quadratic function of the generalized velocities ($T^* = T_2^*$). We have met this equation earlier [Equ.(1.23)], and it is interesting to relate the above conditions to the earlier ones: Indeed, (1.65) implies that the potential does not depend explicitly on t, and $T^* = T_2^*$ implies that the kinematical constraints do not depend explicitly on t [see (1.38) and (1.39)].

1.9.2 Ignorable coordinate

Another first integral can be obtained if a generalized coordinate (say q_s) does not appear explicitly in the Lagrangian of a conservative system (the Lagrangian contains $\dot{q}_s$ but not q_s, so that $\partial L/\partial q_s = 0$). Such a coordinate is called *ignorable*. From Lagrange's equation (1.46),

$$\frac{d}{dt}\left(\frac{\partial L}{\partial \dot{q}_s}\right) = \frac{\partial L}{\partial q_s} = 0$$

It follows that

$$p_s = \frac{\partial L}{\partial \dot{q}_s} = C^t$$

and, since V does not depend explicitly on the velocities, this can be rewritten

$$p_s = \frac{\partial L}{\partial \dot{q}_s} = \frac{\partial T^*}{\partial \dot{q}_s} = C^t \tag{1.72}$$

p_s is the *generalized momentum conjugate to* q_s [by analogy with (1.10)]. Thus, *the generalized momentum associated with an ignorable coordinate is conserved*.

Note that the existence of the first integral (1.72) depends very much on the choice of coordinates, and that it may remain hidden if inappropriate coordinates are used. The ignorable coordinates are also called *cyclic*, because they often happen to be rotational coordinates.

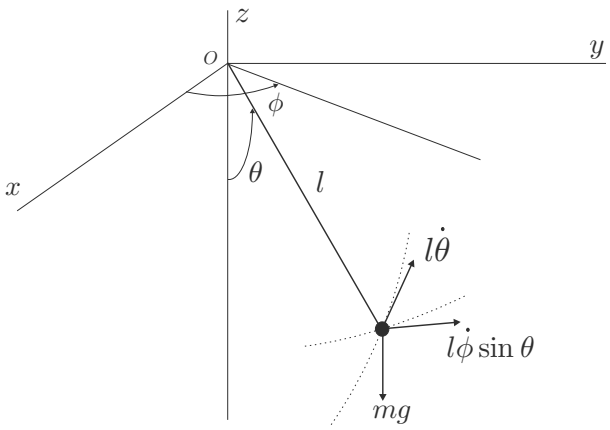

Fig. 1.12. The spherical pendulum.

1.9.3 Example: The spherical pendulum

To illustrate the previous paragraph, consider the spherical pendulum of Fig.1.12. Its configuration is entirely characterized by the two generalized coordinates θ and ϕ. the kinetic coenergy and the potential energy are respectively

$$T^* = \frac{1}{2} m[(l\dot{\theta})^2 + (\dot{\phi} l \sin\theta)^2]$$
$$V = -mgl\cos\theta$$

and the Lagrangian reads

$$L = T^* - V = \frac{1}{2} ml^2[\dot{\theta}^2 + (\dot{\phi}\sin\theta)^2] + mgl\cos\theta$$

The Lagrangian does not depend explicitly on t, nor on the coordinate ϕ. The system is therefore eligible for the two first integrals discussed above. Since the kinetic energy is homogeneous quadratic in $\dot{\theta}$ and $\dot{\phi}$, the conservation of energy (1.71) applies.

As for the ignorable coordinate ϕ, the conjugate generalized momentum is

$$p_\phi = \partial T^* / \partial \dot{\phi} = ml^2 \dot{\phi} \sin^2\theta = C^t$$

This equation simply states the conservation of the angular momentum about the vertical axis Oz (indeed, the moments about Oz of the external forces from the cable of the pendulum and the gravity vanish).

1.10 More on continuous systems

In this section, additional aspects of continuous systems are discussed. The sections on the Green tensor and the geometric stiffness are more specialized and may be skipped without jeopardizing the understanding of subsequent chapters.

1.10.1 Rayleigh-Ritz method

The *Rayleigh-Ritz method*, also called *Assumed Modes method*, is an approximation which allows us to transform a partial differential equation into a set of ordinary differential equations; in other words, it allows us to represent a continuous system by a discrete approximation, which is

expected to approximate the low frequency behavior of the continuous system. To achieve this, it is assumed that the displacement field (assumed one-dimensional here for simplicity, but the approximation applies in three dimensions as well) can be written

$$v(x,t) = \sum_{i=1}^{n} \psi_i(x)\, q_i(t) \tag{1.73}$$

where $\psi_i(x)$ are a set of assumed modes, which are continuous and satisfy the geometric boundary conditions (but not the natural boundary conditions). The n functions of time $q_i(t)$ are the generalized coordinates of the approximate discrete system. If the set of assumed modes is *complete* (such as Fourier series, or power series), the approximation converges towards the exact solution as their number n increases.

To illustrate this method, let us return to the lateral vibration of the Euler-Bernoulli beam. If the transverse displacement is approximated by (1.73), the strain energy (1.30) can be readily transformed into

$$V = \frac{1}{2}\int_0^L EI[\sum_i q_i \psi_i''(x)][\sum_j q_j \psi_j''(x)]dx$$

or

$$V = \frac{1}{2} q^T K q \tag{1.74}$$

where K is the stiffness matrix, defined by

$$K_{ij} = \frac{1}{2}\int_0^L EI\psi_i''(x)\psi_j''(x)dx \tag{1.75}$$

Similarly, the kinetic coenergy is approximated by

$$T^* = \frac{1}{2}\int_0^L \varrho A[\sum_i \dot{q}_i \psi_i(x)][\sum_j \dot{q}_j \psi_j(x)]dx$$

or

$$T^* = \frac{1}{2}\dot{q}^T M \dot{q} \tag{1.76}$$

where the mass matrix is defined as

$$M_{ij} = \frac{1}{2}\int_0^L \varrho A \psi_i(x)\psi_j(x)dx \tag{1.77}$$

The reader familiar with the finite element method will recognize the form of the mass and stiffness matrices, except that the shape functions $\psi_i(x)$

are defined over the entire structure and satisfy the geometric boundary conditions. K and M are symmetric, so that V and T^* exactly fit the forms discussed in section 1.7.1, leading to the differential equation (1.50). Note also that, if the trial functions $\psi_i(x)$ are the vibration modes $\phi_i(x)$ of the system, K and M as defined by (1.75) and (1.77) are both diagonal, because of the orthogonality of the mode shapes, and a set of decoupled equations is obtained.

1.10.2 General continuous system

Anticipating the analysis of piezoelectric structures of chapter 4, we use the notation S_{ij} for the strain tensor and T_{ij} for the stress tensor; these are the standard notations for piezoelectric structures. With these notations, the constitutive equations of a linear elastic material are

$$T_{ij} = c_{ijkl} S_{kl} \tag{1.78}$$

where c_{ijkl} is the tensor of elastic constants. The strain energy density reads

$$U(S_{ij}) = \int_0^{S_{ij}} T_{ij} dS_{ij} \tag{1.79}$$

from which the constitutive equation may be rewritten

$$T_{ij} = \frac{\partial U}{\partial S_{ij}} \tag{1.80}$$

For a linear elastic material

$$U(S_{ij}) = \frac{1}{2} c_{ijkl} S_{ij} S_{kl} \tag{1.81}$$

1.10.3 Green strain tensor

For many problems in mechanical engineering (e.g. the beam theory of section 1.6.1), it is sufficient to consider the infinitesimal definition of strain of linear elasticity. However, problems involving large displacements and prestresses cannot be handled in this way and require a strain measure invariant with respect to the global rotation of the system. In other words, a rigid body motion should produce $S_{ij} = 0$. Such a representation is supplied by the *Green strain tensor*, which is defined as follows: Consider a continuous body and let AB be a segment connecting two

points before deformation, and $A'B'$ be the same segment after deformation; the coordinates are respectively: $A : x_i$, $B : x_i + dx_i$, $A' : x_i + u_i$, $B' : x_i + u_i + d(x_i + u_i)$. If dl_0 is the initial length of AB and dl the length of $A'B'$, it is readily established that

$$dl^2 - dl_0^2 = (\frac{\partial u_i}{\partial x_j} + \frac{\partial u_j}{\partial x_i} + \frac{\partial u_m}{\partial x_i}\frac{\partial u_m}{\partial x_j})dx_i dx_j \tag{1.82}$$

The Green strain tensor is defined as

$$S_{ij} = \frac{1}{2}(\frac{\partial u_i}{\partial x_j} + \frac{\partial u_j}{\partial x_i} + \frac{\partial u_m}{\partial x_i}\frac{\partial u_m}{\partial x_j}) \tag{1.83}$$

It is symmetric, and its linear part is the classical strain measure in linear elasticity; there is an additional quadratic part which accounts for large rotations. Comparing the foregoing equations,

$$dl^2 - dl_0^2 = 2S_{ij}dx_i dx_j \tag{1.84}$$

which shows that if $S_{ij} = 0$, the length of the segment is indeed unchanged, even for large u_i. The Green strain tensor accounts for large rotations; it can be partitioned according to

$$S_{ij} = S_{ij}^{(1)} + S_{ij}^{(2)} \tag{1.85}$$

where $S_{ij}^{(1)}$ is linear in the displacements, and $S_{ij}^{(2)}$ is quadratic.

1.10.4 Geometric strain energy due to prestress

The lateral stiffness of strings and cables is known to depend on their axial tension force. Similarly, long rods subjected to large axial forces have a modified lateral stiffness; compressive forces reduce the natural frequency while traction forces increase it. When the axial compressive load exceeds some threshold, the rod buckles, and the buckling load is that which reduces the natural frequency to 0. The *geometric stiffness* is important for structures subjected to large dead loads which contribute significantly to the strain energy of the system.

Consider a continuous system in a prestressed state (T_{ij}^0, S_{ij}^0) independent of time, and then subjected to a dynamic motion (T_{ij}^*, S_{ij}^*). The total stress and strain state is (Fig.1.13)

$$S_{ij} = S_{ij}^0 + S_{ij}^*$$

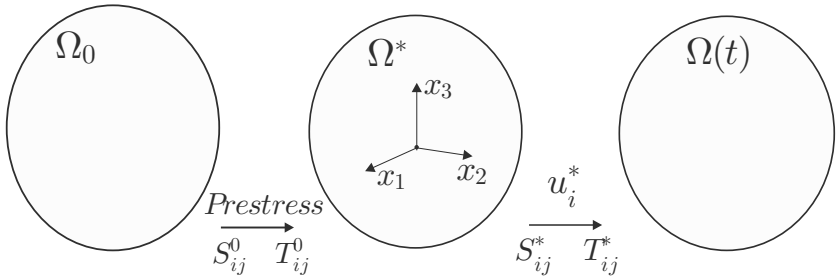

Fig. 1.13. Continuous system in a prestressed state.

$$T_{ij} = T_{ij}^0 + T_{ij}^* \tag{1.86}$$

It is impossible to account for the strain energy associated with the prestress if the linear strain tensor is used. If the Green tensor is used,

$$S_{ij}^* = S_{ij}^{*\,(1)} + S_{ij}^{*\,(2)} \tag{1.87}$$

it can be shown (Geradin & Rixen, 1994) that the strain energy can be written

$$V = V^* + V_g \tag{1.88}$$

where

$$V^* = \frac{1}{2}\int_{\Omega^*} c_{ijkl} S_{ij}^{*\,(1)} S_{kl}^{*\,(1)} d\Omega \tag{1.89}$$

is the additional strain energy due to the linear part of the deformation beyond the prestress (it is the unique term if there is no prestress), and

$$V_g = \int_{\Omega^*} T_{ij}^0 S_{ij}^{*\,(2)} d\Omega \tag{1.90}$$

is the *geometric strain energy due to prestress* involving the prestressed state T_{ij}^0 and the quadratic part of the strain tensor. Unlike V^* which is always positive, V_g may be positive or negative, depending on the sign of the prestress. If V_g is positive, it tends to rigidify the system; it softens it if it is negative, as illustrated below. For a discrete system, V_g takes the general form

$$V_g = \frac{1}{2} x^T K_g x \tag{1.91}$$

where K_g is the *geometric stiffness matrix*, no longer positive definite since V_g may be negative. The geometric stiffness is a significant contributor to the total stiffness of a rotating helicopter blade; the lowering of the natural frequencies of civil engineering structures due to the dead loads is often referred to as the "P-Delta" effect.

1.10.5 Lateral vibration of a beam with axial loads

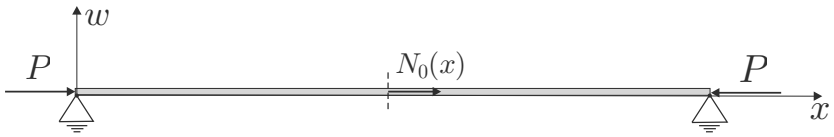

Fig. 1.14. Euler-Bernoulli beam with axial prestress.

Consider again the in-plane vibration of a beam, but subjected to an axial load $N_0(x)$ (positive in traction). The displacement field is

$$u = u_0(x) - z\frac{\partial w}{\partial x}$$

$$v = 0$$

$$w = w(x)$$

The axial preload at x is

$$N_0(x) = AES_0(x) = AE\frac{\partial u_0}{\partial x} \tag{1.92}$$

The Green tensor is in this case

$$S_{11} = S_0 - z\frac{\partial^2 w}{\partial x^2} + \frac{1}{2}[(\frac{\partial u}{\partial x})^2 + (\frac{\partial w}{\partial x})^2] \tag{1.93}$$

and, assuming large rotations but small deformations,

$$\frac{\partial u}{\partial x} \ll \frac{\partial w}{\partial x}$$

and $(\partial u/\partial x)^2$ can be neglected. It follows that the linear part of the Green tensor is

$$S_{ij}^{*\,(1)} = -zw'' \tag{1.94}$$

(as in section 1.6.1), and the quadratic part

$$S_{ij}^{*\,(2)} = \frac{1}{2}(w')^2 \tag{1.95}$$

Accordingly, the additional strain energy due to the linear part

$$V^* = \frac{1}{2}\int_0^L EI(w'')^2 dx \tag{1.96}$$

is identical to (1.30), and the geometric strain energy due to prestress is

$$V_g = \int_V T_0 \frac{1}{2}(w')^2 dV = \frac{1}{2}\int_0^L N_0(x)(w')^2 dx \tag{1.97}$$

where the axial preload $N_0(x)$ is positive in traction.

1.10.6 Example: Simply supported beam in compression

Consider a simply supported beam subjected to a constant axial compression load P. One can estimate the first natural frequency of the system with the Rayleigh-Ritz method, using a single mode approximation:

$$w = q \sin \frac{\pi x}{L} \tag{1.98}$$

With this assumption, the Lagrangian reads

$$L = T^* - (V^* + V_g) = \frac{\varrho AL}{4}\dot{q}^2 - [\frac{\pi^4 EI}{4L^3} - \frac{\pi^2 P}{4L}]q^2 \tag{1.99}$$

Note that V_g contributes negatively to the potential energy because the load P is compressive. The potential energy can be rearranged

$$V^* + V_g = q^2.\frac{\pi^4 EI}{4L^3}[1 - \frac{PL^2}{\pi^2 EI}] = q^2.\frac{\pi^4 EI}{4L^3}[1 - \frac{P}{P_{cr}}] \tag{1.100}$$

where $P_{cr} = \pi^2 EI/L^2$ is the well known Euler's critical buckling load. The Lagrangian (1.99) is that of a single d.o.f. oscillator; the corresponding natural frequency is

$$\omega_1^2 = \frac{\pi^4 EI}{\varrho AL^4}.[1 - \frac{P}{P_{cr}}] \tag{1.101}$$

The first term is the exact value for a simply supported beam without prestress, and the second term is the correction due to the axial loading. One sees that a compressive load reduces ω_1 and, when P reaches P_{cr}, $\omega_1 = 0$; conversely, a traction load tends to increase ω_1. The fact that the *exact* value of the natural frequency has been obtained with an approximation technique is due to the fact that the assumed mode (1.98) is the exact mode shape of the problem. Any other assumption (satisfying the geometric boundary conditions) would have led to a *larger* value of the ω_1, because the Rayleigh-Ritz method tends to overestimate the natural frequencies.

1.11 References

CLOUGH, R.W., PENZIEN, J., *Dynamics of Structures*, McGraw-Hill, 1975.
CRAIG, R.R., Jr., *Structural Dynamics*, Wiley, 1981.
CRANDALL, S.H., KARNOPP, D.C., KURTZ, E.F, Jr., PRIDMORE-BROWN, D.C., *Dynamics of Mechanical and Electromechanical Systems*, McGraw-Hill, N-Y, 1968.
GERADIN, M., RIXEN, D., *Mechanical Vibrations*, Wiley, 1994.
GOLDSTEIN, H., *Classical Mechanics*, Second Edition, Addison-Wesley, 1980.
MEIROVITCH, L., *Methods of Analytical Dynamics*, McGraw-Hill, 1970.
REDDY, J.N., *Energy and Variational Methods in Applied Mechanics*, Wiley, 1984.
WILLIAMS, J.H., Jr., *Fundamentals of Applied Dynamics*, Wiley, 1996.

2

Dynamics of electrical networks

2.1 Introduction

Electrical networks are constituted of passive elements such as resistors, capacitors and inductors, and active ones such as voltage and current sources. The interconnection constraints on electrical networks are represented by Kirchhoff's rules:

Kirchhoff's current rule (KCR) stipulates that no electrical charge can accumulate at a node in the network : the algebraic sum of the currents entering any node must be zero.

Kirchhoff's voltage rule (KVR) translates the fact that the voltage between any two points in a network is independent of the path through the network : the algebraic sum of the voltage drops around any closed loop in a network must be zero.

This chapter presents the variational approach for analyzing electrical networks; this indirect approach can be used as an alternative to the direct approach based on Kirchhoff's rules, but more importantly, it can be combined with the variational approach to mechanical systems to analyze the dynamics of electromechanical systems. The following discussion is within the framework of quasi-static electromagnetic field theory, which assumes that the time variation of the electromagnetic field is slow enough to neglect the interaction between the electric field and the magnetic field. This implies that the size of the device, l, is small in comparison to the wavelength ($l/\lambda \ll 1$).

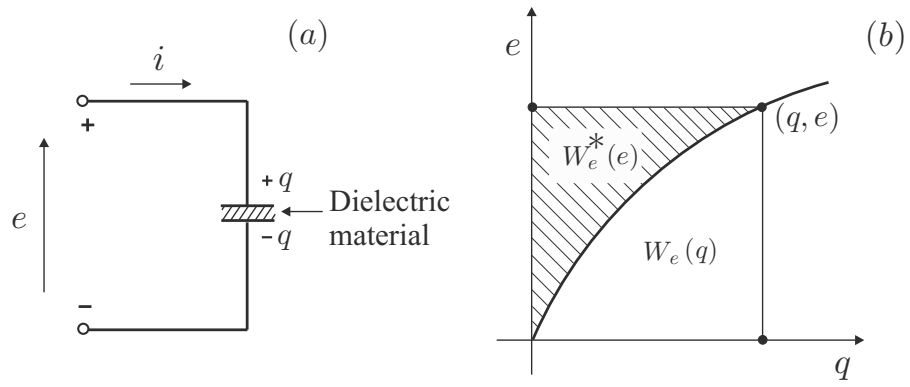

Fig. 2.1. Capacitor (a) network schematic (b) constitutive relation.

2.2 Constitutive equations for circuit elements

2.2.1 The Capacitor

A capacitor is formed by two conducting surfaces separated by a dielectric material (Fig.2.1). When charged, a electric charge of q Coulomb is added to one surface, and taken away from the other surface. The current flowing through the capacitor is the rate of change of the charge in the capacitor:

$$i = \frac{dq}{dt} \tag{2.1}$$

In the process of charging a capacitor, a potential (voltage) difference e is established between the conducting surfaces; the relationship between e and q can be measured statically; it is the constitutive relation of the capacitor, $e(q)$ (Fig.2.1.b).

The electrical energy $W_e(q)$ stored in a capacitor is the work done in charging the capacitor from no charge to q. Since the power input is $P = ei$ (Fig 2.1.a),

$$W_e(q) = \int_0^t ei\, dt = \int_0^q e\, dq \tag{2.2}$$

This integral is the area below the curve in Fig.2.1.b. It follows that

$$e = \frac{dW_e}{dq} \tag{2.3}$$

Usual capacitors are nearly linear, and their constitutive equations can be written

$$q = Ce \tag{2.4}$$

Introducing into (2.2), one gets

$$W_e(q) = \frac{q^2}{2C} \tag{2.5}$$

As for the kinetic energy in section 1.2, a complementary state function can be defined by the Legendre transformation

$$W_e^*(e) = eq - W_e(q) \tag{2.6}$$

$W_e^*(e)$ is called *electrical coenergy function* of the capacitor; it represents the area above the curve in Fig.2.1.b. The total differential of the electrical coenergy is

$$dW_e^* = q\,de + e\,dq - \frac{\partial W_e}{\partial q}dq = q\,de$$

where (2.3) has been used. It follows that

$$q = \frac{dW_e^*}{de} \tag{2.7}$$

and

$$W_e^*(e) = \int_0^e q\,de \tag{2.8}$$

For a linear capacitor with the constitutive equation (2.4),

$$W_e^*(e) = \frac{1}{2}Ce^2 \tag{2.9}$$

2.2.2 The Inductor

When a current flows in a conductor, a magnetic field is produced around the conductor, the strength of the field is proportional to the current. Conversely, when a conductor encloses a region containing a magnetic field, a voltage is induced in the conductor when the magnetic field changes. These induction effects are present in all conductors, but they become very important if the conductor consists of closely packed coils with many turns. In air, the magnetic behavior of a coil is linear (the flux linkage λ is proportional to the current i), but a ferromagnetic core is often added to the coil to enhance the magnetic flux density by several orders of magnitude; the behavior of such coils is nonlinear and often hysteretic.

Faraday's law states that the voltage developed across an inductor is equal to the rate of change of flux linkage λ

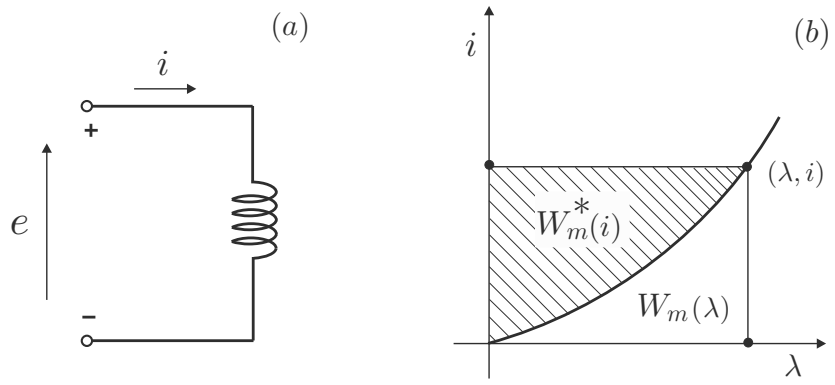

Fig. 2.2. Inductor (a) network schematic (b) constitutive relation.

$$e = \frac{d\lambda}{dt} \tag{2.10}$$

The unit of flux linkage is the *Weber* or *volt-second*. In an ideal inductor, the flux linkage λ depends only on the instantaneous current; a constant current produces a constant λ, so that $e = 0$. Thus, for a constant current, the ideal inductor behaves as a perfect conductor (short-circuit). If the inductor is linear,

$$\lambda = Li \tag{2.11}$$

where L is called inductance; its unit is the *Henry* or *Weber per Ampere*. The magnetic energy $W_m(\lambda)$ stored in an ideal inductor is the work done on the inductor when its magnetic state is changed from no flux linkage to a flux linkage λ. This work is evaluated by integrating the power delivered to the circuit:

$$W_m(\lambda) = \int_0^t ei\, dt = \int_0^\lambda i\, d\lambda \tag{2.12}$$

where (2.10) has been used; it represents the area below the curve of Fig. 2.2.b. It follows that

$$i = \frac{dW_m}{d\lambda} \tag{2.13}$$

If the coil exhibits a linear behavior as in (2.11),

$$W_m(\lambda) = \frac{\lambda^2}{2L} \tag{2.14}$$

A *magnetic coenergy function* W_m^* is defined by the Legendre transformation

$$W_m^*(i) = \lambda i - W_m(\lambda) \tag{2.15}$$

The total differential of the magnetic coenergy is

$$dW^* = \lambda\, di + i\, d\lambda - \frac{dW_m}{d\lambda} d\lambda = \lambda\, di$$

using (2.13). It follows that

$$\lambda = \frac{dW_m^*(i)}{di} \tag{2.16}$$

and

$$W_m^*(i) = \int_0^i \lambda\, di \tag{2.17}$$

It represents the area above the curve of Fig.2.2.b. For a linear inductor (2.11),

$$W_m^*(i) = \frac{1}{2} L i^2 \tag{2.18}$$

2.2.3 Voltage and current sources

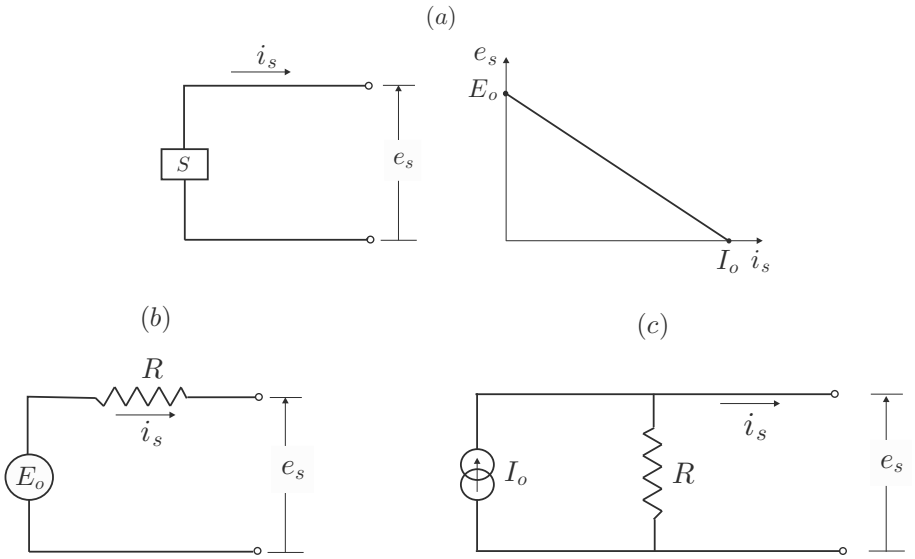

Fig. 2.3. (a) Real source and its voltage-current characteristic. (b) Ideal voltage source model. (c) Ideal current source model.

An ideal voltage source produces a time history of voltage independent of the current flowing through it. An ideal current source produces a prescribed time history of current independent of the voltage across its terminals. A real source behaves as represented in Fig.2.3.a; it has a linear characteristic, between the maximum voltage E_0 when the terminals are open, and the maximum current I_0 when the terminals are short circuited.

$$e_s = E_0 - \frac{E_0}{I_0} i_s$$

A real source can be modelled by ideal sources combined with resistors; in Fig. 2.3.b, an ideal voltage source is connected in series with a resistance R, leading to the characteristic

$$e_s = E_0 - R i_s$$

Alternatively, combining a current source I_0 in parallel with a resistance R, one gets the characteristics

$$e_s = R I_0 - R i_s$$

Thanks to modern power electronics, it is possible to build voltage amplifiers which behave nearly as a perfect voltage source in a given frequency range, and current amplifiers which behave nearly as perfect current sources in a given frequency range.

2.3 Kirchhoff's laws

Electrical networks are constructed by interconnecting passive elements and sources. The interconnections between the elements produce constraints between the variables describing the individual elements; these interconnection laws are known as Kirchhoff's laws.

Kirchhoff's current rule (KCR) state that the sum of the currents flowing into any node must be zero. It is a statement of conservation of electric charge and reflects the fact that electric charge cannot accumulate at a node of the network.

Kirchhoff's voltage rule (KVR) state that the sum of the voltage drops across every element along a closed loop must be zero. This reflects the fact that the electric potential at any point is independent of the path followed to reach that point.

In the analysis of a passive network, the following requirements must be satisfied;

1. Requirements on current variables i_k (coming from KCR), which can be expressed alternatively with charge variables q_k satisfying

$$\frac{dq_k}{dt} = i_k$$

2. Requirements on voltage variables, e_k (coming from KVR), which can be expressed alternatively with flux linkage variables λ_k satisfying

$$\frac{d\lambda_k}{dt} = e_k$$

3. The constitutive equations of individual elements.

The direct method for formulating the dynamic equations of a passive network consists in stating all these requirements analytically. This can be done in either of the following ways.

(a) With independent charge variables q_i, the solution is achieved in three steps:

- Express all current and charges in terms of the independent charge variables q_i (using the KCR).
- Use the constitutive equations to express the voltage or flux linkage across all elements in terms of q_i.
- Use the KVR to obtain a complete set of equations.

(b) A complementary procedure uses a set of independent flux linkages λ_k as independent variables, the solution in three steps proceeds as follows:

- Express all the flux linkages and voltages in terms of the independent λ_k (using the KVR).
- use the constitutive equations to express the currents and charges in all circuit elements in terms of λ_k.
- use the KCR to obtain a complete set of equations.

We shall not pursue the direct approach any further, but rather focus on indirect, variational methods, based on Hamilton's principle.

2.4 Hamilton's principle for electrical networks

In Hamilton's principle, a variational indicator is constructed from the constitutive equations of the network elements. Admissible variations are defined, which satisfy one set of Kirchhoff's rules, and the stationarity of

the variational indicator amounts to satisfying the other set of Kirchhoff's rules. There are two dual forms of Hamilton's principle, depending on the choice of independent variables. In one form, the independent variables are the charges q_i satisfying the KCR, and in the other form, the independent variables are the flux linkages λ_i satisfying the KVR.

In the previous chapter, it was argued that being a fundamental law of physics, Hamilton's principle does not have to be derived, just accepted. We could therefore proceed by first stating the principle for electrical networks and next showing that it implies Kirchhoff's rules. We believe, however, that some kind of derivation, even if it is not in its most general form, will contribute to its understanding. The reader willing to accept Hamilton's principle without discussion may skip the developments of the two following sections and focus on the final results (2.25) and (2.32).

2.4.1 Hamilton's principle, charge formulation

In this formulation, the generalized variables are the charges and currents. Admissible variations δq_i must satisfy Kirchhoff's current rules, and the current and charges variables must satisfy $i_k = \dot{q_k} = dq_k/dt$.

By analogy with Equ.(1.22), we can write the virtual work expression

$$\sum_{i=1}^{M}(e_i - \frac{d\lambda_i}{dt})\delta q_i = 0 \tag{2.19}$$

where M is the number of circuit elements. The first contribution to this sum can be separated into its conservative and non-conservative parts;

$$\sum_{i=1}^{M} e_i \delta q_i = -\delta W_e + \sum_{k=1}^{n_e} E_k \delta q_k \tag{2.20}$$

W_e is the electrical energy function of the system, and E_k represents the generalized voltage corresponding to the nonconservative elements and conjugate to the independent generalized charge variable q_k. n_e is the number of independent generalized charge coordinates. The negative sign on δW_e is due to the fact that when the voltage across a conservative circuit element does work on the circuit, the electrical energy in the element decreases. The second contribution to the sum (2.19) can be rewritten

$$-\sum_{i=1}^{M} \frac{d\lambda_i}{dt}\delta q_i = -\sum_{i=1}^{M} \frac{d}{dt}(\lambda_i \delta q_i) + \sum_{i=1}^{M} \lambda_i \frac{d(\delta q_i)}{dt} \tag{2.21}$$

The first term in the right hand side is a total time derivative which, as we did in section 1.6, can be eliminated by integrating over some interval $[t_1, t_2]$ assuming that the system configuration is known at t_1 and t_2, so that

$$\delta q_i(t_1) = \delta q_i(t_2) = 0 \tag{2.22}$$

The second term at the right hand side of (2.21) is rewritten

$$\sum_{i=1}^{M} \lambda_i \frac{d}{dt} \delta q_i = \sum_{i=1}^{M} \lambda_i \delta i_i = \delta W_m^* \tag{2.23}$$

after permuting d/dt and δ, and using (2.17). Finally, integrating (2.19) between two fixed configurations at t_1 and t_2 and combining Equ.(2.20)-(2.23), one gets

$$\text{V.I.} = \int_{t_1}^{t_2} [\delta W_m^* - \delta W_e + \sum_{i=1}^{n_e} E_k \delta q_k] \, dt \tag{2.24}$$

$$= \int_{t_1}^{t_2} [\delta (W_m^* - W_e) + \sum_{i=1}^{n_e} E_k \delta q_k] \, dt \tag{2.25}$$

The actual path is that which cancels the variational indicator (2.25) with respect to all admissible charge variations δq_i of the path between two instants t_1 and t_2, and such that $\delta q_i(t_1) = \delta q_i(t_2) = 0$.

W_m^* is the magnetic coenergy function of the network, that is the sum of all magnetic coenergies of individual inductors in the network, expressed in terms of the currents i_j; W_e is the electrical energy function of the network, that is the sum of all electrical energies of individual capacitors in the network, expressed in terms of q_j. To be admissible, the current and charges must satisfy Kirchhoff's current law and must satisfy $i_j = dq_j/dt$. W_m^* - W_e is the Lagrangian of the network. There is a complete analogy between (2.25) and (1.26); $\sum E_k \delta q_k$ corresponds to the virtual work of the nonconservative elements, denoted δW_{nc} in (1.26).

2.4.2 Hamilton's principle, flux linkage formulation

We now examine the dual formulation, where the generalized variables are flux linkages λ_k and voltages e_k. Admissible variations must satisfy Kirchhoff's voltage rule, and the flux linkage and voltage variables must satisfy $e_k = d\lambda_k/dt$.

By analogy with (2.19), the virtual work expression reads

$$\sum_{k=1}^{N}(i_k - \frac{dq_k}{dt})\delta\lambda_k = 0 \tag{2.26}$$

where N is the number of circuit elements. The first contribution to this sum can be separated into its conservative and non-conservative parts. From (2.12), one notes that the conservative part corresponds to the magnetic energy W_m of all the conservative elements in the network.

$$\sum_{k=1}^{N} i_k\delta\lambda_k = -\delta W_m + \sum_{k=1}^{n_e} I_k\delta\lambda_k \tag{2.27}$$

I_k are the generalized currents corresponding to the nonconservative elements in the network, and conjugate to the flux linkage coordinates λ_k, n_e is the number of independent flux linkage coordinates. Proceeding as in the previous section, the second contribution to (2.26) can be rewritten

$$-\sum_{k=1}^{N}\frac{dq_k}{dt}\delta\lambda_k = -\sum_{k=1}^{N}\frac{d}{dt}(q_k\delta\lambda_k) + \sum_{k=1}^{N} q_k\frac{d}{dt}(\delta\lambda_k) \tag{2.28}$$

As before, the first term in the right hand side, which is a total time derivative, will vanish after integrating between given system configurations at t_1 and t_2, so that

$$\delta\lambda_k(t_1) = \delta\lambda_k(t_2) = 0 \tag{2.29}$$

The second term in the right hand side of (2.28) is rewritten

$$\sum_{k=1}^{N} q_k\frac{d}{dt}(\delta\lambda_k) = \sum_{k=1}^{N} q_k\delta(\frac{d\lambda_k}{dt}) = \sum_{k=1}^{N} q_k\delta e_k = \delta W_e^* \tag{2.30}$$

where we have used (2.8) and the commutability of δ and $(\dot{})$. Finally, upon integrating Equ.(2.26) between t_1 and t_2, assuming that the configuration is fixed at t_1 and t_2, and combining with (2.27)-(2.30), one gets

$$\text{V.I.} = \int_{t_1}^{t_2}[\delta W_e^* - \delta W_m + \sum_{k=1}^{n_e} I_k\delta\lambda_k]\,dt \tag{2.31}$$

$$\text{V.I.} = \int_{t_1}^{t_2}[\delta(W_e^* - W_m) + \sum_{k=1}^{n_e} I_k\delta\lambda_k]\,dt \tag{2.32}$$

The actual path is that which cancels the variational indicator (2.32) with respect to all admissible flux linkage variations $\delta\lambda_k$ of the path between two instants t_1 and t_2, and such that $\delta\lambda_k(t_1) = \delta\lambda_k(t_2) = 0$.

W_e^* is the electrical coenergy function of the network, that is the sum of all electrical coenergies of individual capacitors in the network, expressed in terms of the voltage e_k; W_m is the magnetic energy function of the network, that is the sum of all magnetic energies of individual inductors in the network, expressed in terms of the independent flux linkage variables λ_k. To be admissible, the voltage and flux linkages must satisfy Kirchhoff's voltage rule and must satisfy $e_k = d\lambda_k/dt$. $W_e^* - W_m$ is the Lagrangian of the network in this formulation.

2.4.3 Discussion

Hamilton's principle for mechanical systems and for electrical networks takes remarkably similar forms. The Lagrangian consists of the coenergy, which depends on the time derivatives of the generalized coordinates, minus the energy, which depends on the generalized coordinates, but not on their time derivatives.

For mechanical systems,

$$L = T^*(\dot{q_i}) - V(q_i) \qquad q_i \equiv \text{generalized displacements}$$

For electrical networks,
(a) charge formulation

$$L = W_m^*(i_k) - W_e(q_k) \qquad q_k = \text{electric charge}, \quad i_k = \dot{q_k}$$

(b) flux linkage formulation

$$L = W_e^*(e_k) - W_m(\lambda_k) \qquad \lambda_k = \text{flux linkage}, \quad e_k = \dot{\lambda_k}$$

The virtual work of the nonconservative elements reads, respectively

$$\delta W_{nc} = Q_i \delta q_i \qquad Q_i = \text{generalized force}$$

$$\delta W_{nc} = E_k \delta q_k \qquad E_k = \text{generalized voltage}$$

$$\delta W_{nc} = I_k \delta \lambda_k \qquad I_k = \text{generalized current}$$

These work expressions are positive if the element supplies energy to the network under the variation, and negative if the element absorbs energy. With the positive directions assumed in Fig.2.4, a resistor R is such that

$$e = -Ri$$

The virtual work expression in the charge formulation is

$$e\,\delta q = -Ri\,\delta q = -R\dot{q}\,\delta q$$

and, in the flux linkage formulation,

$$i\,\delta\lambda = -\frac{e}{R}\delta\lambda = -\frac{1}{R}\dot{\lambda}\,\delta\lambda$$

An ideal voltage source $E(t)$ will contribute

$$e\,\delta q = E(t)\delta q$$

in the charge formulation, but there is no contribution in the flux linkage formulation, because, the time history of the voltage being prescribed at any time, it cannot be altered in any admissible variation of voltage or flux linkage. Although they do not enter the virtual work expression, the voltage sources do enter the flux linkage formulation of Hamilton's principle as part of the admissibility requirements on voltages and flux linkages.

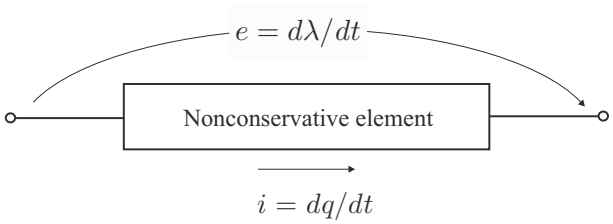

Fig. 2.4. The virtual work increment delivered to the network by the element is $e\,\delta q$ or $i\,\delta\lambda$.

The same considerations apply to an ideal current source $I(t)$ which contributes for $I(t)\delta\lambda$ to the virtual work expression in the flux linkage formulation, but do not contribute in the charge formulation because no variation of current is allowed where it is prescribed. In this latter case, the current sources enter the charge formulation of Hamilton's principle as part of the admissibility requirements.

2.5 Lagrange's equations

Consider a discrete lumped parameter network. Because of the similarity between the formulation of Hamilton's principle for electrical networks and mechanical systems, one can skip the analytical derivation of Lagrange's equations from Hamilton's principle, which follows almost identically that of section 1.7. The most convenient way to satisfy the admissibility conditions on the virtual variations is to select a complete set of independent generalized coordinates. In this way, the admissibility requirements are automatically satisfied.

2.5.1 Lagrange's equations, charge formulation

In the charge formulation of Lagrange's equations, n generalized charge coordinates, q_k, are selected such that their time derivatives, $\dot{q_k}$, constitute independent loop currents in the network. The Lagrangian is

$$L(\dot{q_k}, q_k) = W_m^*(\dot{q_k}) - W_e(q_k) \tag{2.33}$$

where $W_m^*(\dot{q_k})$ is the magnetic coenergy of the network, expressed in terms of the independent loop currents; it is equal to the sum of magnetic coenergies of individual inductors in the network. $W_e(q_k)$ is the electrical energy of the network, expressed in terms of the independent charge variables; it is equal to the sum of electrical energies of individual capacitors in the network. The virtual work of the nonconservative elements is expressed in terms of the independent generalized coordinates according to the work equality

$$\sum_k E_k \delta q_k = \sum_i \epsilon_i \delta q_i$$

where the sum in the left hand side extends to the independent generalized coordinates and that in the right hand side extends to all the nonconservative elements. The resulting Lagrange's equations are

$$\frac{d}{dt}\left(\frac{\partial L}{\partial \dot{q_k}}\right) - \frac{\partial L}{\partial q_k} = E_k \qquad\qquad k = 1, ..., n \tag{2.34}$$

where E_k is the generalized voltage associated with the generalized charge coordinate q_k.

2.5.2 Lagrange's equations, flux linkage formulation

The flux linkage formulation is dual of the charge formulation; n independent flux linkage coordinates λ_k are selected, which automatically satisfy Kirchhoff's voltage rule. The Lagrangian is

$$L(\dot{\lambda_k}, \lambda_k) = W_e^*(\dot{\lambda_k}) - W_m(\lambda_k) \tag{2.35}$$

where $W_e^*(\dot{\lambda_k})$ is the electrical coenergy of the network expressed in terms of the independent voltages $\dot{\lambda_k}$; it is equal to the sum of the electrical coenergies of all capacitors in the network, expressed in terms of voltage variables. $W_m(\lambda_k)$ is the magnetic energy of the network, expressed in terms of the independent flux linkage variables; it is equal to the sum of magnetic energies of all inductors in the network. The virtual work of the nonconservative elements is expressed in terms of the generalized flux linkage coordinates thanks to the work equality

$$\sum_k I_k \, \delta\lambda_k = \sum_i I_i \, \delta\lambda_i$$

where the sum in the left side extends to the independent flux-linkage generalized coordinates and that in the right hand side extends to all nonconservative elements. The resulting Lagrange's equations are

$$\frac{d}{dt}\left(\frac{\partial L}{\partial \dot{\lambda_k}}\right) - \frac{\partial L}{\partial \lambda_k} = I_k \qquad\qquad k = 1, ..., n \tag{2.36}$$

where I_k is the generalized current associated with the generalized flux linkage λ_k.

2.5.3 Example 1

Consider the electrical network of Fig.2.5. We shall write the dynamic equations of the network using successively the flux linkage formulation and the charge formulation.

Flux linkage formulation

We select flux linkage coordinates λ_i at all ungrounded nodes; this leads to 3 independent coordinates λ_1, λ_2, λ_3. Since the voltage drops across the capacitors C_1 and C_2 are respectively $\dot{\lambda_2} - \dot{\lambda_1}$ and $\dot{\lambda_3} - \dot{\lambda_2}$. The electrical coenergy reads

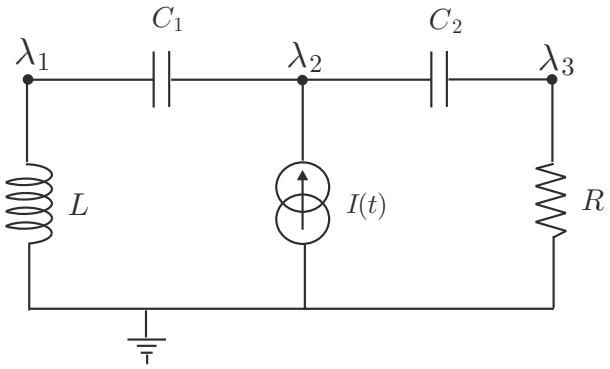

Fig. 2.5. Electrical network, flux linkage formulation.

$$W_e^*(\dot{\lambda_k}) = \frac{1}{2}C_1(\dot{\lambda_2} - \dot{\lambda_1})^2 + \frac{1}{2}C_2(\dot{\lambda_3} - \dot{\lambda_2})^2$$

The flux linkage across the inductor is λ_1 (the grounded node is taken as reference, $\lambda = 0$) and the magnetic energy is

$$W_m(\lambda_k) = \frac{\lambda_1^2}{2L}$$

The Lagrangian is

$$L = W_e^* - W_m = \frac{1}{2}C_1(\dot{\lambda_2} - \dot{\lambda_1})^2 + \frac{1}{2}C_2(\dot{\lambda_3} - \dot{\lambda_2})^2 - \frac{\lambda_1^2}{2L}$$

On the other hand, the virtual work of the nonconservative elements is

$$\delta W_{nc} = I\ \delta\lambda_2 - \frac{\dot{\lambda_3}}{R}\ \delta\lambda_3$$

The first contribution is that of the ideal current generator, and the second is that of the resistor R (the current in the resistor is $\dot{\lambda_3}/R$, and the virtual work is negative because it is a dissipative element). The generalized currents in the Lagrange's equations are respectively $I_1 = 0$, $I_2 = I$ and $I_3 = -\dot{\lambda_3}/R$.

Lagrange's equations (2.36) read

$$\lambda_1 : \qquad C_1(\ddot{\lambda_1} - \ddot{\lambda_2}) + \frac{\lambda_1}{L} = 0$$

$$\lambda_2 : \qquad -C_1\ddot{\lambda_1} + (C_1 + C_2)\ddot{\lambda_2} - C_2\ddot{\lambda_3} = I(t)$$

$$\lambda_3 : \qquad C_2(\ddot{\lambda}_3 - \ddot{\lambda}_2) = -\frac{\dot{\lambda}_3}{R}$$

This system of three ordinary differential equations, in the three variables λ_1, λ_2, λ_3, governs the dynamics of the network.

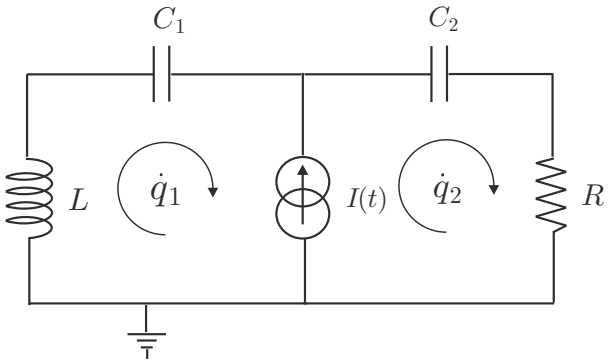

Fig. 2.6. Electrical network, charge formulation.

Charge formulation

We reexamine the problem with a charge formulation. Accordingly, a set of loops is defined (two in this case), and charge variables q_1 and q_2 are associated with every loop, so that $\dot{q_1}$ and $\dot{q_2}$ are the loop currents (the positive direction clockwise adopted in Fig.2.6 is arbitrary). In this case, the two currents $\dot{q_1}$ and $\dot{q_2}$ are not independent, because of the current generator; they must satisfy the admissibility condition

$$\dot{q_2} = \dot{q_1} + I(t) = \dot{q_1} + \dot{q_0}$$

where $I(t) = \dot{q_0}$. Integrating, one gets

$$q_2 = q_1 + q_0$$

We note that q_0 is not a variable, but rather an input to the system (q_0 is the electric charge injected by the current source). It follows that the virtual charge variations are subjected to $\delta q_2 = \delta q_1$, and that this formulation has a single generalized coordinate q_1. The Lagrangian reads

$$L = W_m^*(\dot{q}_1) - W_e(q_1) = \frac{1}{2}L\dot{q}_1^2 - \frac{1}{2C_1}q_1^2 - \frac{1}{2C_2}(q_1 + q_0)^2$$

and the virtual work of the nonconservative elements is

$$\delta W_{nc} = -R\dot{q}_2 \ \delta q_2 = -R(\dot{q}_1 + \dot{q}_0)\delta q_1$$

There is no contribution from the current source in this formulation. Lagrange's equations relative to q_1 is

$$L\ddot{q}_1 + \frac{1}{C_1}q_1 + \frac{1}{C_2}(q_1 + q_0) = -R(\dot{q}_1 + \dot{q}_0)$$

or

$$L\ddot{q}_1 + R\dot{q}_1 + (\frac{C_1 + C_2}{C_1 C_2})q_1 = -R\dot{q}_0 - \frac{q_0}{C_2}$$

with $\dot{q}_0 = I(t)$. Comparing with the flux linkage formulation, we note that, in this case, the charge formulation is more compact and involves only one generalized variable instead of three.

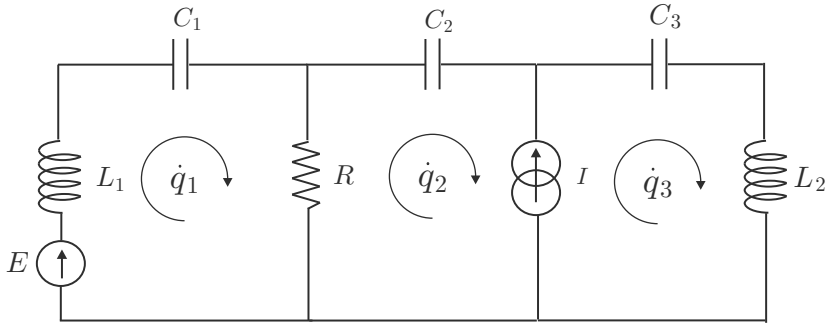

Fig. 2.7. Electrical network, charge formulation.

2.5.4 Example 2

Write the dynamic equation of the electrical network of Fig.2.7 using successively the charge formulation and the flux linkage formulation. This example mixes ideal voltage and current sources, and it will be useful to compare the way they contribute to virtual work of the nonconservative elements. We will restrict ourselves to writing the Lagrangian and the virtual work of the nonconservative elements, since Lagrange's equations can easily be derived from them.

Charge formulation

The current loops are defined as indicated in Fig.2.7. Because of the presence of the current source, the current $\dot{q}_2$ and $\dot{q}_3$ are not independent; they must satisfy the admissibility condition

$$\dot{q}_3 = \dot{q}_2 + I = \dot{q}_2 + \dot{q}_0$$

where $I(t) = \dot{q}_0$. It follows that

$$q_3 = q_2 + q_0$$

and

$$\delta q_3 = \delta q_2$$

since q_0 is not subject to virtual variations. The contributions of all the conservative elements to the magnetic coenergy and electrical energy are as follows

$$W_m^* = \frac{1}{2} L_1 \dot{q}_1^2 + \frac{1}{2} L_2 (\dot{q}_2 + \dot{q}_0)^2$$

$$W_e = \frac{q_1^2}{2C_1} + \frac{q_2^2}{2C_2} + \frac{(q_2 + q_0)^2}{2C_3}$$

and

$$L = W_m^* - W_e$$

The virtual work of the nonconservative elements includes in this case the resistor and voltage source

$$\delta W_{nc} = -R(\dot{q}_1 - \dot{q}_2)(\delta q_1 - \delta q_2) + E\ \delta q_1$$

Note that the current source does not contribute to δW_{nc}, but it appears in both W_m^* and W_e, from $\dot{q}_0$ and q_0 respectively.

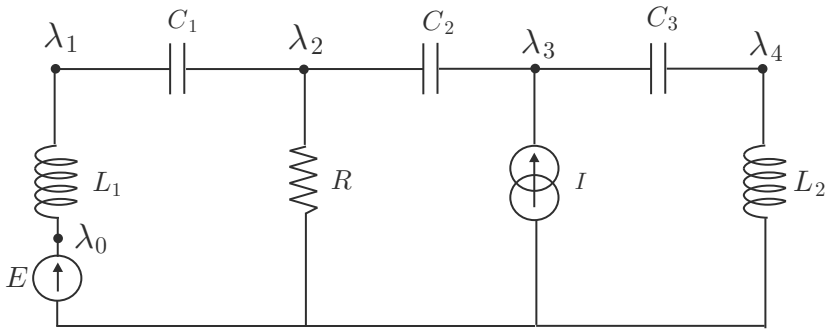

Fig. 2.8. Electrical network, flux linkage formulation.

Flux linkage formulation

A flux linkage coordinate λ_i is selected at each ungrounded node such that $e_i = \dot{\lambda}_i$. The contributions of all the conservative elements to the electrical coenergy and the magnetic energy are respectively:

$$W_e^* = \frac{1}{2}C_1(\dot{\lambda}_2 - \dot{\lambda}_1)^2 + \frac{1}{2}C_2(\dot{\lambda}_3 - \dot{\lambda}_2)^2 + \frac{1}{2}C_3(\dot{\lambda}_4 - \dot{\lambda}_3)^2$$

$$W_m = \frac{(\lambda_1 - \lambda_0)^2}{2L_1} + \frac{\lambda_4^2}{2L_2}$$

and $L = W_e^* - W_m$. The virtual work of the nonconservative elements includes in this case the resistor and the current source.

$$\delta W_{nc} = -\frac{\dot{\lambda}_2}{R}\ \delta\lambda_2 + I\ \delta\lambda_3$$

There is no contribution from the voltage source, because the flux linkage λ_0 is not subject to virtual variations. Thus, the voltage source contributes to the dynamics only through the magnetic energy W_m.

2.6 References

CRANDALL, S.H., KARNOPP, D.C., KURTZ, E.F, Jr., PRIDMORE-BROWN, D.C., *Dynamics of Mechanical and Electromechanical Systems*, McGraw-Hill, N-Y, 1968.
WILLIAMS, J.H., Jr., *Fundamentals of Applied Dynamics*, Wiley, 1996.
WOODSON, H.H., MELCHER, J.R, *Electromechanical Dynamics, Part I: Discrete Systems*, Wiley, 1968.

3

Electromechanical systems

3.1 Introduction

The two preceding chapters have addressed separately the dynamics of mechanical systems and the dynamics of the electrical network. In this chapter, we consider the dynamics of composite systems formed by interconnecting mechanical and electrical variables. The central element in this interconnection is the conversion of mechanical energy into electrical energy, and vice versa, which takes place in electromechanical transducers. Electromechanical transducers are pervasive in modern life, they include microphones, loudspeakers, electrical motors, magnetic suspensions, capacitive accelerometers, and also microelectromechanical systems (MEMS). Piezoelectric transducers will be treated in a separate chapter.

This chapter starts with a review of the constitutive equations of the most frequent lossless lumped parameter electromechanical transducers. It is followed by the statement of Hamilton's principle for electromechanical systems, the Lagrange equations, and a set of examples where the dynamic equations governing a few classical electromechanical systems are established.

3.2 Constitutive relations for transducers

A conservative transducer is a transducer which conserves energy, it is also called *lossless*. There are two types of transducers, those which can *store* energy and those which can only *transfer* energy from one form to the other, without being able to store it. In a transducer which can store energy, the energy can be stored in one form (either mechanically or electrically) and recovered at a later time in another form. On the contrary,

a transfer element transforms one form of energy into the other form, but the instantaneous power at the input is always equal to the instantaneous power at the output. The theory of lumped parameter transducers is based on the quasi-static theory of electromagnetism, which assumes that the physical dimension of the device, l, is much smaller than the electromagnetic wavelength ($l/\lambda \ll 1$). Under this assumption, the field that produces forces in the transducer is either electrical or magnetic, but not both; this allows us to separate the analysis of electrical forces in capacitive transducers, and magnetic forces in inductive transducers.

Note that the electrostatic and electromagnetic forces do not scale down in the same way as the size of the transducer shrinks : the electrostatic forces tend to scale down as l^{-2} and the electrostatic energy as l^{-3}, while the electromagnetic forces scale down as l^{-4} and the electromagnetic energy as l^{-5}. This is why electrostatic transducers are much more used in MEMS.

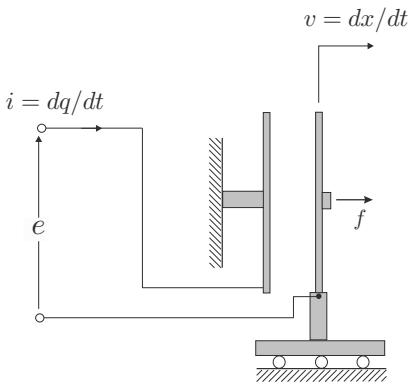

Fig. 3.1. Movable-plate capacitor.

3.2.1 Movable-plate capacitor

A movable plate capacitor is a conservative energy storing transducer which allows electrical energy to be transformed into mechanical energy and vice versa (Fig.3.1). The charge on the capacitor is q and the voltage across the plates is e; the displacement of the movable plate is x and the external force required to hold the movable plate in equilibrium against the electrostatic attraction force is f. The electromechanical transducer is assumed to be perfect, meaning that the electrical side is a pure capac-

itance, and the mechanical construction is massless and without stiffness or damping.

If one takes the movable plate displacement x and the electrical charge q as independent variables, the constitutive relations for a movable-plate capacitor can be given in the form of equations for the voltage and force in terms of x and q:

$$\begin{aligned} e &= e(x, q) \\ f &= f(x, q) \end{aligned} \tag{3.1}$$

The exact form of these equations can be determined either from the electrostatic field theory, or they can be determined experimentally; they must be such that when $q = 0$, there is no electric field and the force f must be zero for all x:

$$f(x, 0) = 0 \tag{3.2}$$

The total power delivered to the capacitor is the sum of the electric power, ei, and the mechanical power, fv. The net work on the capacitor over dt is therefore

$$dW = ei\,dt + fv\,dt = e\,dq + f\,dx \tag{3.3}$$

For a conservative element, this work is converted into stored electrical energy, dW_e, and the total electrical energy $W_e(x, q)$ (it is called *electrical*, although it includes both electrical and mechanical work) is obtained by integrating (3.3) from the reference state to (x, q). Once the electrical energy function $W_e(x, q)$ is known, the constitutive equations can be recovered by differentiation :

$$\frac{\partial W_e}{\partial x} = f \qquad\qquad \frac{\partial W_e}{\partial q} = e \tag{3.4}$$

As in the previous chapter, the complementary state function called *electrical coenergy function* is defined by the Legendre transformation

$$W_e^*(x, e) = eq - W_e(x, q) \tag{3.5}$$

The total differential of the coenergy is

$$dW_e^* = q\,de + e\,dq - \frac{\partial W_e}{\partial x}dx - \frac{\partial W_e}{\partial q}dq$$

and it follows from (3.4) that

$$q = \frac{\partial W_e^*}{\partial e} \qquad\qquad f = -\frac{\partial W_e^*}{\partial x} \tag{3.6}$$

Assuming that the capacitor is electrically linear, one can find the explicit form of the state functions $W_e(x, q)$ and $W_e^*(x, e)$. In this case,

$$e = \frac{q}{C(x)} \tag{3.7}$$

where $C(x)$ is the capacitance corresponding to the position x of the mov-

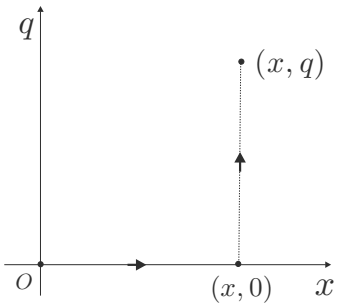

Fig. 3.2. Movable-plate capacitor: integration path for the electrical energy.

able plate (in the simplest case of two flat plates with a constant distance x, neglecting the edge effect, $C(x) = \varepsilon A/x$, where ε is the dielectric constant of the material between the plates and A is the area of the plate). The electrical energy function $W_e(q, x)$ can be obtained by integrating (3.3) from the reference state to (q, x). For a conservative system, this integral is independent of the path followed. If one takes a path consisting of two straight lines $(0, 0) \to (x, 0)$ and $(x, 0) \to (x, q)$ as indicated in Fig. 3.2, we can use the fact that $f = 0$ and $e = 0$ over the first segment, and that $dx = 0$ over the second one, leading to

$$W_e(x, q) = \int_0^q e\, dq = \int_0^q \frac{q}{C(x)} dq = \frac{q^2}{2C(x)} \tag{3.8}$$

and, from the Legendre transformation (3.5) and the constitutive equation (3.7),

$$W_e^*(x, e) = \frac{1}{2} C(x) e^2 \tag{3.9}$$

The constitutive equations of the linear movable plate capacitor follow from (3.4) and (3.6),

$$f = \frac{\partial W_e}{\partial x} = -\frac{q^2}{2C^2}C'(x) \qquad e = \frac{\partial W_e}{\partial q} = \frac{q}{C(x)} \tag{3.10}$$

and

$$f = -\frac{\partial W_e^*}{\partial x} = -\frac{e^2}{2}C'(x) \qquad q = \frac{\partial W_e^*}{\partial e} = Ce \tag{3.11}$$

where $C'(x) = dC(x)/dx$. Note that the state functions (3.8) and (3.9) have been established without knowing the form of $f(x, q)$ in (3.1), using the fact that the system is conservative. Once the explicit forms for W_e and W_e^* have been established, the mechanical force necessary to balance the electrostatic force in the capacitor follows from (3.10) and (3.11).

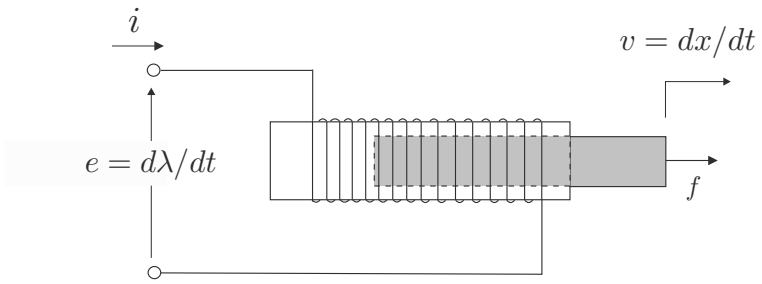

Fig. 3.3. Movable-core inductor.

3.2.2 Movable-core inductor

An ideal movable-core inductor is another conservative energy-storing transducer; it is the magnetic counterpart of the movable-plate capacitor. We use the notation of Fig.3.3, where λ is the flux linkage of the coil, e the voltage at the input, i the input current, x the displacement of the iron core and f the external force required to hold the core in equilibrium against the magnetic attraction. Proceeding as with the movable-plate capacitor, we assume that the electrical side is a perfect inductor, without hysteresis, and that the mechanical construction is massless and without friction. Taking the flux linkage λ and the displacement x as independent variables, we can write the constitutive equations in the form of equations for i and f in terms of λ and x:

$$\begin{aligned} i &= i(x, \lambda) \\ f &= f(x, \lambda) \end{aligned} \tag{3.12}$$

The exact form of the constitutive equations can be determined either from electromagnetic field theory, or from experiments; without hysteresis, (3.12) are assumed to be single-valued functions. Their form must be such that, when $\lambda = 0$, there is no magnetic field and no magnetic attraction. Therefore, the force f balancing the magnetic attraction must be 0 for all x:

$$f(x, 0) = 0 \tag{3.13}$$

The total power delivered to the solenoid is the sum of all the electrical power, ei, and the mechanical power, fv. The net work on the solenoid over dt is therefore

$$dW = ei\,dt + fv\,dt = i\,d\lambda + f\,dx \tag{3.14}$$

For a conservative transducer, this work is converted into stored magnetic energy of the solenoid, dW_m. If the stored magnetic energy is expressed in terms of the independent variables, $W_m(x, \lambda)$,

$$dW_m = \frac{\partial W_m}{\partial \lambda} d\lambda + \frac{\partial W_m}{\partial x} dx \tag{3.15}$$

and, by comparison with (3.14), one recovers the constitutive equations

$$i = \frac{\partial W_m}{\partial \lambda} \qquad\qquad f = \frac{\partial W_m}{\partial x} \tag{3.16}$$

If the system is conservative, the total stored magnetic energy is obtained by integrating (3.14) along any path from the reference state to (x, λ).

As for the movable plate capacitor, the *magnetic coenergy function* is defined by the Legendre transformation

$$W_m^*(x, i) = i\lambda - W_m(x, \lambda) \tag{3.17}$$

Upon taking the total differential of the coenergy and taking into account (3.16), one finds an alternative form of the constitutive equations

$$\lambda = \frac{\partial W_m^*}{\partial i} \qquad\qquad f = -\frac{\partial W_m^*}{\partial x} \tag{3.18}$$

When the constitutive relation between the flux linkage and the current is linear,

$$\lambda = L(x)i \tag{3.19}$$

where $L(x)$ is the inductance of the coil when the core is in the position x. In this case, one can evaluate the magnetic stored energy $W_m(x, \lambda)$ explicitly by integrating (3.14) from the reference state to (x, λ); for a conservative system, this integral is independent of the path, and one can take the path consisting of two straight lines $(0, 0) \to (x, 0)$ and $(x, 0) \to (x, \lambda)$ (Fig. 3.4). Using the fact that $f = 0$, if $\lambda = 0$, one gets

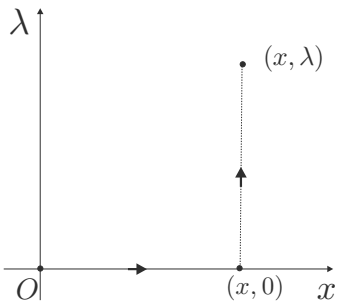

Fig. 3.4. Movable-core inductor: integration path for the magnetic energy.

$$W_m(x, \lambda) = \int_0^\lambda i \, d\lambda = \int_0^\lambda \frac{\lambda}{L(x)} d\lambda = \frac{\lambda^2}{2L(x)} \tag{3.20}$$

The magnetic coenergy is obtained from (3.17), using (3.19) and (3.20):

$$W_m^*(x, i) = \frac{1}{2} L(x) i^2 \tag{3.21}$$

The constitutive relations can be recovered from (3.16) and (3.18):

$$f = \frac{\partial W_m}{\partial x} = -\frac{\lambda^2}{2L^2} L'(x) \qquad i = \frac{\partial W_m}{\partial \lambda} = \frac{\lambda}{L(x)} \tag{3.22}$$

$$f = -\frac{\partial W_m^*}{\partial x} = -\frac{i^2}{2} L'(x) \qquad \lambda = \frac{\partial W_m^*}{\partial i} = L(x) i \tag{3.23}$$

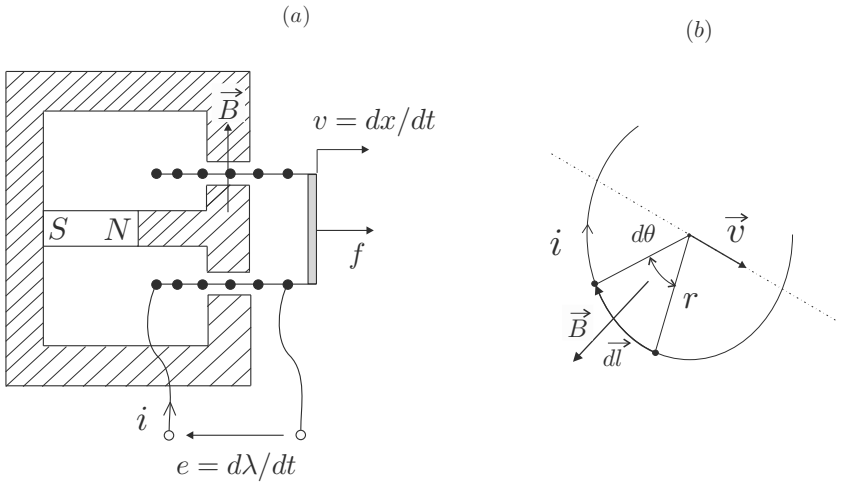

Fig. 3.5. Moving-coil transducer.

3.2.3 Moving-coil transducer

A moving-coil transducer is an energy transformer which converts electrical power into mechanical power and vice versa. The system consists of a permanent magnet (Fig.3.5) which produces a uniform magnetic flux density B normal to the gap, and a coil which is free to move axially within the gap. Let v be the velocity of the coil, f the external force acting to maintain the coil in equilibrium against the electromagnetic forces, e the voltage difference across the coil and i the current into the coil. In this ideal transducer, we neglect the electrical resistance and the self inductance of the coil, as well as its mass and damping (if necessary, these can be handled by adding R and L to the electrical circuit of the coil, or a mass and damper to its mechanical model). The *voice coil* actuator is one of the most popular actuators in mechatronics (e.g. it is used in electromagnetic loudspeakers), but we find it also as a sensor in, for example, geophones.

The constitutive equations of the moving-coil transducer follow from Faraday's law and the Lorentz force law. Faraday's law states that the voltage increment de over some elementary length dl in the direction of the current flow, induced by the motion of the coil is

$$de = \vec{v} \times \vec{B}.\vec{dl} \tag{3.24}$$

On the other hand, a charge particle moving in an electromagnetic field (electric field $\vec{E}$ and magnetic flux density $\vec{B}$) is subjected to the Lorentz force

$$\vec{f} = q(\vec{E} + \vec{v} \times \vec{B}) \tag{3.25}$$

In the macroscopic world, this force is dominated by its magnetic contribution, and the electrostatic contribution can be omitted. If we consider a current formed by a very large number of charged particles (the electrons) moving along the conductor, the total force of the field acting on an elementary length dl of the conductor is

$$\vec{df} = i\vec{dl} \times \vec{B} \tag{3.26}$$

Applying (3.24) to an elementary length $dl = rd\theta$ of one turn of the coil [$\vec{B}$, $\vec{v}$ and $\vec{dl}$ are mutually orthogonal, Fig.3.5.(b)], one finds that the voltage increment in the direction of the current flow is

$$de = \vec{v} \times \vec{B}.\vec{dl} = -vBrd\theta$$

Integrating over θ, assuming that B is uniform in the gap, the voltage drop in the coil, in the direction of the current, is

$$e = 2\pi nrBv = Tv \tag{3.27}$$

where

$$T = 2\pi nrB \tag{3.28}$$

is the *transducer constant*, equal to the product of the length of the coil exposed to the magnetic flux, $2\pi nr$, and the magnetic flux density B. On the other hand, the Lorentz force of the magnetic field acting on the element $dl = rd\theta$ of one turn of the coil with a current i follows from (3.26).

$$df = ird\theta B \tag{3.29}$$

The force f defined in Fig.3.5(a) is the external force required to *balance* the total force of the magnetic field on n turns of the conductor; integrating (3.29) over the length of the conductor exposed to the magnetic flux density, one finds

$$f = -i\,2\pi nrB = -Ti \tag{3.30}$$

where T is again the transducer constant (3.28). Equ.(3.27) and (3.30) are the constitutive equations of the movable-coil transducer (Fig.3.6).

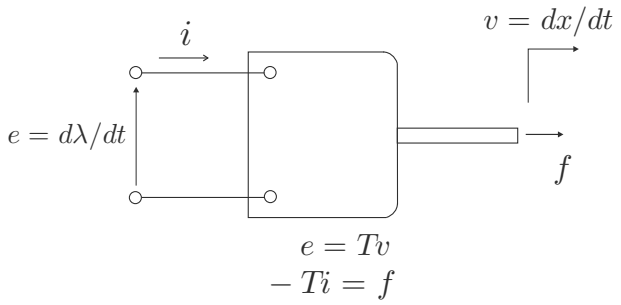

Fig. 3.6. Symbolic representation of a moving-coil transducer.

Notice that the transducer constant T appearing in Faraday's law (3.27), expressed in $volt.sec/m$, is the same as that appearing in the Lorentz force (3.30), expressed in N/Amp.

The total power delivered to the moving-coil transducer is equal to the sum of the electric power, ei, and the mechanical power, fv. Combining with (3.27) and (3.30), one gets

$$ei + fv = Tvi - Tiv = 0 \tag{3.31}$$

Thus, at any time, there is an equilibrium between the electrical power absorbed by the device and the mechanical power delivered (and vice versa). The moving-coil transducer cannot store energy, and behaves as a perfect electromechanical converter. In practice, however, the transfer is never perfect due to eddy currents, flux leakage and magnetic hysteresis, leading to different values of T in (3.27) and (3.30).

Proceeding as for the movable core inductor, it follows from (3.31) that the magnetic energy W_m remains constant, equal to its reference value that can be taken as $W_m = 0$. The constitutive equation (3.27) can be written equivalently in terms of flux linkage

$$\lambda = T(x - x_0) \tag{3.32}$$

where x_0 is an arbitrary reference state. This allows us to write the coenergy function (3.17)

$$W_m^*(x, i) = \lambda i - W_m(x, \lambda) = Ti(x - x_0) \tag{3.33}$$

Using (3.18), we recover the constitutive equations

$$f = -\frac{\partial W_m^*}{\partial x} = -Ti \qquad\qquad \lambda = \frac{\partial W_m^*}{\partial i} = T(x - x_0) \tag{3.34}$$

In this section, the constitutive equations for ideal transducers have been discussed. The models of real transducers usually involve additional elements on the electrical side as well as on the mechanical side of the transducer, to represent the electrical resistance, capacitance and inductance, and the mechanical inertia, stiffness and damping; we will see a few examples shortly. Before that, we shall examine how the dynamic equations of electromechanical systems can be derived from a general form of Hamilton's principle and the Lagrange equations.

3.3 Hamilton's principle

Hamilton's principle has been examined for mechanical systems and electrical networks in the previous chapters. A single formulation based on virtual displacements compatible with the kinematical constraints has been examined for mechanical systems, while two dual approaches have been considered for electrical networks; the charge formulation is based on admissible charge variations compatible with Kirchhoff's current rule, and the flux linkage formulation is based on admissible flux linkage variations compatible with Kirchhoff's voltage rule. In all cases, the Lagrangian was defined as the difference between the coenergy function (which depends on the time derivatives of the generalized coordinates) and the energy function (which depends on the generalized coordinates but not on their time derivatives), see section 2.4.3. The actual path is that which cancels the variational indicator with respect to all admissible variations of the generalized coordinates, between two instants at which the configuration is fixed.

For electromechanical systems, a variational indicator is now constructed as the sum of the mechanical indicator (1.26) and an electrical indicator, either (2.24) or (2.31), depending on the formulation. The actual path is that which cancels the variational indicator with respect to all admissible variations of the generalized coordinates, both mechanical and electrical, compatible with the kinematics and compatible with the electrical requirements (depending on the formulation). As before, the system configuration is fixed at t_1 and t_2.

3.3.1 Displacement and charge formulation

In this case, the admissibility requirements include the kinematical constraints on the virtual displacements δx_i and velocities, and Kirchhoff's

current rule on the virtual variations of charges δq_i and currents. The variational indicator is

$$\text{V.I.} = \int_{t_1}^{t_2} \left[\delta(T^* + W_m^* - V - W_e) + \sum f_i \delta x_i + \sum e_j \delta q_j \right] dt \qquad (3.35)$$

The actual path is that which cancels the variational indicator (3.35) with respect to all admissible variations δx_i and δq_i of the path between two instants t_1 and t_2 at which $\delta x_i(t_1) = \delta x_i(t_2) = \delta q_i(t_1) = \delta q_i(t_2) = 0$. In (3.35) the kinetic coenergy T^* and the magnetic coenergy W_m^* have been grouped; they depend on the time derivative of the generalized coordinates, respectively $\dot{x}_i$ and $i_k = \dot{q}_k$. On the contrary, the potential energy V and the electrical energy W_e do not depend on the time derivative of the generalized variables, but only on x_i and q_k. The Lagrangian is equal to the total coenergy minus the total energy.

$$L = T^* + W_m^* - V - W_e \qquad (3.36)$$

3.3.2 Displacement and flux linkage formulation

In this case, the admissibility requirements on the mechanical variables are unchanged: the virtual displacements δx_i must be compatible with the kinematics. The admissible flux linkage variations $\delta \lambda_i$ must be compatible with Kirchhoff's voltage rule. The variational indicator is

$$\text{V.I.} = \int_{t_1}^{t_2} \left[\delta(T^* + W_e^* - V - W_m) + \sum f_i \delta x_i + \sum i_j \delta \lambda_j \right] dt \qquad (3.37)$$

The actual path is that which cancels the variational indicator (3.37) with respect to all admissible variations δx_i and $\delta \lambda_i$ of the path between t_1 and t_2 at which $\delta x_i(t_1) = \delta x_i(t_2) = \delta \lambda_i(t_1) = \delta \lambda_i(t_2) = 0$. The Lagrangian is now

$$L = T^* + W_e^* - V - W_m \qquad (3.38)$$

with the kinetic coenergy T^* and the electrical coenergy W_e^* depending on the time derivative of the generalized coordinates, $\dot{x}_i$ and $\dot{\lambda}_k = e_k$, while the potential energy and the magnetic energy do not depend explicitly on $\dot{x}_i$ and $\dot{\lambda}_k$, but only on x_i and λ_k.

3.4 Lagrange's equations

If the system can be described by a complete set of independent coordinates describing both the mechanical (z_i) and the electrical part (q_k or λ_k) of the system, the admissibility conditions are automatically fulfilled and the Lagrange equations can be derived from Hamilton's principle as we already did in section 2.5.

3.4.1 Displacement and charge formulation

Let z_i be a complete set of m independent mechanical coordinates and q_k a complete set of n independent charge coordinates. The Lagrangian

$$L(\dot{z}_i, z_i, \dot{q}_k, q_k) = T^* + W_m^* - V - W_e \tag{3.39}$$

accounts for all the conservative elements in the system and

$$\delta W_{nc} = \sum_{i=1}^{m} Q_i \delta z_i + \sum_{k=1}^{n} E_k \delta q_k \tag{3.40}$$

is the virtual work of all the nonconservative elements. It follows from Hamilton's principle that

$$\frac{d}{dt}\left(\frac{\partial L}{\partial \dot{z}_i}\right) - \frac{\partial L}{\partial z_i} = Q_i \qquad i = 1, ..., m \tag{3.41}$$

$$\frac{d}{dt}\left(\frac{\partial L}{\partial \dot{q}_k}\right) - \frac{\partial L}{\partial q_k} = E_k \qquad k = 1, ..., n \tag{3.42}$$

The demonstration follows closely that of the previous chapters and is omitted.

3.4.2 Displacement and flux linkage formulation

Similarly, let z_i be a complete set of m independent mechanical generalized coordinates and λ_k a complete set of n independent flux linkage coordinates. The Lagrangian

$$L(\dot{z}_i, z_i, \dot{\lambda}_k, \lambda_k) = T^* + W_e^* - V - W_m \tag{3.43}$$

accounts for all the conservative elements in the system and

$$\delta W_{nc} = \sum_{i=1}^{m} Q_i \delta z_i + \sum_{k=1}^{n} I_k \delta \lambda_k \tag{3.44}$$

is the virtual work of all the nonconservative elements in the systems. It follows from Hamilton's principle that

$$\frac{d}{dt}\left(\frac{\partial L}{\partial \dot{z}_i}\right) - \frac{\partial L}{\partial z_i} = Q_i \qquad i = 1, ..., m \tag{3.45}$$

$$\frac{d}{dt}\left(\frac{\partial L}{\partial \dot{\lambda}_k}\right) - \frac{\partial L}{\partial \lambda_k} = I_k \qquad k = 1, ..., n \tag{3.46}$$

3.4.3 Dissipation function

As in (1.51), it is customary to define the electrical dissipation function in such a way that the contribution to the right hand side of the Lagrange equation from the dissipative elements (the resistors) can be written respectively

$$E_k = -\frac{\partial D}{\partial \dot{q}_k} \tag{3.47}$$

in the charge formulation, or

$$I_k = -\frac{\partial D}{\partial \dot{\lambda}_k} \tag{3.48}$$

in the flux linkage formulation. The dissipation functions of a single resistor R are respectively,

$$D(\dot{q}) = \frac{1}{2} R \dot{q}^2 \qquad \text{(charge formulation)} \tag{3.49}$$

$$D(\dot{\lambda}) = \frac{1}{2}\frac{\dot{\lambda}^2}{R} \qquad \text{(flux linkage formulation)} \tag{3.50}$$

With these definitions Equ.(3.42) and (3.46) become respectively

$$\frac{d}{dt}\left(\frac{\partial L}{\partial \dot{q}_k}\right) + \frac{\partial D}{\partial \dot{q}_k} - \frac{\partial L}{\partial q_k} = E_k \tag{3.51}$$

$$\frac{d}{dt}\left(\frac{\partial L}{\partial \dot{\lambda}_k}\right) + \frac{\partial D}{\partial \dot{\lambda}_k} - \frac{\partial L}{\partial \lambda_k} = I_k \tag{3.52}$$

The Lagrangian formulation for lumped electromechanical systems is summarized in Table 3.1. We now illustrate with a few examples.

<table>
<tr><td colspan="2">Mechanical Part

Generalized displacements: z_i
Kinetic coenergy: $T^* = \frac{1}{2}\dot{z}^T M \dot{z}$
Strain energy: $V = \frac{1}{2} z^T K z$
Dissipation function (Viscous damping): $D = \frac{1}{2}\dot{z}^T C \dot{z}$
External forces: $\delta W_{nc} = \sum Q_i z_i$
Lagrange's equation: $\frac{d}{dt}\left(\frac{\partial L}{\partial \dot{z}_i}\right) + \frac{\partial D}{\partial \dot{z}_i} - \frac{\partial L}{\partial z_i} = Q_i$</td></tr>
<tr><td>Electrical Part
Charge formulation</td><td>Flux linkage formulation</td></tr>
<tr><td>Generalized coordinates: Electric charges q_k
Magnetic coenergy of an inductor: $W_m^* = \frac{1}{2} L \dot{q}^2$
Electrical energy of a capacitor: $W_e = \frac{q^2}{2C}$
Moving coil transducer: $W_m^* = T\dot{q}(x - x_0)$
Dissipation function of a resistor: $D = \frac{1}{2} R \dot{q}^2$
Voltage source: $\delta W_{nc} = E(t)\delta q$
Current source: $\delta W_{nc} = 0$</td><td>Generalized coordinates: Flux linkages λ_k
Electrical coenergy of a capacitor: $W_e^* = \frac{1}{2} C \dot{\lambda}^2$
Magnetic energy of an inductor: $W_m = \frac{\lambda^2}{2L}$
Dissipation function of a resistor: $D = \frac{\dot{\lambda}^2}{2R}$
Voltage source: $\delta W_{nc} = 0$
Current source: $\delta W_{nc} = I(t)\delta\lambda$</td></tr>
<tr><td>Lagrangian: $L = T^* + W_m^* - V - W_e$</td><td>Lagrangian: $L = T^* + W_e^* - V - W_m$</td></tr>
</table>

Table 3.1. Lagrange's equations for electromechanical systems

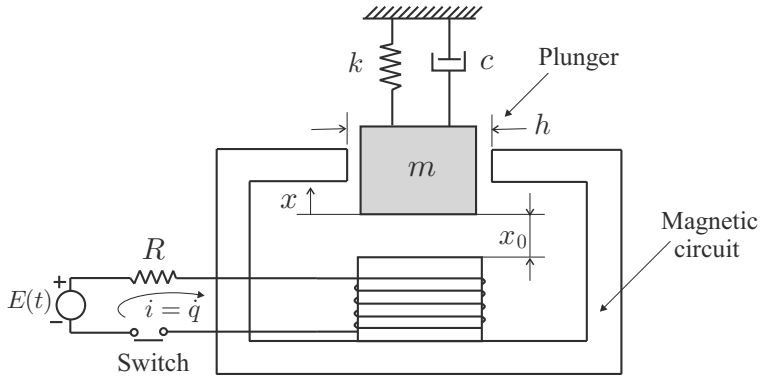

Fig. 3.7. Electromagnetic plunger.

3.5 Examples

3.5.1 Electromagnetic plunger

The electromagnetic plunger is used for tripping current breakers and various types of relays and valves. A movable plunger is driven by an electromagnet (Fig.3.7). The nominal gap of the plunger is x_0, when the current is zero (this corresponds to the unstretched position of the spring); when the switch is closed, the current in the coil produces a magnetic force which attracts the plunger down towards the electromagnet, to close the magnetic circuit at $x = -x_0$. The plunger is modelled as a spring-mass system of mass m, stiffness k and viscous damping c. We also assume that the electromagnet has a variable inductance

$$L(x) = \frac{L_0}{1 + (x_0 + x)/h} \tag{3.53}$$

(h is defined in Fig.3.7). In the charge formulation of the Lagrange equations, the generalized variables are respectively the displacement x of the plunger measured from the nominal position, and the charge q corresponding to the current loop shown in Fig. 3.7. The Lagrangian reads

$$L = T^* + W_m^* - V - W_e = \frac{1}{2}m\dot{x}^2 + \frac{1}{2}L(x)\dot{q}^2 - \frac{1}{2}kx^2 \tag{3.54}$$

and the dissipation function is the sum of the mechanical contribution of the viscous damper and the electrical one of the resistor

$$D = \frac{1}{2}c\dot{x}^2 + \frac{1}{2}R\dot{q}^2 \tag{3.55}$$

The only remaining contributor to the virtual work of the non-conservative forces is the voltage source

$$\delta W_{nc} = E(t)\delta q \tag{3.56}$$

The partial derivatives of the Lagrangian and of the dissipation function are respectively

$$\begin{aligned} \frac{\partial L}{\partial \dot{x}} &= m\dot{x} & \frac{\partial L}{\partial x} &= L'(x)\frac{\dot{q}^2}{2} - kx \\ \frac{\partial L}{\partial \dot{q}} &= L(x)\dot{q} & \frac{\partial L}{\partial q} &= 0 \\ \frac{\partial D}{\partial \dot{x}} &= c\dot{x} & \frac{\partial D}{\partial \dot{q}} &= R\dot{q} \end{aligned}$$

and Lagrange's equations read

$$\begin{aligned} m\ddot{x} + c\dot{x} + kx - L'(x)\frac{\dot{q}^2}{2} &= 0 \\ \frac{d}{dt}\left[L(x)\dot{q}\right] + R\dot{q} &= E \end{aligned} \tag{3.57}$$

3.5.2 Electromagnetic loudspeaker

The loudspeaker converts electrical energy into acoustical energy; in an electromagnetic loudspeaker, this is achieved with a voice coil actuating a membrane which, in turn, displaces the surrounding air. The low frequency behavior of the loudspeaker can be modelled as in Fig.3.8. The mechanical part is represented by a spring-mass system (which, obviously is appropriate only at low frequency); the mechanical constants m, k and c are chosen to account for the fluid-coupling effect of the membrane. The mechanical side is connected to the electrical side through a moving-coil transducer which, as we have seen in section 3.2.3, is a perfect energy transformer, with transducer constant T. The electrical side is modelled by a voltage source in series with a RL circuit.

With the charge formulation of the Lagrange equations and the generalized coordinates x and q ($i = \dot{q}$), the various energy contributors to the Lagrangian are:

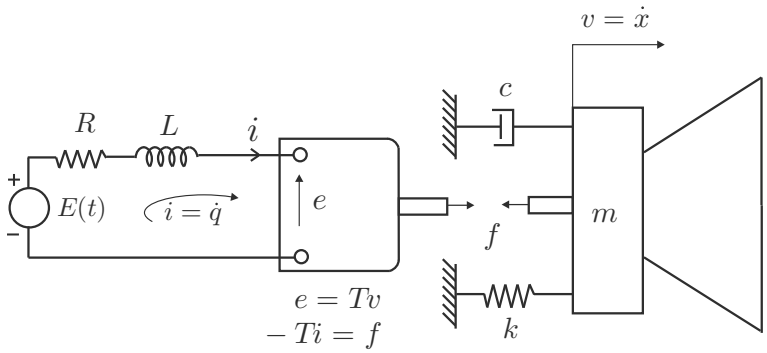

Fig. 3.8. Electromagnetic loudspeaker.

$$T^* = \frac{1}{2}m\dot{x}^2$$

$$V = \frac{1}{2}kx^2$$

$$W_m^* = \frac{1}{2}L\dot{q}^2 + T\dot{q}(x - x_0) \tag{3.58}$$

The first term is the magnetic coenergy in the inductor L and the second corresponds to the moving coil transducer, (3.33). The dissipation function is

$$D = \frac{1}{2}c\dot{x}^2 + \frac{1}{2}R\dot{q}^2$$

and the virtual work of the voltage source is

$$\delta W_{nc} = E(t)\delta q$$

The partial derivatives of the Lagrangian, $L = T^* + W_m^* - V$, and of the dissipation function are respectively

$$\frac{\partial L}{\partial \dot{x}} = m\dot{x} \qquad \frac{\partial L}{\partial x} = -kx + T\dot{q} \qquad \frac{\partial D}{\partial \dot{x}} = c\dot{x}$$

$$\frac{\partial L}{\partial \dot{q}} = L\dot{q} + T(x - x_0) \qquad \frac{\partial L}{\partial q} = 0 \qquad \frac{\partial D}{\partial \dot{q}} = R\dot{q}$$

It follows that Lagrange's equations read

$$m\ddot{x} + c\dot{x} + kx - T\dot{q} = 0$$
$$T\dot{x} + L\ddot{q} + R\dot{q} = E(t) \tag{3.59}$$

Note that, since the moving coil transducer acts as a perfect energy transformer, the set-up of Fig.3.8 could be used as a microphone as well, to convert the acoustic pressure into an output voltage (the membrane would be the pressure sensitive element). However, capacitive microphones are more popular.

3.5.3 Capacitive microphone

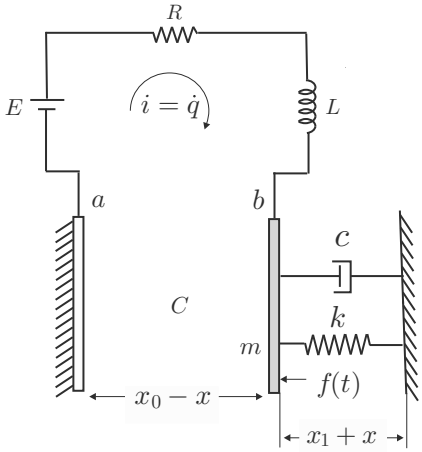

Fig. 3.9. Capacitive microphone.

A condenser microphone consists of a movable plate mounted on a circular spring parallel to a fixed back plate. These two plates form a variable capacitor charged by a constant voltage source through a RL circuit. The voltage drop in the resistor R is supposed to give an electrical image of the pressure (force) acting on the moving plate. The dynamics of the moving plate is modelled by a spring-mass system of constants m, k, c, Fig.3.9. At equilibrium, the electric charge q_0 in the capacitor produces an attractive force between the two plates, which is balanced by the extension of the spring attached to the moving plate; let x_0 be the distance between the two plates and x_1 be the spring extension at equilibrium. We analyze the vibration about the equilibrium position, assuming that the moving plate capacitance varies according to

$$C(x) = \frac{\varepsilon A}{x_0 - x} \tag{3.60}$$

The electrostatic force f_e between the two plates of the capacitor is given by (3.4)

$$f_e = -\left(\frac{\partial W_e}{\partial x}\right)_0 = -\frac{\partial}{\partial x}\left[\frac{q^2}{2C(x)}\right]_0 = \frac{q_0^2}{2\varepsilon A} \tag{3.61}$$

It is balanced by the spring extension kx_1. Thus, at equilibrium,

$$kx_1 = \frac{q_0^2}{2\varepsilon A} \tag{3.62}$$

Using the charge formulation and the generalized coordinates x and q ($i = \dot{q}$), the various energy contributions to the Lagrangian are

$$\begin{aligned} T^* &= \frac{1}{2}m\dot{x}^2 \\ V &= \frac{1}{2}k(x + x_1)^2 \\ W_m^* &= \frac{1}{2}L\dot{q}^2 \\ W_e &= \frac{1}{2C}(q_0 + q)^2 = \frac{x_0 - x}{2\varepsilon A}(q_0 + q)^2 \end{aligned} \tag{3.63}$$

where x is measured with respect to the equilibrium position and q is the excess of charge with respect to the equilibrium charge q_0. The dissipation function is

$$D = \frac{1}{2}c\dot{x}^2 + \frac{1}{2}R\dot{q}^2$$

and

$$\delta W_{nc} = E(t)\delta q + f\delta x$$

The Lagrangian is

$$L = \frac{1}{2}m\dot{x}^2 + \frac{1}{2}L\dot{q}^2 - \frac{1}{2}k(x + x_1)^2 - \frac{x_0 - x}{2\varepsilon A}(q_0 + q)^2$$

The partial derivatives are respectively

$$\frac{\partial L}{\partial \dot{x}} = m\dot{x} \qquad \frac{\partial L}{\partial x} = -k(x + x_1) + \frac{(q_0 + q)^2}{2\varepsilon A} \qquad \frac{\partial D}{\partial \dot{x}} = c\dot{x}$$

$$\frac{\partial L}{\partial \dot{q}} = L\dot{q} \qquad \frac{\partial L}{\partial q} = -\frac{x_0 - x}{\varepsilon A}(q_0 + q) \qquad \frac{\partial D}{\partial \dot{q}} = R\dot{q}$$

and Lagrange's equations read

$$m\ddot{x} + c\dot{x} + k(x + x_1) - \frac{(q_0 + q)^2}{2\varepsilon A} = f \tag{3.64}$$

$$L\ddot{q} + R\dot{q} + \frac{x_0 - x}{\varepsilon A}(q_0 + q) = E \tag{3.65}$$

At equilibrium, $x = \dot{x} = \ddot{x} = 0 = q = \dot{q} = \ddot{q} = f$, and (3.64) reduces to (3.62), and (3.65) to

$$E = \frac{x_0 q_0}{\varepsilon A} \tag{3.66}$$

Assuming that $q \ll q_0$ and $x \ll x_0$ (we restrict ourselves to small disturbances with respect to the equilibrium),

$$(q_0 + q)^2 \simeq {q_0}^2 + 2q_0 q$$

$$(x_0 - x)(q_0 + q) \simeq x_0 q_0 - q_0 x + x_0 q$$

and (3.64) and (3.65) become respectively

$$m\ddot{x} + c\dot{x} + kx - \frac{q_0 q}{\varepsilon A} = f \tag{3.67}$$

$$L\ddot{q} + R\dot{q} - \frac{q_0 x}{\varepsilon A} + \frac{x_0 q}{\varepsilon A} = 0 \tag{3.68}$$

where (3.62) and (3.66) have been used.

$$C_0 = \frac{\varepsilon A}{x_0} \qquad \text{and} \qquad T = \frac{q_0}{\varepsilon A} \tag{3.69}$$

are respectively the nominal capacitance at equilibrium and the electromechanical coupling factor between the mechanical part and the electrical part of the system (T is expressed in *Newton/Coulomb*, or in *Volt/meter*). With this notation, the equations governing the small vibrations about the equilibrium are

$$m\ddot{x} + c\dot{x} + kx - Tq = f \tag{3.70}$$

$$L\ddot{q} + R\dot{q} + q/C_0 - Tx = 0 \tag{3.71}$$

from which one can easily compute the transfer function between the output (voltage drop in the resistor, $R\dot{q}$), and the acoustic force f acting on the moving plate. This is left as an exercise. We now examine three systems which are particularly important in vibration control technology: the proof-mass actuator, the electrodynamic isolator and the geophone.

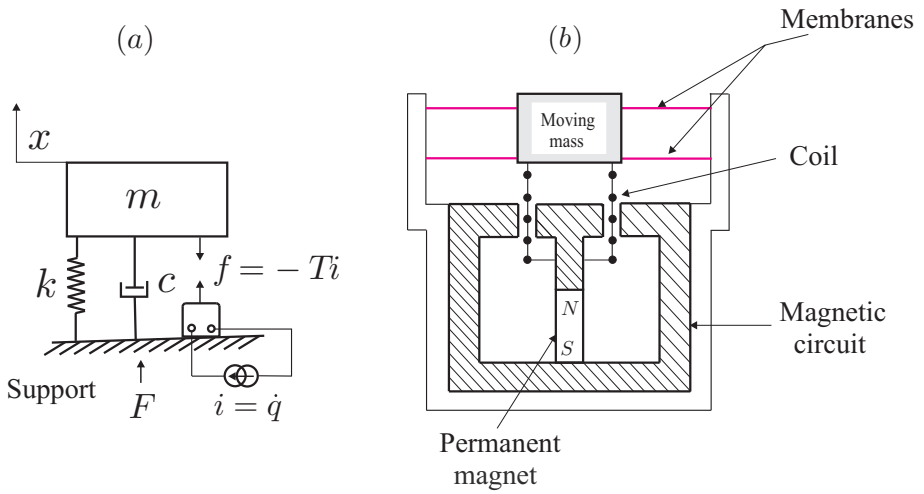

Fig. 3.10. Proof-mass actuator (a) model (b) conceptual design of an electrodynamic actuator.

3.5.4 Proof-mass actuator

A proof-mass actuator (Fig.3.10) is an inertial actuator which is used in various applications of vibration control. A reaction mass m is connected to the support structure by a spring k, a damper c and a force actuator f which can be either magnetic or hydraulic. In the electromagnetic actuator discussed here, the force actuator consists of a moving-coil transducer of constant T excited by a current generator i; the spring is achieved with membranes which also guide the linear motion of the moving mass. The system is readily modelled as in Fig.3.10(a); in a charge formulation, the system has a single generalized coordinate, x; q is not a generalized variable because a current source is used, which enforces $\dot{q} = i$. The various

contributions to the Lagrangian are the same as for the electromagnetic loudspeaker:

$$L = T^* + W_m^* - V = \frac{1}{2}m\dot{x}^2 + \frac{1}{2}L\dot{q}^2 + T\dot{q}(x - x_0) - \frac{1}{2}kx^2$$

and the dissipation function is also identical

$$D = \frac{1}{2}c\dot{x}^2 + \frac{1}{2}R\dot{q}^2$$

Note, however, that although the inductance L of the coil has been included in W_m^* and its resistance has been included in D, they will not appear in the final results, because q is no longer a generalized variable [this is why they have been omitted in Fig.3.10(a)]. Since we use a current source, we have also $\delta W_{nc} = 0$. The Lagrange equation relative to the x coordinate is readily obtained:

$$m\ddot{x} + c\dot{x} + kx = Ti$$

or, in the Laplace domain,

$$x = \frac{Ti}{ms^2 + cs + k} \tag{3.72}$$

(s is the Laplace variable). The total force applied to the support is equal and opposite to that applied to the mass:

$$F = -ms^2x = \frac{-ms^2Ti}{ms^2 + cs + k}$$

It follows that the transfer function between the total force F and the current i applied to the coil is

$$\frac{F}{i} = \frac{s^2T}{s^2 + 2\xi_p\omega_p s + \omega_p^2} \tag{3.73}$$

where T is the transducer constant (in *Newton/Ampere*), $\omega_p = (k/m)^{1/2}$ is the natural frequency of the spring-mass system and ξ_p is the damping ratio, which in practice is fairly high (the negative sign has been removed because it is irrelevant). The Bode plots of (3.73) are shown in Fig.3.11; one sees that the system behaves like a high-pass filter with a high frequency asymptote equal to the transducer constant T; above some critical frequency $\omega_c \simeq 2\omega_p$, the proof-mass actuator can be regarded as an *ideal force generator*. It has no authority over the rigid body modes and the operation at low frequency requires a large stroke, which is technically difficult. Medium to high frequency actuators (40 Hz and more) are relatively easy to obtain with low cost components (loudspeaker technology).

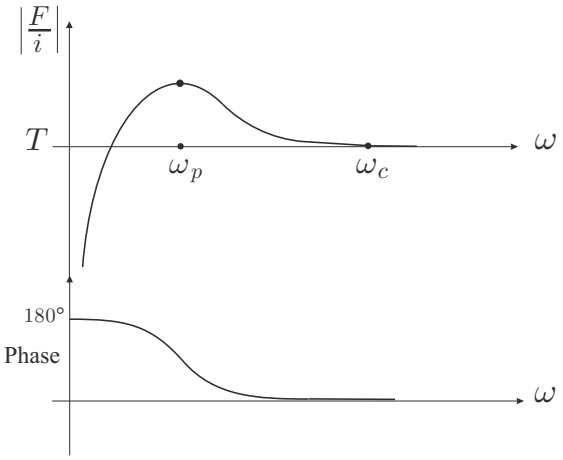

Fig. 3.11. Bode plot F/i of the proof-mass actuator.

3.5.5 Electrodynamic isolator

Consider the system of Fig.3.12(a): two masses m_1 and m_2 are connected by a spring k in parallel with a moving coil transducer of transduction constant T ($T = 2\pi nrB$). This system constitutes a single axis electrodynamic isolator. The mass m_1 is subjected to the disturbance force d, and the mass m_2 is that of the payload that must be isolated from the disturbance. Note that *no mechanical damper is involved in the isolator* (the damping turns out to be detrimental to the high frequency behavior of the isolator).

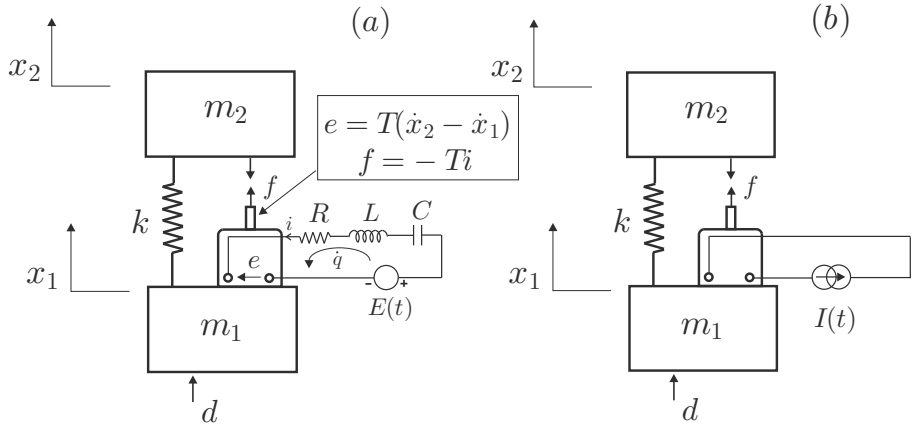

Fig. 3.12. Single axis electrodynamic isolator (a)voltage source (b)current source.

Using once again the charge formulation of Lagrange's equations and the generalized coordinates x_1, x_2 and q, we can write the Lagrangian

$$L = T^* + W_m^* - V - W_e$$
$$= \frac{1}{2}m_1\dot{x}_1^2 + \frac{1}{2}m_2\dot{x}_2^2 + \frac{1}{2}L\dot{q}^2 + T\dot{q}(x_2 - x_1 - x_0) - \frac{1}{2}k(x_2 - x_1)^2 - \frac{q^2}{2C} \quad (3.74)$$

where x_0 is an arbitrary reference state, see (3.33). The dissipation function is

$$D = \frac{1}{2}R\dot{q}^2 \quad (3.75)$$

and

$$\delta W_{nc} = d\,\delta x_1 + E\,\delta q \quad (3.76)$$

Lagrange's equations read

$$m_1\ddot{x}_1 + k(x_1 - x_2) + T\dot{q} = d \quad (3.77)$$

$$m_2\ddot{x}_2 + k(x_2 - x_1) - T\dot{q} = 0 \quad (3.78)$$

$$L\ddot{q} + T(\dot{x}_2 - \dot{x}_1) + R\dot{q} + \frac{q}{C} = E \quad (3.79)$$

The simplest situation is that where the moving coil transducer is shunted on a resistor R; in this case, the electrical circuit consists of a single resistor R and no voltage source is used. Equation (3.79) can be simplified to

$$T(\dot{x}_2 - \dot{x}_1) + R\dot{q} = 0 \quad (3.80)$$

which produces

$$T\dot{q} = -\frac{T^2(\dot{x}_2 - \dot{x}_1)}{R} \quad (3.81)$$

substituting in (3.77) and (3.78), one finds

$$m_1\ddot{x}_1 + \frac{T^2}{R}(\dot{x}_1 - \dot{x}_2) + k(x_1 - x_2) = d \quad (3.82)$$

$$m_2\ddot{x}_2 + \frac{T^2}{R}(\dot{x}_2 - \dot{x}_1) + k(x_2 - x_1) = 0 \quad (3.83)$$

In this case, the electrical system behaves like a viscous damper of constant T^2/R.

If the moving coil transducer is connected to a current source [Fig. 3.12(b)], q is no longer a generalized variable, since $\dot{q} = i$; the Lagrangian of the system is

$$L = \frac{1}{2}m_1\dot{x}_1^2 + \frac{1}{2}m_2\dot{x}_2^2 + Ti(x_2 - x_1 - x_0) - \frac{1}{2}k(x_2 - x_1)^2 \qquad (3.84)$$

and $\delta W_{nc} = d\,\delta x_1$. The Lagrange equations are in this case:

$$m_1\ddot{x}_1 + k(x_1 - x_2) + Ti = d \qquad (3.85)$$

$$m_2\ddot{x}_2 + k(x_2 - x_1) - Ti = 0 \qquad (3.86)$$

These equations are the starting point for the analysis of an active suspension.

3.5.6 The *Sky-hook* damper

Equation (3.83) defines a passive isolator where the damping is achieved by dissipating the electrical energy produced by the moving coil transducer into a resistor R. The *transmissibility* of the isolator is defined as the transfer function between the displacement of the disturbance source, x_1, and that of the payload, x_2. From (3.83), one finds easily

$$\frac{X_2(s)}{X_1(s)} = \frac{T^2 s/R + k}{m_2 s^2 + T^2 s/R + k} = \frac{2\xi\omega_n s + \omega_n^2}{s^2 + 2\xi\omega_n s + \omega_n^2} \qquad (3.87)$$

where $\omega_n^2 = k/m_2$ and $T^2/Rm_2 = 2\xi\omega_n$. The transducer constant T and the resistor R can be selected to smooth the resonance peak, but the damping also spoils the high frequency behavior of the isolator, because the asymptotic decay rate of the transmissibility (3.87) is $\sim s^{-1}$, leading to a high frequency attenuation of −20 dB/decade.

The *sky-hook damper* is a feedback strategy which allows one to eliminate the resonance peak while preserving the asymptotic decay rate $\sim s^{-2}$. It is based on the system of Fig.3.12(b); an absolute acceleration sensor is attached to m_2 and is used to generate a feedback control force proportional to the absolute velocity (an absolute velocity sensor can also be used)

$$I = -g\dot{x}_2$$

Combining with (3.86), one easily gets (in Laplace form)

$$m_2 s^2 x_2 + k(x_2 - x_1) + Tgsx_2 = 0 \qquad (3.88)$$

or

$$\frac{X_2(s)}{X_1(s)} = \frac{k}{m_2 s^2 + Tgs + k} = \frac{\omega_n^2}{s^2 + 2\xi\omega_n s + \omega_n^2} \qquad (3.89)$$

where $2\xi\omega_n = Tg/m_2$ in this case. Compared with (3.87), this result indicates that the feedback gain g can be adjusted to eliminate the resonance, while the asymptotic decay rate is $\sim s^{-2}$ (independent of g), corresponding to a high frequency attenuation of −40 dB/decade.

3.5.7 Geophone

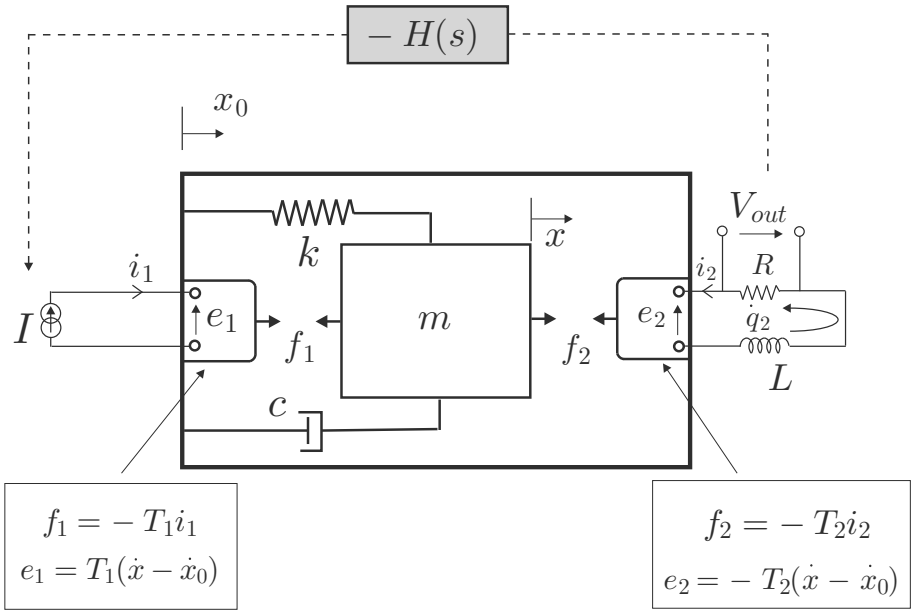

Fig. 3.13. Servo geophone involving two moving-coil transducers.

A geophone is a transducer which behaves as an *absolute velocity sensor* above some cut-off frequency depending on the mechanical structure of the transducer. A servo geophone has the additional feature that an internal feedback loop allows one to program the cut-off frequency of the transducer for the targeted application. The system is represented in Fig.3.13; it consists of a spring-mass system (m, k, c) connected to the sensor frame and to two independent moving-coil transducers. One of them (with transducer constant T_1, on the left side in Fig.3.13) is connected to a current source $I(t)$ and is used in the internal feedback loop of the system. The other one, of transduction constant T_2 is used as sensor. The inductance L represents that of the coil; the voltage drop in the resistor is the output V_{out} of the geophone. Let x_0 be the absolute displacement of the frame (it is the input of the system) and x be that of the mass m. Note that the loop current $\dot{q}_1 = i_1$ is subjected to the constraint $\dot{q}_1 = I$ of the current source. Thus, in a charge formulation of Lagrange's equations, there are only two generalized variables, x and q_2. The Lagrangian of the system is

$$L = \frac{1}{2}m\dot{x}^2 + T_1 I(x - x_0) - T_2\dot{q}_2(x - x_0) + \frac{1}{2}L\dot{q}_2^2 - \frac{1}{2}k(x - x_0)^2 \quad (3.90)$$

and the dissipation function is

$$D = \frac{1}{2}c(\dot{x} - \dot{x}_0)^2 + \frac{1}{2}R\dot{q}_2^2 \quad (3.91)$$

The contributions of the two moving coil transducers to the Lagrangian have opposite signs because of the positive sign adopted for x (the arbitrary reference position appearing in (3.33) has been set to zero). Lagrange's equations read

$$m\ddot{x} + c(\dot{x} - \dot{x}_0) + k(x - x_0) - T_1 I + T_2\dot{q}_2 = 0 \quad (3.92)$$

$$L\ddot{q}_2 - T_2(\dot{x} - \dot{x}_0) + R\dot{q}_2 = 0 \quad (3.93)$$

Upon introducing the relative displacement $y = x - x_0$, we can write these equations

$$m\ddot{y} + c\dot{y} + ky - T_1 I + T_2\dot{q}_2 = -m\ddot{x}_0 \quad (3.94)$$

$$L\ddot{q}_2 + R\dot{q}_2 - T_2\dot{y} = 0 \quad (3.95)$$

Taking the Laplace transform of (3.95), one gets

$$V_{out} = Rs\, q_2 = \frac{RT_2 s}{Ls + R}\, y \quad (3.96)$$

and, if the resistance R is large ($R \to \infty$)

$$V_{out} \simeq T_2 s\, y \quad (3.97)$$

From (3.94),

$$(ms^2 + cs + k)y + T_2 s q_2 = T_1 I - ms^2 x_0 \quad (3.98)$$

Combining with (3.96)

$$\left[ms^2 + \left(c + \frac{{T_2}^2}{Ls + R}\right)s + k\right] y = T_1 I - ms^2 x_0 \quad (3.99)$$

If R is large, the contribution of the moving coil transducer to the viscous damping, $T_2^2/(Ls + R)$, can be neglected (or combined with c), leading to the approximation

$$(ms^2 + cs + k)y = T_1 I - ms^2 x_0 \tag{3.100}$$

Combining with (3.97),

$$(ms^2 + cs + k)V_{out} = T_2 T_1 sI - T_2 ms^3 x_0 \tag{3.101}$$

Next, if we include a proportional plus integral (PI) feedback controller between V_{out} and the input current I:

$$I = -H(s)V_{out} = -(g_1 + \frac{g_2}{s})V_{out} \tag{3.102}$$

where g_1 and g_2 are respectively the proportional and integral control gains. From (3.102),

$$T_2 T_1 sI = -(T_2 T_1 g_1 s + T_2 T_1 g_2)V_{out} \tag{3.103}$$

and, substituting into (3.101), one gets

$$\left[ms^2 + (c + T_2 T_1 g_1)s + (k + T_2 T_1 g_2)\right] V_{out} = -T_2 ms^3 x_0 \tag{3.104}$$

or

$$\frac{V_{out}}{s\, x_0} = \frac{-T_2 ms^2}{ms^2 + (c + T_2 T_1 g_1)s + k + T_2 T_1 g_2} \tag{3.105}$$

Thus, *the transfer function between the output voltage V_{out} and the absolute frame velocity sx_0 is a second order high-pass filter of asymptotic gain T_2*, the transducer gain of the moving coil transducer on the right hand side of Fig.3.13. Beyond some corner frequency, the system behaves as an absolute velocity sensor. Without feedback control ($g_1 = g_2 = 0$), the corner frequency of the sensor is fixed by the mechanical resonance of the sensor, $(k/m)^{1/2}$, but if a PI controller is used, the corner frequency and the damping ratio of the transfer function can be set arbitrarily by selecting g_1 and g_2 in the appropriate manner. In particular, the mechanical spring k can be softened with a negative value of g_2. The transducer gain T_1 is also a design parameter.

3.5.8 One-axis magnetic suspension

A reluctance force always appears between two media of different magnetic permittivity (like iron and air); it is orthogonal to the interface and its magnitude

$$f = -\frac{\partial W_m^*}{\partial x}$$

increases with the difference in permittivity between the two media. The reluctance force has already been examined in the electromagnetic plunger, in section 3.5.1; it is also central in magnetic suspensions where it is used to levitate a body by balancing the gravity force and thus eliminating friction. Consider the elementary one-axis model of Fig.3.14, where the ideal current source reflects the fact that the magnetic suspensions are usually controlled with current amplifiers.

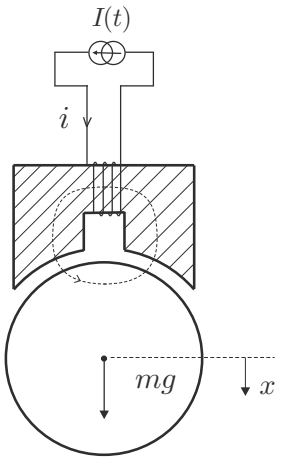

Fig. 3.14. One-axis magnetic suspension.

If one uses a charge formulation of Lagrange's equations, x is the single generalized variables; the Lagrangian of the system is

$$L = T^* - V + W_m^* = \frac{1}{2}m\dot{x}^2 + mgx + \frac{1}{2}L(x)i^2 \tag{3.106}$$

and Lagrange's equation reads

$$m\ddot{x} - mg - \frac{i^2}{2}L'(x) = 0 \tag{3.107}$$

This expresses the equilibrium between the inertia force, the gravity and the reluctance attraction force (reluctance forces are always attractive). The set point (x_0, i_0) is the static equilibrium point where the reluctance force balances the gravity force

$$mg = -\frac{{i_0}^2}{2} L'(x_0) \tag{3.108}$$

Let us consider the variation of the magnetic attraction force about the set point.

$$f(i,x) = -\frac{\partial W_m^*}{\partial x} = f(i_0,x_0) + \left(\frac{\partial f}{\partial i}\right)_{i_0,x_0}(i-i_0) + \left(\frac{\partial f}{\partial x}\right)_{i_0,x_0}(x-x_0) + h.o.t$$

$$= -\frac{i_0^2}{2} L'(x_0) - L'(x_0) i_0 \Delta i - \frac{i_0^2}{2} L''(x_0) \Delta x \tag{3.109}$$

where Δi is the current increment and Δx is the displacement with respect to the set point (i_0, x_0). The first term is balanced by gravity and the reluctance force increment reads

$$\Delta f = -L'(x_0)\, i_0 \Delta i - \frac{i_0^2}{2} L''(x_0) \Delta x = k_i \Delta i + k_x \Delta x \tag{3.110}$$

where k_i is the *force to current factor* and k_x is the *bearing stiffness* about the set point; they are illustrated in Fig.3.15. A negative stiffness k_x means that any disturbance load acting on the system will produce a deviation from the set point which, in turn, will increase the imbalance and the deviation from the set point. Such a system is mechanically unstable and requires a feedback loop between the displacement increment Δx and the current increment Δi to achieve stability.

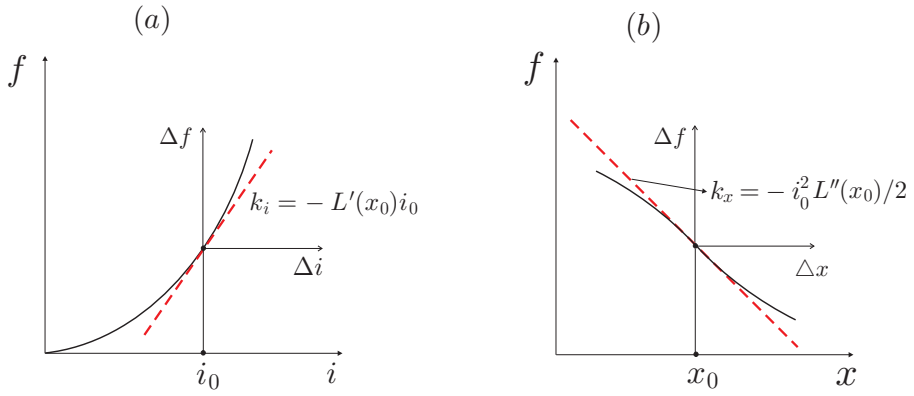

Fig. 3.15. Variation of the magnetic force about the set point (a)with the input current (x_0 fixed) (b)with the distance to the set point (i_0 fixed).

3.6 General electromechanical transducer

3.6.1 Constitutive equations

The constitutive behavior of a wide class of electromechanical transducers can be modelled as in Fig.3.16, where the black box represents the conversion mechanism between electrical energy and mechanical energy, and vice versa. In Laplace form, the constitutive equations read

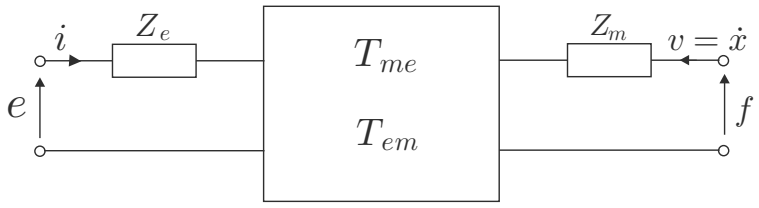

Fig. 3.16. Electrical analog schematic representation of an electromechanical transducer.

$$e = Z_e i + T_{em} v \tag{3.111}$$

$$f = T_{me} i + Z_m v \tag{3.112}$$

where e is the Laplace transform of the input voltage across the electrical terminals, i the input current, f the force applied to the mechanical terminals, and v the velocity of the mechanical part. Z_e is the blocked electrical impedance, measured for $v = 0$; T_{em} is the transduction coefficient representing the electromotive force (voltage) appearing in the electrical circuit per unit velocity in the mechanical part (in *volt.sec/m*). T_{me} is the transduction coefficient representing the force acting on the mechanical terminals to balance the electromagnetic force induced per unit current input on the electrical side (in *N/Amp*), and Z_m is the mechanical impedance, measured when the electrical side is open ($i = 0$). As an example, it is easy to check that the electromagnetic loudspeaker equations (3.59) can be written in this form with $Z_e = Ls + R$, $Z_m = ms + c + k/s$, $T_{em} = T$ and $T_{me} = -T$. The same representation applies also to the piezoelectric transducer analyzed in the next chapter.

In absence of external force ($f = 0$), v can be eliminated between the two foregoing equations, leading to

$$e = (Z_e - \frac{T_{em} T_{me}}{Z_m}) i$$

$-T_{em}T_{me}/Z_m$ is called the *motional impedance*. The total driving point electrical impedance is the sum of the blocked and the motional impedances.

3.6.2 Self-sensing

Equation (3.111) shows that the voltage drop across the electrical terminals of any electromechanical transducer is the sum of a contribution proportional to the current applied and a contribution proportional to the velocity of the mechanical terminals. Thus, if $Z_e i$ can be measured and subtracted from e, a signal proportional to the velocity is obtained. This suggests the bridge structure of Fig.3.17. The bridge equations are as follows: for the branch containing the transducer,

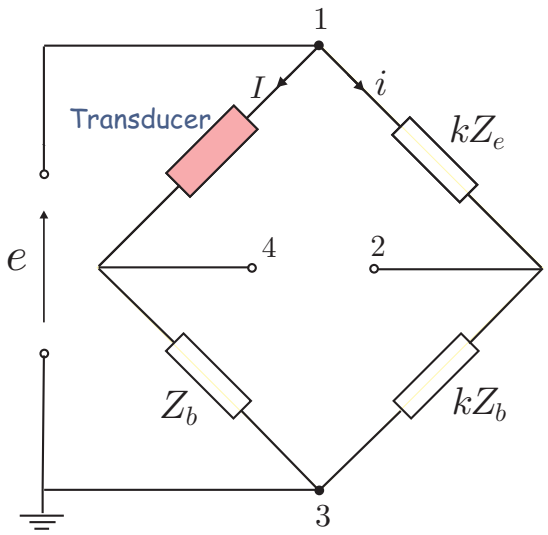

Fig. 3.17. Bridge circuit for self-sensing actuation.

$$e = Z_e I + T_{em} v + Z_b I$$

$$I = \frac{1}{Z_e + Z_b}(e - T_{em} v)$$

$$V_4 = Z_b I = \frac{Z_b}{Z_e + Z_b}(e - T_{em} v)$$

For the other branch,

$$e = kZ_e i + kZ_b i$$

$$V_2 = kZ_b i = \frac{Z_b}{Z_e + Z_b}\, e$$

and the bridge output

$$V_4 - V_2 = \left(\frac{-Z_b\, T_{em}}{Z_e + Z_b}\right) v \tag{3.113}$$

is indeed a linear function of the velocity v of the mechanical terminals. Note, however, that $-Z_b\, T_{em}/(Z_e + Z_b)$ acts as a filter; the bridge impedance Z_b must be adapted to the transducer impedance Z_e to avoid amplitude distortion and phase shift between the output voltage $V_4 - V_2$ and the transducer velocity in the frequency band of interest. The self-sensing piezoelectric actuator will be examined in more detail in chapter 6.

3.7 References

CRANDALL, S.H., KARNOPP, D.C., KURTZ, E.F, Jr., PRIDMORE-BROWN, D.C., *Dynamics of Mechanical and Electromechanical Systems*, McGraw-Hill, N-Y, 1968.

D'AZZO, J.J., HOUPIS, C.H., *Feedback Control System Analysis & Synthesis*, Second Edition, McGraw-Hill, N-Y, 1966.

DE BOER, E., Theory of Motional Feedback, *IRE Transactions on Audio*, 15-21, Jan.-Feb., 1961.

HUNT, F.V., *Electroacoustics: The Analysis of Transduction, and its Historical Background*, Harvard Monographs in Applied Science, No 5, 1954. Reprinted, Acoustical Society of America, 1982.

KARNOPP, D.C., TRIKHA, A.K., Comparative study of optimization techniques for shock and vibration isolation, *Trans. ASME, J. of Engineering for Industry, Series B*, 91, 1128-1132, 1969.

PRATT, J., FLATAU, A., Development and analysis of self-sensing magnetostrictive actuator design, SPIE Smart Materials and Structures Conference, Vol.1917, 1993.

SCHWEITZER, G., BLEULER, H., TRAXLER, A., *Active Magnetic Bearings*, vdf Hochschulverlag AG an der ETH Zürich, 1994.

WILLIAMS, J.H., Jr., *Fundamentals of Applied Dynamics*, Wiley, 1996.

WOODSON, H.H., MELCHER, J.R, *Electromechanical Dynamics, Part I: Discrete Systems*, Wiley, 1968.

4

Piezoelectric systems

4.1 Introduction

Piezoelectric materials belong to the so-called *smart materials*, or *multi-functional materials*, which have the ability to respond significantly to stimuli of different physical natures. Figure 4.1 lists various effects that are observed in materials in response to various inputs: mechanical, electrical, magnetic, thermal, light. The coupling between the physical fields of different types is expressed by the non-diagonal cells in the figure; if its magnitude is sufficient, the coupling can be used to build discrete or distributed transducers of various types, which can be used as sensors, actuators, or even integrated in structures with various degrees of tailoring and complexity (e.g. as fibers), to make them controllable or responsive to their environment (e.g. for shape morphing, precision shape control, damage detection, dynamic response alleviation,...).

Figure 4.2 summarizes the mechanical properties of a few smart materials which are considered for actuation in structural control applications. Figure 4.2(a) shows the maximum (blocked) stress versus the maximum (free) strain; the diagonal lines in the diagram indicate a constant energy density. Figure 4.2(b) shows the specific energy density (i.e. energy density by unit mass) versus the maximum frequency; the diagonal lines indicate a constant specific power density. Note that all the material characteristics vary by several orders of magnitude. Among them all, the piezoelectric materials are undoubtedly the most mature and those with the most applications.

This chapter begins with the analysis of a one-dimensional discrete piezoelectric transducer and the energy conversion process between mechanical energy and electrical energy. The constitutive equations are

Output / Input	Strain	Electric charge	Magnetic flux	Temperature	Light
Stress	Elasticity	Piezo-electricity	Magneto-striction		Photo-elasticity
Electric field	Piezo-electricity	Permittivity			Electro -optic effect
Magnetic field	Magneto-striction	Magneto-electric effect	Permeability		Magneto -optic
Heat	Thermal expansion	Pyro-electricity		Specific heat	
Light	Photostriction	Photo-voltaic effect			Refractive index

Fig. 4.1. Stimulus-Response relations indicating various effects in materials. The smart materials correspond to the non-diagonal cells.

examined, and the analytical forms of the electromechanical energy and co-energy functions are established. Next, the integration of a piezoelectric transducer into a mechanical system is considered, and the Lagrangian formulation of the dynamic equations is addressed; it is then extended to the case of a structure with a finite number of piezoelectric transducers. The remainder of this chapter is devoted to the constitutive equations of a general piezoelectric material and Hamilton's principle for a piezoelectric structure. Finally, the Lagrangian formulation is illustrated with Rosen's piezoelectric transformer.

4.2 Piezoelectric transducer

The piezoelectric effect was discovered by Pierre and Jacques Curie in 1880. The direct piezoelectric effect consists in the ability of certain crystalline materials to generate an electrical charge in proportion to an externally applied force; the direct effect is used in force transducers. According to the inverse piezoelectric effect, an electric field parallel to the direction of polarization induces an expansion of the material. The piezoelectric effect is anisotropic; it can be exhibited only by materials whose crystal structure has no center of symmetry; this is the case for some ceramics

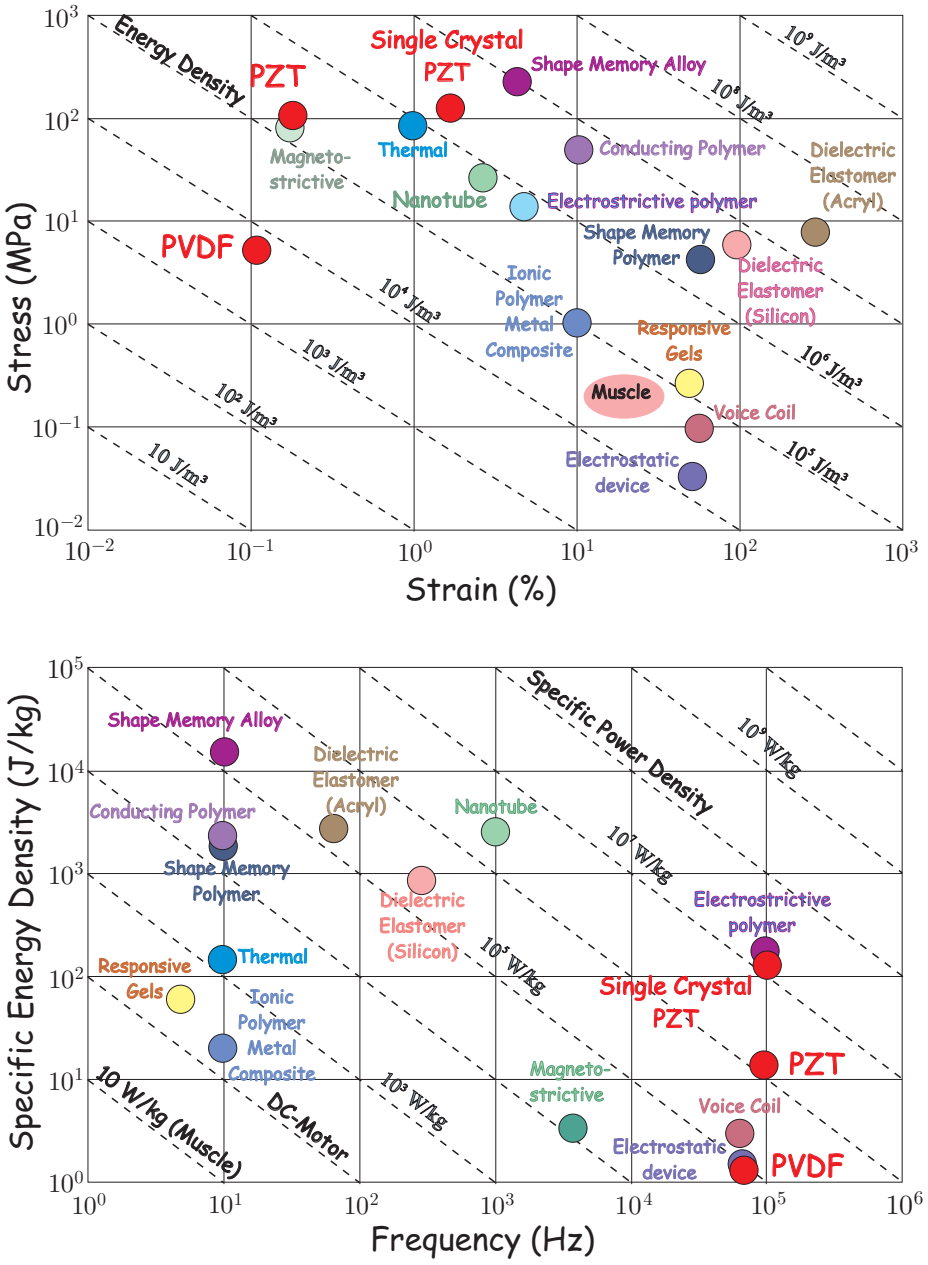

Fig. 4.2. (a) Maximum stress vs. maximum strain of various smart material actuators. (b) Specific energy density vs. maximum frequency (by courtesy of R. Petricevic, *Neue Materialen Würzburg*).

below a certain temperature called the *Curie temperature*; in this phase, the crystal has built-in electric dipoles, but the dipoles are randomly orientated and the net electric dipole on a macroscopic scale is zero. During the poling process, when the crystal is cooled in the presence of a high electric field, the dipoles tend to align, leading to an electric dipole on a macroscopic scale. After cooling and removing of the poling field, the dipoles cannot return to their original position; they remain aligned along the poling direction and the material body becomes permanently piezoelectric, with the ability to convert mechanical energy to electrical energy and vice versa; this property will be lost if the temperature exceeds the Curie temperature or if the transducer is subjected to an excessive electric field in the direction opposed to the poling field.

The most popular piezoelectric materials are *Lead-Zirconate-Titanate (PZT)* which is a ceramic, and *Polyvinylidene fluoride (PVDF)* which is a polymer. In addition to the piezoelectric effect, piezoelectric materials exhibit a *pyroelectric* effect, according to which electric charges are generated when the material is subjected to temperature; this effect is used to produce heat detectors; it will not be discussed here.

In this section, we consider a transducer made of a one-dimensional piezoelectric material of constitutive equations (we use the notations of the IEEE Standard on Piezoelectricity)

$$D = \varepsilon^T E + d_{33} T \tag{4.1}$$

$$S = d_{33} E + s^E T \tag{4.2}$$

where D is the electric displacement (charge per unit area, expressed in $Coulomb/m^2$), E the electric field (V/m), T the stress (N/m^2) and S the strain. ε^T is the dielectric constant (permittivity) under constant stress, s^E is the compliance when the electric field is constant (inverse of the Young's modulus) and d_{33} is the piezoelectric constant, expressed in m/V or $Coulomb/Newton$; the reason for the subscript 33 is that, by convention, index 3 is always aligned to the poling direction of the material, and we assume that the electric field is parallel to the poling direction. More complicated situations will be considered later. Note that the same constant d_{33} appears in (4.1) and (4.2).

In the absence of external force, a transducer subjected to a voltage with the same polarity as that during poling produces an elongation, and

a voltage opposed to that during poling makes it shrink (inverse piezoelectric effect). In (4.2), this amounts to a positive d_{33}. Conversely (direct piezoelectric effect), if we consider a transducer with open electrodes ($D = 0$), according to (4.1), $E = -(d_{33}/\varepsilon^T)T$, which means that a traction stress will produce a voltage with polarity opposed to that during poling, and a compressive stress will produce a voltage with the same polarity as that during poling.

4.3 Constitutive relations of a discrete transducer

Equations (4.1) and (4.2) can be written in a matrix form

$$\left\{ \begin{array}{c} D \\ S \end{array} \right\} = \left[\begin{array}{cc} \varepsilon^T & d_{33} \\ d_{33} & s^E \end{array} \right] \left\{ \begin{array}{c} E \\ T \end{array} \right\} \tag{4.3}$$

where (E, T) are the independent variables and (D, S) are the dependent variables. If (E, S) are taken as the independent variables, Equ.(4.1) and (4.2) can be rewritten

$$D = \frac{d_{33}}{s^E} S + \varepsilon^T \left(1 - \frac{{d_{33}}^2}{s^E \varepsilon^T} \right) E$$

$$T = \frac{1}{s^E} S - \frac{d_{33}}{s^E} E$$

or

$$\left\{ \begin{array}{c} D \\ T \end{array} \right\} = \left[\begin{array}{cc} \varepsilon^T (1 - k^2) & e_{33} \\ -e_{33} & c^E \end{array} \right] \left\{ \begin{array}{c} E \\ S \end{array} \right\} \tag{4.4}$$

where $c^E = 1/s^E$ is the Young's modulus under $E = 0$ (short circuited electrodes), in N/m^2 (Pa); $e_{33} = d_{33}/s^E$, product of d_{33} by the Young modulus, is the constant relating the electric displacement to the strain for short-circuited electrodes (in $Coulomb/m^2$), and also that relating the compressive stress to the electric field when the transducer is blocked ($S = 0$).

$$k^2 = \frac{{d_{33}}^2}{s^E \varepsilon^T} = \frac{{e_{33}}^2}{c^E \varepsilon^T} \tag{4.5}$$

k is called the *electromechanical coupling factor* of the material; it measures the efficiency of the conversion of mechanical energy into electrical energy, and vice versa, as discussed below. From (4.4), we note that $\varepsilon^T(1 - k^2)$ is the dielectric constant under zero strain.

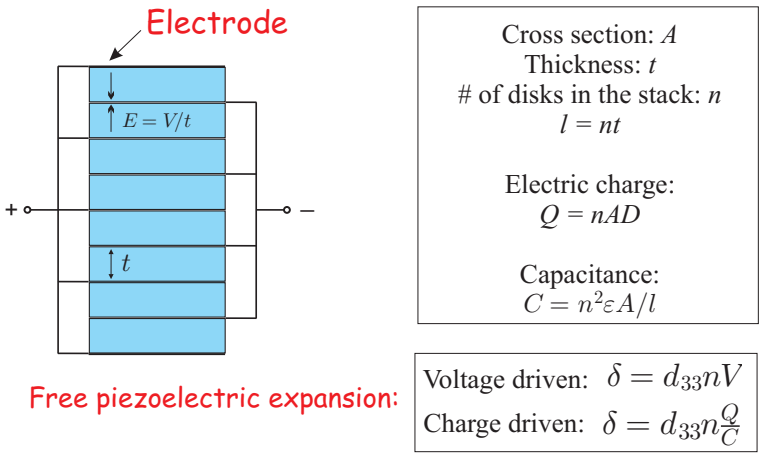

Fig. 4.3. Piezoelectric linear transducer.

If one assumes that all the electrical and mechanical quantities are uniformly distributed in a linear transducer formed by a stack of n disks of thickness t and cross section A (Fig.4.3), the global constitutive equations of the transducer are obtained by integrating Equ.(4.3) and (4.4) over the volume of the transducer; one easily finds

$$\begin{Bmatrix} Q \\ \Delta \end{Bmatrix} = \begin{bmatrix} C & nd_{33} \\ nd_{33} & 1/K_a \end{bmatrix} \begin{Bmatrix} V \\ f \end{Bmatrix} \tag{4.6}$$

or

$$\begin{Bmatrix} Q \\ f \end{Bmatrix} = \begin{bmatrix} C(1-k^2) & nd_{33}K_a \\ -nd_{33}K_a & K_a \end{bmatrix} \begin{Bmatrix} V \\ \Delta \end{Bmatrix} \tag{4.7}$$

where $Q = nAD$ is the total electric charge on the electrodes of the transducer, $\Delta = Sl$ is the total extension ($l = nt$ is the length of the transducer), $f = AT$ is the total force and V the voltage applied between the electrodes of the transducer, resulting in an electric field $E = V/t = nV/l$. $C = \varepsilon^T An^2/l$ is the capacitance of the transducer with no external load ($f = 0$), $K_a = A/s^E l$ is the stiffness with short-circuited electrodes ($V = 0$). Note that the electromechanical coupling factor can be written alternatively

$$k^2 = \frac{{d_{33}}^2}{s^E \varepsilon^T} = \frac{n^2 {d_{33}}^2 K_a}{C} \tag{4.8}$$

Equation (4.6) can be inverted

$$\begin{Bmatrix} V \\ f \end{Bmatrix} = \frac{K_a}{C(1-k^2)} \begin{bmatrix} 1/K_a & -nd_{33} \\ -nd_{33} & C \end{bmatrix} \begin{Bmatrix} Q \\ \Delta \end{Bmatrix} \tag{4.9}$$

from which we can see that the stiffness with open electrodes ($Q = 0$) is $K_a/(1-k^2)$ and the capacitance for a fixed geometry ($\Delta = 0$) is $C(1-k^2)$. Note that typical values of k are in the range $0.3-0.7$; for large k, the stiffness changes significantly with the electrical boundary conditions, and similarly the capacitance depends on the mechanical boundary conditions.

Next, let us write the total stored electromechanical energy and coenergy functions in the same way as we did for the movable plate capacitor in chapter 3.

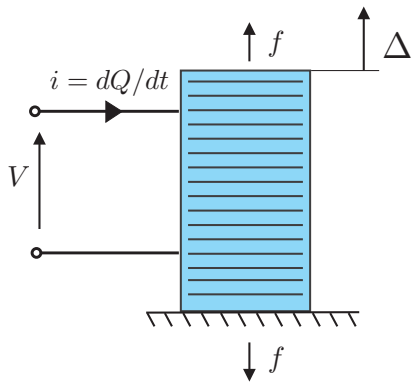

Fig. 4.4. Discrete Piezoelectric transducer.

Consider the discrete piezoelectric transducer of Fig.4.4; the total power delivered to the transducer is the sum of the electric power, Vi and the mechanical power, $f\dot{\Delta}$. The net work on the transducer is

$$dW = Vidt + f\dot{\Delta}dt = VdQ + fd\Delta \tag{4.10}$$

For a conservative element, this work is converted into stored energy, dW_e, and the total stored energy, $W_e(\Delta, Q)$ can be obtained by integrating (4.10) from the reference state to the state (Δ, Q). Since the system is conservative, the integration can be done along any path leading from $(0, 0)$ to (Δ, Q). Upon differentiating $W_e(\Delta, Q)$,

$$dW_e(\Delta, Q) = \frac{\partial W_e}{\partial \Delta} d\Delta + \frac{\partial W_e}{\partial Q} dQ \tag{4.11}$$

and, comparing with (4.10), we recover the constitutive equations

$$f = \frac{\partial W_e}{\partial \Delta} \qquad\qquad V = \frac{\partial W_e}{\partial Q} \tag{4.12}$$

Substituting f and V from (4.9) into (4.10), one gets

$$\begin{aligned} dW_e &= V\,dQ + f\,d\Delta \\ &= \frac{Q\,dQ}{C(1-k^2)} - \frac{nd_{33}K_a}{C(1-k^2)}(\Delta\,dQ + Q\,d\Delta) + \frac{K_a}{1-k^2}\Delta\,d\Delta \end{aligned}$$

which is the total differential of

$$W_e(\Delta, Q) = \frac{Q^2}{2C(1-k^2)} - \frac{nd_{33}K_a}{C(1-k^2)}Q\Delta + \frac{K_a}{1-k^2}\frac{\Delta^2}{2} \tag{4.13}$$

This is the analytical expression of the stored electromechanical energy for the discrete piezoelectric transducer. Equations (4.12) recover the constitutive equations (4.9). The first term on the right hand side of (4.13) is the electrical energy stored in the capacitance $C(1-k^2)$ (corresponding to a fixed geometry, $\triangle = 0$); the third term is the elastic strain energy stored in a spring of stiffness $K_a/(1-k^2)$ (corresponding to open electrodes, $Q = 0$); the second term is the piezoelectric energy. Referring to Fig.4.5, the last term in (4.13) corresponds to integrating (4.10) over the horizontal segment from $(0,0)$ to $(\Delta, 0)$, while the other two result from integrating on the vertical segment, from $(\Delta, 0)$ to (Δ, Q).

As with the movable plate capacitor, the coenergy function is defined by the Legendre transformation

$$W_e^*(\Delta, V) = VQ - W_e(\Delta, Q) \tag{4.14}$$

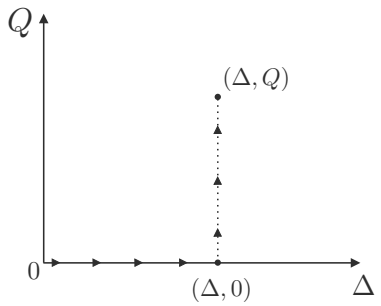

Fig. 4.5. Integration path from $(0,0)$ to (Δ, Q).

The total differential of the coenergy is

$$dW_e^* = Q\,dV + V\,dQ - \frac{\partial W_e}{\partial \Delta}d\Delta - \frac{\partial W_e}{\partial Q}dQ$$

$$dW_e^* = Q\,dV - f\,d\Delta \tag{4.15}$$

where Equ.(4.12) have been used. It follows that

$$Q = \frac{\partial W_e^*}{\partial V} \qquad \text{and} \qquad f = -\frac{\partial W_e^*}{\partial \Delta} \tag{4.16}$$

Introducing the constitutive equations (4.7) into (4.15),

$$dW_e^* = \left[C(1-k^2)V + nd_{33}K_a\Delta\right]dV + (nd_{33}K_aV - K_a\Delta)\,d\Delta$$

$$= C(1-k^2)V\,dV + nd_{33}K_a\,(\Delta dV + V\,d\Delta) - K_a\Delta\,d\Delta$$

which is the total differential of

$$W_e^*(\Delta, V) = C(1-k^2)\frac{V^2}{2} + nd_{33}K_aV\Delta - K_a\frac{\Delta^2}{2} \tag{4.17}$$

This is the analytical form of the coenergy function for the discrete piezoelectric transducer. The first term on the right hand side of (4.17) is recognized as the electrical coenergy in the capacitance $C(1-k^2)$ (corresponding to a fixed geometry, $\Delta = 0$); the third is the strain energy stored in a spring of stiffness K_a (corresponding to short-circuited electrodes, $V = 0$). The second term of (4.17) is the piezoelectric coenergy; using the fact that the uniform electric field is $E = nV/l$ and the uniform strain is $S = \Delta/l$, it can be rewritten

$$\int_\Omega Se_{33}E\,d\Omega \tag{4.18}$$

where the integral extends to the volume Ω of the transducer. Recall that, in the flux linkage formulation of the Lagrange equations, $V = \dot{\lambda}$.

4.3.1 Interpretation of k^2

Consider a piezoelectric transducer subjected to the following mechanical cycle: first, it is loaded with a force F with short-circuited electrodes; the resulting extension is

$$\Delta_1 = \frac{F}{K_a}$$

where $K_a = A/(s^E l)$ is the stiffness with short-circuited electrodes. The energy stored in the system is

$$W_1 = \int_0^{\Delta_1} f\, dx = \frac{F\Delta_1}{2} = \frac{F^2}{2K_a}$$

At this point, the electrodes are open and the transducer is unloaded according to a path of slope $K_a/(1-k^2)$, corresponding to the new electrical boundary conditions,

$$\Delta_2 = \frac{F(1-k^2)}{K_a}$$

The energy recovered in this way is

$$W_2 = \int_0^{\Delta_2} f\, dx = \frac{F\Delta_2}{2} = \frac{F^2(1-k^2)}{2K_a}$$

leaving $W_1 - W_2$ stored in the transducer. The ratio between the remaining stored energy and the initial stored energy is

$$\frac{W_1 - W_2}{W_1} = k^2$$

Similarly, consider the following electrical cycle: first, a voltage V is applied to the transducer which is mechanically unconstrained ($f = 0$). The electric charges appearing on the electrodes are

$$Q_1 = CV$$

where $C = \varepsilon^T An^2/l$ is the unconstrained capacitance, and the energy stored in the transducer is

$$W_1 = \int_0^{Q_1} v\, dq = \frac{VQ_1}{2} = \frac{CV^2}{2}$$

At this point, the transducer is blocked mechanically and electrically unloaded from V to 0. The electrical charges are removed according to

$$Q_2 = C(1-k^2)V$$

where the capacitance for fixed geometry has been used. The energy recovered in this way is

$$W_2 = \int_0^{Q_2} v\, dq = \frac{C(1-k^2)V^2}{2}$$

leaving $W_1 - W_2$ stored in the transducer. Here again, the ratio between the remaining stored energy and the initial stored energy is

$$\frac{W_1 - W_2}{W_1} = k^2$$

Although the foregoing relationships provide a clear physical interpretation of the electromechanical coupling factor, they do not bring a practical way of measuring k^2; the experimental determination of k^2 is often based on impedance (or admittance) measurements, as discussed in the next section.

4.4 Structure with a discrete piezoelectric transducer

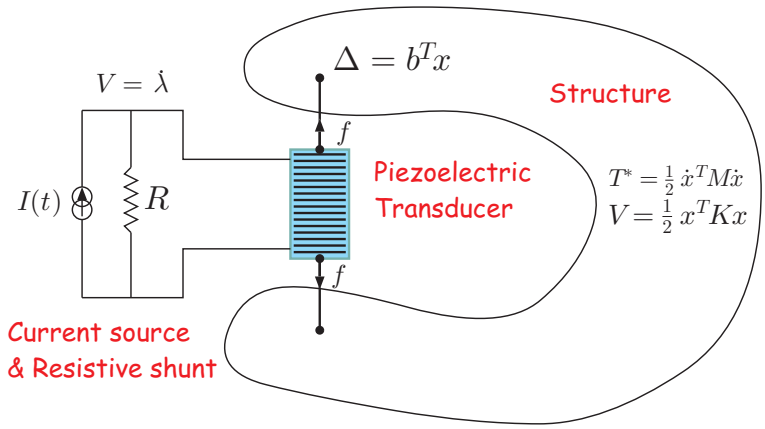

Fig. 4.6. Linear structure equipped with a piezoelectric transducer, a current source and a shunted resistor.

Consider the linear structure of Fig.4.6, assumed undamped for simplicity, and equipped with a discrete piezoelectric transducer as discussed in the previous section. It is also assumed that the transducer is connected to a current source $I(t)$ and is shunted with a resistor R. Using a flux linkage formulation for the electrical quantities, the Lagrangian of the system reads (Table 3.1):

$$L = T^* + W_e^* - V \tag{4.19}$$

where

$$T^* = \frac{1}{2}\dot{x}^T M \dot{x} \tag{4.20}$$

is the kinetic coenergy of the structure,

$$V = \frac{1}{2}x^T K x \tag{4.21}$$

is the strain energy in the structure, excluding the piezoelectric transducer, and

$$W_e^*(\dot{\lambda}) = \frac{1}{2}C(1-k^2)\dot{\lambda}^2 + nd_{33}K_a\dot{\lambda}\Delta - \frac{1}{2}K_a\Delta^2 \tag{4.22}$$

is the coenergy function of the piezoelectric transducer, given by (4.17), where $\dot{\lambda} = V$ is the voltage at the electrodes of the transducer. Combining these equations and taking into account that $\Delta = b^T x$, where b is the projection vector relating the end displacements of the transducer to the global coordinate system, we can write the Lagrangian

$$L = \frac{1}{2}\dot{x}^T M \dot{x} - \frac{1}{2}x^T(K + K_a b b^T)x + C(1-k^2)\frac{\dot{\lambda}^2}{2} + nd_{33}K_a\dot{\lambda}b^T x \tag{4.23}$$

The virtual work of the non-conservative forces is

$$\delta W_{nc} = I\delta\lambda - \frac{\dot{\lambda}}{R}\delta\lambda + F\delta x \tag{4.24}$$

where I is the current source intensity and F is the vector of external forces applied to the structure. Note that the resistor can be handled alternatively by the dissipation function

$$D = \frac{\dot{\lambda}^2}{2R}$$

In this case, it disappears from the virtual work equation. Similarly, if the viscous damping of the structure is included in the analysis, an additional contribution (1.53) appears in the dissipation function. These equations are the starting point of the Lagrangian formulation of the system dynamics. The Lagrange equations relative to the generalized coordinates x and λ give respectively

$$M\ddot{x} + (K + K_a b b^T)x = bK_a nd_{33}V + F \tag{4.25}$$

$$\frac{d}{dt}[C(1-k^2)V + nd_{33}K_a b^T x] + \frac{V}{R} = I \tag{4.26}$$

where $V = \dot{\lambda}$. These two equations govern the system dynamics when a current source is used. We assume $F = 0$ in what follows.

4.4.1 Voltage source

If a *voltage* source is used instead of a current source, λ ceases to be a generalized variable (see Table 3.1) and the shunted resistor becomes irrelevant (and useless). In this case, Equ.(4.25) applies alone. In absence of external forces, if one defines the unconstrained expansion $\delta = nd_{33}V$ under the voltage V [see Equ.(4.6)], it is rewritten

$$M\ddot{x} + (K + K_a bb^T)x = bK_a\delta \tag{4.27}$$

Thus, the effect of the piezoelectric transducer on the structure can be represented by a pair of *self-equilibrating* forces applied axially to the ends of the transducer; as for thermal loads, their magnitude is equal to the product of the stiffness of the transducer (under short-circuited boundary conditions in this case, K_a) and the unconstrained piezoelectric expansion, δ[1]. From (4.27), note that if the electrodes of the transducer are short-circuited, $\delta = 0$, and the eigenvalue problem is

$$M\ddot{x} + (K + K_a bb^T)x = 0 \tag{4.28}$$

or alternatively in Laplace form

$$Ms^2x + (K + K_a bb^T)x = 0 \tag{4.29}$$

Thus, $K + K_a bb^T$ is the global stiffness matrix when the transducer is short-circuited.

4.4.2 Current source

If one considers the case of a pure current source, $R \to \infty$ in (4.26). Upon transforming in the Laplace domain and eliminating V between (4.26) and (4.25), one finds easily after some algebra that the governing equation is.

$$\left[Ms^2 + (K + K_a bb^T) + \frac{(nd_{33}K_a)^2}{C(1-k^2)}bb^T\right]x = bnd_{33}\frac{K_a}{1-k^2}\frac{I}{sC}$$

and, taking into account(4.8),

$$\left[Ms^2 + \left(K + \frac{K_a}{1-k^2}bb^T\right)\right]x = b\frac{K_a}{1-k^2}nd_{33}\frac{I}{sC} \tag{4.30}$$

[1] this is the *thermal analogy*

Note that I/s is the electric charge Q, and, by setting $f = 0$ in Equ.(4.9), one sees that $\delta = nd_{33}Q/C$ is the free expansion of the transducer under Q. Thus, as for a voltage source, the effect of the piezoelectric transducer on the structure can be represented by a pair of self-equilibrating piezoelectric forces; the magnitude is equal to the product of the free expansion δ and the stiffness of the transducer. Note, however, that the stiffness of the transducer involved here is that with open electrodes, $K_a/(1-k^2)$ [see Equ.(4.9) with $(Q = 0)$] .

If the electrodes of the transducer are open, setting $I = 0$ in (4.30), one obtains the eigenvalue problem

$$\left[Ms^2 + \left(K + \frac{K_a}{1-k^2}bb^T\right)\right] x = 0 \tag{4.31}$$

Thus, the global stiffness matrix when the transducer has open electrodes is $K + \dfrac{K_a}{1-k^2}bb^T$.

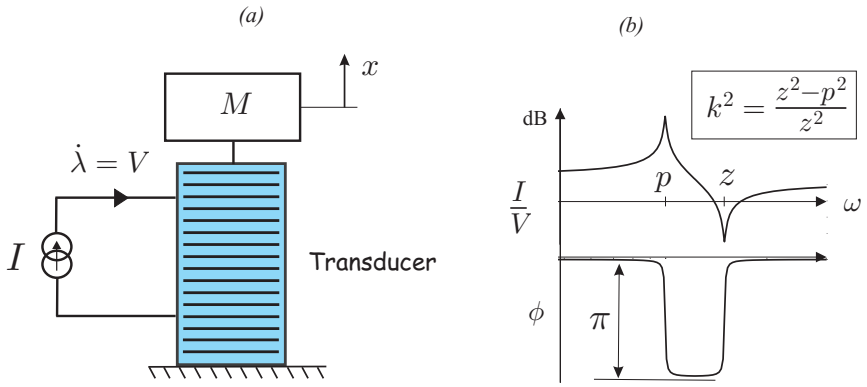

Fig. 4.7. (a) Elementary dynamical model of the piezoelectric transducer. (b) Typical admittance FRF of the transducer, in the vicinity of its natural frequency.

4.4.3 Admittance of the piezoelectric transducer

We have just seen that the effect of the piezoelectric transducer on the natural frequencies of the structure depends on its electrical boundary conditions; the stiffness is larger with open electrodes than with short-circuited electrodes, and the difference depends on the electromechanical coupling factor. Consider the system of Fig.4.7(a), which is the simplest

possible dynamical model of the piezoelectric transducer; from (4.25) and (4.26) (with $b = 1$), the governing equations are (in the Laplace domain):

$$(Ms^2 + K_a)x = K_a n d_{33} V$$
$$s[C(1 - k^2)V + n d_{33} K_a x] = I$$

Upon substituting x from the first to the second equation and using the definition (4.8) of the electromechanical coupling factor, we obtain the admittance (inverse of the impedance):

$$\frac{I}{V} = sC(1 - k^2)\left[\frac{Ms^2 + K_a/(1 - k^2)}{Ms^2 + K_a}\right] \tag{4.32}$$

The numerator vanishes at the transmission zeros ($\pm jz$) such that

$$z^2 = \frac{K_a/(1 - k^2)}{M} \tag{4.33}$$

z is the natural frequency with open electrodes. Similarly, the denominator vanishes at the poles ($\pm jp$) such that

$$p^2 = \frac{K_a}{M} \tag{4.34}$$

p is the natural frequency with short-circuited electrodes. This was expected since $I = 0$ with open electrodes and $V = 0$ with short-circuited electrodes. This is a general statement; we will see later that when the transducer is placed in a multiple d.o.f. structure, the poles and zeros in the admittance FRF are solutions of the eigenvalue problems (4.29) and (4.31), respectively. Combining (4.33) and (4.34), one finds that

$$\frac{z^2 - p^2}{z^2} = k^2 \tag{4.35}$$

which constitutes a practical way to determine the electromechanical coupling factor from admittance (or impedance) FRF measurements (Fig.4.7(b)).

4.4.4 Prestressed transducer

In most practical applications, the piezoelectric transducer is encapsulated inside a mechanical structure which protects it from the environment and introduces compression prestresses (the normal operating mode of the

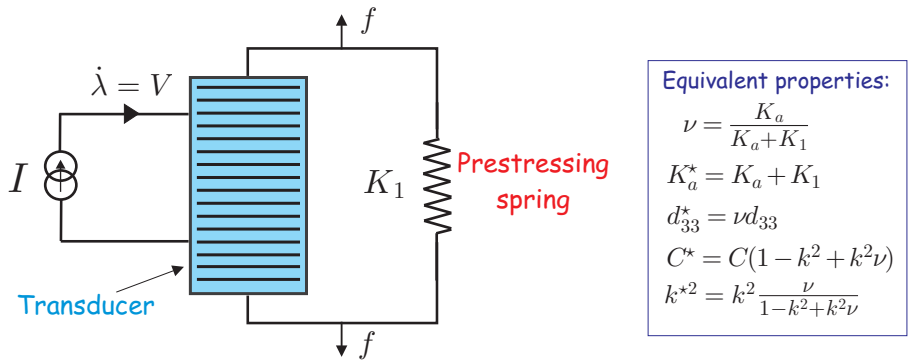

Fig. 4.8. Prestressed piezoelectric transducer.

stacked design is in compression); this can be represented a linear spring K_1 operating in parallel with the transducer (Fig.4.8). The equivalent properties of this transducer can be obtained from those of the original one by noting that the short-circuited stiffness now becomes $K_a^* = K_a + K_1$ while the constant volume capacitance remains unchanged, $C(1 - k^2)$. On the other hand, the joint coenergy function of the transducer and the spring reads

$$W_e^*(\Delta, V) = C(1-k^2)\frac{V^2}{2} + nd_{33}K_aV\Delta - (K_a + K_1)\frac{\Delta^2}{2} \tag{4.36}$$

(equal to the coenergy of the piezoelectric transducer minus the strain energy of the spring) and, from (4.16), the constitutive equations are

$$\left\{ \begin{array}{c} Q \\ f \end{array} \right\} = \left[\begin{array}{cc} C(1-k^2) & nd_{33}K_a \\ -nd_{33}K_a & K_a + K_1 \end{array} \right] \left\{ \begin{array}{c} V \\ \Delta \end{array} \right\} \tag{4.37}$$

Examining the behavior under $f = 0$, one finds

$$\Delta = nd_{33}\frac{K_a}{K_a + K_1}V = nd_{33}\,\nu\,V$$

$$Q = C(1-k^2)V + \frac{n^2d_{33}^2K_a^2}{K_a + K_1}V = C(1-k^2+k^2\nu)V$$

where $\nu = K_a/(K_a+K_1)$ is the *fraction of strain energy* in the transducer. Thus, the effective piezoelectric coefficient and the capacitance under $f = 0$ are respectively

$$d_{33}^* = \nu\, d_{33} \tag{4.38}$$

$$C^* = C(1 - k^2 + k^2\nu) \tag{4.39}$$

Using the definition (4.8) of the electromechanical coupling factor, one finds that it is reduced according to

$$k^{*2} = \frac{n^2 {d_{33}^*}^2 K_a^*}{C^*} = k^2 \frac{\nu}{1 - k^2 + k^2\nu} \tag{4.40}$$

It can be verified that, since the constant volume capacitance is not affected by the spring K_1,

$$C^*(1 - k^{*2}) = C(1 - k^2)$$

and that the stiffness with open electrodes is

$$\frac{K_a^*}{1 - k^{*2}} = \frac{K_a}{1 - k^2} + K_1$$

The value of k^{*2} can be determined experimentally as explained in the previous section.

4.4.5 Active enhancement of the electromechanical coupling

The electromechanical coupling factor is a very important material property, because it controls the conversion between the mechanical energy and the electrical energy. The role of k^2 in piezoelectric transformers and in passive damping of vibration by shunted piezoelectric transducers on passive electrical networks will be stressed later in this book. In this section, a way of increasing the electromechanical coupling factor by shunting a (synthetic) *negative* capacitance on the transducer (Fig.4.9) is examined, and the equivalent properties of the system are established.

Consider the system of Fig.4.9 where a piezoelectric transducer is in parallel with a negative capacitance. The joint coenergy is the sum of that of the piezoelectric transducer and that of the negative capacitance:

$$W_e^*(\dot{\lambda}) = \frac{1}{2}C(1 - k^2)\dot{\lambda}^2 + nd_{33}K_a\dot{\lambda}\Delta - \frac{1}{2}K_a\Delta^2 - \frac{1}{2}C_1\dot{\lambda}^2$$

The equivalent piezoelectric transducer is defined as having the same n, d_{33} and K_a (stiffness with short-circuited electrodes), and a capacitance C^* and electromechanical coupling factor k^* such that the coenergy function can be written as in Equ.(4.17):

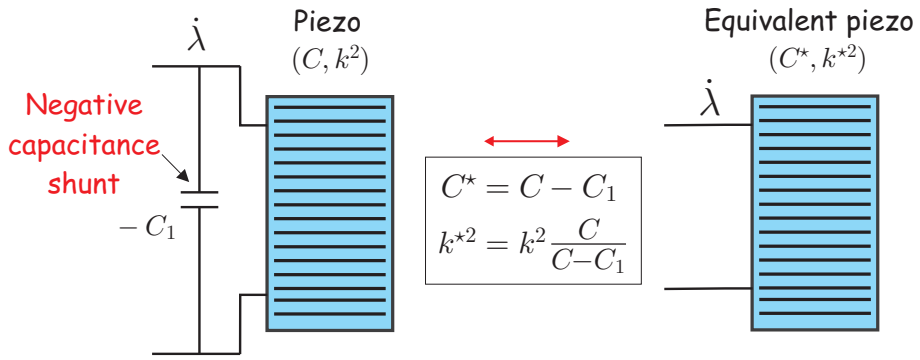

Fig. 4.9. Piezoelectric transducer shunted on a negative capacitance $-C_1$ and equivalent properties.

$$W_e^*(\dot{\lambda}) = \frac{1}{2}C^*(1-k^{*2})\dot{\lambda}^2 + nd_{33}K_a\dot{\lambda}\Delta - \frac{1}{2}K_a\Delta^2$$

This implies that

$$C^*(1-k^{*2}) = C(1-k^2) - C_1 \tag{4.41}$$

Besides, from the definition (4.8) of the electromechanical coupling factor, one must have

$$k^2 = \frac{n^2 d_{33}^2 K_a}{C} \qquad k^{*2} = \frac{n^2 d_{33}^2 K_a}{C^*}$$

which implies

$$Ck^2 = C^* k^{*2} \tag{4.42}$$

From (4.41) and (4.42), one finds the properties of the equivalent transducer:

$$C^* = C - C_1 \tag{4.43}$$

$$k^{*2} = k^2 \frac{C}{C - C_1} \tag{4.44}$$

Note that since $k^{*2} < 1$, one must have $C_1 < C(1-k^2)$. Thus if a perfect negative capacitance can be synthesized, the composite system formed by a piezoelectric transducer in parallel with a negative capacitance behaves like a equivalent piezoelectric transducer (Fig.4.9) with the reduced capacitance C^* given by (4.43) and the increased electromechanical coupling factor k^{*2} given by (4.44). In these circumstances, the negative capacitive shunting can be seen as a way of improving the conversion properties of the piezoelectric transducer. A negative capacitance can be synthesized as indicated in Fig.4.10; it is an active circuit involving an operational amplifier.

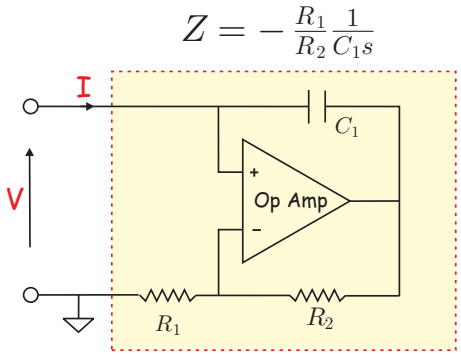

Fig. 4.10. Synthesis of a negative capacitance (from Philbrick Researches, Inc.)

4.5 Multiple transducer systems

Consider the case (Fig.4.11) where n_T identical piezoelectric transducers shunted with identical admittances Y_{SH} are imbedded into a structure (to be subsequently controlled in a decentralized manner, with identical control for all loops). Let $\lambda = (\lambda_1 \ldots, \lambda_i, \ldots)^T$ be the vector of flux linkage electrical coordinates and $\Delta = (\Delta_1 \ldots, \Delta_i, \ldots)^T$ the vector of transducer extensions; Δ can be expressed in global coordinates as

$$\Delta = B^T x \tag{4.45}$$

where B is the appropriate projection matrix. The Lagrangian of the system is

$$L = T^* - V + \sum_{i=1}^{n_T} W_e^*(i) \tag{4.46}$$

where T^* and V refer to the structure and the other term is the sum of the coenergies of all the transducers.

$$L = \frac{1}{2}\dot{x}^T M\dot{x} - \frac{1}{2}x^T Kx + \sum_{i=1}^{n_T}\left[C(1-k^2)\frac{\dot{\lambda}_i^2}{2} + nd_{33}K_a\dot{\lambda}_i\Delta_i - \frac{K_a}{2}\Delta_i^2\right]$$

$$= \frac{1}{2}\dot{x}^T M\dot{x} - \frac{1}{2}x^T Kx + \frac{1}{2}C(1-k^2)\dot{\lambda}^T\dot{\lambda} + nd_{33}K_a\dot{\lambda}^T\Delta - \frac{1}{2}K_a\Delta^T\Delta$$

Combining with (4.45), we can write the Lagrangian

$$L = \frac{1}{2}\dot{x}^T M\dot{x} - \frac{1}{2}x^T(K + K_a BB^T)x + \frac{1}{2}C(1-k^2)\dot{\lambda}^T\dot{\lambda} + nd_{33}K_a\dot{\lambda}^T B^T x \tag{4.47}$$

The virtual work of non conservative forces is

$$\delta W_{nc} = \delta\lambda^T I - Y_{SH}\delta\lambda^T\dot{\lambda} \tag{4.48}$$

In these equations, λ and I are vectors of dimension n_T while $C, K_a, Y_{SH}, \ldots$ are scalar quantities, common to all loops. From (4.47) and (4.48), the Lagrange's equations read (with $V = \dot{\lambda}$)

$$M\ddot{x} + (K + K_a B B^T)x = nK_a d_{33} BV \tag{4.49}$$

$$\frac{d}{dt}[C(1-k^2)V + nd_{33}K_a B^T x] + Y_{SH}V = I \tag{4.50}$$

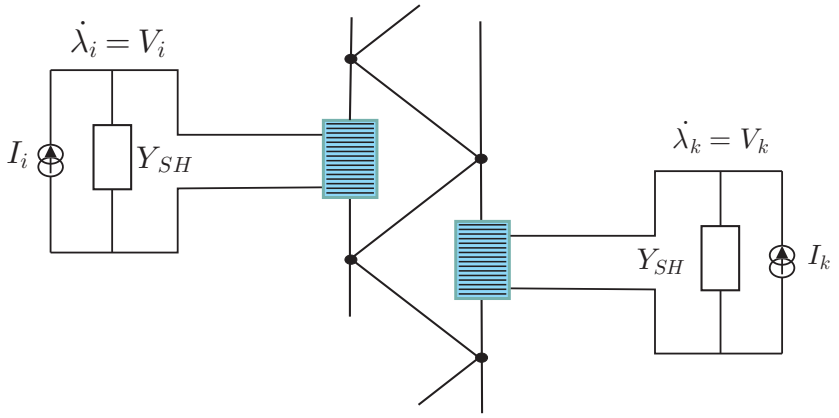

Fig. 4.11. Structure equipped with multiple transducers.

4.6 General piezoelectric structure

The Lagrangian of a structure involving a finite number of discrete piezoelectric transducers can be written in the general form

$$L = \frac{1}{2}\dot{x}^T M\dot{x} - \frac{1}{2}x^T K_{xx}x + \frac{1}{2}\dot{\lambda}^T C_{\phi\phi}\dot{\lambda} + \dot{\lambda}^T K_{\phi x}x \tag{4.51}$$

[compare with (4.47)]. In this equation, M is the mass matrix, K_{xx} is the stiffness matrix (including the mechanical part of the transducers with short circuited electrical boundary conditions), $C_{\phi\phi}$ is the matrix of capacitance of the transducers (for fixed displacements) and $K_{\phi x}$ is the

coupling matrix of piezoelectric properties, relating the mechanical and electrical variables.

If the transducers are connected to voltage sources $\phi = \dot{\lambda}$, the flux linkages are not generalized coordinates, $\delta W_{nc} = f^T \delta x$, and the Lagrange equation reads

$$M\ddot{x} + K_{xx}x - K_{\phi x}^T \phi = f \tag{4.52}$$

$K_{\phi x}^T \phi$ are the self-equilibrating piezoelectric loads associated with the voltage distribution ϕ. The eigenvalue problem,

$$\left(Ms^2 + K_{xx}\right) x = 0 \tag{4.53}$$

corresponds to short-circuited electrical boundary conditions. On the other hand, if the transducers are connected to current sources I and a passive network of admittance matrix Y,

$$\delta W_{nc} = f^T \delta x + I^T \delta\lambda - \dot{\lambda}^T Y\, \delta\lambda \tag{4.54}$$

or alternatively, for a resistive network, the dissipation function may be used:

$$D = \frac{1}{2}\dot{\lambda}^T Y \dot{\lambda} \tag{4.55}$$

In this case, the Lagrange equations are

$$x: \qquad M\ddot{x} + K_{xx}x - K_{\phi x}^T \dot{\lambda} = f \tag{4.56}$$

$$\lambda: \qquad C_{\phi\phi}\ddot{\lambda} + K_{\phi x}\dot{x} + Y\dot{\lambda} = I \tag{4.57}$$

In the Laplace domain, with the notation $\phi = \dot{\lambda}$,

$$Ms^2 x + K_{xx}x - K_{\phi x}^T \phi = f \tag{4.58}$$

$$C_{\phi\phi}\phi + K_{\phi x}x + Y\phi/s = I/s \tag{4.59}$$

If $Y = 0$ (no shunted resistor network), ϕ can be substituted from (4.59) into (4.58), leading to

$$\left[Ms^2 + \left(K_{xx} + K_{\phi x}^T C_{\phi\phi}^{-1} K_{\phi x}\right)\right] x = f + K_{\phi x}^T C_{\phi\phi}^{-1}\, I/s \tag{4.60}$$

Once again, $K_{\phi x}^T C_{\phi\phi}^{-1}\, I/s$ are the self-equilibrating piezoelectric loads associated with the electric charge I/s. The stiffness matrix $K_{xx} + K_{\phi x}^T C_{\phi\phi}^{-1} K_{\phi x}$ corresponds to open electrodes electrical boundary conditions, with eigenvalue problem

$$\left[Ms^2 + (K_{xx} + K_{\phi x}^T C_{\phi\phi}^{-1} K_{\phi x})\right] x = 0 \tag{4.61}$$

4.7 Piezoelectric material

4.7.1 Constitutive relations

The constitutive equations of a general piezoelectric material are

$$T_{ij} = c_{ijkl}^E S_{kl} - e_{kij} E_k \tag{4.62}$$

$$D_i = e_{ikl} S_{kl} + \varepsilon_{ik}^S E_k \tag{4.63}$$

where T_{ij} and S_{kl} are the components of the stress and strain tensors, respectively, c_{ijkl}^E are the elastic constants under constant electric field (Hooke's tensor), e_{ikl} the piezoelectric constants (in $Coulomb/m^2$) and ε_{ij}^S the dielectric constant under constant strain. These formulae use classical tensor notations, where all indices $i, j, k, l = 1, 2, 3$, and there is a summation on all repeated indices. The above equations are a generalization of (4.4), with S_{kl} and E_j as independent variables; they can be written alternatively with T_{kl} and E_j as independent variables:

$$S_{ij} = s_{ijkl}^E T_{kl} + d_{kij} E_k \tag{4.64}$$

$$D_i = d_{ikl} T_{kl} + \varepsilon_{ik}^T E_k \tag{4.65}$$

where s_{ijkl}^E is the tensor of compliance under constant electric field, d_{ikl} the piezoelectric constants (in $Coulomb/Newton$) and ε_{ik}^T the dielectric constant under constant stress. The difference between the properties under constant stress and under constant strain has been stressed in section 4.3. As an alternative to the above tensor notations, it is customary to use the engineering vector notations

$$T = \begin{Bmatrix} T_{11} \\ T_{22} \\ T_{33} \\ T_{23} \\ T_{31} \\ T_{12} \end{Bmatrix} \qquad S = \begin{Bmatrix} S_{11} \\ S_{22} \\ S_{33} \\ 2S_{23} \\ 2S_{31} \\ 2S_{12} \end{Bmatrix} \tag{4.66}$$

With these notations, Equ.(4.62) (4.63) can be written in matrix form

$$\{T\} = [c]\{S\} - [e]\{E\}$$

$$\{D\} = [e]^T\{S\} + [\varepsilon]\{E\} \tag{4.67}$$

and (4.64), (4.65),

$$\begin{aligned} \{S\} &= [s]\{T\} + [d]\{E\} \\ \{D\} &= [d]^T\{T\} + [\varepsilon]\{E\} \end{aligned} \tag{4.68}$$

where the superscript T stands for the transposed; the other superscripts have been omitted, but can be guessed from the equation itself. Assuming that the coordinate system coincides with the orthotropy axes of the material and that the direction of polarization coincides with direction 3, the explicit form of (4.68) is:

Actuation:

$$\begin{Bmatrix} S_{11} \\ S_{22} \\ S_{33} \\ 2S_{23} \\ 2S_{31} \\ 2S_{12} \end{Bmatrix} = \begin{bmatrix} s_{11} & s_{12} & s_{13} & 0 & 0 & 0 \\ s_{12} & s_{22} & s_{23} & 0 & 0 & 0 \\ s_{13} & s_{23} & s_{33} & 0 & 0 & 0 \\ 0 & 0 & 0 & s_{44} & 0 & 0 \\ 0 & 0 & 0 & 0 & s_{55} & 0 \\ 0 & 0 & 0 & 0 & 0 & s_{66} \end{bmatrix} \begin{Bmatrix} T_{11} \\ T_{22} \\ T_{33} \\ T_{23} \\ T_{31} \\ T_{12} \end{Bmatrix} + \begin{bmatrix} 0 & 0 & d_{31} \\ 0 & 0 & d_{32} \\ 0 & 0 & d_{33} \\ 0 & d_{24} & 0 \\ d_{15} & 0 & 0 \\ 0 & 0 & 0 \end{bmatrix} \begin{Bmatrix} E_1 \\ E_2 \\ E_3 \end{Bmatrix} \tag{4.69}$$

Sensing:

$$\begin{Bmatrix} D_1 \\ D_2 \\ D_3 \end{Bmatrix} = \begin{bmatrix} 0 & 0 & 0 & 0 & d_{15} & 0 \\ 0 & 0 & 0 & d_{24} & 0 & 0 \\ d_{31} & d_{32} & d_{33} & 0 & 0 & 0 \end{bmatrix} \begin{Bmatrix} T_{11} \\ T_{22} \\ T_{33} \\ T_{23} \\ T_{31} \\ T_{12} \end{Bmatrix} + \begin{bmatrix} \varepsilon_{11} & 0 & 0 \\ 0 & \varepsilon_{22} & 0 \\ 0 & 0 & \varepsilon_{33} \end{bmatrix} \begin{Bmatrix} E_1 \\ E_2 \\ E_3 \end{Bmatrix} \tag{4.70}$$

Typical values of the piezoelectric constants for piezoceramics (PZT) and piezopolymers (PVDF) are given Table 4.1. Examining the actuator equation (4.69), we note that when an electric field E_3 is applied parallel to the direction of polarization, an extension is observed along the same direction; its amplitude is governed by the piezoelectric coefficient d_{33}. Similarly, a shrinkage is observed along the directions 1 and 2 perpendicular to the electric field, the amplitude of which is controlled by d_{31} and d_{32}, respectively (shrinkage, because d_{31} and d_{32} are negative). Piezoceramics have an isotropic behaviour in the plane, $d_{31} = d_{32}$; on the con-

trary, when PVDF is polarized under stress, its piezoelectric properties are highly anisotropic, with $d_{31} \sim 5d_{32}$. Equation (4.69) also indicates that an electric field E_1 normal to the direction of polarization 3 produces a shear deformation S_{13}, controlled by the piezoelectric constant d_{15} (similarly, a shear deformation S_{23} occurs if an electric field E_2 is applied; it is controlled by d_{24}). An interesting feature of this type of actuation is that d_{15} is the largest of all piezoelectric coefficients (500 $10^{-12}C/N$ for PZT). The various modes of operation associated with the piezoelectric coefficients d_{33}, d_{31} and d_{15} are illustrated in Fig.4.12.

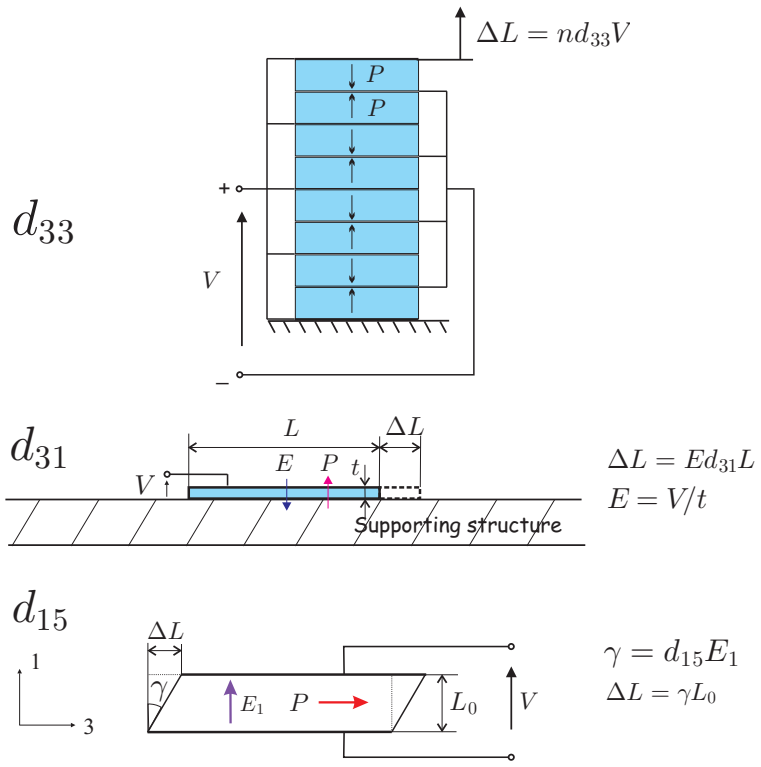

Fig. 4.12. Actuation modes of piezoelectric actuators. P indicates the direction of polarization.

4.7.2 Coenergy density function

With an approach parallel to that of the discrete transducer in section 4.3, the total stored energy density in a unit volume of material is the

sum of the mechanical work and the electrical work,

$$dW_e(S,D) = \{dS\}^T\{T\} + \{dD\}^T\{E\} \tag{4.71}$$

[compare with (4.10)]. For a conservative system, $W_e(S,D)$ can be obtained by integrating (4.71) from the reference state to the state (S,D); since the system is conservative, the integration can be done along any path from $(0,0)$ to (S,D). Upon differentiating $W_e(S,D)$ and comparing with (4.71) we recover the constitutive equations

$$\{T\} = \left\{\frac{\partial W_e}{\partial S}\right\} \qquad \text{and} \qquad \{E\} = \left\{\frac{\partial W_e}{\partial D}\right\} \tag{4.72}$$

which are the distributed counterparts of (4.12). The *coenergy density function* is defined by the Legendre transformation

$$W_e^*(S,E) = \{E\}^T\{D\} - W_e(S,D) \tag{4.73}$$

[compare with (4.14)]. The total differential is

$$\begin{aligned} dW_e^* &= \{dE\}^T\{D\} + \{E\}^T\{dD\} - \{dS\}^T\left\{\frac{\partial W_e}{\partial S}\right\} - \{dD\}^T\left\{\frac{\partial W_e}{\partial D}\right\} \\ &= \{dE\}^T\{D\} - \{dS\}^T\{T\} \end{aligned} \tag{4.74}$$

where (4.72) have been used. It follows that

$$\{D\} = \left\{\frac{\partial W_e^*}{\partial E}\right\} \qquad \text{and} \qquad \{T\} = -\left\{\frac{\partial W_e^*}{\partial S}\right\} \tag{4.75}$$

Substituting (4.67) into (4.74),

$$dW_e^* = \{dE\}^T[e]^T\{S\} + \{dE\}^T[\varepsilon]\{E\} - \{dS\}^T[c]\{S\} + \{dS\}^T[e]\{E\} \tag{4.76}$$

which is the total differential of

$$W_e^*(S,E) = \frac{1}{2}\{E\}^T[\varepsilon]\{E\} + \{S\}^T[e]\{E\} - \frac{1}{2}\{S\}^T[c]\{S\} \tag{4.77}$$

[compare with (4.17)]. The first term in the right hand side is the electrical coenergy stored in the dielectric material (ε is the matrix of permittivity under constant strain); the third term is the strain energy stored in the elastic material (c is the matrix of elastic constants under constant electric

Material properties	PZT	PVDF
Piezoelectric constants		
$d_{33}(10^{-12}C/N$ or $m/V)$	300	−25
$d_{31}(10^{-12}C/N$ or $m/V)$	−150	*uni-axial*: $d_{31} = 15$ $d_{32} = 3$ *bi-axial*: $d_{31} = d_{32} = 3$
$d_{15}(10^{-12}C/N$ or $m/V)$	500	0
$e_{31} = d_{31}/s^E(C/m^2)$	−7.5	0.025
Electromechanical coupling factor		
k_{33}	0.7	
k_{31}	0.3	∼0.1
k_{15}	0.7	
Dielectric constant $\varepsilon^T/\varepsilon_0$ $(\varepsilon_0 = 8.85\ 10^{-12}F/m)$	1800	10
Max. Electric field (V/mm)	2000	$5\ 10^5$
Max. operating (Curie) T° $(^\circ C)$	80°−150°	90°
Density (Kg/m^3)	7600	1800
Young's modulus $1/s^E$ (GPa)	50	2.5
Maximum stress (MPa)		
Traction	80	200
Compression	600	200
Maximum strain	Brittle	50%

Table 4.1. Typical properties of piezoelectric materials.

field); the second term is the piezoelectrical coenergy, which generalizes (4.18) in three dimensions. Taking the partial derivatives (4.75), one recovers the constitutive equations (4.67). In that sense, the analytical form of the coenergy density function, (4.77) together with (4.75), can be seen as an alternative definition of the linear piezoelectricity. In the literature,

$$H(S, E) = -W_e^*(S, E) \tag{4.78}$$

is known as the *electric enthalpy density*.

4.8 Hamilton's principle

We follow a displacement/flux linkage formulation as in section 3.3.2. The admissibility requirements are, as before, that the virtual displacements δu_i must be compatible with the kinematics of the system, and the admissible flux linkage variations $\delta\lambda_k$ must be compatible with Kirchhoff's voltage rule. The variational indicator is

$$\text{V.I.} = \int_{t_1}^{t_2} [\delta(T^* + W_e^*) + \delta W_{nc}]dt = 0 \tag{4.79}$$

$T^* + W_e^*$ is the Lagrangian. The actual path is that which cancels the variational indicator (4.79) with respect to all admissible variations δu_i and $\delta\lambda_k$ of the path between t_1 and t_2, where $\delta u_i(t_1) = \delta u_i(t_2) = \delta\lambda_k(t_1) = \delta\lambda_k(t_2) = 0$.

$$T^* = \frac{1}{2}\int_\Omega \varrho\{\dot{u}\}^T\{\dot{u}\}d\Omega \tag{4.80}$$

and

$$W_e^* = \frac{1}{2}\int_\Omega \left(\{E\}^T[\varepsilon]\{E\} + 2\{S\}^T[e]\{E\} - \{S\}^T[c]\{S\}\right) d\Omega \tag{4.81}$$

The virtual work of nonconservative forces has contributions from external forces and applied currents; for discrete systems,

$$\delta W_{nc} = \sum_i f_i\delta x_i + \sum_k I_k\delta\lambda_k \tag{4.82}$$

For continuous systems, the virtual work of external forces has contributions from volume forces and surface forces.

$$\int_\Omega f_i\delta u_i d\Omega + \int_{S_2} t_i\delta u_i dS \tag{4.83}$$

(S_2 is the part of surface where external forces are applied). The virtual work of external applied currents can be integrated by part with respect to time:

$$\int_{t_1}^{t_2}\sum_k I_k\delta\lambda_k\, dt = Q_k\delta\lambda_k\Big]_{t_1}^{t_2} - \int_{t_1}^{t_2} Q_k\delta\dot{\lambda}_k\, dt \tag{4.84}$$

where, Q_k is the electric charge associated with I_k, $\dot{Q}_k = I_k$. Taking into account that $\delta\lambda_k(t_1) = \delta\lambda_k(t_2) = 0$ and using the notation $\phi_k = \dot{\lambda}_k$ for the

potential associated with the flux linkage λ_k, we can write the electrical part of δW_{nc}

$$\delta W_{nc} = -Q_k \, \delta\phi_k \tag{4.85}$$

For continuous systems, if surface charges are prescribed over S_3, this can be rewritten

$$-\int_{S_3} \bar{\sigma} \, \delta\phi \, dS \tag{4.86}$$

where $\bar{\sigma}$ is the surface charge density. Putting together (4.83)-(4.86), we find

$$\delta W_{nc} = \int_\Omega f_i \delta u_i d\Omega + \int_{S_2} t_i \delta u_i dS - Q_k \delta\phi_k - \int_{S_3} \bar{\sigma} \, \delta\phi \, dS \tag{4.87}$$

The contribution of the kinetic coenergy to the variational indicator can be rewritten

$$\begin{aligned} \int_{t_1}^{t_2} \delta T^* dt &= \int_{t_1}^{t_2} dt \int_\Omega \varrho \, \delta\dot{u}_i \dot{u}_i \, d\Omega \\ &= \int_\Omega \varrho \delta u_i \dot{u}_i \Big]_{t_1}^{t_2} d\Omega - \int_{t_1}^{t_2} dt \int_\Omega \varrho \, \delta u_i \ddot{u}_i \, d\Omega \end{aligned} \tag{4.88}$$

The first term vanishes because $\delta u(t_1) = \delta u(t_2) = 0$. The coenergy term δW_e^* reads

$$\begin{aligned} \delta W_e^* &= \int_\Omega (\{\delta E\}^T [\varepsilon] \{E\} + \{\delta E\}^T [e]^T \{S\} + \{\delta S\}^T [e] \{E\} - \{\delta S\}^T [c] \{S\}) d\Omega \\ &= \int_\Omega \left[\{\delta E\}^T \Big([\varepsilon] \{E\} + [e]^T \{S\} \Big) + \{\delta S\}^T \Big([e] \{E\} - [c] \{S\} \Big) \right] d\Omega \end{aligned}$$

and, taking into account the constitutive equations (4.67)

$$\begin{aligned} \delta W_e^* &= \int_\Omega \Big(\{\delta E\}^T \{D\} - \{\delta S\}^T \{T\} \Big) \, d\Omega \\ &= \int_\Omega \left(\delta E_i D_i - \delta S_{ij} T_{ij} \right) d\Omega \end{aligned} \tag{4.89}$$

Taking into account the relationship between the electric field and the electric potential, on one hand, and that between the strain and the displacement on the other hand;

$$E_i = -\phi_{,i}$$

and

$$S_{ij} = \frac{1}{2}(u_{i,j} + u_{j,i})$$

where the subscript notation, i is used for the partial derivative $\dfrac{\partial}{\partial x_i}$.

$$\begin{aligned}\delta W_e^* &= \int_\Omega (-\delta\phi_{,i} D_i - \delta u_{i,j} T_{ij})\, d\Omega \\ &= \int_\Omega [-(\delta\phi D_i)_{,i} + \delta\phi D_{i,i} - (\delta u_i T_{ij})_{,j} + \delta u_i T_{ij,j}]\, d\Omega\end{aligned}$$

Upon using the *divergence theorem*,

$$\int_\Omega \frac{\partial A_i}{\partial x_i}\, d\Omega = \int_\Omega A_{i,i}\, d\Omega = \int_S A_i n_i\, dS \tag{4.90}$$

where n_i is the outward normal to the surface, one finds

$$\delta W_e^* = \int_\Omega (\delta\phi D_{i,i} + \delta u_i T_{ij,j})\, d\Omega - \int_S (\delta\phi D_i n_i + \delta u_i T_{ij} n_j) dS \tag{4.91}$$

Combining (4.87),(4.88) and (4.91), the variational indicator reads

$$\begin{aligned}0 = &\int_\Omega [\delta\phi\, D_{i,i} + \delta u_i(-\varrho\ddot{u}_i + T_{ij,j} + f_i)]\, d\Omega \\ &- \int_S [\delta\phi(D_i n_i + \bar{\sigma}) + \delta u_i(T_{ij} n_j - t_i)]\, dS\end{aligned} \tag{4.92}$$

Thus, since the virtual variations $\delta\phi$ and the virtual displacements δx_i are arbitrary within the volume Ω, one must have

$$D_{i,i} = \mathrm{div}\{D\} = 0 \tag{4.93}$$

which is *Gauss's law* (we have assumed that there is no volume charge within the dielectric medium), and

$$T_{ij,j} + f_i = \varrho\ddot{u}_i \tag{4.94}$$

which is mechanical equilibrium equation with volume forces f_i.
On the external surface,

$$T_{ij} n_j = t_i \qquad \text{on} \quad S_2 \tag{4.95}$$

$$D_i n_i = -\bar{\sigma} \qquad \text{on} \quad S_3 \tag{4.96}$$

The above discussion is somewhat tedious, but it shows that cancelling the variational indicator (4.79) is equivalent to enforcing Gauss's equation (4.93) and the dynamic equilibrium (4.94) within the volume of the material, and the natural boundary conditions on the part of the surface where external loads and electric charges are applied, (4.95) and (4.96). Hamilton's principle is the starting point for the finite element formulation of piezoelectric structures.

4.9 Rosen's piezoelectric transformer

Piezoelectric transformers were first introduced by Rosen in 1956; they have been very successful for low power applications such as power supply of laptop computers. Due to the high energy density of piezoelectric materials, the high electromechanical coupling factors and the high quality factor of the mechanical resonance (low damping), they tend to be lighter and more efficient than wire wound transformers whose efficiency tends to decrease rapidly as the size is reduced. Besides, they are free from electromagnetic interference and the solid-state nature of piezoelectric transformers is the key to mass production.

The principle of Rosen's piezoelectric transformer is shown in Fig.4.13; the left side is the driving section; the input a.c. voltage generates an axial vibration thanks to the d_{31} coefficient. The axial vibration is transmitted to the power generating section which is polarized in the axial direction and generates the output voltage thanks to the d_{33} coefficient. The system is supposed to work at an axial resonance of the free-free mechanical system. We analyze this system as an application of Lagrange's equation, using the Rayleigh-Ritz method discussed in section 1.10. We assume that

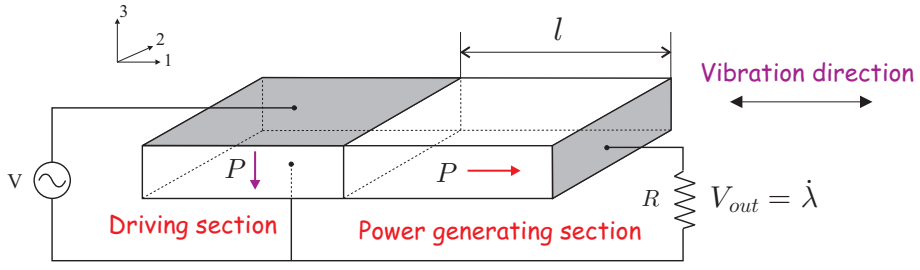

Fig. 4.13. Principle of Rosen's piezoelectric transformer. P indicates the direction of polarization.

the system works at the resonance of the second axial mode and that the axial displacements are close to those of a uniform bar (Fig.4.14)

$$u = l\, z(t)\, \phi(x) = l\, z(t)\, \cos\frac{\pi x}{l} \tag{4.97}$$

The system has one generalized mechanical coordinate, the amplitude $z(t)$ of the assumed mode, and one generalized electrical coordinate, the flux linkage λ associated with the output voltage, $\dot{\lambda} = V_{out}$. Following the general approach of Hamilton's principle, we write the Lagrangian as the sum of the kinetic coenergy T^* and the coenergy function W_e^* defined respectively by (4.80) and (4.81)

$$L = T^* + W_e^* = T^* + W_{e,left}^* + W_{e,right}^* \tag{4.98}$$

where the contributions of the driving section and the power generating section to the coenergy function have been separated. T^* can be calculated for the entire system starting from the assumed displacement field (4.97)

$$\begin{aligned} \dot{u} &= l\dot{z}\, \phi(x) = l\dot{z} \cos\frac{\pi x}{l} \\ T^* &= \frac{1}{2}\int_0^{2l} \varrho A \dot{u}^2 dx = \frac{\varrho A}{2} l^2 \dot{z}^2 \int_0^{2l} \phi^2(x) dx = \frac{\varrho A}{2} l^3 \dot{z}^2 \end{aligned} \tag{4.99}$$

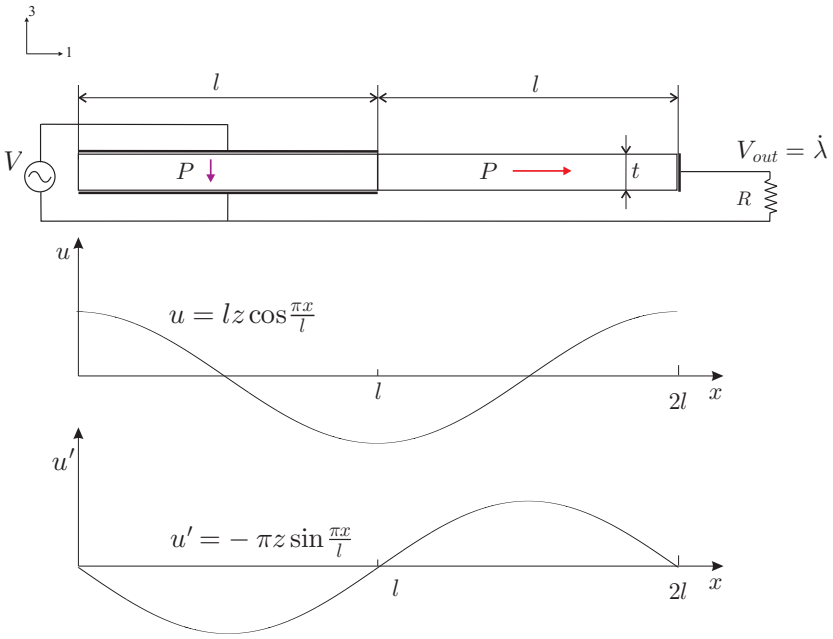

Fig. 4.14. Assumed axial displacements in the transformer.

where A is the cross-section and ϱ the mass density of the bar. Since the electrical states of the driving section and the power generating section; are different, the coenergy function is partitioned:

(a) Driving section

The input voltage V is applied between electrodes which extend over the entire length of the driving section; we therefore assume that the electric field E_3 is uniform over the entire volume, $E_3 = V/t$. From (4.81),

$$W^*_{e,left} = \int_0^l A(\frac{1}{2}\varepsilon^S_{33}E_3^2 + S_1 e_{31}E_3 - \frac{1}{2}c^E_{11}S_1^2)dx \tag{4.100}$$

with

$$E_3 = \frac{V}{t} \qquad\qquad S_1 = u' = l\,\phi'(x)z \tag{4.101}$$

Note that E_3 is the electric field in direction 3 while S_1 is the strain along the axis of the bar. Substituting (4.101) into (4.100) and integrating over $[0, l]$, one gets

$$W^*_{e,left} = \frac{Al}{2}\varepsilon^S_{33}\left(\frac{V}{t}\right)^2 - 2Al\,e_{31}\left(\frac{V}{t}\right)z - Al\frac{\pi^2}{4}c^E_{11}z^2 \tag{4.102}$$

(b) Power generating section

We assume that all quantities are constant over the cross-section of the bar. According to the constitutive equation (4.63)

$$D_1 = \varepsilon^S_{33}E_1 + e_{33}S_1$$

or

$$E_1 = \frac{1}{\varepsilon^S_{33}}D_1 - \frac{e_{33}}{\varepsilon^S_{33}}S_1 \tag{4.103}$$

where the use of the subscript 3 in the properties reflects the fact that, in the power generating section, the polarization is along the axis 1. On the other hand, since there is no volume charge in the dielectric material, Gauss's law states that $\mathrm{div}\{D\} = 0$, that is

$$\frac{\partial D_1}{\partial x} = 0$$

Thus D_1 is constant along the power generating section. Integrating (4.103), one gets

$$V_{out} = \dot{\lambda} = \int_l^{2l} -E_1 dx = -\frac{D_1 l}{\varepsilon^S_{33}} + \frac{e_{33}}{\varepsilon^S_{33}}\int_l^{2l} S_1 dx$$

and, upon using (4.101),

$$V_{out} = \dot{\lambda} = -\frac{D_1 l}{\varepsilon_{33}^S} + \frac{e_{33}}{\varepsilon_{33}^S} 2\, l\, z$$

Substituting D_1 from this expression into (4.103), one gets the electric field in terms of the generalized variables z and $\dot{\lambda}$:

$$E_1 = -\frac{\dot{\lambda}}{l} + \frac{e_{33}}{\varepsilon_{33}^S}(2 - l\phi')z \tag{4.104}$$

The coenergy density is in this case

$$W^*_{e,right} = \frac{1}{2}\varepsilon_{33}^S E_1^2 + S_1 e_{33} E_1 - \frac{1}{2} c_{11}^E S_1^2 \tag{4.105}$$

where, once again, the subscripts reflects the fact that the polarization is along axis 1; upon substituting S_1 from (4.101) and E_1 from (4.104), and integrating from l to $2l$, one finds

$$W^*_{e,right} = \frac{Al}{2}\varepsilon_{33}^S \left(\frac{\dot{\lambda}}{l}\right)^2 - 2Ale_{33}\left(\frac{\dot{\lambda}}{l}\right) z + Alz^2 \frac{e_{33}^2}{\varepsilon_{33}^S}\left(2 - \frac{\pi^2}{4}\right) - Al\frac{\pi^2}{4} c_{11}^E z^2 \tag{4.106}$$

Upon adding the various contributions (4.99),(4.102) and (4.106), the Lagrangian reads

$$\begin{aligned} L &= T^* + W^*_{e,left} + W^*_{e,right} \\ &= \varrho\frac{Al^3}{2}\dot{z}^2 + \frac{Al}{2}\varepsilon_{33}^S\left(\frac{V}{t}\right)^2 - 2A\, l\, e_{31}\left(\frac{V}{t}\right) z - \frac{Al\pi^2}{4} c_{11}^E z^2 + \frac{Al}{2}\varepsilon_{33}^s\left(\frac{\dot{\lambda}}{l}\right)^2 \\ &\quad -2A\, l\, e_{33}\left(\frac{\dot{\lambda}}{l}\right) z + A\, l\, \frac{e_{33}^2}{\varepsilon_{33}^s}\left(2 - \frac{\pi^2}{4}\right) z^2 - \frac{Al\pi^2}{4} c_{11}^E z^2 \end{aligned} \tag{4.107}$$

The dissipation function is

$$D = \frac{\dot{\lambda}^2}{2R} \tag{4.108}$$

The partial derivatives of the Lagrangian with respect to z are:

$$\frac{\partial L}{\partial \dot{z}} = \varrho A l^3 \dot{z}$$

$$\frac{\partial L}{\partial z} = -2A\,l\,e_{31}\left(\frac{V}{t}\right) - 2A\,l\,e_{33}\left(\frac{\dot{\lambda}}{l}\right) + A\,l\frac{e_{33}^2}{\varepsilon_{33}^s}\left(4-\frac{\pi^2}{2}\right)z - A\,l\pi^2 c_{11}^E z$$

The Lagrange equation relative to z is

$$\varrho l^2\ddot{z} + \pi^2 c_{11}^E z - \frac{e_{33}^2}{\varepsilon_{33}^S}\left(4-\frac{\pi^2}{2}\right)z + 2\,e_{33}\left(\frac{\dot{\lambda}}{l}\right) = -2\,e_{31}\left(\frac{V}{t}\right) \qquad (4.109)$$

The partial derivatives of L with respect to the generalized coordinate λ are

$$\frac{\partial L}{\partial \dot{\lambda}} = A\varepsilon_{33}^s\frac{\dot{\lambda}}{l} - 2Ae_{33}z$$

$$\frac{\partial L}{\partial \lambda} = 0 \qquad\qquad \frac{\partial D}{\partial \dot{\lambda}} = \frac{\dot{\lambda}}{R}$$

and the Lagrange equation relative to the coordinate λ is

$$\frac{A}{l}\varepsilon_{33}^S\ddot{\lambda} - 2Ae_{33}\dot{z} + \frac{\dot{\lambda}}{R} = 0 \qquad (4.110)$$

With open output electrodes, $R \to \infty$. Substituting $V_{out} = \dot{\lambda}$ and transforming into the Laplace domain,

$$\varepsilon_{33}^s\,s\,\frac{V_{out}}{l} = 2e_{33}\,s\,z$$

or

$$\frac{V_{out}}{l} = \frac{2e_{33}}{\varepsilon_{33}^S}z \qquad (4.111)$$

Substituting into (4.109),

$$\varrho l^2 s^2 z + \left(\pi^2 c_{11}^E + \frac{\pi^2}{2}\frac{e_{33}^2}{\varepsilon_{33}^S}\right)z = -2e_{31}\left(\frac{V}{t}\right) \qquad (4.112)$$

or

$$\varrho l^2 s^2 z + a\,c_{11}^E z = -2e_{31}\left(\frac{V}{t}\right) \qquad (4.113)$$

where the factor

$$a = \pi^2 + \frac{\pi^2}{2}\frac{e_{33}^2}{c_{11}^E\varepsilon_{33}^S} = \pi^2\left[1 + \frac{k_{33}^2}{2(1-k_{33}^2)}\right] = \pi^2\frac{1-k_{33}^2/2}{1-k_{33}^2} \qquad (4.114)$$

accounts for the increase in stiffness due to the piezoelectric transformation. In writing (4.114), we have used the fact that

$$\varepsilon_{33}^S = \varepsilon_{33}^T(1 - k_{33}^2) \qquad \text{and} \qquad k_{33}^2 = \frac{e_{33}^2}{c_{11}^E \varepsilon_{33}^T} \tag{4.115}$$

(c_{11}^E is in fact c_{33}^E in the power generating section). The natural frequency of the system is

$$\omega_n^2 = \frac{c_{11}^E a}{\varrho l^2} \tag{4.116}$$

and (4.113) can be rewritten

$$z = \frac{-2e_{31}\,(V/t)}{a\,c_{11}^E\,(1 + s^2/\omega_n^2)} \tag{4.117}$$

This is the transfer function between the input voltage V and the modal amplitude z; it has been obtained by neglecting the structural damping in the system. In fact, the transformer is supposed to operate at the mechanical resonance ω_n, where the damping cannot be ignored. Near the resonance, (4.117) must be replaced by

$$z = \frac{-2e_{31}\,(V/t)}{a\,c_{11}^E\,(1 + 2\xi s/\omega_n + s^2/\omega_n^2)} \tag{4.118}$$

The amplitude at resonance is

$$z = \frac{2\,e_{31}}{a\,c_{11}^E} Q_m \frac{V}{t} \tag{4.119}$$

where $Q_m = 1/2\xi$ is known as the *Quality factor* of the oscillation (it represents the amplification of the harmonic response at resonance with respect to the static ones). Introducing in (4.111), one gets

$$\frac{V_{out}}{l} = \frac{4e_{33}e_{31}}{ac_{11}^E\varepsilon_{33}^S} Q_m \frac{V}{t}$$

Finally, using (4.114-115), the step-up voltage ratio of the transformer becomes

$$r = \frac{V_{out}}{V} = \frac{4}{\pi^2}\,\frac{k_{33}k_{31}}{(1 - k_{33}^2/2)}\,Q_m\,\frac{l}{t} \tag{4.120}$$

Thus, the voltage amplification ratio r is proportional to the length to thickness ratio, l/t, the electromechanical coupling factors k_{33} and k_{31} and the mechanical quality factor Q_m.

4.10 References

ALLIK, H., HUGHES, T.J.R., Finite Element method for piezoelectric vibration, *Int. J. for Numerical Methods in Engineering*, Vol.2, 151-157, 1970.

CADY, W.G., *Piezoelectricity: an Introduction to the Theory and Applications of Electromechanical Phenomena in Crystals*, McGrawHill, 1946.

EER NISSE, E.P., Variational method for electrostatic vibration analysis, *IEEE Trans. on Sonics and Ultrasonics*, Vol. SU-14, No 4, 153-160 October 1967.

FORWARD, R.L., US Patent 4,158,787, June 1979.

IEEE Standard on Piezoelectricity, ANSI/IEEE Std 176-1987.

PHILBRICK RESEARCHES, Inc., *Application Manual for Computing Amplifiers for Modelling, Measuring, Manipulating & Much Else*, Nimrod Press, Boston, 1965.

Philips Application Book on Piezoelectric Ceramics, (J. Van Randeraat & R.E. Setterington, Edts), Mullard Limited, London, 1974.

Physik Intrumente catalogue, Products for Micropositioning (*PI* GmbH, FRG).

PIEFORT, V., *Finite element modelling of piezoelectric active structures*, PhD Thesis, Université Libre de Bruxelles, Active Structures Laboratory, 2001.

ROSEN, C.A., Ceramic transformers and filters, Proc. Electronic Component Symposium, p.205-211 (1956).

TIERSTEN, H.F., Hamilton's principle for linear piezoelectric media, *Proceedings of the IEEE*, 1523-1524, August 1967.

UCHINO, K., *Ferroelectric Devices*, Marcel Dekker, 2000.

5

Piezoelectric laminates

5.1 Piezoelectric beam actuator

Consider the piezoelectric beam of Fig.5.1; it is covered with a single piezoelectric layer of uniform thickness h_p, polarized along the z axis; the supporting structure is acting as electrode on one side and there is an electrode of variable width $b_p(x)$ on the other side. The voltage difference between the electrodes is controlled, so that the part of the piezoelectric material located between the electrodes is subjected to an electric field E_3 parallel to the polarization (note that the piezoelectric material which is not covered by the electrode on both sides is useless as active material). We denote by $w(x,t)$ the transverse displacements of the beam; according to the Euler-Bernoulli assumption, the stress and strain fields are uniaxial, along Ox; the axial strain S_1 is related to the curvature $w^{''}$ by

$$S_1 = -zw^{''} \tag{5.1}$$

where z is the distance to the neutral axis. We also assume that the piezoelectric layer is thin enough, so that E_3 is constant across the thickness.

5.1.1 Hamilton's principle

The kinetic coenergy reads

$$T^* = \frac{1}{2}\int_0^l \varrho A\dot{w}^2 dx \tag{5.2}$$

where A is the cross-section of the beam. Both the electric field and the strain vectors have a single non-zero component, respectively E_3 and S_1; the coenergy function (4.77) is therefore

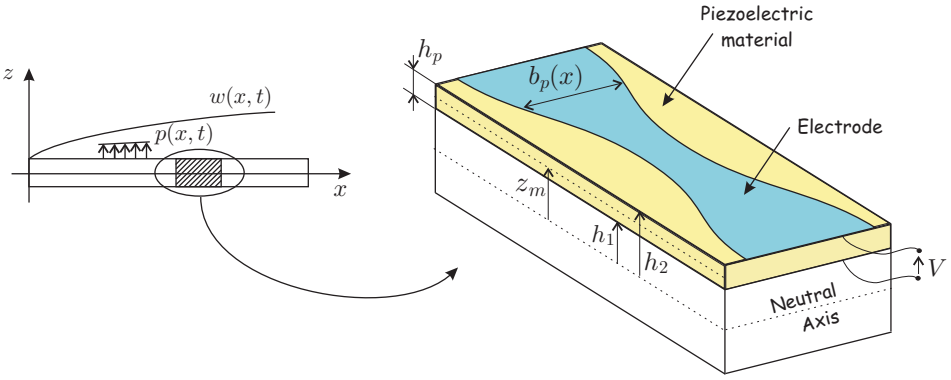

Fig. 5.1. Piezoelectric beam covered by a single piezoelectric layer with an electrode profile of width $b(x)$.

$$W_e^* = \frac{1}{2}\int_0^l dx \int_A \left(\varepsilon_{33}E_3^2 + 2S_1 e_{31}E_3 - c_{11}S_1^2\right) dA \tag{5.3}$$

and, combining with (5.1),

$$W_e^* = \frac{1}{2}\int_0^l dx \int_A \left(\varepsilon_{33}E_3^2 - 2w'' z e_{31}E_3 - c_{11}w''^2 z^2\right) dA \tag{5.4}$$

The first contribution to W_e^* is restricted to the piezoelectric part of the beam under the electrode area; the integral over the cross section can be written $\varepsilon_{33}E_3^2 b_p h_p$. The second contribution is also restricted to the piezoelectric layer; taking into account that

$$\int_A z dA = \int_{h_1}^{h_2} b_p\, z\, dz = b_p h_p z_m$$

where z_m is the distance between the mid-plane of the piezoelectric layer and the neutral axis (Fig.5.1), it can be written $-2w'' e_{31}E_3 b_p h_p z_m$. The third term in W_e^* can be rewritten by introducing the bending stiffness (we give up the classical notation EI of chapter 1 to avoid confusion)

$$\mathcal{D} = \int_A c_{11} z^2 dA \tag{5.5}$$

Thus, W_e^* reads

$$W_e^* = \frac{1}{2}\int_0^l \left(\varepsilon_{33}E_3^2 b_p h_p - 2w'' e_{31}E_3 b_p h_p z_m - \mathcal{D}w''^2\right) dx$$

Next, we can apply Hamilton's principle, recalling that only the vertical displacement is subject to virtual changes, δw, since the electric potential is fixed (voltage control). Integrating by part the kinetic energy with respect to time and taking into account that $\delta w(x,t_1)=\delta w(x,t_2)=0$,

$$\int_{t_1}^{t_2}\delta T^*dt=\int_{t_1}^{t_2}dt\int_0^l\varrho A\dot{w}\,\delta\dot{w}\,dx=-\int_{t_1}^{t_2}dt\int_0^l\varrho A\ddot{w}\,\delta w\,dx$$

Similarly,

$$\delta W_e^*=\int_0^l[-\delta w^{''}\left(e_{31}E_3b_ph_pz_m\right)-\mathcal{D}w^{''}\delta w^{''}]dx$$

and, integrating by part twice with respect to x,

$$\delta W_e^*=-(e_{31}E_3b_ph_pz_m)\delta w'\Big]_0^l+(e_{31}E_3b_ph_pz_m)^{'}\delta w\Big]_0^l-\int_0^l(e_{31}E_3b_ph_pz_m)^{''}\delta w dx$$

$$-\mathcal{D}w^{''}\delta w^{'}\Big]_0^l+\left(\mathcal{D}w^{''}\right)^{'}\delta w\Big]_0^l-\int_0^l\left(\mathcal{D}w^{''}\right)^{''}\delta w\,dx$$

The virtual work of nonconservative forces is

$$\delta W_{nc}=\int_0^l p(x,t)\delta w\,dx$$

where $p(x,t)$ is the distributed transverse load applied to the beam. Introducing in Hamilton's principle (4.79), one gets that

$$\text{V.I.}=\int_{t_1}^{t_2}dt\int_0^l\left[-\varrho A\ddot{w}-\left(e_{31}E_3b_ph_pz_m\right)^{''}-\left(\mathcal{D}w^{''}\right)^{''}+p\right]\delta w\,dx$$

$$-\left[\left(e_{31}E_3b_ph_pz_m+\mathcal{D}w^{''}\right)\delta w^{'}\right]_0^l+\left[\{(e_{31}E_3b_ph_pz_m)^{'}+\left(\mathcal{D}w^{''}\right)^{'}\}\delta w\right]_0^l=0$$

for all admissible variations δw compatible with the kinematics of the system.

5.1.2 Piezoelectric loads

It follows from the previous equation that the differential equation governing the problem is

$$\varrho A\ddot{w} + \left(\mathcal{D}w''\right)'' = p - \left(e_{31}E_3 b_p h_p z_m\right)'' \tag{5.6}$$

If one takes into account that only b_p depends on the spatial variable x and that $E_3 h_p = V$, the voltage applied between the electrodes of the piezoelectric layer, it becomes

$$\varrho A\ddot{w} + \left(\mathcal{D}w''\right)'' = p - e_{31}V z_m b_p''(x) \tag{5.7}$$

This equation indicates that the effect of the piezoelectric layer is equivalent to a *distributed load proportional to the second derivative of the width of the electrode.*

Examining the remaining terms, one must also have

$$\begin{gathered}\left(e_{31}E_3 b_p h_p z_m + \mathcal{D}w''\right)\delta w' = 0 \\ \left[\left(e_{31}E_3 b_p h_p z_m\right)' + \left(\mathcal{D}w''\right)'\right]\delta w = 0 \quad \text{at } x = 0 \text{ and } x = l\end{gathered} \tag{5.8}$$

The first condition states that at an end where the rotation is free, one must have

$$e_{31}V b_p z_m + \mathcal{D}w'' = 0 \tag{5.9}$$

This means that the effect of the piezoelectric layer is that of a *bending moment proportional to the width of the electrode.* Similarly, the second condition states that at an end where the displacement is free, one must have

$$e_{31}V b_p' z_m + \left(\mathcal{D}w''\right)' = 0 \tag{5.10}$$

Since $\left(\mathcal{D}w''\right)'$ represents the transverse shear force along the beam, this means that the effect of the piezoelectric layer is that of a *point force proportional to the first derivative of the electrode width.* One should always keep in mind that the piezoelectric loading consists of internal forces which are always *self-equilibrated.*

Figure 5.2 shows a few examples of electrode shapes and the corresponding piezoelectric loading. A rectangular electrode [Fig.5.2(a)] is equivalent to a pair of bending moments M_p applied at the ends of the electrode. A triangular electrode [Fig.5.2(b)] is equivalent to a pair of point forces P and a bending moment M_p; note that if the beam is clamped on the left side, the corresponding loads will be taken by the

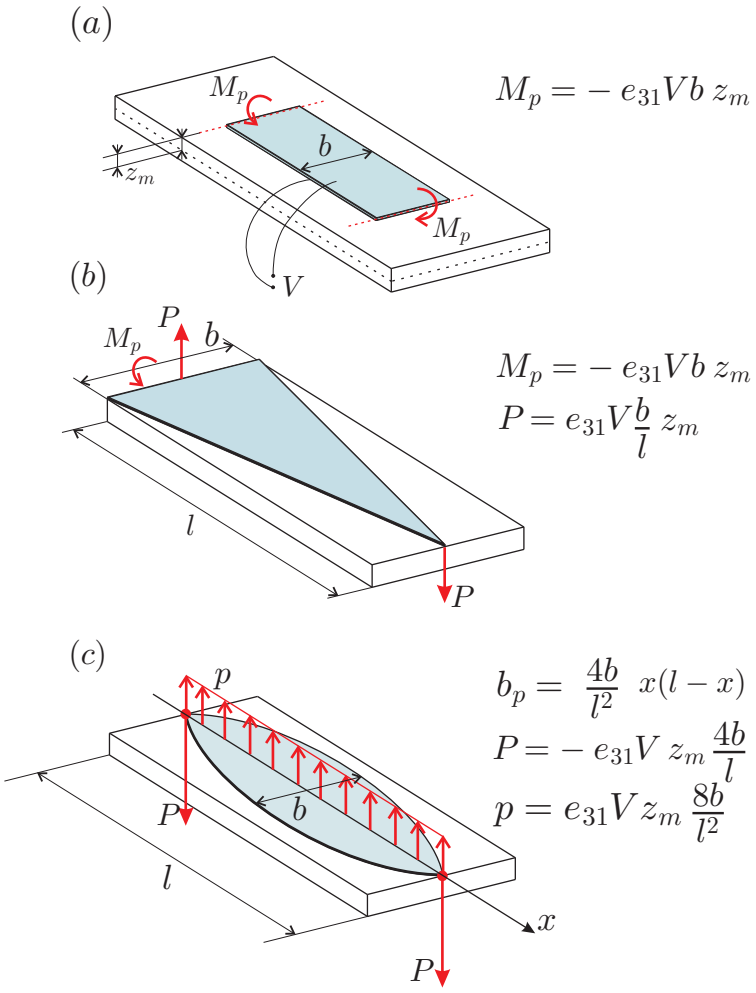

Fig. 5.2. Examples of electrode shapes and corresponding piezoelectric loading: (a) rectangular electrode, (b) triangular electrode, (c) parabolic electrode. The piezoelectric loading is always self-equilibrated.

support, and the only remaining force is the point load at the right end. A parabolic electrode [Fig.5.2(c)] is equivalent to a uniform distributed load p and a pair of point forces P at the ends.

As another example, consider the electrode shape of Fig.5.3. It consists of a rectangular part of length l_1, followed by a part with constant slope, of length l_2. According to the foregoing discussion, this is equivalent to bending moments M_1 and M_2 at the extremities of the electrodes, and point forces P at the location where there is a sudden change in the first

derivative $b^{'}(x)$. Once again, the piezoelectric loading is self-equilibrated.

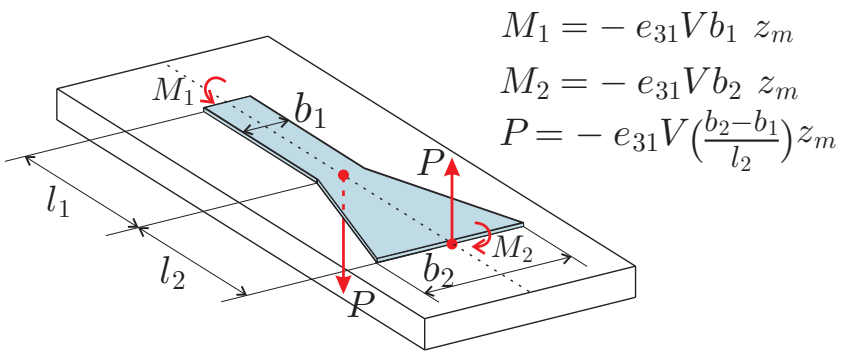

Fig. 5.3. Self-equilibrated equivalent piezoelectric loading for an electrode with a sudden change in $b_p'(x)$.

5.2 Laminar sensor

5.2.1 Current and charge amplifiers

When used in sensing mode, a piezoelectric transducer is coupled to an operational amplifier [Fig.5.4(a)] to form either a current amplifier [Fig.5.4(b)], or a charge amplifier [Fig.5.4(c)]. An operational amplifier is an active electrical circuit working as a high gain linear voltage amplifier with infinite input resistance (so that the input currents i_- and i_+ are essentially zero), and zero output resistance, so that the output voltage e_0 is essentially proportional to the voltage difference $e_+ - e_-$; the open loop gain A is usually very high, which means that the allowable input voltage is very small (millivolt). As a result, when the electrodes of a piezoelectric transducer are connected to an operational amplifier, they can be regarded as short-circuited and the electric field through the piezo can be considered as $E_3 = 0$. Then, it follows from the constitutive equation (4.63) that the electric displacement is proportional to the strain

$$D_3 = e_{31}S_1 \tag{5.11}$$

5.2.2 Distributed sensor output

If one assumes that the piezoelectric sensor is thin with respect to the beam, the strain can be regarded as uniform over its thickness,

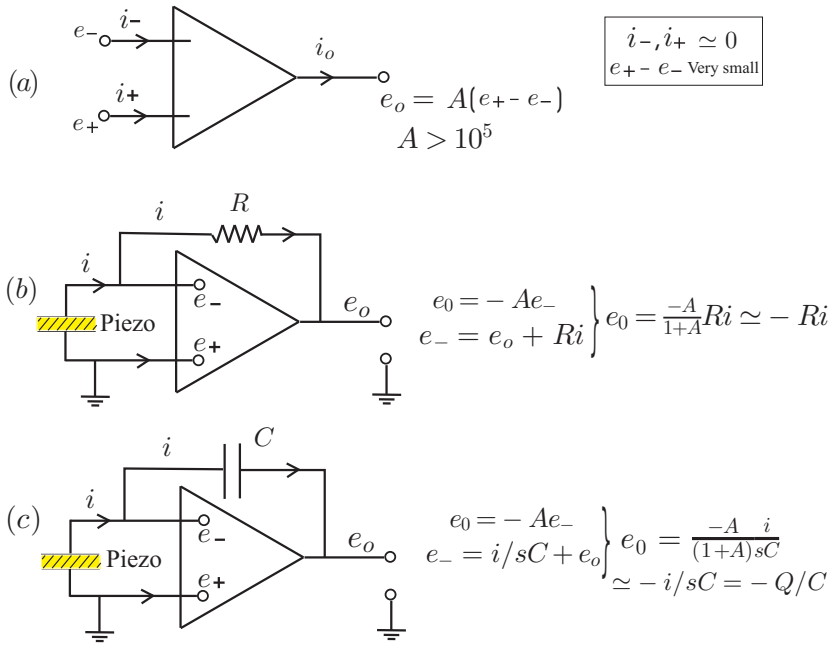

Fig. 5.4. (a) Operational amplifier, (b) Current amplifier, (c) Charge amplifier.

$S_1 = -z_m w''$, and $E_3 = 0$ is enforced by the charge amplifier; integrating over the electrode area (Fig.5.1), one gets

$$Q = \int D_3 dA = -\int_a^b b_p(x) z_m e_{31} w'' dx = -z_m e_{31} \int_a^b b_p(x) w'' dx \quad (5.12)$$

with a constant polarization profile e_{31}. It is assumed that the sensor extends from $x = a$ to $x = b$ over the beam. Thus, the amount of electric charge is proportional to the *weighted average of the curvature*, the weighing function being the width of the electrode. For an electrode with constant width,

$$Q = -z_m e_{31} b_p [w'(b) - w'(a)] \quad (5.13)$$

The sensor output is proportional to the *difference of slopes* (i.e. rotations) at the extremities of the sensor strip. We note that this result is dual of that of Fig.5.2(a), where the piezoelectric transducer is used in actuation mode.

Equation (5.12) can be integrated by parts, twice, leading to

$$\int_a^b w^{''} b_p(x)dx = w^{'} b_p \Big]_a^b - w b_p^{'} \Big]_a^b + \int_a^b w\, b^{''} dx \tag{5.14}$$

If, as an example, one considers the case of a cantilever beam clamped at $x = 0$ and covered with a piezoelectric strip and an electrode of triangular shape extending over the whole length as in Fig.5.2.b ($a = 0$ and $b = l$), $w(0) = w^{'}(0) = 0$ (cantilever beam) and $b_p^{''} = 0$, $b_p(l) = 0$, $b_p^{'} = -b_p(0)/l$ (triangular electrode). Substituting into (5.14) and (5.12), one gets

$$Q = -z_m e_{31} \frac{b_p(0)}{l} w(l) \ \sim \ w(l) \tag{5.15}$$

Thus, the output signal is proportional to the *tip displacement* of the cantilever beam. Once again, this result is dual of that obtained in actuation mode (the piezoelectric loading is a point force at the tip). Similarly, if one considers a parabolic electrode as in Fig.5.2(c) and if the beam is such that $w(0) = w(l) = 0$ (this includes pinned-pinned, pinned-clamped, etc), we have $b_p(0) = b_p(l) = 0$ and $b_p^{''}(x) = -8b/l^2$ and, substituting into (5.14),

$$Q = z_m e_{31} \frac{8b}{l^2} \int_0^l w(x)dx \ \sim \ \int_0^l w(x)dx \tag{5.16}$$

Thus, the output signal is proportional to the *volume displacement*, which is, once again, dual of the uniform distributed load in actuation mode. All the above results are based on the beam theory which is essentially one-dimensional; their accuracy in practical applications will depend very much on the relevance of these assumptions for the applications concerned. This issue is important in applications, especially in collocated control systems.

5.2.3 Charge amplifier dynamics

According to Fig.5.4.c, the output voltage is proportional to the amount of electric charge generated on the electrode; the amplifier gain is fixed by the capacitance C. This relation is correct at frequencies beyond some corner frequency depending on the amplifier construction, but does not apply statically (near $\omega = 0$). If a refined model of the charge amplifier is required, this behavior can be represented by adding a second order high-pass filter

$$F(s) = \frac{s^2}{s^2 + 2\xi_c \omega_c s + \omega_c^2} \tag{5.17}$$

with appropriate parameters ω_c and ξ_c. For frequencies well above the corner frequency ω_c, $F(s)$ behaves like a unit gain.

5.3 Spatial modal filters

5.3.1 Modal actuator

According to (5.7), a piezoelectric layer with an electrode of width $b_p(x)$ is equivalent to a distributed transverse load proportional to $b_p^{''}(x)$. Let

$$w(x,t) = \sum_i z_i(t)\phi_i(x) \tag{5.18}$$

be the modal expansion of the transverse displacements, where $z_i(t)$ are the modal amplitudes, and $\phi_i(x)$ the mode shapes, solutions of the eigenvalue problem

$$\left[\mathcal{D}\phi_i^{''}(x)\right]^{''} - \omega_i^2 \varrho A \phi_i = 0 \tag{5.19}$$

They satisfy the orthogonality conditions

$$\int_0^l \varrho A\, \phi_i(x)\phi_j(x)dx = \mu_i \delta_{ij} \tag{5.20}$$

$$\int_0^l \mathcal{D}\, \phi_i^{''}(x)\phi_j^{''}(x)dx = \mu_i \omega_i^2 \delta_{ij} \tag{5.21}$$

where μ_i is the modal mass, ω_i the natural frequency of mode i, and δ_{ij} is the Kronecker delta index ($\delta_{ij} = 1$ if $i = j$, $\delta_{ij} = 0$ if $i \neq j$). Substituting (5.18) into (5.7) (assuming $p = 0$), one gets

$$\varrho A \sum_i \ddot{z}_i \phi_i + \sum_i z_i (\mathcal{D}\phi_i^{''})^{''} = -e_{31} V b_p^{''} z_m$$

or using (5.19),

$$\varrho A \sum_i \ddot{z}_i \phi_i + \varrho A \sum_i z_i \omega_i^2 \phi_i = -e_{31} V b_p^{''} z_m$$

where the sums extend over all modes. Upon multiplying by $\phi_k(x)$, integrating over the length of the beam, and using the orthogonality condition (5.20), one finds easily the equation governing the modal amplitude z_k:

$$\mu_k(\ddot{z}_k + \omega_k^2 z_k) = -e_{31} V z_m \int_0^l b_p^{''}(x)\phi_k(x)dx \tag{5.22}$$

The right hand side is the modal force p_k applied by the piezoelectric strip to mode k. From the first orthogonality condition (5.20), it is readily seen that if the electrode profile is chosen in such a way that

$$b_p'' \sim \varrho A \phi_l(x) \tag{5.23}$$

all the modal forces p_k vanish, except p_l:

$$p_k \sim -e_{31} V z_m \int_0^l \varrho A \phi_l \phi_k dx \sim -e_{31} V z_m \mu_l \delta_{kl} \tag{5.24}$$

such an electrode profile will excite only mode l; it constitutes a *modal actuator* (for mode l).

5.3.2 Modal sensor

Similarly, if the piezoelectric layer is used as a sensor, the electric charge appearing on the sensor is given by (5.12). Introducing the modal expansion (5.18),

$$Q = -z_m e_{31} \sum_i z_i(t) \int_0^l b_p(x) \phi_i''(x) dx \tag{5.25}$$

Comparing this equation with the second orthogonality conditions (5.21), one sees that any specific mode can be made unobservable by choosing the electrode profile in such a way that the integral vanishes. If the electrode profile is chosen according to

$$b_p(x) \sim \mathcal{D} \phi_l''(x) \tag{5.26}$$

(proportional to the distribution of the bending moment of mode l), the output charge becomes

$$Q \sim -z_m e_{31} \mu_l \omega_l^2 z_l(t) \tag{5.27}$$

It contains only a contribution from mode l. This electrode profile constitutes a *modal sensor*. Note that, for a uniform beam, (5.19) implies that the mode shapes satisfy $\phi_i^{IV}(x) \sim \phi_i(x)$. It follows that the electrode profile of a modal sensor also satisfies that of a modal actuator: from (5.26),

$$b_p''(x) \sim \phi_l^{IV}(x) \sim \phi_l(x) \tag{5.28}$$

which satisfies (5.23). Figure 5.5 illustrates the electrode profile of modal filters used for a uniform beam with various boundary conditions; the change of sign indicates a change in polarity of the piezoelectric strip, which is equivalent to negative values of $b_p(x)$. As an alternative, the

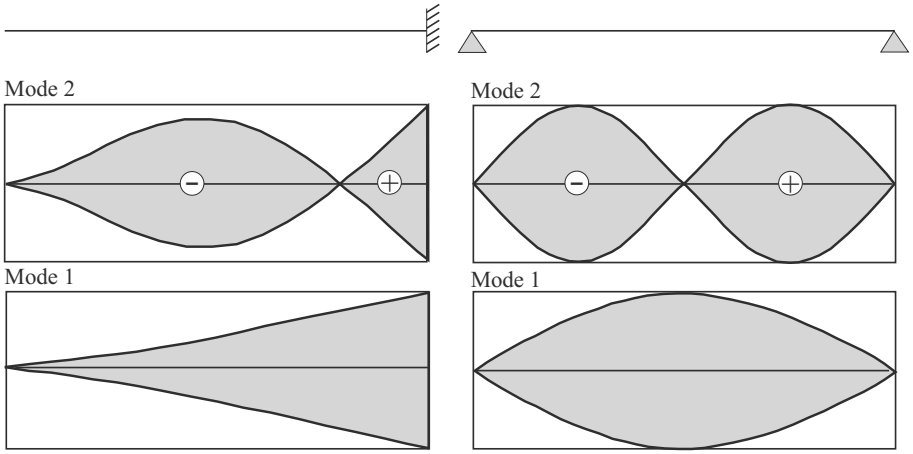

Fig. 5.5. Electrode profile of modal filters for the first two modes of a uniform beam for various boundary conditions: (a) cantilever, (b) simply supported.

part of the sensor with negative polarity can be bonded on the opposite side of the beam, with the same polarity. The reader will notice that the electrode shape of the simply supported beam is the same as the mode shape itself, while for the cantilever beam, the electrode shape is that of the mode shape of a beam clamped at the opposite end.

Modal filters constitute an attractive option for *spillover* alleviation, because they allow one to minimize the controllability and observability of a known set of modes. The limits of the beam approximation in practical applications will be discussed at the end of this chapter.

5.4 Active beam with collocated actuator-sensor

Consider a beam provided with a pair of rectangular piezoelectric actuator and sensor (Fig.5.6). They are collocated in the sense of the Euler-Bernoulli beam theory, which means that they extend over the same length along the beam. The system can, for example, be modelled by finite elements; the mesh is such that there is a node at both ends of the piezos (each node has two degrees of freedom, one translation y_i and one rotation θ_i). We seek the open-loop FRF between the voltage $V(t)$ applied to the actuator, and the output voltage $v_0(t)$ of the sensor (assumed to be connected to a charge amplifier).

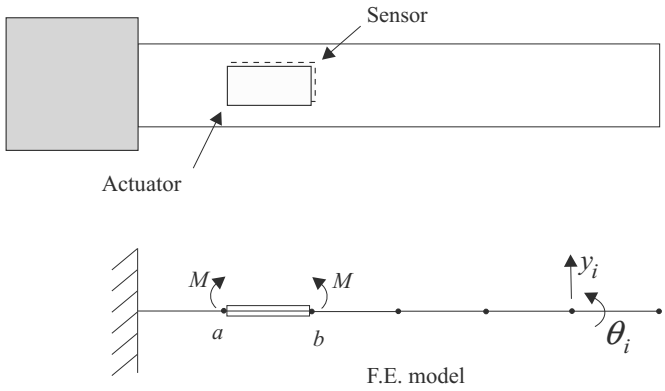

Fig. 5.6. Active cantilever beam with collocated piezoelectric actuator and sensor.

5.4.1 Frequency response function

According to the foregoing sections, the rectangular piezoelectric actuator is equivalent to a pair of torques M with opposite signs and proportional to V:

$$M = g_a V \tag{5.29}$$

where g_a is the actuator gain which can be computed from the actuator size and the material properties (Fig 5.2). In the general form of the equation of motion (1.50), the external force is

$$f = bM = bg_a V \tag{5.30}$$

where the influence vector b has the form $b^T = (.., 0, -1, 0, 1, ...)$; the only non-zero components correspond to the rotational degrees of freedom of the nodes located at $x = a$ and $x = b$ in the model. In modal coordinates, the system dynamics is governed by a set of independent second order equations

$$\ddot{z}_k + 2\xi_k \omega_k \dot{z}_k + \omega_k^2 z_k = \frac{\phi_k^T f}{\mu_k} = \frac{p_k}{\mu_k} \tag{5.31}$$

where ω_k is the natural frequency of mode k, ξ_k the modal damping ratio and μ_k the modal mass. Using the Laplace variable s, we can write it alternatively as

$$z_k = \frac{p_k}{\mu_k (s^2 + 2\xi_k \omega_k s + \omega_k^2)} \tag{5.32}$$

The modal forces p_k represent the work of the external loading on the various mode shapes:

$$p_k = \phi_k^T f = \phi_k^T b g_a V = g_a V \Delta\theta_k^a \tag{5.33}$$

where $\Delta\theta_k^a = \phi_k^T b$ is the relative rotation (difference of slope) between the extremities of the actuator, for mode k. Similarly, according to (5.13), the sensor output is also proportional to the difference of slope, that is the relative rotation of the extremities of the sensor, $\triangle\theta^s$. In modal coordinates,

$$v_0 = g_s \Delta\theta^s = g_s \sum_i z_i \Delta\theta_i^s \tag{5.34}$$

where g_s is the sensor gain, depending on the sensor size, material properties and on the charge amplifier gain, and $\Delta\theta_i^s$ are the modal components of the relative rotation between the extremities of the sensor. Note that if the sensor and the actuator extend over the same length of the beam, they can be considered as *collocated* in the sense of the Euler-Bernoulli beam theory, and

$$\Delta\theta_i^s = \Delta\theta_i^a = \Delta\theta_i \tag{5.35}$$

Combining the actuator equation (5.33), the sensor equation (5.34) with the equation of structural dynamics in modal coordinates (5.32), one easily gets the FRF between the actuator voltage V and the sensor output v_0 by substituting $s = j\omega$.

$$\frac{v_0}{V} = G(\omega) = g_a g_s \sum_{i=1}^{n} \frac{\Delta\theta_i^2}{\mu_i \left(\omega_i^2 - \omega^2 + 2j\xi_i\omega_i\omega\right)} \tag{5.36}$$

5.4.2 Pole-zero pattern

For an undamped system, the FRF is purely real:

$$\frac{v_0}{V} = G(\omega) = g_a g_s \sum_{i=1}^{n} \frac{\Delta\theta_i^2}{\mu_i \left(\omega_i^2 - \omega^2\right)} \tag{5.37}$$

All the residues of the modal expansion of the open loop FRF are positive and one can check that $dG(\omega)/d\omega \geq 0$ ($\omega \geq 0$), so that $G(\omega)$ is an increasing function of ω between resonances. Near the resonance ω_i, $G(\omega)$ jumps from $+\infty$ at ω_i^- to $-\infty$ at ω_i^+ and its behavior must be similar to that of Fig.5.7, with *alternating poles (resonances) and zeros (anti-resonances)* on the imaginary axis, Fig.5.8(a). Actually, for a lightly damped system, the poles and zeros are slightly in the left half plane [Fig.5.8(b)].

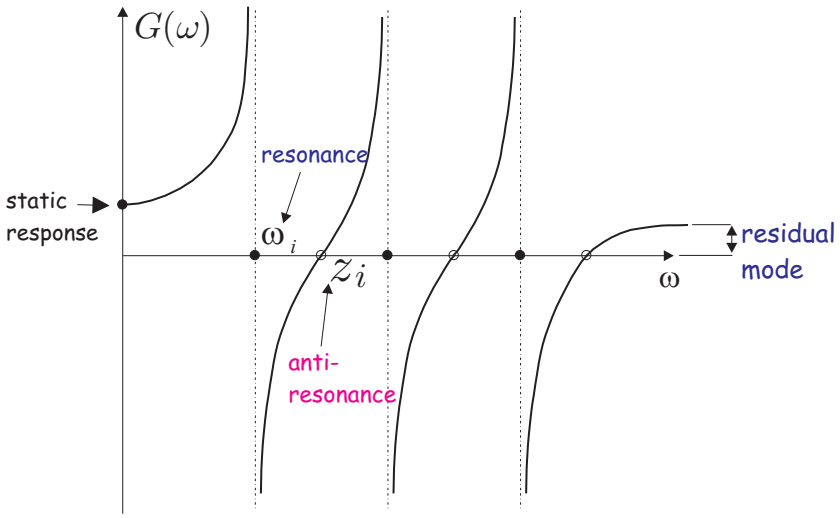

Fig. 5.7. Typical FRF of an undamped collocated system (truncated after 3 modes).

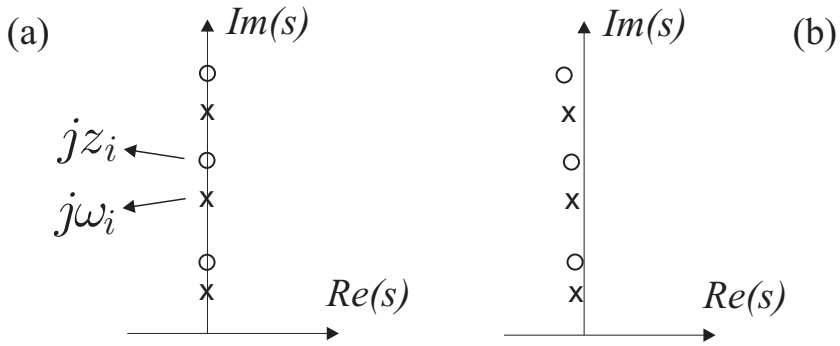

Fig. 5.8. Pole/zero pattern of a structure with collocated actuator/sensor: (a) undamped, (b) lightly damped (only the upper half of the complex plane is shown; the diagram is symmetrical with respect to the real axis).

A collocated control system always exhibits Bode and Nyquist plots similar to those of Fig.5.9: every flexible mode introduces a circle in the Nyquist diagram, which is more or less centered on the imaginary axis which is intersected at ω_i and z_i; the radius is proportional to ξ_i^{-1}. In the Bode plot, a 180° phase lag occurs at every natural frequency (pole), and is compensated by a 180° phase lead at every imaginary zero, and the phase always oscillates between 0 and −180°. This *interlacing* property of the poles and zeros is of fundamental importance in control system design for lightly damped vibrating systems, because it is possible to

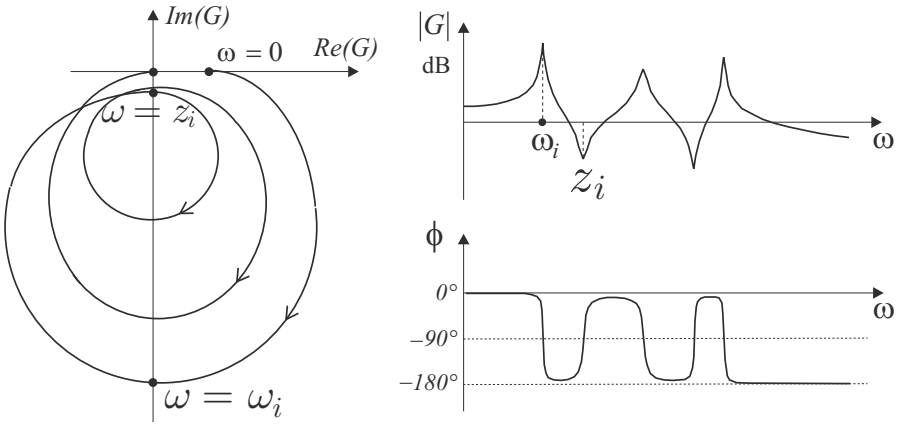

Fig. 5.9. Nyquist diagram and Bode plots of a lightly damped structure with collocated actuator and sensor pair.

find a fixed controller with guaranteed stability, irrespective to changes in the mass and stiffness distribution of the system. Figure 5.10 shows typical experimental results obtained with a system similar to that of Fig.5.6. Observe that $G(\omega)$ does not exhibit any roll-off (decay) at high frequency; this indicates a *feedthrough* component in the system, which is not apparent from the modal expansion (5.36) (according to which the high frequency behavior is as ω^{-2}). We will come back to this shortly. [1]

5.4.3 Modal truncation

Let us now examine the modal truncation of (5.36) which normally includes all the modes of the system (a finite number n with a discrete model, or infinite if one looks at the system as a distributed one). Obviously, if one wants an accurate model in some frequency band $[0, \omega_c]$, all the modes which belong to this frequency band must be included in the truncated expansion, but the high frequency modes cannot be completely ignored. Indeed, if one rewrites (5.36)

$$G(\omega) = g_a g_s \sum_{i=1}^{n} \frac{\Delta\theta_i^2}{\mu_i \omega_i^2}.H_i(\omega) \tag{5.38}$$

where

[1] Another observation is that a small linear shift appears in the phase diagram, due to the fact that these results have been obtained digitally (the sampling is responsible for a small delay in the system).

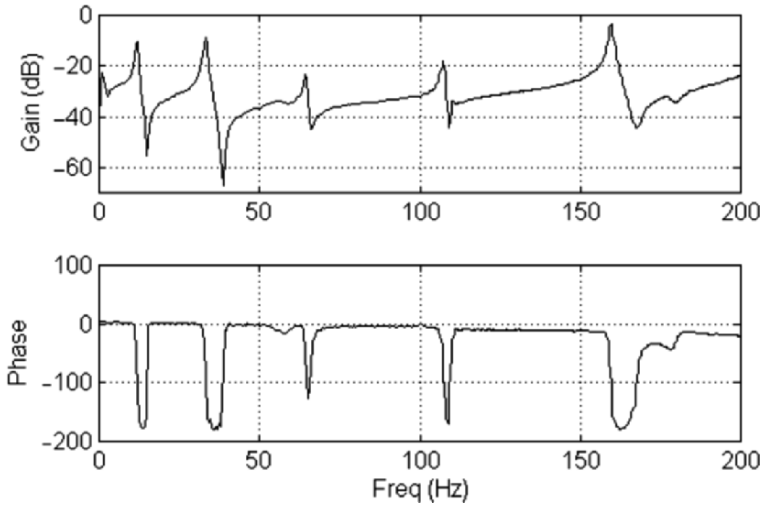

Fig. 5.10. Experimental open-loop FRF $G(\omega)$ of a piezoelectric beam similar to that of Fig.5.6.

$$H_i(\omega) = \sum_{i=1}^{n} \frac{1}{1 - \omega^2/\omega_i^2 + 2j\xi_i\omega/\omega_i} \tag{5.39}$$

is the *dynamic amplification* of mode i. For any mode with a natural frequency ω_i substantially larger than ω_c, $H_i(\omega) \simeq 1$ within $[0, \omega_c]$ and the sum (5.38) may be replaced by

$$G(\omega) = g_a g_s \sum_{i=1}^{m} \frac{\Delta\theta_i^2}{\mu_i \omega_i^2}.H_i(\omega) + g_a g_s \sum_{i=m+1}^{n} \frac{\Delta\theta_i^2}{\mu_i \omega_i^2} \tag{5.40}$$

where m has been selected in such a way that $\omega_m \gg \omega_c$. This equation recognizes the fact that, at low frequency, the high frequency modes respond in a *quasi-static* manner. The sum over the high frequency modes can be eliminated by noting that the static gain satisfies

$$G(0) = g_a g_s \sum_{i=1}^{n} \frac{\Delta\theta_i^2}{\mu_i \omega_i^2} \tag{5.41}$$

leading to

$$G(\omega) = g_a g_s \sum_{i=1}^{m} \frac{\Delta\theta_i^2}{\mu_i \omega_i^2}.H_i(\omega) + [G(0) - g_a g_s \sum_{i=1}^{m} \frac{\Delta\theta_i^2}{\mu_i \omega_i^2}] \tag{5.42}$$

The term between brackets, independent of ω, which corresponds to the high frequency modes is often called the *residual mode*. This equation can be written alternatively

$$G(\omega) = G(0) + g_a g_s \sum_{i=1}^{m} \frac{\Delta\theta_i^2}{\mu_i \omega_i^2}.[H_i(\omega) - 1]$$

or

$$G(\omega) = G(0) + g_a g_s \sum_{i=1}^{m} \frac{\Delta\theta_i^2}{\mu_i \omega_i^2} \frac{(\omega^2 - 2j\xi_i\omega_i\omega)}{(\omega_i^2 - \omega^2 + 2j\xi_i\omega_i\omega)} \tag{5.43}$$

The feedthrough component observed in Fig.5.10 is clearly apparent in (5.42) and (5.43). Note that the above equations require the static gain $G(0)$, but do not require the knowledge of the high frequency modes.

It is important to emphasize the fact that the quasi-static correction has a significant impact on the open-loop zeros of $G(\omega)$, and consequently on the performance of the control system. Referring to Fig.5.7, it is clear that neglecting the residual mode (quasi-static correction) amounts to shifting the diagram $G(\omega)$ along the vertical axis; this operation alters the location of the zeros which are at the crossing of $G(\omega)$ with the horizontal axis. Including the quasi-static correction tends to bring the zeros closer to the poles which, in general, tends to reduce the performance of the control system. Thus, it is a fairly general statement to say that *neglecting the residual mode (high frequency dynamics) tends to overestimate the performance of the control system*. Finally, note that since the piezoelectric loads are self-equilibrated, they would not affect the rigid body modes if there were any.

5.5 Piezoelectric laminate

In the first part of this chapter, the partial differential equation governing the dynamics of a piezoelectric beam, and the equivalent piezoelectric loads were established from Hamilton's principle. A similar approach can be used for piezoelectric laminates, but it is lengthy and cumbersome. The analytical expression for the equivalent piezoelectric loads and the sensor output can be obtained alternatively, as in the classical analysis of laminate composites, by using the appropriate constitutive equations; this is essentially the approach followed by (C.K. Lee, 1990).

5.5.1 Two dimensional constitutive equations

Consider a two dimensional piezoelectric laminate in a plane (x, y): the poling direction z is normal to the laminate and the electric field is also applied along z. In the piezoelectric orthotropy axes, the constitutive equations (4.62) (4.63) read

$$\{T\} = [c]\{S\} - \begin{Bmatrix} e_{31} \\ e_{32} \\ 0 \end{Bmatrix} E_3 \tag{5.44}$$

$$D_3 = \{e_{31}\ e_{32}\ 0\}\{S\} + \varepsilon E_3 \tag{5.45}$$

where

$$\{T\} = \begin{Bmatrix} T_{11} \\ T_{22} \\ T_{12} \end{Bmatrix} \qquad \{S\} = \begin{Bmatrix} S_{11} \\ S_{22} \\ 2S_{12} \end{Bmatrix} = \begin{Bmatrix} \partial u/\partial x \\ \partial v/\partial y \\ \partial u/\partial y + \partial v/\partial x \end{Bmatrix} \tag{5.46}$$

are the stress and strain vector, respectively, $[c]$ is the matrix of elastic constants under constant electric field, E_3 is the component of the electric field along z, D_3 is the z component of the electric displacement and ε the dielectric constant under constant strain (ε^S).

5.5.2 Kirchhoff theory

Following the Kirchhoff theory (e.g. Agarwal and Broutman, 1990), we assume that a line originally straight and normal to the midplane remains so in the deformed state. This is equivalent to neglecting the shear deformations S_{23} and S_{31}. If the midplane undergoes a displacement $u_0\ , v_0\ , w_0\ ,$ a point located on the same normal at a distance z from the midplane undergoes the displacements (Fig.5.11)

$$\begin{aligned} u &= u_0 - z\frac{\partial w_0}{\partial x} \\ v &= v_0 - z\frac{\partial w_0}{\partial y} \\ w &= w_0 \end{aligned} \tag{5.47}$$

The corresponding strains are

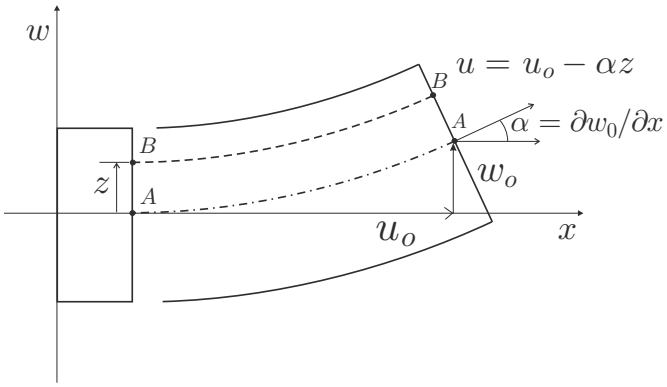

Fig. 5.11. Kinematics of a Kirchhoff shell.

$$\{S\} = \{S^0\} + z\{\kappa\} \tag{5.48}$$

where

$$\{S^0\} = \begin{Bmatrix} S^0_{11} \\ S^0_{22} \\ 2S^0_{12} \end{Bmatrix} = \begin{Bmatrix} \partial u_0/\partial x \\ \partial v_0/\partial y \\ \partial u_0/\partial y + \partial v_0/\partial x \end{Bmatrix} \tag{5.49}$$

are the midplane strains and

$$\{\kappa\} = \begin{Bmatrix} \kappa_{11} \\ \kappa_{22} \\ \kappa_{12} \end{Bmatrix} = -\begin{Bmatrix} \partial^2 w_0/\partial x^2 \\ \partial^2 w_0/\partial y^2 \\ 2\partial^2 w_0/\partial x \partial y \end{Bmatrix} \tag{5.50}$$

are the curvatures (the third component represents twisting). The stresses in the laminate vary from layer to layer (because of varying stiffness properties) and it is convenient to integrate over the thickness to obtain an equivalent system of forces and moments acting on the cross sections:

$$\{N\} = \int_{-h/2}^{h/2} \{T\} dz \qquad \{M\} = \int_{-h/2}^{h/2} \{T\} z\, dz \tag{5.51}$$

The positive direction of the resultant forces and moments is given in Fig.5.12. $\{N\}$ and $\{M\}$ are respectively a force per unit length, and a moment per unit length.

5.5.3 Stiffness matrix of a multi-layer elastic laminate

Before analyzing a piezoelectric laminate, let us recall the stiffness matrix of a multi-layer elastic laminate (Fig.5.13). If $[c]_k$ represents the stiffness

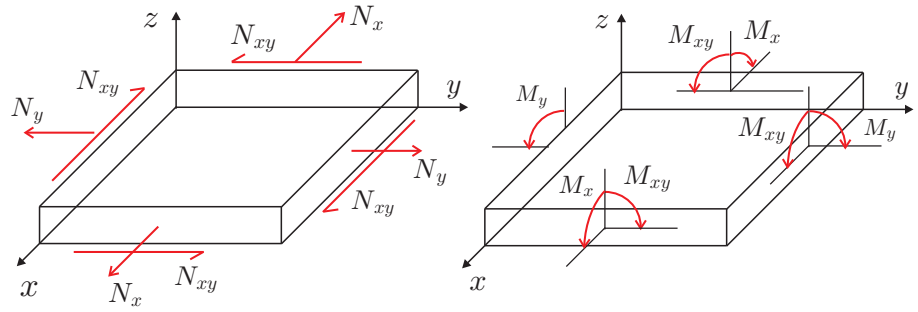

Fig. 5.12. Resultant forces and moments.

matrix of the material of layer k, expressed in global coordinates, the constitutive equation within layer k is

$$\{T\} = [c]_k\{S\} = [c]_k\{S^0\} + z[c]_k\{\kappa\} \tag{5.52}$$

Upon integrating over the thickness of the laminate, one gets

$$\begin{Bmatrix} N \\ M \end{Bmatrix} = \begin{bmatrix} A & B \\ B & D \end{bmatrix} \begin{Bmatrix} S^0 \\ \kappa \end{Bmatrix} \tag{5.53}$$

with

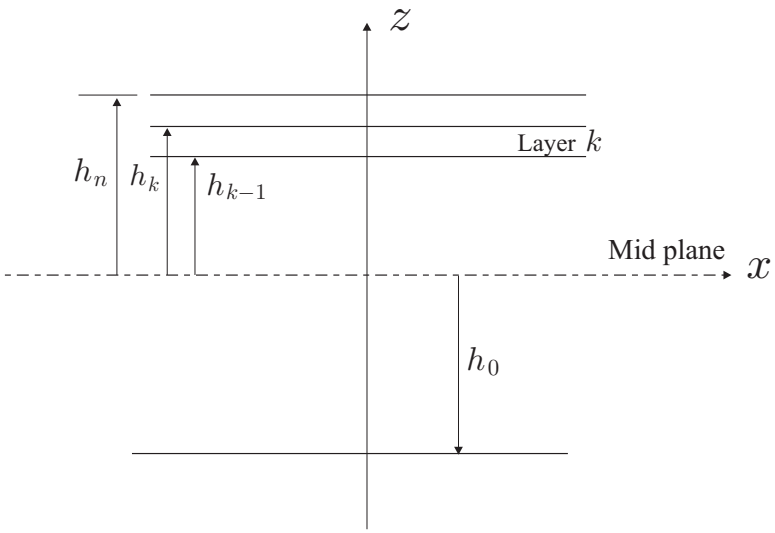

Fig. 5.13. Geometry of a multilayered laminate.

$$A = \sum_{k=1}^{n} [c]_k (h_k - h_{k-1})$$
$$B = \frac{1}{2} \sum_{k=1}^{n} [c]_k (h_k^2 - h_{k-1}^2) \tag{5.54}$$
$$D = \frac{1}{3} \sum_{k=1}^{n} [c]_k (h_k^3 - h_{k-1}^3)$$

where the sum extends over all the layers of the laminate; this is a classical result in laminate composites. A is the extensional stiffness matrix relating the in-plane resultant forces to the midplane strains; D is the bending stiffness matrix relating the moments to the curvatures, and B is the coupling stiffness matrix, which introduces coupling between bending and extension in a laminated plate; from (5.54), it is readily seen that B vanishes if the laminate is symmetric, because two symmetric layers contribute equally, but with opposite signs to the sum.

5.5.4 Multi-layer laminate with a piezoelectric layer

Next, consider a multi-layer laminate with a single piezoelectric layer (Fig.5.14); the constitutive equations of the piezoelectric layer are (5.44) and (5.45). Upon integrating over the thickness of the laminate as in the previous section, assuming that the global axes coincide with orthotropy axes of the piezoelectric layer, one gets

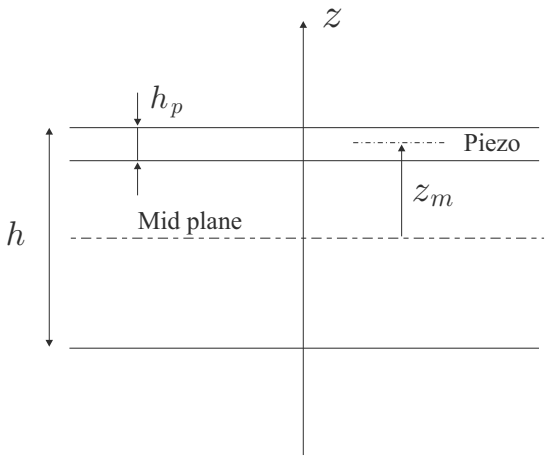

Fig. 5.14. Piezoelectric layer.

$$\left\{ \begin{matrix} N \\ M \end{matrix} \right\} = \begin{bmatrix} A & B \\ B & D \end{bmatrix} \left\{ \begin{matrix} S^0 \\ \kappa \end{matrix} \right\} + \begin{bmatrix} I_3 \\ z_m I_3 \end{bmatrix} \left\{ \begin{matrix} e_{31} \\ e_{32} \\ 0 \end{matrix} \right\} V \tag{5.55}$$

$$D_3 = \{e_{31}\ e_{32}\ 0\}[I_3\ \ z_m I_3] \left\{ \begin{matrix} S^0 \\ \kappa \end{matrix} \right\} - \varepsilon\, V/h_p \tag{5.56}$$

where V is the difference of potential between the electrodes of the piezoelectric layer ($E_3 = -V/h_p$), h_p the thickness of the piezoelectric layer, z_m the distance between the midplane of the piezoelectric layer and the midplane of the laminated; I_3 is the unity matrix of rank 3 and A,B,D are given by (5.54), including the piezoelectric layer.[2] In writing (5.56), it has been assumed that the thickness of the piezoelectric layer is small with respect to that of the laminate, so that the strain can be regarded as uniform across its thickness.

5.5.5 Equivalent piezoelectric loads

If there is no external load, $\{N\}$ and $\{M\}$ vanish and (5.55) can be rewritten

$$\begin{bmatrix} A & B \\ B & D \end{bmatrix} \left\{ \begin{matrix} S^0 \\ \kappa \end{matrix} \right\} = - \begin{bmatrix} I_3 \\ z_m I_3 \end{bmatrix} \left\{ \begin{matrix} e_{31} \\ e_{32} \\ 0 \end{matrix} \right\} V \tag{5.57}$$

The right hand side are the equivalent piezoelectric loads. If the material is isotropic, $e_{31} = e_{32}$, and the equivalent piezoelectric loads are *hydrostatic* (i.e. they are independent of the orientation of the facet within the part covered by the electrode). Overall, they consist of an *in-plane force normal to the contour of the electrode, and a constant moment acting on the contour of the electrode* (Fig.5.15); the force per unit length and moment per unit length are respectively

$$N_p = -e_{31} V \qquad\qquad M_p = -e_{31} z_m V \tag{5.58}$$

[2] the piezoelectric layer contributes to A, B and D with the stiffness properties under constant electric field.

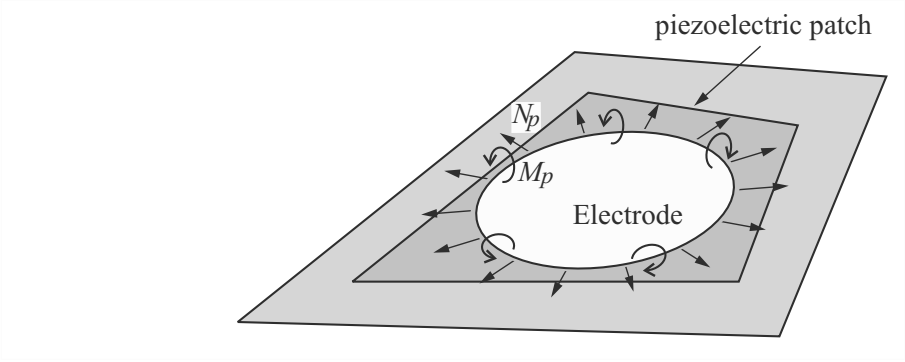

Fig. 5.15. Equivalent piezoelectric loads $N_p = -e_{31}V$, $M_p = -e_{31}z_mV$ for an isotropic piezoelectric actuator.

5.5.6 Sensor output

On the other hand, if the piezoelectric layer is used as a sensor and if its electrodes are connected to a charge amplifier which enforces $V{\sim}0$ (Fig.5.4), the sensor equation (5.56) becomes

$$D_3 = \{e_{31}\ e_{32}\ 0\}[I_3\ \ z_mI_3]\left\{\begin{array}{c} S^0 \\ \kappa \end{array}\right\} \tag{5.59}$$

Upon substituting the midplane strains and curvature from (5.49) (5.50), and integrating over the electrode area, one gets

$$Q = \int_\Omega D_3 d\Omega = \int_\Omega \left[e_{31}\frac{\partial u_0}{\partial x} + e_{32}\frac{\partial v_0}{\partial y} - z_m\left(e_{31}\frac{\partial^2 w}{\partial x^2} + e_{32}\frac{\partial^2 w}{\partial y^2}\right)\right] d\Omega \tag{5.60}$$

The integral extends over the electrode area (the part of the piezo not covered by the electrode does not contribute to the signal). The first part of the integral is the contribution of the *membrane strains*, while the second is due to *bending*.

If the piezoelectric properties are isotropic ($e_{31} = e_{32}$), the surface integral can be further transformed into a contour integral using the divergence theorem; the previous equation is rewritten

$$\begin{aligned} Q &= e_{31}\int_\Omega \text{div}\ \vec{u}_0\ d\Omega - e_{31}z_m\int_\Omega \text{div. }\vec{\text{grad}}\, w\ d\Omega \\ &= e_{31}\int_C \vec{n}.\vec{u}_0\, dl - e_{31}z_m\int_C \vec{n}.\ \vec{\text{grad}}\, w\ dl \end{aligned}$$

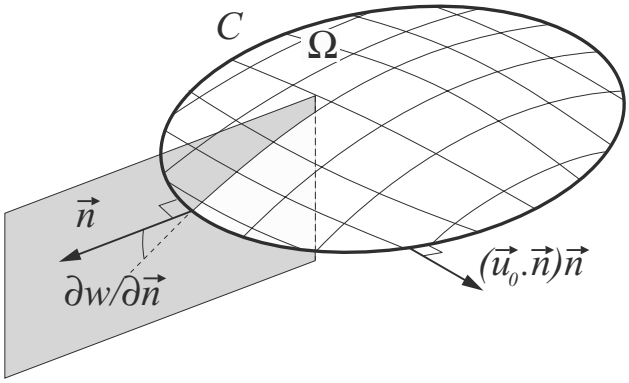

Fig. 5.16. Contributions to the sensor output for an isotropic piezoelectric layer. Ω is the electrode area.

where $\vec{n}$ is the outward normal to the contour of the electrode in its plane. Alternatively,

$$Q = e_{31} \int_C (\vec{u}_0.\vec{n} - z_m \frac{\partial w}{\partial \vec{n}}) dl \tag{5.61}$$

This integral extends over the contour of the electrode (Fig.5.16); the first contribution is the component of the mid-plane, *in-plane displacement normal to the contour* and the second one is associated with the *slope along the contour*.

Once again, the duality between the equivalent piezoelectric loads generated by the transducer used as actuator, and the sensor output when the transducer is connected to a charge amplifier must be pointed out.

5.5.7 Remarks

1. In this chapter, we have analyzed successively the piezoelectric beam according to the assumption of Euler-Bernoulli, and piezoelectric laminate according to Kirchhoff's assumption. The corresponding piezoelectric loads have been illustrated in Fig.5.2 and 5.15, respectively; the sensor output, when the transducer is used in sensing mode, can be deduced by *duality*: *a bending moment normal to the contour in actuation mode corresponds to the slope along the contour in sensing mode, and the in-plane force normal to the contour in actuation mode corresponds to the in-plane displacement normal to the contour in sensing mode*. Figure 5.17 illustrates the equivalent piezoelectric loads according to both theories for a rectangular isotropic piezoceramic patch acting on a structure extending along one dimension: according to the beam theory, the equivalent

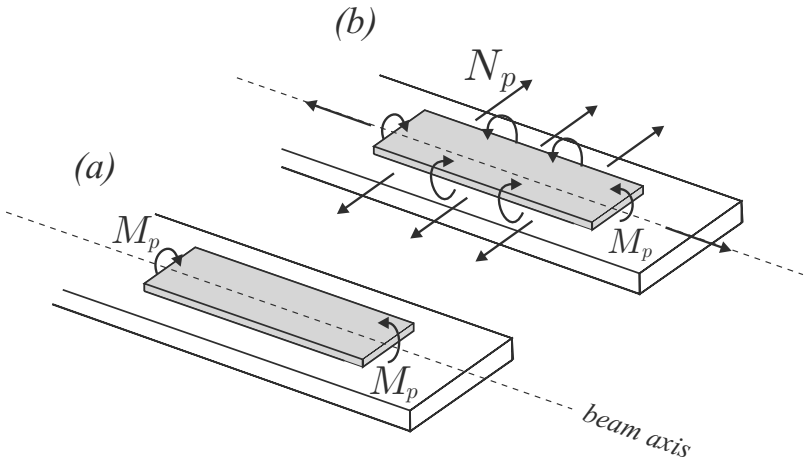

Fig. 5.17. Equivalent piezoelectric loads of a rectangular piezoelectric patch bonded on a beam: (a) beam theory, (b) laminate theory.

piezoelectric loads consist of a pair of torques applied to the end of the electrode (Fig.5.17.a), while according to the laminate theory, the torque is applied along the whole contour of the electrode and it is supplemented by an in-plane force N_p normal to the contour (Fig.5.17.b). If the structure extends dominantly along one axis, and if one is interested in the structural response *far away* from the actuator (e.g. tip displacement), it is reasonable to think that the piezoelectric loads of the beam theory are indeed the dominant ones. However, in active vibration control, one is often interested in configurations where the dual actuator and sensor are close to being *collocated*, to warrant alternating poles and zeros in the open-loop FRF, for a wide frequency range (the perfectly dual and collocated case was considered in section 5.4); in this case, it turns out that the contributions to the piezoelectric loading and to the sensor output which are ignored in the beam theory are significant, and neglecting them usually leads to significant errors in the open-loop zeros of the control system. This issue is discussed extensively in (Preumont, 2002).

2. Similarly, experiments conducted on a cantilever beam excited by a PZT patch on one side and covered with an isotropic PVDF film on the other side, with an electrode shaped as a modal filter for the first mode according to the theory of modal sensor developed in section 5.3, have revealed significant discrepancies between the measured FRF and that predicted by the beam theory; however, the FRF could be predicted quite accurately by the laminated plate theory (Preumont et al., 2003).

3. The Kirchhoff theory presented here mostly aimed at introducing the equivalent piezoelectric loads (5.58) and the sensor output equations (5.60) and (5.61). Mindlin shell finite elements have been considered in (Piefort, 2001) and implemented in an industrial computer code (SAMCEF). A deeper discussion of the finite element formulation of multi-layer piezoelectric shells can be found in (Benjeddou, 2000, Garcia Lage et al., 2004, Heyliger et al., 1996) and the literature quoted in these papers. The newly available PZT fibers (with interdigitated electrodes or not), which are usually supplied in a soft polymer cladding, seem to be particularly difficult to model accurately, due to the stiffness discrepancy between the supporting structure, the PZT fibers and the soft polymer interface; this is the subject of on-going research.

4. For beams, modal filtering has been achieved by shaping the width of the electrode. This concept cannot be directly transposed to plates. Spatial filtering of two-dimensional structures requires the tailoring of the piezoelectric constant, which is impossible in practice (the material can be polarized or not, but the polarization cannot be controlled). This problem has been solved by using a *porous electrode*; the fraction of electrode area is adjusted to achieve homogenized piezoelectric constants which produce the desired spatial filtering; the theory and the design procedure is described in (Preumont et al., 2003, 2005).

5.6 References

AGARWAL, B.D., BROUTMAN, L.J., *Analysis and Performance of Fiber Composites*, Wiley, 2nd Ed., 1990.

BENJEDDOU, A., Advances in piezoelectric finite element modeling of adaptive structural element: a survey, *Computers and Structures*, 76, 347-363, 2000.

BURKE, S.E., HUBBARD, J.E., Active vibration control of a simply supported beam using spatially distributed actuator. *IEEE Control Systems Magazine*, August, 25-30, 1987.

CRAWLEY, E.F., LAZARUS, K.B., Induced strain actuation of isotropic and anisotropic plates, *AIAA Journal*, Vol.29, No 6, pp.944-951, 1991.

DIMITRIADIS, E.K., FULLER, C.R., ROGERS, C.A., Piezoelectric actuators for distributed vibration excitation of thin plates, *Trans. ASME, J. of Vibration and Acoustics*, Vol.113, pp.100-107, January 1991.

GARCIA LAGE, R., MOTA SOARES, C.M., MOTA SOARES, C.A., REDDY, J.N., Layerwise partial mixed finite element analysis of magneto-electro-elastic plates, *Computers an Structures*, 82, 1293-1301, 2004.

HEYLIGER, P., PEI, K.C., SARAVANOS, D., Layerwise mechanics and finite element model for laminated piezoelectric shells, *AIAA Journal*, Vol.34, No 11, 2353-2360, November 1996.

HWANG, W.-S., PARK, H.C., Finite element modeling of piezoelectric sensors and actuators, *AIAA Journal*, Vol.31, No.5, pp.930-937, May 1993.

LEE, C.-K., Theory of laminated piezoelectric plates for the design of distributed sensors/actuators - Part I: Governing equations and reciprocal relationships, *J. of Acoustical Society of America*, Vol.87, No.3, 1144-1158, March 1990.

LEE, C.-K., CHIANG, W.-W., O'SULLIVAN, T.C., Piezoelectric modal sensor/actuator pairs for critical active damping vibration control, *J. of Acoustical Society of America*, Vol. 90, No 1, 374-384, July 1991.

LEE, C.-K., MOON, F.C., Modal sensors/actuators, *Trans. ASME, J. of Applied Mechanics*, Vol.57, pp.434-441, June 1990.

LERCH, R., Simulation of piezoelectric devices by two- and three-dimensional finite elements, *IEEE Transactions on Ultrasonics, Ferroelectrics, and Frequency Control*, Vol 37, No 3, May 1990.

PIEFORT, V., *Finite element modelling of piezoelectric active structures*, PhD Thesis, Université Libre de Bruxelles, Active Structures Laboratory, 2001.

PREUMONT, A., *Vibration Control of Active Structures, An Introduction*, 2nd Edition, Kluwer, 2002.

PREUMONT, A., FRANÇOIS, A., DE MAN, P., PIEFORT, V., Spatial filters in structural control, *Journal of Sound and Vibration*, 265, 61-79, 2003.

PREUMONT, A., FRANÇOIS, A., DE MAN, P., LOIX, N., HENRIOULLE, K., Distributed sensors with piezoelectric films in design of spatial filters for structural control, *Journal of Sound and Vibration*, 282, 701-712, 2005.

REX, J., ELLIOTT, S.J., The QWSIS, A new sensor for structural radiation control, MOVIC-1, Yokohama, Sept. 1992.

6

Active and passive damping with piezoelectric transducers

6.1 Introduction

Damping is essential in limiting the detrimental effects of mechanical resonances. This is illustrated in Fig.6.1 which shows, for a single d.o.f. oscillator, the influence of the fraction of critical damping ξ on *(i)* the dynamic amplification at resonance (expressed in dB) and *(ii)* the number of cycles N necessary to reduce the amplitude of the impulse response by 50%. Typical damping values encountered in various fields of structural engineering are also indicated in Fig.6.1.

In this chapter, we consider a structure with one or several piezoelectric transducers, and investigate how they can be used to introduce damping, actively or passively. *Active* damping requires the introduction of a sensor and a feedback control loop, which brings in all the classical control issues such as stability, robustness, etc... In this analysis, we focus on *collocated* actuator/sensor pairs, to benefit from the alternating pole/zero pattern of the open-loop transfer function. Indeed, thanks to this property, it is possible to find control laws with *guaranteed stability*, irrespective of variations in the parameters of the structure. *Passive* damping can also be achieved with a piezoelectric transducer, by first transforming the energy of the mechanical vibration into electrical energy, and then dissipating this electrical energy in a passive electrical network. Good performance can be achieved if one locates the transducer in order to maximize the mechanical energy stored in it, and if one can maximize the energy conversion from mechanical energy to electrical energy. The former depends essentially on the structural design; the ability of a vibration mode to concentrate the vibrational energy into the transducer is measured by the *fraction of modal strain energy*, ν_i; the ability to transform the strain energy into

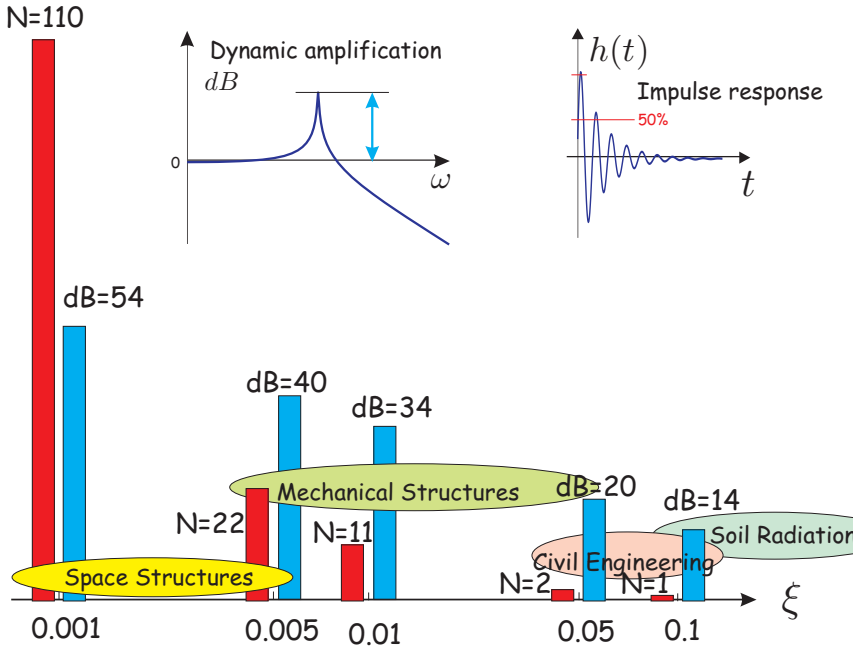

Fig. 6.1. Dynamic amplification at resonance (in dB) and number of cycles N to reduce the amplitude of the impulse response by 50% as a function of the damping ratio ξ (the damping scale is logarithmic).

electrical energy is measured by the *electromechanical coupling factor*, k; it is a material parameter; recent improvements in piezoelectric materials have led to electromechanical coupling factors k_{33} of 0.7 and more, making them a very attractive option for passive damping. ν_i and k are often combined in the *generalized electromechanical coupling factor*, K_i.

In the first part of this chapter, we consider the active damping of a structure equipped with a discrete piezoelectric transducer and a collocated force sensor; the feedback control law known as the *Integral Force Feedback* (IFF) is shown to have guaranteed stability. The implementations based on voltage control and current control are compared, and the modal damping ratio is estimated via a root locus technique; it is noted that the performances of the voltage control implementation depend only on the fraction of modal strain energy, while the current control implementation depends also on the electromechanical coupling factor. Next, the passive control via resistive shunting is considered and it is shown that the problem can be formulated with the same root-locus approach as the IFF. Passive control via inductive shunting is also considered, where a

RL shunt is added to the capacitive piezoelectric transducer, to form a resonant circuit acting as a vibration absorber; damping performances are significantly enhanced when the electrical circuit is properly tuned, but they drop rapidly below the resistive shunting when the system is de-tuned. The chapter ends with a brief discussion of the self-sensing actuator, how it can be used for shaping transfer functions, and a few alternative control strategies (Lead and PPF).

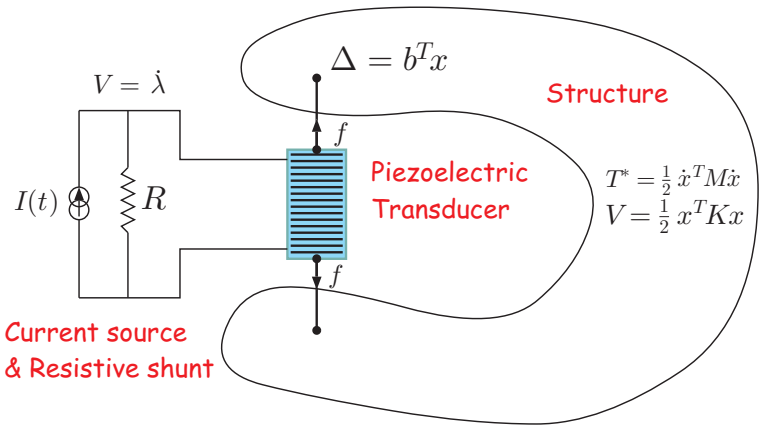

Fig. 6.2. Piezoelectric linear transducer.

6.2 Active strut, open-loop FRF

Consider the system of Fig.6.2, formed by a linear structure equipped with an active strut consisting of a piezoelectric transducer used as actuator and a force sensor measuring the total force f in the strut. The actuator is connected to a voltage source or a current source, while the force sensor can be visualized as another piezoelectric transducer connected to a charge amplifier (Fig.6.3). According to the the constitutive equation (4.6), if $V = 0$ is enforced at the electrodes of the sensor, $Q = [nd_{33}]^s f$. Following Fig.5.4.c, the output voltage of the charge amplifier is proportional to the force f applied on the sensor:

$$y = -\frac{Q}{C_1} = -\frac{[nd_{33}]^s f}{C_1} = g_s f \tag{6.1}$$

where $[nd_{33}]^s$ refers to the sensor and C_1 is the capacitance of the charge amplifier; g_s is the sensor gain.

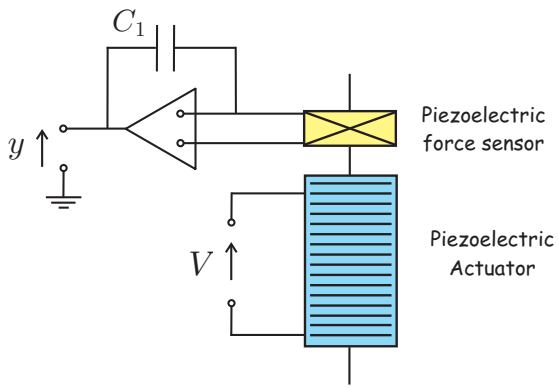

Fig. 6.3. Active strut consisting of a piezoelectric transducer and a piezoelectric force sensor.

The system of Fig.6.2 has already been analyzed in Chapter 4; if the transducer is controlled with a voltage source, the dynamics of the system is governed by Equ.(4.27):

$$M\ddot{x} + (K + K_a bb^T)x = bK_a\delta \tag{6.2}$$

where $\delta = nd_{33}V$ is the unconstrained expansion of the actuator under voltage V. K is the stiffness matrix of the structure excluding the axial stiffness of the actuator (but including the sensor), and b is the projection vector of the actuator in the global coordinate system. The right hand side of this equation are the piezoelectric loads. In Laplace variable, it can be rewritten

$$x = (Ms^2 + K + K_a bb^T)^{-1} bK_a\delta \tag{6.3}$$

$(Ms^2 + K + K_a bb^T)^{-1}$ is the *dynamic flexibility matrix* of the system. Let ϕ_i be the normal modes, solutions of the eigenvalue problem

$$(K + K_a bb^T - \omega_i^2 M)\phi_i = 0 \tag{6.4}$$

They satisfy the usual orthogonality conditions

$$\phi_i^T M \phi_j = \mu_i \delta_{ij} \tag{6.5}$$

$$\phi_i^T (K + K_a bb^T)\phi_j = \mu_i \omega_i^2 \delta_{ij} \tag{6.6}$$

If the global displacements are expanded into modal coordinates,

$$x = \sum_j \alpha_j \phi_j \tag{6.7}$$

where α_i are the modal amplitudes, (6.2) becomes

$$\sum_j s^2 \alpha_j M \phi_j + \sum_j \alpha_j (K + K_a b b^T) \phi_j = b K_a \delta \tag{6.8}$$

Left multiplying by ϕ_i^T and taking into account the orthogonality conditions, one finds

$$\alpha_i = \frac{\phi_i^T}{\mu_i(\omega_i^2 + s^2)} b K_a \delta \tag{6.9}$$

and

$$x = \sum_{i=1}^{n} \frac{\phi_i \phi_i^T}{\mu_i(\omega_i^2 + s^2)} b K_a \delta \tag{6.10}$$

By comparison with (6.3), the modal expansion of the dynamic flexibility matrix is obtained:

$$(M s^2 + K + K_a b b^T)^{-1} = \sum_{i=1}^{n} \frac{\phi_i \phi_i^T}{\mu_i(\omega_i^2 + s^2)} \tag{6.11}$$

On the other hand, according to the second constitutive equation (4.6) of the actuator,

$$\Delta = b^T x = n d_{33} V + f/K_a = \delta + f/K_a \tag{6.12}$$

(this equation states that the total displacement at the end nodes of the actuator is the sum of the piezoelectric expansion and the elastic displacement). Combining with the collocated sensor equation (6.1),

$$y = g_s f = g_s K_a (b^T x - \delta) \tag{6.13}$$

Substituting (6.10), one finds the modal expansion of the open-loop transfer function of the system

$$\frac{y}{\delta} = g_s K_a [\sum_{i=1}^{n} \frac{(b^T \phi_i)^2 K_a}{\mu_i \omega_i^2} \frac{1}{(s^2/\omega_i^2 + 1)} - 1] \tag{6.14}$$

Note that $b^T \phi_i$ is the actuator extension when the system vibrates according to mode i; the ratio

$$\nu_i = \frac{(b^T \phi_i)^2 K_a}{\mu_i \omega_i^2} = \frac{\phi_i^T (K_a b b^T) \phi_i}{\phi_i^T (K + K_a b b^T) \phi_i} \tag{6.15}$$

is readily interpreted as the ratio between (twice) the strain energy in the actuator and (twice) the total strain energy when the structure vibrates

according to mode i; ν_i is the *fraction of modal strain energy*. With this definition, the open-loop transfer function is rewritten

$$\frac{y}{\delta} = g_s K_a [\sum_{i=1}^{n} \frac{\nu_i}{(s^2/\omega_i^2 + 1)} - 1] \tag{6.16}$$

and, substituting $s = j\omega$, we obtain the open-loop FRF

$$\frac{y}{\delta} = G(\omega) = g_s K_a [\sum_{i=1}^{n} \frac{\nu_i}{(1 - \omega^2/\omega_i^2)} - 1] \tag{6.17}$$

where the sum extends to all structural modes of the structure. ν_i is the residue of mode i in the modal expansion of the open-loop FRF; it can be regarded as a compound index of controllability and observability of mode i. ν_i is readily available from commercial finite element codes. This result has been obtained by neglecting the structural damping; for a lightly damped structure with modal damping ξ_i, it becomes

$$\frac{y}{\delta} = g_s K_a [\sum_{i=1}^{n} \frac{\nu_i}{(1 + 2j\xi_i\omega/\omega_i - \omega^2/\omega_i^2)} - 1] \tag{6.18}$$

Combining (6.17) with (6.12), one gets the FRF between the piezoelectric free expansion δ and the total displacement of the actuator

$$\frac{\Delta}{\delta} = \sum_{i=1}^{n} \frac{\nu_i}{1 - \omega^2/\omega_i^2} \tag{6.19}$$

Considering the static response of the system, it is readily seen from (6.2) that, at $\omega = 0$,

$$\Delta = b^T (K + K_a b b^T)^{-1} b K_a \delta \tag{6.20}$$

Thus, writing (6.19) for $\omega = 0$, one gets

$$(\frac{\Delta}{\delta})_{\omega=0} = \sum_{i=1}^{n} \nu_i = b^T (K + K_a b b^T)^{-1} b K_a = \frac{K_a}{K^*} \tag{6.21}$$

where K^* is the stiffness of the system (structure + short-circuited actuator) seen from the end points of the transducer ($K_a < K^*$). This result is helpful if one wants to truncate the modal expansion after m modes. Using the same reasoning as in section 5.4.3, for $\omega \ll \omega_m$, one can use the approximation

$$\frac{y}{\delta} = G(\omega) \simeq g_s K_a [\sum_{i=1}^{m} \frac{\nu_i}{(1-\omega^2/\omega_i^2)} + \sum_{i=m+1}^{n} \nu_i - 1] \tag{6.22}$$

and, from (6.21), the residual mode can be expressed in terms of the static stiffness and the fraction of modal strain energy of the low frequency modes

$$\sum_{i=m+1}^{n} \nu_i = \frac{K_a}{K^*} - \sum_{i=1}^{m} \nu_i \tag{6.23}$$

leading to

$$G(\omega) \simeq g_s K_a [\sum_{i=1}^{m} \frac{\nu_i \, \omega^2}{(\omega_i^2 - \omega^2)} + \frac{K_a}{K^*} - 1] \tag{6.24}$$

With damping, this results becomes

$$G(\omega) \simeq g_s K_a [\sum_{i=1}^{m} \frac{\nu_i \, (\omega^2 - 2\xi_i \omega_i \omega)}{(\omega_i^2 - \omega^2 + 2j\xi_i \omega_i \omega)} + \frac{K_a}{K^*} - 1] \tag{6.25}$$

Note that the modal truncation must be considered with care if one wants to predict accurately the performance of the control system, and the discussion of section 5.4.3 applies fully here.

6.3 Active damping via IFF

6.3.1 Voltage control

Equation (6.2) governing the dynamics of the system is rewritten in Laplace form

$$Ms^2 x + (K + K_a b b^T) x = b K_a \delta \tag{6.26}$$

The output equation of the force sensor is given by (6.13):

$$y = f = g_s K_a (\Delta - \delta) = g_s K_a (b^T x - \delta) \tag{6.27}$$

The *Integral Force Feedback (IFF)* consists of

$$\delta = \frac{g}{g_s K_a s} \, y \tag{6.28}$$

(note that it is a positive feedback); $1/s$ is the integral effect; the constant $g_s K_a$ at the denominator is for normalization purpose. Combining these three equations, one easily gets the closed-loop characteristic equation

$$[Ms^2 + (K + K_a bb^T) - \frac{g}{s+g}(K_a bb^T)]x = 0 \tag{6.29}$$

The asymptotic roots for $g \to 0$ (open-loop poles) satisfy

$$[Ms^2 + (K + K_a bb^T)]x = 0 \tag{6.30}$$

The solutions of this eigenvalue problem are the natural frequencies ω_i of the global structure *when the electrodes of the transducer are short-circuited*. On the other hand, the asymptotic roots for $g \to \infty$ (open-loop zeros, z_i) are solutions of the eigenvalue problem

$$[Ms^2 + K]x = 0 \tag{6.31}$$

which corresponds to the situation where *the axial contribution of the transducer to the stiffness has been removed*. Note that, depending on the design of its connections with the structure, the transducer may contribute to the stiffness matrix by more than its axial component $K_a bb^T$; all but the axial component must be included in K to achieve an accurate prediction of the zeros z_i. In particular, the rotary stiffness of flexible joints approximating spherical joints in precision structures may sometimes have a significant impact on the zeros.

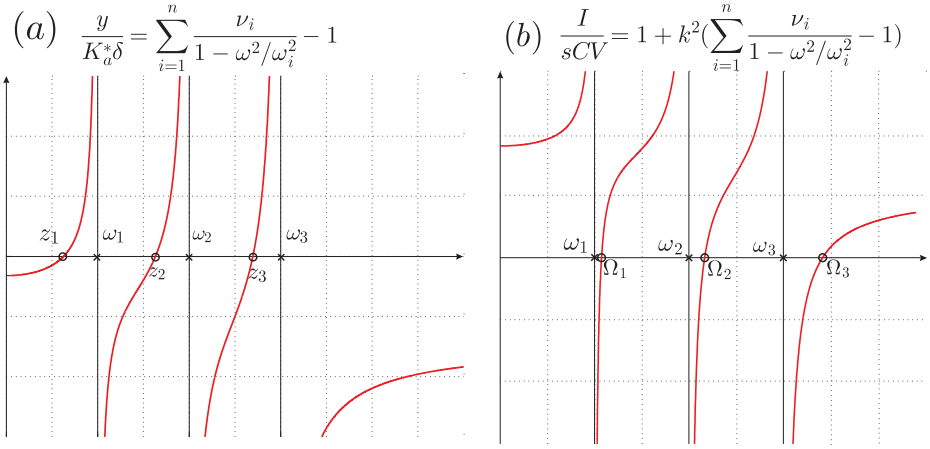

Fig. 6.4. (a) Open-loop FRF of the active strut mounted in the structure (undamped). (b) Admittance of the transducer mounted in the structure.

6.3.2 Modal coordinates

The closed-loop equation is transformed to modal coordinates by the change of variables $x = \Phi\alpha$, where $\Phi = (\dots \phi_i \dots)$ is the matrix of the mode shapes; we assume that they have been normalized in such a way that $\Phi^T M \Phi = I$; the mode shapes are solutions of the eigenvalue problem (6.30); the second orthogonality condition reads

$$\Phi^T (K + K_a b b^T) \Phi = \omega^2 = diag(\omega_i^2) \tag{6.32}$$

where ω_i are the natural frequencies of the structure with short-circuited electrodes. The modal expansion of the open-loop transfer function has been obtained earlier in (6.17); the fact that all the residues ν_i in the open-loop FRF are positive guarantees alternating poles and zeros, beginning with a zero (Fig.6.4(a)). The root locus plot corresponding to the IFF is shown in Fig.6.5.

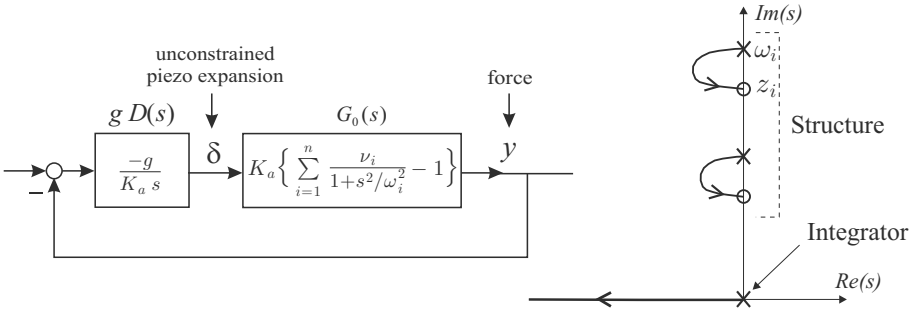

Fig. 6.5. (a) Block diagram of the IFF. (b) Typical root locus (for two modes).

Transforming (6.29) in modal coordinates, $x = \Phi\alpha$, one gets

$$[Is^2 + \omega^2 - \frac{g}{s+g} \Phi^T (K_a b b^T) \Phi]\alpha = 0 \tag{6.33}$$

(after using the orthogonality conditions). The matrix $\Phi^T (K_a b b^T) \Phi$ is in general fully populated; assuming that it is diagonally dominant, and neglecting the off-diagonal terms, it can be rewritten

$$\Phi^T (K_a b b^T) \Phi \simeq diag(\nu_i \omega_i^2) \tag{6.34}$$

after using the definition (6.15) of the fraction of modal strain energy, and (6.33) is reduced to a set of uncoupled equations:

$$s^2 + \omega_i^2 - \frac{g}{s+g}\nu_i\omega_i^2 = 0 \tag{6.35}$$

Denoting

$$z_i^2 = \omega_i^2(1-\nu_i) \tag{6.36}$$

we can transform Equ.(6.35) into

$$1 + g\frac{s^2+z_i^2}{s(s^2+\omega_i^2)} = 0 \tag{6.37}$$

which shows that every mode follows a root locus with poles at $\pm j\omega_i$ and at $s = 0$, and zeros at $\pm jz_i$ (Fig.6.6). From Equ.(6.31), we know that the zeros are the natural frequencies of the structure when the axial contribution of the transducer to the stiffness matrix has been removed. The maximum modal damping is given by

$$\xi_i^{max} = \frac{\omega_i - z_i}{2z_i} \tag{6.38}$$

and it is achieved for $g = \omega_i\sqrt{\omega_i/z_i}$. Comparing Fig.6.6 with Fig.6.5(b), one sees that the approximation consisting of neglecting the off-diagonal terms in (6.34) is essentially equivalent to assuming that the zeros are given by (6.36), and that every single loop from ω_i to z_i in Fig.6.5(b) can be drawn independently of the other neighboring loops. Note that, since equation (6.36) relating the zeros z_i, the poles ω_i and the fraction

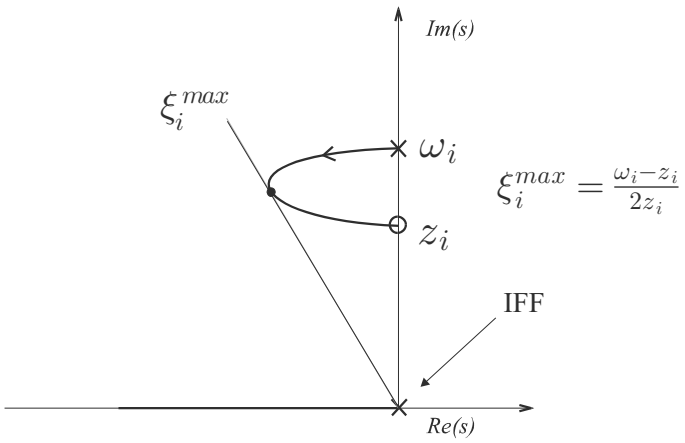

Fig. 6.6. Root locus of the IFF, voltage control (only half of the locus is shown).

of modal strain energy ν_i is approximate, one can use the roots of (6.31) as z_i when drawing the root locus (6.37).[1]

6.3.3 Current control

The case of a pure current source has been considered in section 4.4.2. The system dynamics is governed by Equ.(4.30)

$$\left[Ms^2 + \left(K + \frac{K_a}{1-k^2} bb^T\right)\right] x = b \frac{K_a}{1-k^2} n d_{33} \frac{I}{sC} \tag{6.39}$$

In this equation, $\delta = nd_{33}I/sC = nd_{33}Q/C$ is the free extension of the actuator under the electric charge Q. From the constitutive equation (4.9), the sensor equation reads:

$$y = g_s f = g_s \frac{K_a}{1-k^2}(b^T x - \delta) \tag{6.40}$$

which is very much the same as (6.13), except that the stiffness is now that for open electrodes. We use an IFF control on the charge Q, which is equivalent to a proportional controller on I:

$$\delta = \frac{g}{g_s[K_a/(1-k^2)]s}\, y \tag{6.41}$$

(again, the constant at the denominator is for normalization). Combining these three equations as we already did in the previous section, one finds easily that the closed-loop poles are solutions of the eigenvalue problem

$$[Ms^2 + (K + \frac{K_a}{1-k^2} bb^T) - \frac{g}{s+g} \frac{K_a}{1-k^2} bb^T]x = 0 \tag{6.42}$$

The asymptotic roots for $g = 0$ (open-loop poles) satisfy

$$[Ms^2 + (K + \frac{K_a}{1-k^2} bb^T)]x = 0 \tag{6.43}$$

The solutions are the natural frequencies of the global structure, Ω_i, *when the transducer electrodes are open*. On the other hand, the asymptotic

[1] The root locus of Fig.6.6 is almost unchanged if the pole at the origin is moved slightly to the left along the real axis; this may help to prevent saturation due to integral control; it is not critical if a piezoelectric force sensor is used, because the charge amplifier behaves like a high-pass filter.

roots when $g \to \infty$ (open-loop zeros, z_i) are again solutions of the eigenvalue problem (6.31). Following the same procedure as in the previous section, we can transform Equ.(6.42) into modal coordinates; it is readily found that the closed-loop poles are solutions of

$$1 + g\frac{s^2 + z_i^2}{s(s^2 + \Omega_i^2)} = 0 \tag{6.44}$$

which is the same as (6.37), except that the natural frequencies Ω_i with open electrodes are used instead of ω_i (with short-circuited electrodes). The root locus is again that of Fig.6.6, and the maximum damping ratio is given by (6.38) with Ω_i instead of ω_i:

$$\xi_i^{max} = \frac{\Omega_i - z_i}{2z_i} \tag{6.45}$$

Note that, assuming that the displacement mode shapes ϕ_i are independent of the electric boundary conditions,

$$\Omega_i^2 = \phi_i^T(K + \frac{K_a}{1-k^2}bb^T)\phi_i = \phi_i^T(K + K_a bb^T)\phi_i + \frac{k^2}{1-k^2}\phi_i^T K_a bb^T \phi_i \tag{6.46}$$

or, using (6.15),

$$\Omega_i^2 \simeq \omega_i^2(1 + \frac{k^2}{1-k^2}\nu_i) \tag{6.47}$$

6.4 Admittance of the piezoelectric transducer

The admittance of the transducer alone has already been investigated in section 4.4.3, to establish the relationship between the electromechanical coupling factor and the natural frequencies with open and short-circuited boundary conditions. Here, we consider a more complex situation where the transducer is mounted in a structure (that we assume undamped, as usual, to simplify the equations as much as we can). The dynamics of this system was already examined in section 4.4; with $R \to \infty$ and $F = 0$ in (4.25) and (4.26),

$$(Ms^2 + K + K_a bb^T)x = bK_a n d_{33} V \tag{6.48}$$

$$I = sC(1-k^2)V + snd_{33}K_a b^T x \tag{6.49}$$

The first equation governs the dynamics of the structure, and the second is the constitutive equation of the piezoelectric transducer. From (6.48)

$$x = (Ms^2 + K + K_a bb^T)^{-1} bK_a nd_{33} V \tag{6.50}$$

and, using the modal expansion of the dynamic flexibility matrix, (6.11), one gets

$$\Delta = b^T x = \sum_{i=1}^{n} \frac{b^T \phi_i \phi_i^T b}{\mu_i(\omega_i^2 + s^2)} \, nd_{33} K_a V \tag{6.51}$$

$$I = sC(1-k^2)V + snd_{33}K_a \{\sum_{i=1}^{n} \frac{b^T \phi_i \phi_i^T b}{\mu_i(\omega_i^2 + s^2)}\} \, nd_{33} K_a V \tag{6.52}$$

or

$$I = sC(1-k^2)V + sCk^2 \{\sum_{i=1}^{n} \frac{\nu_i}{1 + s^2/\omega_i^2}\} \, V \tag{6.53}$$

after using (4.8) and (6.15). Finally, the reduced admittance FRF is obtained

$$\frac{I}{sCV} = 1 + k^2 (\sum_{i=1}^{n} \frac{\nu_i}{1 - \omega^2/\omega_i^2} - 1) \tag{6.54}$$

It is represented in Fig.6.4(b). This figure can in fact be obtained by translating the diagram of Fig.6.4(a) along the vertical axis. Again, the diagram exhibits alternating poles and zeros (all the residues are positive), but in reverse order (it begins with a pole at ω_1). The poles are the same as those of the open-loop FRF, that is the natural frequencies of the structure with short-circuited electrodes. Let us consider the zeros: they are solution of (6.49) with $I = 0$

$$0 = sC(1-k^2)V + snd_{33}K_a b^T x \tag{6.55}$$

Substituting V from this equation into (6.48) and using the definition (4.8) of the electromechanical coupling factor, one finds that the zeros are solutions of

$$(Ms^2 + K + \frac{K_a}{1-k^2} bb^T) x = 0 \tag{6.56}$$

This equation is identical to (6.43), meaning that the zeros of the admittance are the poles of the system when the transducer electrodes are open, Ω_i. Thus, in a single admittance (or impedance) measurement, the natural frequencies ω_i with short-circuited electrodes and Ω_i with open electrodes can be determined.

6.5 Damping via resistive shunting

Return to Equ.(4.25)(4.26) and set $F = 0$ and $I = 0$ (the current source is removed); the governing equations are, in the Laplace domain

$$(Ms^2 + K + K_a bb^T)x = bK_a n d_{33} V \tag{6.57}$$

$$[sRC(1-k^2)+1]V = -sRnd_{33}K_a b^T x \tag{6.58}$$

Eliminating V and using the definition of k^2, one gets the characteristic equation

$$[Ms^2 + (K + K_a bb^T) + \frac{k^2 K_a bb^T}{(1-k^2)+1/sRC}]x = 0 \tag{6.59}$$

When $R = 0$, it is identical to (6.30), leading to the frequencies ω_i (short-circuited). For $R \to \infty$, it becomes identical to (6.43), leading to Ω_i (open electrodes). Upon transforming into modal coordinates, exactly as we did in the previous sections, and denoting $\varrho = RC$, one finds that every mode follows the characteristic equation

$$s^2 + \omega_i^2 + \frac{k^2 \nu_i \omega_i^2}{1 - k^2 + 1/\varrho s} = 0 \tag{6.60}$$

which, after using (6.47), can be rewritten

$$1 + \frac{1}{\varrho(1-k^2)} \; \frac{s^2 + \omega_i^2}{s(s^2 + \Omega_i^2)} = 0 \tag{6.61}$$

Thus, although resistive shunting is by no means a feedback control, the solution of the characteristic equation has been written in the form of a classical root locus, with $1/\varrho(1-k^2)$ acting as the feedback gain. This root locus has once again the shape of Fig.6.6, with open-loop poles at $\pm j\Omega_i$ (open electrodes) and open-loop zeros at $\pm j\omega_i$ (short-circuited electrodes). As in Fig.6.6, the maximum achievable damping is given by

$$\xi_i^{max} = \frac{\Omega_i - \omega_i}{2\ \omega_i} \simeq \frac{\Omega_i^2 - \omega_i^2}{4\ \omega_i^2} \tag{6.62}$$

and, using again Equ.(6.47),

$$\xi_i^{max} \simeq \frac{k^2 \nu_i}{4(1-k^2)} \tag{6.63}$$

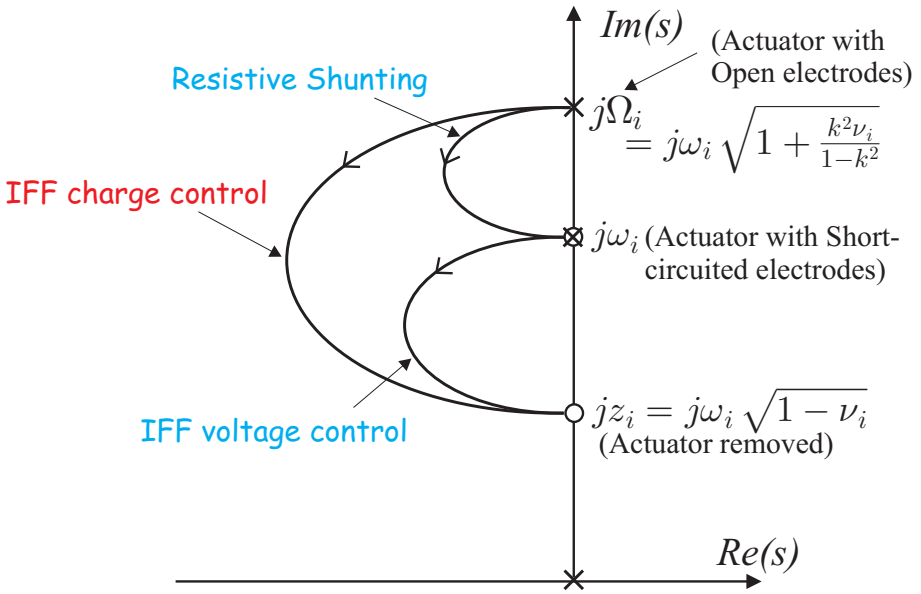

Fig. 6.7. Root locus plots corresponding to various control configurations.

This equation points out the influence of the fraction of modal strain energy ν_i and the electromechanical coupling factor k on passive damping with resistive shunting. Note that all the modes cannot be optimally damped simultaneously, because there is a single tuning parameter ϱ.

Figure 6.7 and Table 6.1 summarize the results of the three control configurations. Column 4 of Table 6.1 gives an approximation of the maximum achievable modal damping based on (6.62); these expressions show clearly the influence of the fraction of modal strain energy ν_i and that of the electromechanical coupling factor k. Figure 6.8 shows a chart of the maximum achievable modal damping for the three control strategies, as a function of ν_i and k; the contour lines correspond to constant modal damping. Note that: *(i)* For the IFF with voltage control, the maximum damping is independent of the electromechanical coupling factor. *(ii)* The IFF with charge control gives always better performances than with voltage control; the advantage increases with k. *(iii)* Significant modal damping with resistive shunting can be achieved only when the electromechanical coupling factor is large; piezoelectric materials with $k \geq 0.7$ are available.

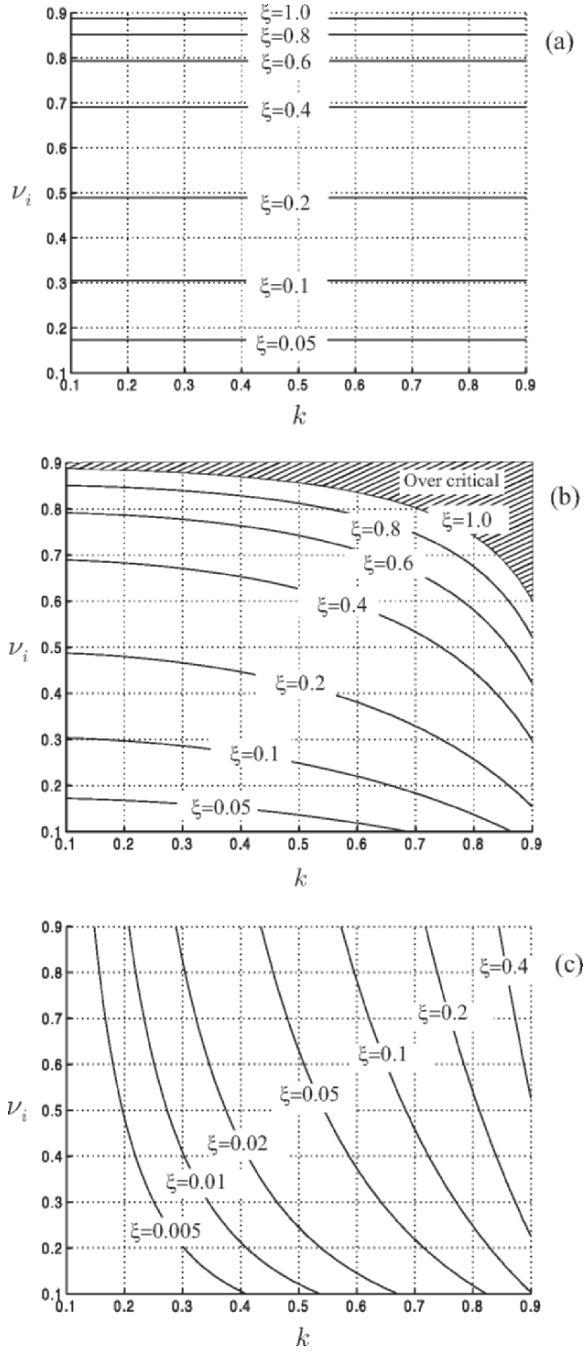

Fig. 6.8. Maximum achievable modal damping as a function of ν_i and k. (a) IFF voltage control, (b) IFF charge control, (c) Resistive shunting.

Table 6.1. Open-loop poles and zeros and maximum achievable modal damping in the root locus of Fig.6.7. The inductive shunting is added for comparison.

Control	Open-loop poles	Open-loop zeros	Max. Damping ξ_i
IFF (Voltage control)	$\pm j\omega_i$ *(short-circuit)*	$\pm jz_i \simeq \pm j\omega_i\sqrt{1-\nu_i}$	$\frac{\nu_i}{4(1-\nu_i)}$
IFF (Charge control)	$\pm j\Omega_i \simeq \pm j\omega_i\sqrt{1+\frac{k^2\nu_i}{1-k^2}}$	$\pm jz_i$ *(transducer removed)*	$\frac{\nu_i}{4(1-\nu_i)(1-k^2)}$
Resistive shunting	$\pm j\Omega_i$ (*open electrodes*)	$\pm j\omega_i$	$\frac{k^2\nu_i}{4(1-k^2)}$
Inductive shunting	p_1, p_2	0, $\pm j\Omega_i$	$\frac{1}{2}\sqrt{\frac{k^2\nu_i}{1-k^2}}$

6.5.1 Damping enhancement via negative capacitance shunting

Equation (6.63) indicates that the damping performance of the resistive shunting depends critically of the electromechanical coupling factor and Fig.6.8(c) shows that when k is larger than 0.7, significant damping (say > 0.05) can be achieved for reasonable values of ν_i. On the other hand, the active enhancement of the electromechanical coupling factor via a synthetic negative capacitance has been addressed in section 4.4.5; If the piezoelectric transducer is shunted on a negative capacitance $-C_1$ [such that $C_1 < C(1-k^2)$], it behaves like an equivalent transducer with properties given by (4.43) and (4.44):

$$C^* = C - C_1 \qquad\qquad k^{*2} = k^2\frac{C}{C-C_1}$$

Thus, the damping effectiveness of the resistive shunting can be improved by placing a negative capacitance in parallel with the transducer. The performances can again be predicted by the root locus (6.61) where k^* is used in (6.47) to evaluate Ω_i^2. The maximum damping is still given by

(6.63) with k^* instead of k. The idea of using a negative synthetic capacitance to enhance the damping seems to have been originally proposed by (Forward, 1979); some stability problems remain and this topic is still under investigation.

6.5.2 Generalized electromechanical coupling factor

The admittance function of a piezoelectric transducer mounted in a structure exhibits alternating poles at ω_i and zeros at Ω_i [Fig.6.4(b)]. By analogy with (4.35), the *generalized electromechanical coupling factor* (of mode i) is defined as

$$K_i^2 = \frac{\Omega_i^2 - \omega_i^2}{\Omega_i^2} \tag{6.64}$$

Using (6.47), one finds

$$K_i^2 = \frac{k^2 \nu_i}{1 - k^2 + k^2 \nu_i} \tag{6.65}$$

K_i^2 combines material data with information about the structure; $K_i^2 = k^2$ if $\nu_i = 1$. Note that, in the literature, the definition

$$K_i^2 = \frac{\Omega_i^2 - \omega_i^2}{\omega_i^2} = \frac{k^2 \nu_i}{1 - k^2} \tag{6.66}$$

is often used instead of (6.64). The difference between the two definitions is insignificant in most practical applications, but (6.66) does not supply $K_i = k$ if $\nu_i = 1$. Note also that the maximum performance of resistive shunting, (6.63), is directly related to the generalized electromechanical coupling factor.

6.6 Inductive shunting

Inductive shunting constitutes an alternative way of enhancing the modal damping; the shunt consists of an inductor and a resistor in series which are combined with the capacitance of the piezoelectric transducer to create a damped electrical resonance; if the electrical resonance is tuned on the mechanical resonance, the resonant shunt acts as a vibration absorber as in Den Hartog's tuned mass damper. The theory of inductive shunting was first developed by (Hagood & von Flotow, 1991).

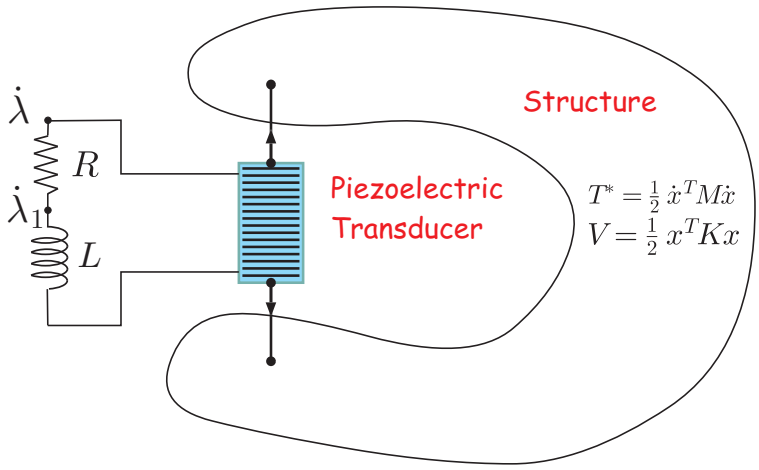

Fig. 6.9. Inductive shunting.

Consider the system of Fig.6.9, where the piezoelectric transducer is shunted on a RL circuit. The electrical variables are λ and λ_1. The Lagrangian reads in this case

$$L = \frac{1}{2}\dot{x}^T M\dot{x} - \frac{1}{2}x^T(K + K_a bb^T)x + C(1-k^2)\frac{\dot{\lambda}^2}{2} + nd_{33}K_a\dot{\lambda}b^T x - \frac{1}{2}\lambda_1^2/L \tag{6.67}$$

The virtual work of the non-conservative forces is

$$\delta W_{nc} = -\frac{\dot{\lambda} - \dot{\lambda}_1}{R}\,\delta(\dot{\lambda} - \dot{\lambda}_1) \tag{6.68}$$

or one can use alternatively the dissipation function

$$D = \frac{1}{2}\frac{(\dot{\lambda} - \dot{\lambda}_1)^2}{R} \tag{6.69}$$

Upon writing Lagrange's equations, one finds (in Laplace form):

$$Ms^2 x + (K + K_a bb^T)x = bK_a nd_{33}s\lambda \tag{6.70}$$

$$s[C(1-k^2)s\lambda + nd_{33}K_a b^T x] + \frac{s(\lambda - \lambda_1)}{R} = 0 \tag{6.71}$$

$$\frac{\lambda_1}{L} + \frac{s(\lambda_1 - \lambda)}{R} = 0 \tag{6.72}$$

λ_1 can be eliminated between the last two equations, leading to

$$[sC(1-k^2)+Y_{SH}]\lambda = -nd_{33}K_a b^T x \tag{6.73}$$

where

$$Y_{SH} = (R+Ls)^{-1} \tag{6.74}$$

is the admittance of the shunt. Substituting λ into the first equation, one finds the eigenvalue problem

$$[Ms^2 + (K + K_a bb^T) + \frac{k^2}{(1-k^2)} \cdot \frac{K_a bb^T}{[1 + Y_{SH}/sC(1-k^2)]}]x = 0 \tag{6.75}$$

with

$$\frac{Y_{SH}}{sC(1-k^2)} = \frac{1}{(R+Ls)sC(1-k^2)} = \frac{1/LC(1-k^2)}{s^2+(R/L)s} = \frac{\omega_e^2}{s^2+2\xi_e\omega_e s} \tag{6.76}$$

after defining the electrical frequency

$$\omega_e^2 = \frac{1}{LC(1-k^2)} \tag{6.77}$$

and the electrical damping

$$2\xi_e\omega_e = \frac{R}{L} \tag{6.78}$$

Upon transforming into modal coordinates, using the same notation as in the previous sections, one finds that every mode is governed by the characteristic equation

$$s^2 + \omega_i^2 + \frac{k^2\nu_i\omega_i^2}{1-k^2}[\frac{s^2+2\xi_e\omega_e s}{s^2+2\xi_e\omega_e s+\omega_e^2}] = 0 \tag{6.79}$$

or

$$s^2 + \Omega_i^2 + \frac{k^2\nu_i\omega_i^2}{1-k^2}[\frac{-\omega_e^2}{s^2+2\xi_e\omega_e s+\omega_e^2}] = 0 \tag{6.80}$$

where, as usual, ω_i is the natural frequency with short-circuited electrodes and Ω_i that with open electrodes. Thus, the characteristic equation can be rearranged into

$$(s^2+\Omega_i^2)(s^2+2\xi_e\omega_e s+\omega_e^2) - \frac{k^2\nu_i}{1-k^2}\omega_i^2\omega_e^2 = 0 \tag{6.81}$$

or

$$s^4 + 2\xi_e\omega_e s^3 + (\Omega_i^2+\omega_e^2)s^2 + 2\Omega_i^2\xi_e\omega_e s + \omega_i^2\omega_e^2 = 0 \tag{6.82}$$

This can be rewritten in a root locus form

$$1 + 2\xi_e\omega_e \frac{s(s^2+\Omega_i^2)}{s^4+(\Omega_i^2+\omega_e^2)s^2+\omega_i^2\omega_e^2} = 0 \tag{6.83}$$

In this formulation, $2\xi_e\omega_e$ plays the role of the gain in a classical root locus. Note that, for large R, the poles tend to $\pm j\Omega_i$, as expected. For $R = 0$ (i.e. $\xi_e = 0$), they are the solutions p_1 and p_2 of the characteristic equation $s^4 + (\Omega_i^2 + \omega_e^2)s^2 + \omega_i^2\omega_e^2 = 0$ which accounts for the classical double peak of resonant dampers, with p_1 above $j\Omega_i$ and p_2 below $j\Omega_i$. Figure 6.10 shows the root locus for a fixed value of ω_i/Ω_i and various values of the electrical tuning, expressed by the ratio

$$\alpha_e = \frac{\omega_e\omega_i}{\Omega_i^2} \tag{6.84}$$

The locus consists of two loops, starting respectively from p_1 and p_2; one of them goes to $j\Omega_i$ and the other goes to the real axis, near $-\Omega_i$. If $\alpha_e > 1$ [Fig.6.10(a)], the upper loop starting from p_1 goes to the real axis, and that starting from p_2 goes to $j\Omega_i$, and the upper pole is always more heavily damped than the lower one (note that, if $\omega_e \to \infty$, $p_1 \to \infty$ and $p_2 \to j\omega_i$; the lower branch of the root locus becomes that of the resistive shunting). The opposite situation occurs if $\alpha_e < 1$ [Fig.6.10(b)]: the upper loop goes from p_1 to $j\Omega_i$ and the lower one goes from p_2 to the real axis; the lower pole is always more heavily damped. If $\alpha_e = 1$ [Fig.6.10(c)], the two poles are always equally damped until the two branches touch each other in Q. This double root is achieved for

$$\alpha_e = \frac{\omega_e\omega_i}{\Omega_i^2} = 1,\ \xi_e^2 = 1 - \frac{\omega_i^2}{\Omega_i^2} \tag{6.85}$$

This can be regarded as the optimum tuning of the inductive shunting (note that, comparing with (6.64), $\xi_e^2 = K_i^2$; thus, the optimum electrical damping ratio exactly matches the generalized electromechanical coupling factor). The corresponding eigenvalues satisfy

$$s^2 + \Omega_i^2 + \Omega_i(\frac{\Omega_i^2}{\omega_i^2} - 1)^{1/2}s = 0 \tag{6.86}$$

For various values of ω_i/Ω_i (or K_i), the optimum poles at Q move along a circle of radius Ω_i [Fig.6.10(d)]. The corresponding damping ratio can be obtained easily by identifying the previous equation with the classical form of the damped oscillator, $s^2 + 2\xi_i\Omega_i s + \Omega_i^2 = 0$, leading to

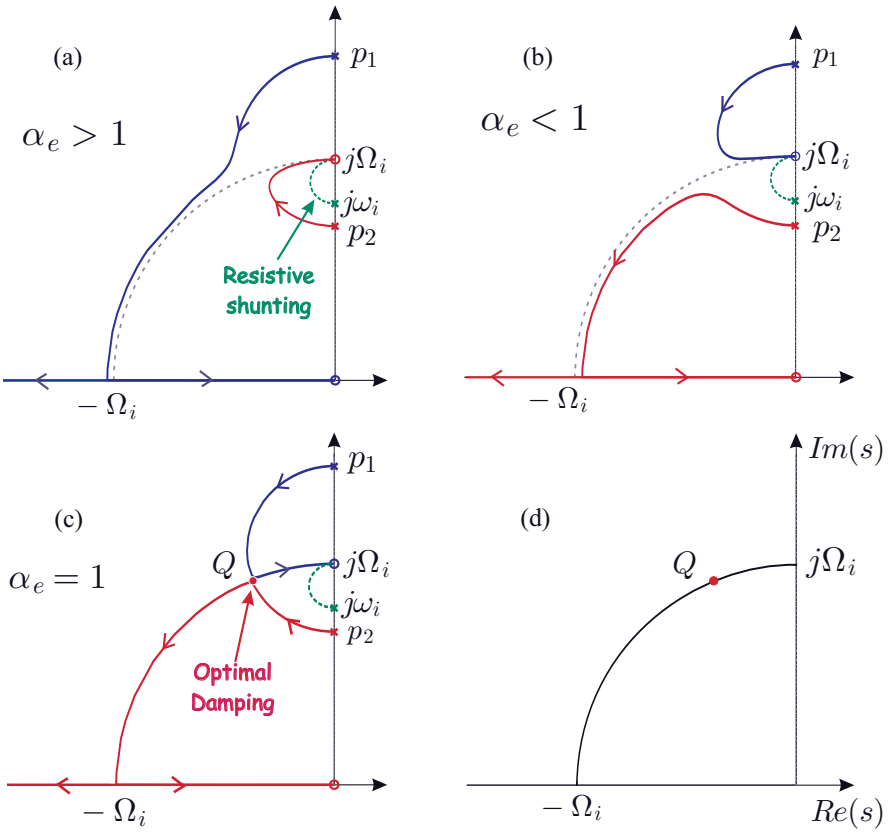

Fig. 6.10. Root locus plot for inductive shunting (only the upper half is shown). The optimum damping at Q is achieved for $\alpha_e = 1$ and $\xi_e = K_i^2$; the maximum modal damping is $\xi_i \simeq K_i/2$.

$$\xi_i = \frac{1}{2}\left(\frac{\Omega_i^2}{\omega_i^2} - 1\right)^{1/2} = \frac{1}{2}\left(\frac{K_i^2}{1 - K_i^2}\right)^{1/2} \simeq \frac{K_i}{2} \tag{6.87}$$

Using (6.47), we can express the optimum damping ratio in terms of the electromechanical coupling factor and the fraction of modal strain energy:

$$\xi_i = \frac{1}{2}\left(\frac{k^2 \nu_i}{1 - k^2}\right)^{1/2} \tag{6.88}$$

This value is significantly higher than that achieved with purely resistive shunting [it is exactly the square-root of (6.63)]; it has been added to Table 6.1 for comparison. Note, however, that it is much more sensitive to the tuning of the electrical parameters on the targeted modes. This is

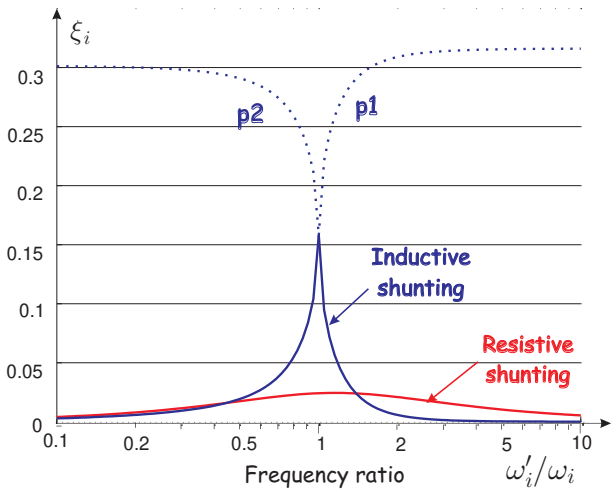

Fig. 6.11. Evolution of the damping ratio of the inductive and resistive shunting with the de-tuning of the structural mode. ω_i is the natural frequency for which the shunt has been optimized, ω_i' is the actual value ($k = 0.5$, $\nu_i = 0.3$).

illustrated in Fig.6.11, which displays the evolution of the damping ratio ξ_i when the actual natural frequency ω_i' moves away from the nominal frequency ω_i for which the shunt has been optimized (the damping ratio associated with p_1 and p_2 is plotted in dotted lines; the ratio ω_i'/Ω_i' is kept constant in all cases). One sees that the performance of the inductive shunting drops rapidly below that of the resistive shunting when the de-tuning increases. Note that, for low frequency modes, the optimum inductance value can be very large; such large inductors can be synthesized electronically. The multimodal passive damping via resonant shunt has been investigated by (Hollkamp, 1994).

All the dissipation mechanisms considered in this chapter are based on linear time-invariant filters. Recently, promising alternative nonlinear methods based on state switching have been proposed. The transducer is connected to a solid-state switch device which discharges periodically the piezoelectric element on a small inductor, producing a voltage inversion (Guyomar & Richard, 2005).

6.6.1 Alternative formulation

Throughout our analysis of piezoelectric structures, we have adopted a flux linkage formulation for the electrical variables. However, we could also have used a charge formulation. In most cases, this would have led to

more electrical variables, but in the particular case of inductive shunting, the charge formulation is in fact more compact, because there is a single electrical variable instead of two in the flux linkage formulation. Let $\dot{q}$ be the current in the single current loop of Fig.6.9; the Lagrangian of the system is in this case [2]

$$L = T^* + W_m^* - V - W_e \tag{6.89}$$

where T^* and V refer, as usual, to the mechanical part of the system, W_m^* is the magnetic coenergy of the inductor, $W_m^* = (1/2)L\dot{q}^2$, and W_e is the electromechanical energy of the piezoelectric transducer, given by (4.13).

$$L = \frac{1}{2}\dot{x}^T M\dot{x} + \frac{1}{2}L\dot{q}^2 - \frac{1}{2}x^T Kx - \frac{q^2}{2C(1-k^2)} + \frac{nd_{33}K_a}{C(1-k^2)}\, qb^T x - \frac{K_a}{1-k^2}\frac{(b^T x)^2}{2} \tag{6.90}$$

The dissipation function is in this case $D = (1/2)R\dot{q}^2$. The Lagrange equations relative to the coordinates x and q are respectively

$$M\ddot{x} + (K + \frac{K_a}{1-k^2}\, bb^T)x - \frac{bnd_{33}K_a}{C(1-k^2)}\, q = 0 \tag{6.91}$$

$$L\ddot{q} + R\dot{q} + \frac{q}{C(1-k^2)} - \frac{nd_{33}K_a}{C(1-k^2)}\, b^T x = 0 \tag{6.92}$$

Using (6.77) and (6.78), (6.92) is rewritten

$$\ddot{q} + 2\xi_e\omega_e\dot{q} + \omega_e^2 q - \omega_e^2 nd_{33}K_a b^T x = 0$$

or, in Laplace form,

$$q = \frac{\omega_e^2}{s^2 + 2\xi_e\omega_e s + \omega_e^2}\, nd_{33}K_a b^T x \tag{6.93}$$

Introducing in (6.91), one finds

$$(Ms^2 + K + \frac{K_a}{1-k^2}\, bb^T)x + \frac{k^2}{1-k^2}K_a bb^T x[\frac{-\omega_e^2}{s^2 + 2\xi_e\omega_e s + \omega_e^2}] = 0 \tag{6.94}$$

and, after transformation into modal coordinates, one recovers Equ.(6.80); the rest of the discussion of the previous section applies.

[2] see (3.39)

6.7 Decentralized control

One way to increase the damping is to use multiple transducer systems controlled in a decentralized manner (Fig.4.11); this allows one to preserve the robustness properties of individual loops with respect to the parametric uncertainty, and minimizes the sensitivity with respect to sensor and actuator failure by leaving the remaining loops unaffected if one of them breaks. The dynamics of a structure with n_T identical piezoelectric transducers has been analyzed in section 4.5; the governing equations are (4.49) and (4.50).

We first consider the case where the transducers, assumed to be identical, are connected to voltage sources, and the IFF controller relies on independent force feedback loops with identical gains. With voltage sources, λ are no longer generalized variables, and the system dynamics is governed by

$$Ms^2x + (K + K_aBB^T)x = BK_a\delta = K_aBnd_{33}V \tag{6.95}$$

where V is the vector of voltages applied and B is the $(n \times n_T)$ projection matrix relating the end displacements of the transducers to the global coordinate system, $\Delta = B^Tx$, and δ is the vector of unconstrained piezoelectric displacements. As in the single-input single-output (SISO) case discussed earlier, the output equation of the force sensor is

$$y = f = g_sK_a(\Delta - \delta) = g_sK_a(B^Tx - \delta) \tag{6.96}$$

and the IFF control law is

$$\delta = \frac{g}{g_sK_as}\,y \tag{6.97}$$

These equations are formally identical to those of the SISO case, except that δ and y are vector quantities; it is assumed that the control gain g is the same for all control loops. Combining the above equations, we obtain the closed-loop characteristic equation

$$[Ms^2 + (K + K_aBB^T) - \frac{g}{s+g}(K_aBB^T)]x = 0 \tag{6.98}$$

As in the SISO case, the asymptotic roots for $g \to 0$ (open-loop poles), solution of

$$[Ms^2 + (K + K_aBB^T)]x = 0 \tag{6.99}$$

are the natural frequencies ω_i of the global structure with short-circuited electrodes. On the other hand, the asymptotic roots for $g \to \infty$ (open-loop zeros, z_i) are solutions of

$$[Ms^2 + K]x = 0 \tag{6.100}$$

which, again, corresponds to the situation where the axial contribution of the transducer to the global stiffness matrix has been removed. A notable difference with respect to the SISO case, however, is the fact that the poles and zeros are no longer guaranteed to be alternating along the imaginary axis, and it is not always simple to determine the asymptotic value of a specific mode without following the entire locus. The formulation into modal coordinates follows exactly section 6.3.2, except that the fraction of modal strain energy is defined by

$$\Phi^T(K_a B B^T)\Phi \simeq diag(\nu_i \omega_i^2) \tag{6.101}$$

and contains contributions from all transducers. The results of Table 6.1 still apply in this case, with ν_i being the fraction of modal strain energy for all the transducers.[3]

The case of the current sources and the resistive shunting can be treated similarly; again, if one assumes that all shunting loops use the same resistor, all the results of Table 6.1 apply. The actuator placement aims at maximizing the fraction of modal strain energy in the set of modes that are targeted for control. An interesting option consists of integrating piezoelectric transducers into a *Stewart-Gough platform*, which can be used as an interface between independent substructures; this application is discussed in (Preumont, 2002, Abu Hanieh, 2003). Another application is the control of large trusses with cables attached to active tendons; it has been explored in (Preumont, Achkire, Bossens, 1997-2001); once again, the cable network is designed to maximize the fraction of modal strain energy in the active tendons.

6.8 General piezoelectric structure

The dynamics of a general piezoelectric structure has been analyzed in section 4.6. The governing equations are

$$Ms^2 x + K_{xx} x - K_{\phi x}^T V = 0 \tag{6.102}$$

$$sC_{\phi\phi} V + sK_{\phi x} x + Y_{SH} V = I \tag{6.103}$$

For passive shunting, $I = 0$ and V can be eliminated from the previous equations, leading to the eigenvalue problem

[3] within the limits of the approximation (6.101).

$$[Ms^2 + K_{xx} + sK_{\phi x}^T(sC_{\phi\phi} + Y_{SH})^{-1}K_{\phi x}]x = 0 \qquad (6.104)$$

There are numerous practical situations where $C_{\phi\phi}$ and Y_{SH} are diagonal matrices [e.g. a structure with a set of PZT or MFC (Macro Fiber Composite) patches shunted independently] and the foregoing equation can be reduced to a form essentially similar to (6.59). The two asymptotes for $Y_{SH} \to \infty$ and $Y_{SH} = 0$ are again the eigenvalue problems with short-circuited electrodes and open electrodes, respectively.

6.9 Self-sensing

The active strut of Fig.6.3 consists of two transducers, one used as actuator, and one as force sensor. It is possible to combine the sensor and the actuator into a single element called a *self-sensing actuator* (Dosch, Inman & Garcia, 1992). The general principle of self-sensing has already been discussed at the end of Chapter 3; here the special case of a piezoelectric transducer is considered. Since the impedance of a piezoelectric transducer is essentially that of a capacitor, the bridge structure is that of Fig.6.12, with all elements being capacitors (C_2 and C_3). The control voltage is V_c and the sensor output is $V_1 - V_2$. By an appropriate choice of the capacitance C_3, one can make the sensor output proportional to the force f applied to the transducer, or to the strain, that is the relative displacement Δ of its end points. Moreover, we will see that the transmission zeros depend on the capacitance C_3 which can therefore be used for shaping the open-loop transfer function.

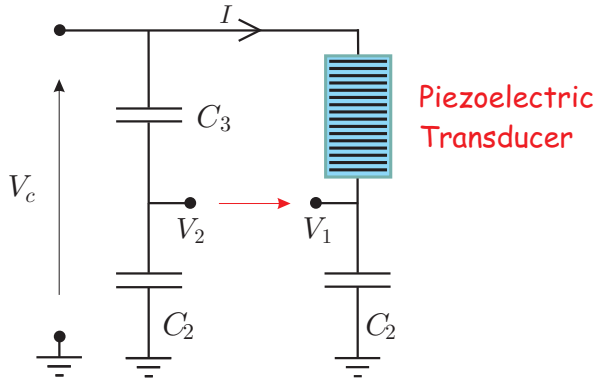

Fig. 6.12. Self-sensing actuator.

6.9.1 Force sensing

The self-sensing actuator consists of a bridge (Fig.6.12); one element of the right branch of the bridge is the transducer itself, while the other branch is made of known capacitors. According to the constitutive equation of the transducer, (4.6),

$$I/s = Q = CV + nd_{33}f \tag{6.105}$$

where C is the unconstrained capacitance ($f = 0$) and $V = V_c - V_1$ is the voltage difference at the transducer electrodes. It follows that

$$V = \frac{I}{Cs} - \frac{nd_{33}}{C}f \tag{6.106}$$

On the other hand, $V_1 = I/C_2 s$ and

$$V_c = V + V_1 = (\frac{1}{C} + \frac{1}{C_2})\frac{I}{s} - \frac{nd_{33}}{C}f$$

or

$$I = \frac{CC_2 s}{C + C_2}V_c + \frac{C_2 s}{C + C_2}nd_{33}f$$

and

$$V_1 = \frac{I}{C_2 s} = \frac{C}{C + C_2}V_c + \frac{nd_{33}}{C + C_2}f \tag{6.107}$$

In the left branch of the bridge

$$V_2 = \frac{C_3}{C_3 + C_2}V_c \tag{6.108}$$

and

$$V_1 - V_2 = [\frac{C}{C + C_2} - \frac{C_3}{C_3 + C_2}]V_c + \frac{nd_{33}}{C + C_2}f \tag{6.109}$$

It follows that, if C_3 is selected in such a way that $C_3 = C$, the output

$$V_1 - V_2 = \frac{nd_{33}}{C + C_2}f \tag{6.110}$$

is proportional to the *force* applied to the transducer.

6.9.2 Displacement sensing

Alternatively, let us start from the constitutive equation (4.7)

$$I/s = Q = C^S V + nd_{33}K_a\Delta \tag{6.111}$$

where $C^S = C(1-k^2)$ is the blocked capacitance ($\Delta = 0$). Following the same procedure as above,

$$V = \frac{I}{C^S s} - \frac{nd_{33}K_a}{C^S}\Delta$$

$$V_c = V_1 + V = \frac{I}{C_2 s} + \frac{I}{C^S s} - \frac{nd_{33}K_a}{C^S}\Delta$$

or

$$I = \frac{C^S C_2 s}{C^S + C_2}V_c + \frac{C_2 s}{C^S + C_2}nd_{33}K_a\Delta$$

and

$$V_1 = \frac{I}{C_2 s} = \frac{C^S}{C^S + C_2}V_c + \frac{nd_{33}K_a}{C^S + C_2}\Delta \tag{6.112}$$

Equation (6.108) still applies to the other branch of the bridge and the output is

$$V_1 - V_2 = [\frac{C^S}{C^S + C_2} - \frac{C_3}{C_3 + C_2}]V_c + \frac{nd_{33}K_a}{C^S + C_2}\Delta \tag{6.113}$$

It follows that, if C_3 is selected in such a way that $C_3 = C^S = C(1-k^2)$, the output voltage

$$V_1 - V_2 = \frac{nd_{33}K_a}{C^S + C_2}\Delta \tag{6.114}$$

is proportional to the *relative displacement* Δ at the end nodes of the transducer.

6.9.3 Transfer function

We have just seen that the output of the self-sensing actuator depends of the value of the capacitance C_3 in the measurement bridge; $C_3 = C$, the unconstrained capacitance of the transducer, leads to an output signal proportional to the force acting on the transducer, and $C_3 = C^S = C(1-k^2)$, the blocked capacitance, leads to an output signal proportional to the relative displacement of the end nodes of the transducer. This suggests

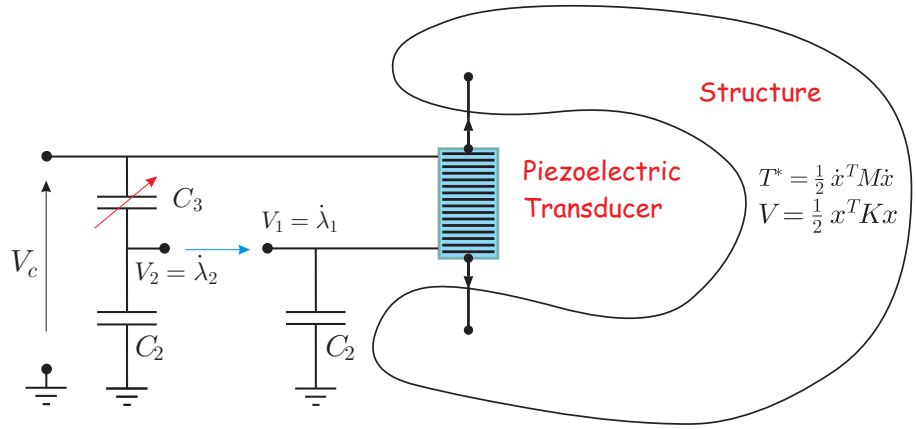

Fig. 6.13. Self-sensing actuator mounted in a structure.

that the transmission zeros depend on the value of the capacitance C_3. This point is investigated in this section.

Consider the self-sensing actuator inserted in a structure as in Fig.6.13; the capacitance C_3 can be varied and its influence on the open-loop zeros of the transfer function $(V_1 - V_2)/V_c$ is investigated. The Lagrangian of the system reads in this case

$$L = \frac{1}{2}\dot{x}^T M\dot{x} - \frac{1}{2}x^T(K + K_a bb^T)x + C(1-k^2)\frac{(V_c - \dot{\lambda}_1)^2}{2} + nd_{33}K_a(V_c - \dot{\lambda}_1)b^T x$$

$$+ \frac{1}{2}C_3(V_c - \dot{\lambda}_2)^2 + \frac{1}{2}C_2(\dot{\lambda}_2^2 + \dot{\lambda}_1^2) \tag{6.115}$$

There are two electrical variables, λ_1 and λ_2; proceeding as in section 4.4, the Lagrange's equations read (in Laplace form)

$$Ms^2 x + (K + K_a bb^T)x = bK_a nd_{33}(V_c - V_1) \tag{6.116}$$

$$s[-C(1-k^2)(V_c - V_1) - nd_{33}K_a b^T x + C_2 V_1] = 0 \tag{6.117}$$

$$s[-C_3(V_c - V_2) + C_2 V_2] = 0 \tag{6.118}$$

after substituting $V_1 = \dot{\lambda}_1$ and $V_2 = \dot{\lambda}_2$. The first equation governs the dynamics of the structure, while the other two express the KCR in the two branches of the bridge. The third equation immediately provides

$$\frac{V_2}{V_c} = \frac{1}{1 + C_2/C_3} \tag{6.119}$$

The transfer function between V_c and V_1 can be obtained as follows; from (6.117)

$$V_1 = \frac{nd_{33}K_a b^T x + C(1-k^2)V_c}{C(1-k^2)+C_2} \tag{6.120}$$

Introducing in (6.116), one gets easily

$$\{Ms^2 + K + K_a bb^T[1 + \frac{k^2}{1-k^2+r}]\}x = bnd_{33}K_a[\frac{r}{1-k^2+r}]V_c \tag{6.121}$$

where we have used (4.8) and defined $r = C_2/C$. This equation is very similar to (4.30). Upon transforming into modal coordinates as in section 6.3.2, $x = \Phi\alpha$, one finds easily the modal equation

$$[s^2 + \omega_i^2 + \nu_i\omega_i^2\frac{k^2}{1-k^2+r}]\alpha_i = \phi_i^T bnd_{33}K_a[\frac{r}{1-k^2+r}]V_c \tag{6.122}$$

This equation shows that the open-loop poles lie somewhere between those of the system with short circuited electrodes, ω_i (corresponding to $r \to \infty$) and those of the system with open electrodes, Ω_i (corresponding to $r = 0$). To make this equation more compact, let us define

$$\omega_i^{*2} = \omega_i^2 + \nu_i\omega_i^2\frac{k^2}{1-k^2+r} \tag{6.123}$$

ω_i^* are the natural frequencies of the system when the driving voltage source is short-circuited, $V_c = 0$. With this notation, the structural displacements can be expressed

$$x = \sum \frac{\phi_i\phi_i^T b}{(s^2+\omega_i^{*2})}nd_{33}K_a[\frac{r}{1-k^2+r}]V_c$$

and, combining with (6.120), one gets

$$\frac{V_1}{V_c} = \sum_i \frac{\nu_i\omega_i^2}{(s^2+\omega_i^{*2})}\frac{k^2 r}{(1-k^2+r)^2} + \frac{1-k^2}{1-k^2+r} \tag{6.124}$$

where the definition (6.15) of ν_i has been used. Combining with (6.119), one gets the open-loop transfer function

$$G(s) = \frac{V_1 - V_2}{V_c} = \sum_i \frac{\nu_i\omega_i^2}{(s^2+\omega_i^{*2})}\frac{k^2 r}{(1-k^2+r)^2} + [\frac{1-k^2}{1-k^2+r} - \frac{1}{1+rC/C_3}] \tag{6.125}$$

One sees that all the residues of the modal expansion are positive; this guarantees alternating poles and zeros in the transfer function. On the other hand, the feedthrough component (between brackets) has a magnitude which is controlled by the ratio C/C_3; by making C_3 a variable element, it is possible to change the magnitude of the feedtrough and consequently the location of the zeros. This brings a degree of tailoring on the open-loop transfer function. To illustrate this, consider the asymptotic situation where $r \gg 1$; in this case, the previous equation can be simplified into

$$G(s) = \frac{V_1 - V_2}{V_c} = \frac{1}{r}[\sum_i \frac{\nu_i \omega_i^2 k^2}{(s^2 + \omega_i^{*2})} + (1 - k^2 - C_3/C)] \tag{6.126}$$

At $s = 0$,

$$G(0) = \frac{1}{r}[\sum_i \frac{\nu_i \omega_i^2 k^2}{\omega_i^{*2}} + (1 - k^2 - C_3/C)] \tag{6.127}$$

Because $\omega_i < \omega_i^*$ [from (6.123)] and $\sum_i \nu_i < 1$ [from (6.21)], the first term is positive and smaller than k^2. It follows that $C_3 = C$ leads to $G(0) < 0$, while $C_3 = C(1 - k^2)$ cancels the feedthrough term, leading

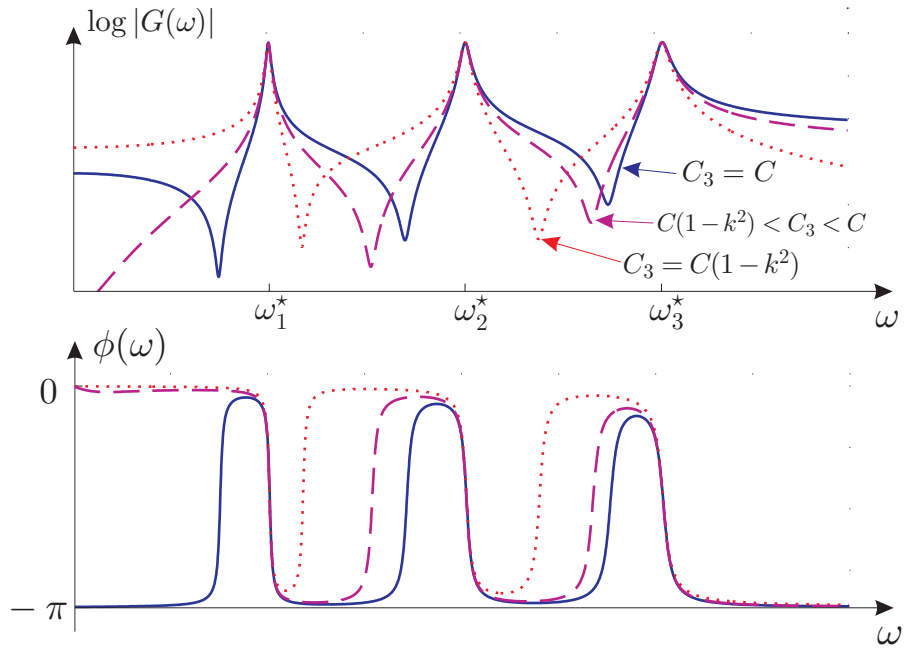

Fig. 6.14. Self-sensing actuator: effect of the capacitance C_3 on the open-loop FRF.

to $G(0) > 0$. Thus, if $C_3 = C$, $G(s)$ exhibits alternating poles and zeros on the imaginary axis, starting with a zero, while if $C_3 = C(1 - k^2)$, it starts with a pole. This is illustrated in Fig.6.14 which shows the effect of C_3 on a typical open-loop FRF (this figure has been generated with the following data: $\omega_1 = 1$, $\omega_2 = 2$, $\omega_3 = 3$, $\nu_1 = \nu_2 = \nu_3 = 0.2$, $k = 0.5$, $r = 1$, and a uniform damping $\xi_i = 0.01$).

6.10 Other active damping strategies

In Fig.6.14, all the FRF exhibit alternating poles and zeros; however, they differ in the way the pole-zero pattern starts at low frequency. The FRF corresponding to $C_3 = C$ starts with a low frequency zero and is identical to that of Fig.6.4(a) or Fig.6.5(b); the IFF is a very effective control strategy for this situation. On the other hand, for $C_3 = C(1-k^2)$, the FRF starts with a low frequency pole, and the IFF strategy would be unstable for this pole-zero configuration; alternative strategies applicable in this case are discussed below.

6.10.1 Lead control

The first case to consider is that where the open-loop FRF exhibits some roll-off at high frequency, usually -40 dB/decade, corresponding to the open-loop transfer function having two poles in excess of zeros (decays as ω^{-2} at high frequency). The modal expansion of the open-loop transfer function is

$$G(s) = \sum_{i=1}^{n} \frac{b^T \phi_i \phi_i^T b}{\mu_i (s^2 + {\omega_i}^2)} \tag{6.128}$$

This corresponds typically to the case of a point force actuator collocated with a displacement sensor. The pole-zero pattern is that of Fig.6.15; this system can be damped with a *lead compensator*:

$$H(s) = g \frac{s+z}{s+p} \qquad (p \gg z) \tag{6.129}$$

The block diagram of the control system is shown in Fig.6.16. This controller takes its name from the fact that it produces a phase lead in the frequency band between z and p, bringing active damping to all the modes belonging to $z < \omega_i < p$. All the branches of the root locus belong to the left-half plane, which means that the closed-loop system has guaranteed stability, at least if perfect actuator and sensor dynamics are assumed.

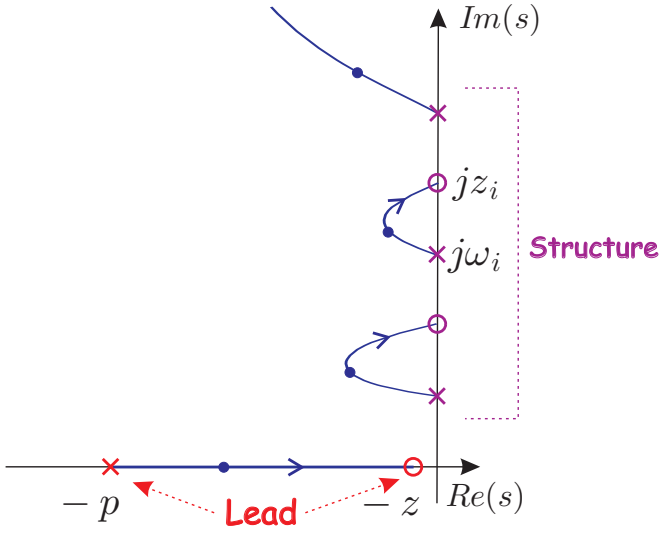

Fig. 6.15. Root locus of the lead compensator applied to a structure with collocated actuator and sensor (open-loop transfer function with two poles in excess of zeros).

The controller does not have any roll-off, but the roll-off of the structure is enough to guarantee gain stability at high frequency.

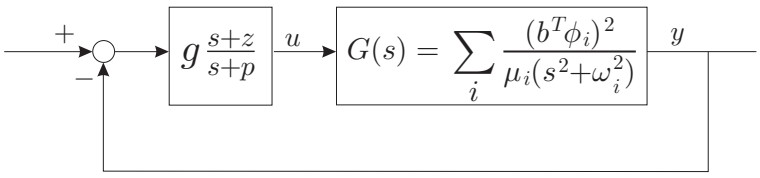

Fig. 6.16. Block diagram of the lead compensator applied to a structure with collocated actuator and sensor (open-loop transfer function with two poles in excess of zeros).

6.10.2 Positive Position Feedback (PPF)

The situation where the open-loop FRF has a roll-off of -40 dB/decade is not the most frequent one when piezoelectric actuators are used. Figure 5.10 shows a typical experimental open-loop FRF corresponding to an active cantilever beam with collocated PZT actuator and sensor patches, similar to that of Fig.5.6. As observed earlier, this open-loop FRF does not roll-off at high frequency, and this was attributed to a feedthrough term in the system equation; a similar situation occurs in (6.125). When

the open-loop transfer function has a feedtrough component, the system stability requires that the compensator includes some roll-off.[4] The *Positive Position Feedback* was proposed (Goh & Caughey, 1985, Fanson & Caughey, 1990) to achieve just that, for systems similar to that of Fig.5.6. The controller consists of a second order filter

$$H(s) = \frac{-g}{s^2 + 2\xi_f \omega_f s + \omega_f^2} \tag{6.130}$$

where the damping ξ_f is usually high (0.5 to 0.7), and the filter frequency ω_f is adapted to target a specific mode. The block diagram of the control system is shown in Fig.6.17; the negative sign in $H(s)$, which produces a positive feedback, is the origin of the name of this controller.

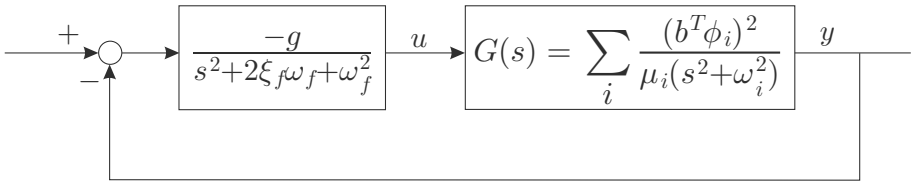

Fig. 6.17. Block diagram of the PPF controller applied to a structure with collocated actuator and sensor (the open-loop transfer function has the same number of poles and zeros).

Figure 6.18 shows typical root loci when the PPF poles are targeted to mode 1 and mode 2, respectively (i.e. ω_f close to ω_1 or ω_2, respectively). One sees that the whole locus is contained in the left half plane, except one part on the positive real axis, but that part of the locus is reached only for large values of g, which are not used in practice. The stability condition can be established as follows: the characteristic equation of the closed loop system reads

$$\psi(s) = 1 + gH(s)G(s) = 1 - \frac{g}{s^2 + 2\xi_f \omega_f s + \omega_f^2} \{ \sum_{i=1}^{n} \frac{b^T \phi_i \phi_i^T b}{\mu_i (s^2 + \omega_i{}^2)} \} = 0$$

or

$$\psi(s) = s^2 + 2\xi_f \omega_f s + \omega_f^2 - g \{ \sum_{i=1}^{n} \frac{b^T \phi_i \phi_i^T b}{\mu_i (s^2 + \omega_i{}^2)} \} = 0$$

According to the Routh-Hurwitz criterion for stability, if one of the

[4] in the IFF control discussed earlier, there is a feedthrough in $G(s)$, but the controller $1/s$ has a -20 dB/decade roll-off.

coefficients of the power expansion of the characteristic equation becomes negative, the system is unstable. It is not possible to write the power expansion $\psi(s)$ explicitly for an arbitrary value of n, however, one can see easily that the constant term (in s^0) is

$$a_n = \psi(0) = \omega_f^2 - g\sum_{i=1}^{n} \frac{b^T \phi_i \phi_i^T b}{\mu_i {\omega_i}^2}$$

In this case, a_n becomes negative when the static loop gain becomes larger than 1. The stability condition is therefore

$$gG(0)H(0) = \frac{g}{\omega_f^2}\{\sum_{i=1}^{n} \frac{b^T \phi_i \phi_i^T b}{\mu_i {\omega_i}^2}\} < 1 \tag{6.131}$$

Note that it is independent of the structural damping in the system. Since the instability occurs for large gains which are not used in practice, the PPF can be regarded as unconditionally stable. Unlike the lead controller of the previous section which controls all the modes which belong to $z < \omega_i < p$, the PPF filter must be tuned on the targeted mode (it is therefore essential to know the natural frequency accurately), and the authority on the modes with very different frequencies is substantially reduced. Several PPF filters can be used in parallel, to target several modes simultaneously, but they must be tuned with care, because of the cross coupling between the various loops.

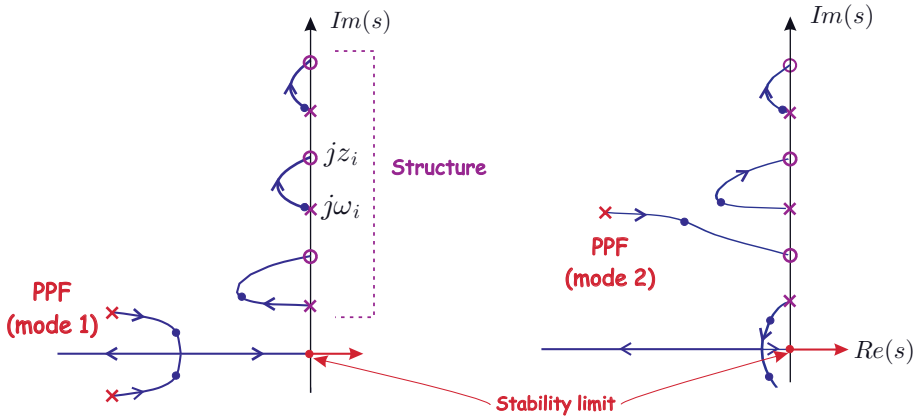

Fig. 6.18. Root locus of the PPF controller applied to a structure with collocated actuator and sensor (the open-loop transfer function has the same number of poles and zeros). (a) Targeted at mode 1. (b) Targeted at mode 2. (For clarity, different scales are used for the real and the imaginary axes.)

6.11 Remark

Throughout this chapter, structural damping has been ignored; this assumption has led to fairly simple analytical results for the closed-loop modal active damping. In the presence of light structural damping, the passive and active damping can simply be added.

In the absence of structural damping, the closed-loop stability has been achieved as a result of the collocation, leading to a fixed, alternating pole-zero pattern, and because perfect actuator and sensor dynamics have been assumed. For non-collocated control systems, this approach is not sufficient, because it is not possible to stabilize (by feedback) a distributed flexible structure if the structural damping is ignored, due to *spillover* (some destabilization always occurs outside the bandwidth of the controller, as expressed by the *Bode Integrals*). Similarly, the actuator and sensor dynamics alters the pole-zero pattern of the control system and, here again, structural damping is necessary to achieve closed-loop stability with imperfect actuator-sensor dynamics.

6.12 References

ABU HANIEH, A., *Active isolation and damping of vibrations via Stewart platform*, PhD Thesis, Université Libre de Bruxelles, Active Structures Laboratory, 2003.

ACHKIRE, Y., *Active tendon control of cable-stayed bridges*, PhD Thesis, Université Libre de Bruxelles, Active Structures Laboratory, 1997.

ANDERSON, E.H., HAGOOD, N.W., Simultaneous piezoelectric sensing/actuation: analysis and application to controlled structures, *Journal of Sound and Vibration*, 174, 617-639, 1994.

AUBRUN, J.N. Theory of the control of structures by low-authority controllers, *AIAA J. Guidance and Control*, Vol.3, No 5, 444-451, Sept.-Oct. 1980.

BALAS, M.J., Active Control of Flexible Systems, *Journal of Optimization Theory and Applications*, Vol.25, No 3, 415-436, 1978.

BALAS, M.J., Direct Velocity Feedback Control of Large Space Structures, *AIAA J. of Guidance and Control*, Vol.2, No 3, 252-253, 1979.

BOSSENS, F., *Contrôle actif des structures câblées: de la théorie à l'implémentation*, PhD Thesis, Université Libre de Bruxelles, Active Structures Laboratory, 2001.

CANNON, R.H. & ROSENTHAL, D.E., Experiment in Control of Flexible Structures with Noncolocated Sensors and Actuators, *AIAA J. of Guidance and Control*, Vol.7, No 5, 546-553, Sep.-Oct., 1984.
CHEN, W.-K., *Passive and Active Filters*, Wiley, 1986.
CLARK, W.W., Vibration control with state-switched piezoelectric materials, *Journal of Intelligent Material Systems and Structures*, Vol.11, 263-271, April, 2000.
DAVIS, C.L., LESIEUTRE, G.A., A modal strain energy approach to the prediction of resistivity shunted piezoceramic damping, *Journal of Sound and Vibration*, **184**(1), 129-139, 1995.
DELIYANNIS, T., SUN, Y., FIDLER, J.K., *Continuous-Time Active Filter Design*, CRC Press, 1999.
DEN HARTOG, J.P., *Mechanical Vibrations*, McGraw-Hill, 1947.
DÖRLEMANN, C., MUSS, P., SCHUGT, M., UHLENBROCK, R., New high speed current controlled amplifier for PZT multilayer stack actuators, *ACTUATOR-2002*, Bremen, June, 2002.
DOSCH, J., INMAN, D., GARCIA, E., A self-sensing piezoelectric actuator for collocated control, *Journal of Intelligent Material Systems and Structures*, 3, 166-185, 1992.
EDBERG, D.L., BICOS, A.S., FECHTER, J.S., On piezoelectric energy conversion for electronic passive damping enhancement, Proceedings of *Damping'91*, San Diego, 1991.
FANSON, J.L., CAUGHEY, T.K., Positive Position Feedback control of large space structures, *AIAA Journal*, Vol.28, No 4, 717-724, April 1990.
FORWARD, R.L., Electronic damping of vibrations in optical structures, *Journal of Applied Optics*, **18**, 690-697, March, 1979.
FORWARD, R.L., US Patent 4,158,787, June 1979.
GEVARTER, W.B., Basic relations for control of flexible vehicles, *AIAA Journal*, Vol.8, No 4, 666-672, April 1970.
GOH, C.J., CAUGHEY, T.K., On the stability problem caused by finite actuator dynamics in the collocated control of large space structures, *Int. J. Control*, Vol.41, No 3, 787-802, 1985.
GUYOMAR, D., RICHARD, C., Non-linear and hysteretic processing of piezoelement: Application to vibration control, wave control and energy harvesting, *Int. Journal of Applied Electromagnetics and Mechanics*, 21, 193-207, 2005.
HAGOOD, N.W., CRAWLEY, E.F., Experimental investigation of passive enhancement of damping for space structures, *AIAA J. of Guidance*, vol.14, No 6, 1100-1109, Nov.-Dec. 1991.

HAGOOD, N.W., von FLOTOW, A., Damping of structural vibrations with piezoelectric materials and passive electrical networks, *Journal of Sound and Vibration* **146**(2), 243-268, 1991.

HOLLKAMP, J.J., Multimodal passive vibration suppression with piezoelectric materials and resonant shunts, *J. Intell. Material Syst. Structures*, Vol.5, Jan.1994.

HUGHES, P.C., ABDEL-RAHMAN, T.M., Stability of Proportional Plus Derivative Plus Integral Control of Flexible Spacecraft, *AIAA J. of Guidance and Control*, Vol.2, No 6, 499-503, Nov.-Dec., 1979.

MARTIN, G.D. *On the control of flexible mechanical systems*, PhD Thesis, Stanford University, 1978.

MOHEIMANI, S.O.R., A survey of recent innovations in vibration damping and control using shunted piezoelectric transducers, *IEEE Transactions on Control Systems Technology*, Vol.11, No 4, 482-494, July 2003.

PARK, C.H., BAZ, A. Vibration control of beams with negative capacitive shunting of interdigital electrode piezoceramics, *Journal of Vibration and Control*, Vol.11: 331-346, 2005.

PREUMONT, A., DUFOUR, J.P., MALEKIAN, C., Active damping by a local force feedback with piezoelectric actuators, *AIAA J. of Guidance*, Vol.15, No 2, 390-395, March-April, 1992.

PREUMONT, A., ACHKIRE, Y., Active damping of structures with guy cables, *AIAA Journal of Guidance, Control, and Dynamics*, Vol.20, No 2, 320-326, March-April 1997.

PREUMONT, A., ACHKIRE, Y., BOSSENS, F., Active tendon control of large trusses, *AIAA Journal*, Vol.38, No 3, 493-498, March 2000.

PREUMONT, A. *Vibration Control of Active Structures, An Introduction*, (2nd Edition), Kluwer, 2002.

Bibliography

ABU HANIEH, A., *Active isolation and damping of vibrations via Stewart platform*, PhD Thesis, Université Libre de Bruxelles, Active Structures Laboratory, 2003.

ACHKIRE, Y., *Active tendon control of cable-stayed bridges*, PhD Thesis, Université Libre de Bruxelles, Active Structures Laboratory, 1997.

AGARWAL, B.D., BROUTMAN, L.J., *Analysis and Performance of Fiber Composites*, Wiley, 2nd Ed., 1990.

ALLIK, H., HUGHES T.J.R., Finite Element method for piezoelectric vibration, *Int. J. for Numerical Methods in Engineering*, Vol.2, 151-157, 1970.

ANDERSON, E.H., HAGOOD, N.W., Simultaneous piezoelectric sensing/actuation: analysis and application to controlled structures, *Journal of Sound and Vibration*, 174, 617-639, 1994.

AUBRUN, J.N. Theory of the control of structures by low-authority controllers, *AIAA J. Guidance and Control*, Vol.3, No 5, 444-451, Sept.-Oct. 1980.

BALAS, M.J., Active Control of Flexible Systems, *Journal of Optimization Theory and Applications*, Vol.25, No 3, 415-436, 1978.

BALAS, M.J., Direct Velocity Feedback Control of Large Space Structures, *AIAA J. of Guidance and Control*, Vol.2, No 3, 252-253, 1979.

BENJEDDOU, A., Advances in piezoelectric finite element modeling of adaptive structural element: a survey, *Computers and Structures*, 76, 347-363, 2000.

BOSSENS, F., *Contrôle actif des structures câblées: de la théorie à l'implémentation*, PhD Thesis, Université Libre de Bruxelles, Active Structures Laboratory, 2001.

BURKE, S.E., HUBBARD, J.E., Active vibration control of a simply supported beam using spatially distributed actuator. *IEEE Control Systems Magazine*, August, 25-30, 1987.

CADY, W.G., *Piezoelectricity: an Introduction to the Theory and Applications of Electromechanical Phenomena in Crystals*, McGrawHill, 1946.

CANNON, R.H. & ROSENTHAL, D.E., Experiment in Control of Flexible Structures with Noncolocated Sensors and Actuators, *AIAA J. of Guidance and Control*, Vol.7, No 5, 546-553, Sep.-Oct., 1984.

CHEN, W.-K., *Passive and Active Filters*, Wiley, 1986.

CLARK, W.W., Vibration control with state-switched piezoelectric materials, *Journal of Intelligent Material Systems and Structures*, Vol.11, 263-271, April, 2000.

CLOUGH, R.W., PENZIEN, J., *Dynamics of Structures*, McGraw-Hill, 1975.

CRAIG, R.R., Jr., *Structural Dynamics*, Wiley, 1981.

CRANDALL, S.H., KARNOPP, D.C., KURTZ, E.F, Jr., PRIDMORE-BROWN, D.C., *Dynamics of Mechanical and Electromechanical Systems*, McGraw-Hill, N-Y, 1968.

CRAWLEY, E.F., LAZARUS, K.B., Induced strain actuation of isotropic and anisotropic plates, *AIAA Journal*, Vol.29, No 6, pp. 944-951, 1991.

DAVIS, C.L., LESIEUTRE, G.A., A modal strain energy approach to the prediction of resistivity shunted piezoceramic damping, *Journal of Sound and Vibration*, **184**(1), 129-139, 1995.

D'AZZO, J.J., HOUPIS, C.H., *Feedback Control System Analysis & Synthesis*, Second Edition, McGraw-Hill, N-Y, 1966.

DE BOER, E., Theory of Motional Feedback, *IRE Transactions on Audio*, 15-21, Jan.-Feb., 1961.

DELIYANNIS, T., SUN, Y., FIDLER, J.K., *Continuous-Time Active Filter Design*, CRC Press, 1999.

DEN HARTOG, J.P., *Mechanical Vibrations*, McGraw-Hill, 1947.

DIMITRIADIS, E.K., FULLER, C.R., ROGERS, C.A., Piezoelectric actuators for distributed vibration excitation of thin plates, *Trans. ASME, J. of Vibration and Acoustics*, Vol.113, pp. 100-107, January 1991.

DÖRLEMANN, C., MUSS, P., SCHUGT, M., UHLENBROCK, R., New high speed current controlled amplifier for PZT multilayer stack actuators, *ACTUATOR-2002*, Bremen, June, 2002.

DOSCH, J., INMAN, D., GARCIA, E., A self-sensing piezoelectric actuator for collocated control, *Journal of Intelligent Material Systems and Structures*, 3, 166-185, 1992.

EDBERG, D.L., BICOS, A.S., FECHTER, J.S., On piezoelectric energy conversion for electronic passive damping enhancement, Proceedings of *Damping'91*, San Diego, 1991.

EER NISSE, E.P., Variational method for electrostatic vibration analysis, *IEEE Trans. on Sonics and Ultrasonics*, Vol. SU-14, No 4, 153-160 October 1967.

FANSON, J.L., CAUGHEY, T.K., Positive Position Feedback control of large space structures, *AIAA Journal*, Vol.28, No 4, 717-724, April 1990.

FORWARD, R.L., Electronic damping of vibrations in optical structures, *Journal of Applied Optics*, **18**, 690-697, March, 1979.

FORWARD, R.L., US Patent 4,158,787, June 1979.

GARCIA LAGE, R., MOTA SOARES, C.M., MOTA SOARES, C.A., REDDY, J.N., Layerwise partial mixed finite element analysis of magneto-electro-elastic plates, *Computers an Structures*, 82, 1293-1301, 2004.

GERADIN, M., RIXEN, D., *Mechanical Vibrations*, Wiley, 1994.

GEVARTER, W.B., Basic relations for control of flexible vehicles, *AIAA Journal*, Vol.8, No 4, 666-672, April 1970.

GOH, C.J., CAUGHEY, T.K., On the stability problem caused by finite actuator dynamics in the collocated control of large space structures, *Int. J. Control*, Vol.41, No 3, 787-802, 1985.

GOLDSTEIN, H., *Classical Mechanics*, Second Edition, Addison-Wesley, 1980.

GUYOMAR, D., RICHARD, C., Non-linear and hysteretic processing of piezoelement: Application to vibration control, wave control and energy harvesting, *Int. Journal of Applied Electromagnetics and Mechanics*, 21, 193-207, 2005.

HAGOOD, N.W., CRAWLEY, E.F., Experimental investigation of passive enhancement of damping for space structures, *AIAA J. of Guidance*, vol.14, No 6, 1100-1109, Nov.-Dec. 1991.

HAGOOD, N.W., von FLOTOW, A., Damping of structural vibrations with piezoelectric materials and passive electrical networks, *Journal of Sound and Vibration* **146**(2), 243-268, 1991.

HEYLIGER, P., PEI, K.C., SARAVANOS, D., Layerwise mechanics and finite element model for laminated piezoelectric shells, *AIAA Journal*, Vol.34, No 11, 2353-2360, November 1996.

HOLLKAMP, J.J., Multimodal passive vibration suppression with piezoelectric materials and resonant shunts, *J. Intell. Material Syst. Structures*, Vol.5, Jan.1994.

HUGHES, P.C., ABDEL-RAHMAN, T.M., Stability of Proportional Plus Derivative Plus Integral Control of Flexible Spacecraft, *AIAA J. of Guidance and Control*, Vol.2, No 6, 499-503, Nov.-Dec., 1979.

HUNT, F.V., *Electroacoustics: The Analysis of Transduction, and its Historical Background*, Harvard Monographs in Applied Science, No 5, 1954. Reprinted, Acoustical Society of America, 1982.

HWANG, W.-S., PARK, H.C., Finite element modeling of piezoelectric sensors and actuators, *AIAA Journal*, Vol.31, No 5, pp. 930-937, May 1993.

IEEE Standard on Piezoelectricity, ANSI/IEEE Std 176-1987.

KARNOPP, D.C., TRIKHA, A.K., Comparative study of optimization techniques for shock and vibration isolation, *Trans. ASME, J. of Engineering for Industry, Series B*, 91, 1128-1132, 1969.

LEE, C.-K., Theory of laminated piezoelectric plates for the design of distributed sensors/actuators - Part I: Governing equations and reciprocal relationships, *J. of Acoustical Society of America*, Vol. 87, No. 3, 1144-1158, March 1990.

LEE, C.-K., CHIANG, W.-W., O'SULLIVAN, T.C., Piezoelectric modal sensor/actuator pairs for critical active damping vibration control, *J. of Acoustical Society of America*, Vol. 90, No. 1, 374-384, July 1991.

LEE, C.-K., MOON, F.C., Modal sensors/actuators, *Trans. ASME, J. of Applied Mechanics*, Vol.57, pp.434-441, June 1990.

LERCH, R., Simulation of piezoelectric devices by two- and three-dimensional finite elements, *IEEE Transactions on Ultrasonics, Ferroelectrics, and Frequency Control*, Vol. 37, No. 3, May 1990.

MARTIN, G.D. *On the control of flexible mechanical systems*, PhD Thesis, Stanford University, 1978.

MEIROVITCH, L., *Methods of Analytical Dynamics*, McGraw-Hill, 1970.

MOHEIMANI, S.O.R., A survey of recent innovations in vibration damping and control using shunted piezoelectric transducers, *IEEE Transactions on Control Systems Technology*, Vol.11, No 4, 482-494, July 2003.

PARK, C.H., BAZ, A. Vibration control of beams with negative capacitive shunting of interdigital electrode piezoceramics, *Journal of Vibration and Control*, Vol.11: 331-346, 2005.

PHILBRICK RESEARCHES, Inc., *Application Manual for Computing Amplifiers for Modelling, Measuring, Manipulating & Much Else*, Nimrod Press, Boston, 1965.

Philips Application Book on Piezoelectric Ceramics, (J. Van Randeraat & R.E. Setterington, Edts), Mullard Limited, London, 1974.

Physik Intrumente catalogue, Products for Micropositioning (*PI* GmbH, FRG).

PIEFORT, V., *Finite element modelling of piezoelectric active structures*, PhD Thesis, Université Libre de Bruxelles, Active Structures Laboratory, 2001.

PRATT, J., FLATAU, A., Development and analysis of self-sensing magnetostrictive actuator design, SPIE Smart Materials and Structures Conference, Vol.1917, 1993.

PREUMONT, A., DUFOUR, J.P., MALEKIAN, C., Active damping by a local force feedback with piezoelectric actuators, *AIAA J. of Guidance*, Vol.15, No 2, 390-395, March-April, 1992.

PREUMONT,A., ACHKIRE, Y., Active damping of structures with guy cables, *AIAA Journal of Guidance, Control, and Dynamics*, Vol.20, No 2, 320-326, March-April 1997.

PREUMONT, A., ACHKIRE, Y., BOSSENS, F., Active tendon control of large trusses, *AIAA Journal*, Vol.38, No 3, 493-498, March 2000.

PREUMONT, A. *Vibration Control of Active Structures, An Introduction*, (2nd Edition), Kluwer, 2002.

PREUMONT, A., FRANÇOIS, A., DE MAN, P., PIEFORT, V., Spatial filters in structural control, *Journal of Sound and Vibration*, 265, 61-79, 2003.

PREUMONT, A., FRANÇOIS, A., DE MAN, P., LOIX, N., HENRIOULLE, K., Distributed sensors with piezoelectric films in design of spatial filters for structural control, *Journal of Sound and Vibration*, 282, 701-712, 2005.

ROSEN, C.A., Ceramic transformers and filters, Proc. Electronic Component Symposium, p.205-211 (1956).

REDDY, J.N., *Energy and Variational Methods in Applied Mechanics*, Wiley, 1984.

REX, J., ELLIOTT, S.J., The QWSIS, A new sensor for structural radiation control, MOVIC-1, Yokohama, Sept. 1992.

SCHWEITZER, G., BLEULER, H., TRAXLER, A., *Active Magnetic Bearings*, vdf Hochschulverlag AG an der ETH Zürich, 1994.

TIERSTEN, H.F., Hamilton's principle for linear piezoelectric media, *Proceedings of the IEEE*, 1523-1524, August 1967.

UCHINO, K., *Ferroelectric Devices*, Marcel Dekker, 2000.

WILLIAMS, J.H., Jr., *Fundamentals of Applied Dynamics*, Wiley, 1996.

WOODSON, H.H., MELCHER, J.R, *Electromechanical Dynamics, Part I: Discrete Systems*, Wiley, 1968.

Index

absolute velocity sensor, 89
active circuit, 112, 136
active damping, 159
active strut, 161
active tendon, 184
admittance, 109, 166, 170
alternating poles and zeros, 143, 155, 167
anti-resonance, 144
Assumed Modes method, 32

bearing stiffness, 91
blocked electrical impedance, 92
Bode Integrals, 195
Bode plots, 145
bridge, 93, 185
buckling, 38

Campbell diagram, 27
capacitive microphone, 79
charge amplifier, 136, 138, 161
coenergy density function, 118, 119
coenergy function, 102, 103
collocated, 141, 143, 154, 159, 163
condenser microphone, 79
conservation of energy, 11, 30
conservative force, 10
conservative transducer, 61, 62, 65
constitutive equations
  circuit elements, 42
  electromechanical transducer, 92
  linear elastic material, 34
  piezoelectric laminate, 148
  piezoelectric material, 116
  piezoelectric transducer, 99

Curie temperature, 98
current amplifier, 136
current control (IFF), 169
current source, 45

D'Alembert principle, 10
damping, 159
  ratio, 160
decentralized control, 183
degree of freedom, 5
direct piezoelectric effect, 96
dissipation function, 19, 74
distributed sensor, 136
divergence theorem, 123, 153
duality, 154
dynamic amplification, 146, 160
dynamic flexibility matrix, 162

effective force, 10
electric dipoles, 98
electrical
  coenergy, 43, 51, 63
  energy, 42, 49, 63
  enthalpy density, 120
electrode shape, 134
electrodynamic isolator, 84
electromagnetic plunger, 76
electromechanical
  coenergy, 101
  energy, 101
electromechanical converter, 70
electromechanical coupling factor, 81, 99, 100, 103, 109, 111, 129, 160, 173
energy density, 118

energy storing transducer, 62, 65
energy transformer, 68
Euler-Bernoulli beam, 14, 33, 131, 141

Faraday's law, 43, 68
feedthrough, 145, 147, 190
force sensor, 162
force to current factor, 91
fraction of modal strain energy, 160, 164, 167, 173
fraction of strain energy, 110

Gauss's law, 123
generalized coordinates, 4, 17
generalized electromechanical coupling factor, 160, 176, 179
generalized momentum, 31
geometric
  stiffness, 35
  strain energy, 36
geophone, 87
Green strain tensor, 34
gyroscopic
  forces, 17, 25
  system, 17, 24

Hamilton's principle, 11, 121, 131
  charge formulation, 47, 71
  flux linkage formulation, 49, 72
high-pass filter, 138
holonomic constraint, 5, 28
homogenized piezoelectric constant, 156
hydrostatic (loads), 152

ignorable coordinate, 30
impedance (piezoelectric transducer), 109
impulse response, 159
inductive shunting, 176
Integral Force Feedback (IFF), 160, 165
interlacing, 145
inverse piezoelectric effect, 96

Jacobi integral, 29

kinematic constraint, 5
kinetic
  coenergy, 2, 17
  energy, 2
Kirchhoff
  current rule (KCR), 41, 46
  voltage rule (KVR), 41, 46
Kirchhoff plate theory, 148
Kronecker delta index, 139

Lagrange multipliers, 28
Lagrange's equation, 17, 75
  charge formulation, 53, 73
  flux linkage formulation, 54, 73
  with constraints, 27
Lagrangian, 12, 18, 51, 53, 72, 75
  piezoelectric structure, 106, 113, 114, 182
laminar sensor, 136
lead compensator, 191
Lead-Zirconate-Titanate, 98
Legendre transformation, 3, 43, 44, 63, 66, 102, 118
Lorentz force, 68
loudspeaker, 77

magnetic
  coenergy, 44, 49, 66
  energy, 44, 51, 66
  suspension, 89
mechanical impedance, 92
MEMS, 61
MFC, 185
microphone (capacitive), 79
Mindlin shell, 155
modal
  actuator, 139
  filter, 139
  sensor, 140
  truncation, 145
motional impedance, 93
movable core inductor, 65
movable plate capacitor, 62
moving coil transducer, 68
  coenergy function, 70
multi-functional materials, 95
multi-layer laminate, 149

natural boundary conditions, 16, 124
negative capacitance, 111, 112, 175
non-conservative force, 12
non-holonomic constraint, 6, 28
Nyquist diagram, 145

operational amplifier, 112, 136
orthogonality conditions, 139, 162

Painlevé integral, 30
parabolic electrode, 135, 138
passive damping, 159
piezoelectric
  beam, 155
  coenergy, 103
  energy, 102
  laminate, 131, 147, 151
  loads, 133, 152
  materials, 95
  transformer (Rosen's), 124
pole-zero pattern, 143, 191
poling, 98
Polyvinylidene fluoride, 98
porous electrode, 156
Positive Position Feedback (PPF), 193
prestressed piezoelectric transducer, 109
principle of virtual work, 8
proof-mass actuator, 82
PVDF, 98
PZT, 98
  fibers, 156

quality factor, 129
quasi-static correction, 146

Rayleigh-Ritz method, 32, 38, 124
rectangular electrode, 134, 137
reluctance force, 89
residual mode, 147, 165
resistive shunting, 172
resonance, 144
roll-off, 145, 191, 192
root locus, 168, 173, 180, 192, 193
Rosen's piezoelectric transformer, 124
Routh-Hurwitz criterion, 193

SAMCEF, 156
scleronomic constraint, 5
self-equilibrating forces, 107, 115, 134
self-sensing, 93, 185
sky-hook, 86
smart materials, 95
spatial filter, 139, 156
special relativity, 4
spillover, 141, 195
Stewart-Gough platform, 184
stored electromechanical energy, 101
strain energy density, 34

thermal analogy, 107
transducer, 61, 159
  constant (transduction coefficient), 69, 92
transmissibility, 86
triangular electrode, 135, 138

unconstrained expansion, 107

virtual displacement, 7
virtual work, 8, 52–54
voice coil, 68
voltage control (IFF), 165
voltage source, 45
volume displacement, 138